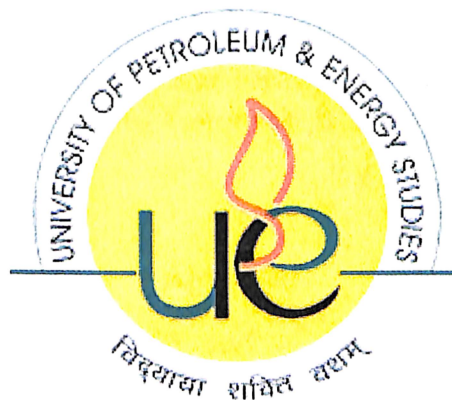


# DESIGN OF NUCLEAR POWER PLANT WITH GAS TURBINE-MODULAR HELIUM COOLED REACTOR

By  
**VELIDI V S S GURUNADH**  
R660209017/500007924



College of Engineering  
University of Petroleum & Energy Studies  
Dehradun  
May, 2011

UPES - Library



---DH306---

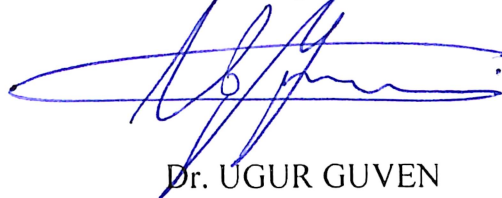
GUR-2011MT

# DESIGN OF NUCLEAR POWER PLANT WITH GAS TURBINE- MODULAR HELIUM COOLED REACTOR

A thesis submitted in partial fulfillment of the requirements for the Degree of  
Master of Technology in  
Energy Systems Engineering

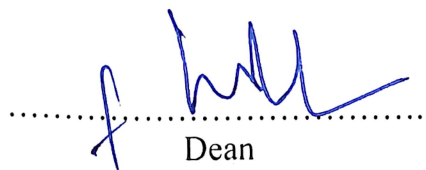
By  
VELIDI V S S GURUNADH  
R660209017/500007924

Under the guidance of



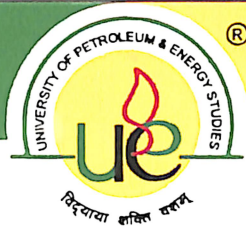
Dr. UGUR GUVEN  
Professor of Aerospace Engineering (Ph.D)  
Nuclear Science and Technology Engineer (M.Sc)  
University of Petroleum & Energy Studies

Approved



.....  
Dean

College of Engineering  
University of Petroleum & Energy Studies  
Dehradun



**UNIVERSITY OF PETROLEUM & ENERGY STUDIES**  
(ISO 9001:2000 Certified)

**CERTIFICATE**

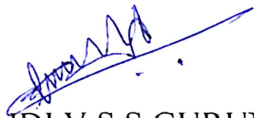
This is to certify that the work contained in this thesis titled “**DESIGN OF NUCLEAR POWER PLANT WITH GAS TURBINE-MODULAR HELIUM COOLED REACTOR**” has been carried out by VELIDI V S S GURUNADH (R660209017/500007924) under my guidance and has not been submitted elsewhere for a degree.

Dr. UGUR GUVEN  
Professor of Aerospace Engineering (Ph.D)  
Nuclear Science and Technology Engineer (M.Sc)  
University of Petroleum & Energy Studies

## ACKNOWLEDGMENTS

I would like to express my deep appreciation and thanks for my guide Dr Ugur Guven. This work is supported by Dr.Kamal Bansal from the day of synopsis to the final day, I am also Thank full to my parents Mr.VG V Subrahmanyam and Ms.V S L V Kameswari, their suport for my higher education. Also I am very much thank full to Mr. Sandeepan, Mr. Pavan kumar for their support.

May 2011



VELIDI V S S GURUNADH  
M.TECH ENERGY SYSTEMS

## TABLE OF CONTENTS

	<u>Page</u>
<b>TABLE OF CONTENTS</b> .....	6
<b>LIST OF TABLES</b> .....	7
<b>LIST OF FIGURES</b> .....	9
<b>ABBREVIATIONS</b> .....	12
<b>NOMENCLATURE</b> .....	13
<b>ABSTRACT</b> .....	14
<b>1. INTRODUCTION</b> .....	15
1.1 Nuclear Fission Reaction .....	19
1.2 Heat Exchange in Fission Reactors .....	20
1.3 Concept of Cooling Reactors .....	26
<b>2. GAS COOLED REACTORS</b> .....	30
2.1 Gas Cooled Reactors Concepts .....	30
2.2 Gas Coolents for Reactors.....	31
2.3 Gas Cooled Reactor Systems .....	33
2.4 Carbon Dioxide Cooling .....	38
<b>3. HELIUM COOLED REACTORS</b> .....	40
3.1 Introduction to Helium Cooled Reactor .....	40
3.2 Properties of Helium .....	42
3.3 Why Helium-Safety Issue-Longevity.....	43
3.4 Nuclear Fuel for Helium Cooled Reactors... <b>Error! Bookmark not defined.</b>	45
3.5 Conduction/ Radiation Cool Down To Boundary and Thermal Inertia .....	59
<b>4. CFD ANALYSIS OF HEAT TRANSFER IN THE NUCLEAR CORE... Error!</b> <b>Bookmark not defined.</b>	<b>68</b>
4.1 Initial Boundary Conditions .....	68
4.2 Fuel Elements Arrangement in a Core .....	69
4.3 3D Modelling on Fuel Pebbles..... <b>Error! Bookmark not defined.</b>	<b>93</b>
<b>5. THERMODYNAMIC ANALYSIS OF GT-MHR</b> <b>Error! Bookmark not defined.</b>	<b>105</b>
5.1 Gas Turbine power conversion system .....	105
5.2 Thermal Design of GT-MHR.....	107
5.3 Helium Gas Turbo Machines .....	<b>Error! Bookmark not defined.</b>
5.4 Reactor Vessel.....	115
5.4 Compact Heat Exchanger .....	117
5.4 Turbine-Compressor Analysis.....	121
<b>6. MATERIAL ANALYSIS FOR HELIUM COOLED REACTORS</b> <b>127</b> <b>Error!</b> <b>Bookmark not defined.</b>	<b>127</b>
6.1 Niobium 1 % Zirconium .....	127
6.2 Hastelloy X.....	129
6.3 Beryllium Oxide .....	131
6.4 Rhenium .....	133
6.5 Crystal Structures .....	134
6.6 Fuel Materials.....	138
6.7 Reactor Shielding Analysis .....	144

6.8 Material Selection of Helium-Cooled Fusion Power Plant Designs .....	145
6.9 Mechanical Design and Reliability .....	148
<b>7. USGAE OF HELIUM COOLED REACTORS IN VARIOUS APPLICATIONS</b> .....	<b>150</b>
7.1 Space Power Applications.....	150
7.2 Hydrogen Production .....	161
7.3 Helium Cooling for Fusion Reactors .....	163
<b>8. RESULTS AND DISCUSSIONS .....</b>	<b>168</b>
<b>REFERENCES.....</b>	<b>Error! Bookmark not defined.170</b>
<b>APPENDICES .....</b>	<b>174</b>

## LIST OF TABLES

	<u>Page</u>
<b>Table 1.1:</b> Properties of various coolents for nuclear reactors <b>Error! Bookmark not defined.</b>	
<b>Table 3.1:</b> Properties of natural Helium .....	42
<b>Table 3.2:</b> Core Evacuation Time for Representative Pebble Densities .....	56
<b>Table 3.3:</b> Thermal Properties of Pebble Material .....	60
<b>Table 3.4:</b> Vessel Conduction Decay Heat Removal .....	62
<b>Table 3.5:</b> Fuel Pebbles Design Parameters for Helium Cooled Reactors .....	64
<b>Table 5.1:</b> Thermal Reactor design Parameters .....	111
<b>Table 5.2:</b> Thermal Cycle Design Perameters .....	111
<b>Table 5.3:</b> Helium Properties for Thermal Cycle Design Parameters .....	113
<b>Table 5.4:</b> Operating Conditions for Compact Heat Exchangers .....	118
<b>Table 5.5:</b> Design Perameters of compressors .....	122
<b>Table 6.1:</b> Critical Energies Compared to Binding Energy of Last Neutron .....	140
<b>Table 6.2:</b> Properties of Different Uranium Isotopes .....	141
<b>Table 6.3:</b> Types and Compsiton of Fuel in the GT-MHR .....	143
<b>Table 6.4:</b> Material Compositon of TRISO Fuel Pebbles .....	144
<b>Table 6.5:</b> Key Design Parameters for Different Structural Materials .....	149
<b>Table 7.1:</b> Distance In our Solar System .....	151
<b>Table 7.2:</b> Space Impulse for 10,000 Kg Space Probe.....	153
<b>Table 7.3:</b> Physiscal Properties of Coolant Materials .....	158
<b>Table A.1:</b> Physical Properties of the Fluid .....	174
<b>Table B.1:</b> Thermodynamic Properties of the Fluid .....	174
<b>Table C.1:</b> Properties of Pyro CarbonThermal Reactor design Parameters .....	176
<b>Table D.1:</b> Model Settings .....	177
<b>Table D.2:</b> Model Zone .....	177
<b>Table E.1:</b> Fluid .....	177
<b>Table E.2:</b> Reactor Inlet .....	178
<b>Table E.3:</b> Reactor Outlet.....	179
<b>Table E.4:</b> Side Walls .....	180
<b>Table E.5:</b> Fuel Pebblesl .....	181
<b>Table F.1:</b> Linear Solverl .....	182
<b>Table G.1:</b> Discretization Scheme .....	182
<b>Table H.1:</b> Material: Titanium (Solid).....	182
<b>Table H.2:</b> Material: Steel (Solid).....	182
<b>Table H.3:</b> Material: Helium (Fluid) .....	183
<b>Table H.4:</b> Material: Air (Fluid) .....	183
<b>Table H.5:</b> Material: Aluminium (Solid) .....	184
<b>Table I.1 :</b> Solution Limits.....	184
<b>Table J.1 :</b> Hydrogen Production Source Analysis.....	184

## LIST OF FIGURES

	<u>Page</u>
<b>Figure 1.1</b> : Neutron Interaction With Fissile Material And Enery Release .....	16
<b>Figure 1.2</b> : Binding Energy Per Nucleon Vs Binding Energy .....	18
<b>Figure 1.3</b> : Yeild of Fission Products According To The Mass Number .....	20
<b>Figure 1.4</b> : Heat Flow In Fuel Element .....	26
<b>Figure 2.1</b> : Gas Cooled Reactor Core Arrangement .....	34
<b>Figure 3.1</b> : Helium Cooled Reactor Coolant Circulating System .....	41
<b>Figure 3.2</b> : Helium Cooled Reactor Fuel Temerature Effect .....	45
<b>Figure 3.3</b> : TRISO Coated Fuel Pebbles .....	46
<b>Figure 3.4</b> : Maximum Temperature Selection For Trisco Coated Fuel Pebbles ...	46
<b>Figure 3.5</b> : Helium Cooled Reactor Fuel Partical Bed Arrangement .....	55
<b>Figure 3.6</b> : Helium Cooled Reactor Fuel Temperature Limits .....	57
<b>Figure 3.7</b> : GT-MHR Radial Temperature Gradient During After-Heat Rejection Maximum .....	61
<b>Figure 3.8</b> : GT-MHR Coolent Flow Variation In Reactor Core .....	63
<b>Figure 3.9</b> : Natural Convection Loop In Side The Reactor .....	67
<b>Figure 4.1</b> : Fuel Pebbels Arrangement In Side The Nucler Core .....	70
<b>Figure 4.2</b> : Fuel Pebbel Structure .....	71
<b>Figure 4.3</b> : 2D Modelling Of Fuel Pebbels In Gambit .....	72
<b>Figure 4.4</b> : Mesh Generation On 2d Model .....	73
<b>Figure 4.5</b> : Mesh Generation On Fuel Pebbles .....	74
<b>Figure 4.6</b> : Grid Displayed In Fluent 2d Model .....	75
<b>Figure 4.7</b> : Absolute Pressure Contours Of 2d Model .....	76
<b>Figure 4.8</b> : Dynamic Pressure Contours Of 2d Model .....	77
<b>Figure 4.9</b> : Relative Total Pressure Inside The Reactor .....	77
<b>Figure 4.10</b> : Pressure Coefficent For A Pebbles System .....	78
<b>Figure 4.11</b> : Static Pressure In Side The Reactor .....	79
<b>Figure 4.12</b> : Relative Y Velocity In Side The Reactor .....	79
<b>Figure 4.13</b> : Relative X Velocity In Side The Reactor .....	80
<b>Figure 4.14</b> : Radial Velocity Contours In Side The Reactor .....	81
<b>Figure 4.15</b> : Tangentail Velcity Contours In Side The Reactor .....	81
<b>Figure 4.16</b> : Velocity Vectors Colared By Relative Velocity Magnitude .....	82
<b>Figure 4.17</b> : Relative Velocity Magnitude .....	83
<b>Figure 4.18</b> : X- Velocity Contours In Side The Reactor .....	83
<b>Figure 4.19</b> : Y- Velocity Contours In Side The Reactor .....	84
<b>Figure 4.20</b> : Vector Colared By Radial Velocity .....	85
<b>Figure 4.21</b> : Velocity Vector Colared By Y Velocity .....	85
<b>Figure 4.22</b> : Velocity Vector Colared By Tangentail Velocity .....	86
<b>Figure 4.23</b> : Velocity Vectors Colored By Steam Function Side The Reactor .....	86
<b>Figure 4.24</b> : Velocity Vectots Colared By X Velocity .....	87
<b>Figure 4.25</b> : Static Temperture Contours .....	87
<b>Figure 4.26</b> : Relative Total Temperature .....	88



<b>Figure 4.27</b> : Outer Surface Wall Temperature .....	88
<b>Figure 4.28</b> : Inner Surface Wall Temperature .....	89
<b>Figure 4.29</b> : Contours Of Internal Energy .....	90
<b>Figure 4.30</b> : Contours of Entropy .....	90
<b>Figure 4.31</b> : Stream Fucntion .....	91
<b>Figure 4.32</b> : Total Energy Contours .....	92
<b>Figure 4.33</b> : Y-Wall Shear Stress .....	92
<b>Figure 4.34</b> : X-Wall Shear Stress Development .....	93
<b>Figure 4.35</b> : Gambit Modelling Based On 3d .....	94
<b>Figure 4.36</b> : Meshed Model For 3d Simulation .....	95
<b>Figure 4.37</b> : Turbulance Kinetic Energy .....	96
<b>Figure 4.38</b> : Turbulence Kinetic Energy .....	97
<b>Figure 4.39</b> : Turbulent Intensity .....	98
<b>Figure 4.40</b> : Total Temperature Between Fuel Pebbles .....	98
<b>Figure 4.41</b> : Internal Energy Development In Between Pebbels .....	99
<b>Figure 4.42</b> : Static Temperature In Between Pebbles .....	100
<b>Figure 4.43</b> : Velocity Vector Colored By Radial Velocity .....	100
<b>Figure 4.44</b> : Wall Temperature Effect On Pebbles .....	101
<b>Figure 4.45</b> : Wall Shear Stress Development .....	102
<b>Figure 4.46</b> : Total Pressure Development In Side The 3d Model .....	102
<b>Figure 4.47</b> : Relative Total Pressures .....	103
<b>Figure 4.48</b> : Total Turbulence Kinetic Energy .....	104
<b>Figure 4.49</b> : Total Temperature Contours .....	104
<b>Figure 5.1</b> : GT-MHR Power Conversion Unit .....	106
<b>Figure 5.2</b> : GT-MHR Thermodynamic Cycle Design .....	110
<b>Figure 5.3</b> : T-S Diagram For GT-MHR Cycle .....	112
<b>Figure 5.4</b> : P-V Diagram For GT-MHR Cycle .....	112
<b>Figure 5.5</b> : GT-MHR Model Design .....	114
<b>Figure 5.6</b> : Reactor Core Design For GT-MHR Plant .....	116
<b>Figure 5.7</b> : Uranium Enrichment With Respect To Its Work Requirement .....	120
<b>Figure 5.8</b> : Turbine And Compressor Arrangement On Shaft.....	124
<b>Figure 5.9</b> : PBMR Power Converstion System .....	126
<b>Figure 6.1</b> : Niobium 1 % Zerconium Mechanical Properties .....	128
<b>Figure 6.2</b> : Niobium 1 % Zerconium Thermal Properties .....	129
<b>Figure 6.3</b> : Hast-X Mechanical Properties .....	130
<b>Figure 6.4</b> : Hast-X Thermal Properties .....	131
<b>Figure 6.5</b> : Beo Mechanical Properties .....	132
<b>Figure 6.6</b> : Beo Thermal Properties .....	132
<b>Figure 6.7</b> : Uranium Enrichment With Respect To Its Work Requirement .....	141
<b>Figure 6.8</b> : Uranium Enrichment With Respect To Its Weight Requirement .....	142
<b>Figure 7.1</b> : Gas Core Reactor Cycle .....	159
<b>Figure 7.2</b> : Cavitated Gas Core Nuclear Reactor Fuel Elements .....	160
<b>Figure 7.3</b> : Hydrogen Production Cycle With Steam Reforming .....	162
<b>Figure 7.4</b> : Fusion Blancet Used In Helium Cooled Reactor .....	166

## ABBREVIATIONS

ITER	: International Thermonuclear Experimental Reactor
HEU	: Highly enriched uranium
IAEA	: International Atomic Energy
KWt	: Thermal Power Generated
FIMA	: Fissions per Initial Metal Atom.
DF	: Derived Fuel
DU	: Depleted Uranium
FP	: Fission product
FR	: Fast Reactor
GA	: General Atomic
GC	: Graphite-Carbon
GT-MHR	: Gas turbine modular helium cooled reactor
HLW	: High level radioactive waste
HTGR	: High Temperature gas cooled reactor
LLW	: Low level radioactive waste
LWR	: Light water reactor
MHA-bt	: Modular Helium accelerator -base transmutation
MHR	: Modular Helium cooled reactor
MHR-bt	: Modular Helium cooled reactor-base transmutation
MHTGR	: Modular high temperature gas cooled reactor
MOX	: Mixed oxide
NCS	: Nuclear Criticality safety
PWR	: Pressurized water reactor
SNR	: Spent Nuclear Fuel
TF	: Transmutation fuel
TRISO	: Particle Coating
TRU	: Transuranium

## NOMENCLATURE

<b>E</b>	: Energy
<b>f</b>	: Friction factor
<b>h</b>	: Effective heat transfer coefficient, W/m <sup>2</sup> -C
<b>k</b>	: Thermal conductivity of the material, W/m-C
<b>L</b>	: Length of the heat sink, m
<b>m</b>	: Mass of a neutron
<b>v</b>	: Velocity in a substance
<b>V</b>	: Volume flow rate, m <sup>3</sup> /s
<b>n1, n2</b>	: Exponents larger than 3
<b>q<sub>max</sub></b>	: Maximum heat flux, W/m <sup>2</sup>
<b>T<sub>in</sub></b>	: Inlet temperature of coolant, C
<b>T<sub>max</sub></b>	: Maximum permitted surface temperature, C
<b>C<sub>p</sub></b>	: Specific heat of helium, J/g-C
<b>W</b>	: Pumping power = $M(\Delta P/\rho)$ , W
<b>ΔP</b>	: Pressure drop, Pa
<b>δ</b>	: Thickness of the wall facing heat flux, m
<b>ρ</b>	: Density of helium, kg/m
<b>v</b>	: The number of neutrons per fission (2.43)
<b>x</b>	: Fast fission factor
<b>p</b>	: Response escape probability
<b>f</b>	: Thermal utilization factor
<b>H</b>	: Reproduction factor
<b>K<sup>*</sup></b>	: Four factor
<b>K</b>	: Infinite multiplication factor
<b>N<sub>1</sub></b>	: Number of atoms of fuel / cm <sup>3</sup>
<b>N<sub>2</sub></b>	: Number of atoms/cm <sup>3</sup> of moderator
<b>N<sub>3</sub></b>	: Number of atoms/cm <sup>3</sup> of coolant
<b>Σ<sub>a</sub></b>	: Macroscopic cross section of the material being analyzed
<b>σ<sub>a</sub></b>	: Microscopic cross section for the material analyzed
<b>Q</b>	: Heat Flux
<b>Q</b>	: Heat Transfer Rate, W/m <sup>2</sup>
<b>A</b>	: Area, m <sup>2</sup>
<b>k = C<sub>p</sub>/C<sub>v</sub></b>	: The specific Heat Ratio
<b>C<sub>p</sub></b>	: Specific heat in a constant pressure process
<b>C<sub>v</sub></b>	: Specific heat in a constant volume process
<b>R</b>	: Individual gas constant
<b>P</b>	: Power
<b>D</b>	: Diameter
<b>k</b>	: Conductivity
<b>l</b>	: Length
<b>ΔT</b>	: Temperature

## Abstract

The current generations of nuclear power plants are based on light water reactors and steam cycle power conversion systems. This work concentrates on design of next generation nuclear power plants having a potential of efficiency closer to 50 % using more efficient prime mover with a nuclear closed Brayton cycle (NCBC). The Gas Turbine-Modular Helium Reactor (GT-MHR) is a new turbine generating system powered by a passively-safe nuclear reactor. It eliminates the need to make steam to produce electricity, and frees us from the pollution and waste of fossil-fuel generating plants. Because helium is naturally inert and single-phase, the helium-cooled reactor can operate at much higher temperatures than today's conventional nuclear plants. The higher the turbines operating temperature, the more efficient the plant becomes mandated by the laws of thermodynamics. To this is added the efficiency of the helium directly driving the turbine, instead of having to go through a large heat exchanger to produce steam.

The combination of the gas turbine and the modular helium reactor, the MHR and the gas turbine represents the ultimate in simplicity, safety, and economy. The reactor coolant directly drives the turbine which turns the generator. The GT-MHR power plant is essentially contained in two interconnected pressure vessels enclosed within a below-ground concrete containment structure. One vessel contains the reactor system and is based on the MHR. The second vessel contains the power conversion system. The turbo-machine consists of a generator, turbine, and two compressor sections mounted on a single shaft rotating on magnetic bearings. The active magnetic bearings control shaft stability while eliminating the need for lubricants within the primary system. The vessel also contains three compact heat exchangers.

## CHAPTER 1

### INTRODUCTION

Nuclear power generation with fission is a most common type of method, but in order to create fission reaction there are several types of techniques available. The idea of designing a nuclear reactor is more of about designing a controlled chain reaction in terms of neutron interaction with matter. The penetration of matter by charged particles such as alpha particles or protons, produced from radioactivity or by electrical acceleration, is relatively slight because of the electrostatic force between the incident particles and the electrons of the target atoms [30]. Neutrons have no charge and can move through matter for long distance without being stopped, only by collisions with nuclei, neutrons can be absorbed by lose of energy. To demonstrate neutron in motion electron-volt energy unit is used, in order to find out the energy levels in the neutron the following equation 1 is used.

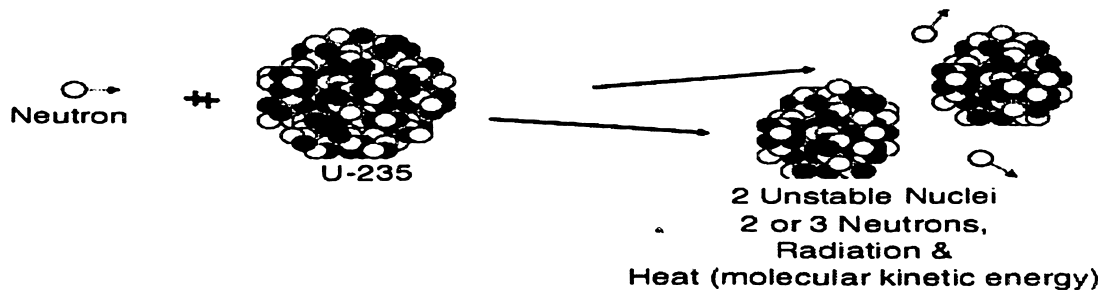
$$E = \frac{1}{2}mv^2 \quad (1)$$

In nuclear fission a small fraction of the weight of the fissionable material is converted into energy, from the theory of relativity the mass of a moving body should increase as its velocity increases [15]. For a body of rest mass  $m_0$ , its mass  $m$  at any velocity  $v$  will be given as

$$m = \frac{m_0}{\sqrt{1 - \frac{v^2}{c^2}}} \quad (2)$$

In the fission reaction the incident neutron enters the heavy target nucleus, forming a compound nucleus that is excited to such a high energy level ( $E_{exc} > E_{crit}$ ) that the nucleus "splits" into two large fragments plus some neutrons. An example of a typical fission reaction is shown in figure 1.1. A large amount of energy is released in the form of radiation and fragment kinetic energy [37]. The measure of how far the energy level of a nucleus is above its ground state is called the excitation energy ( $E_{exc}$ ). For fission to occur, the excitation energy must be above a particular value for that

nuclide. The critical energy ( $E_{crit}$ ) is the minimum excitation energy required for fission to occur.



(Source: nuclear Reactor physics, Raymond I. Murray)

**Figure 1.1** Neutron Interaction With Fissile Material And Energy Release.

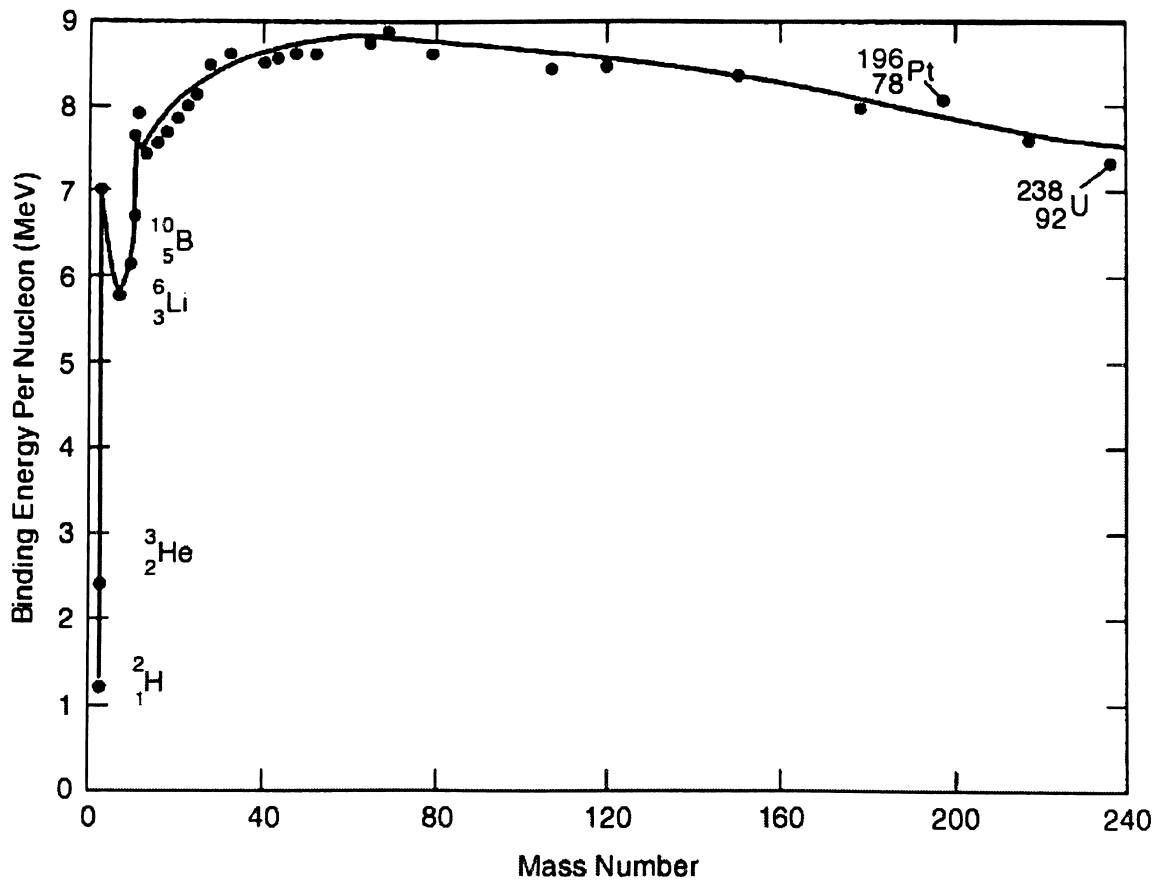
A fissile material is composed of nuclides for which fission is possible with neutrons of any energy level. What is especially significant about these nuclides is their ability to be fissioned with zero kinetic energy neutrons (thermal neutrons). Thermal neutrons have very low kinetic energy levels (essentially zero) because they are roughly in equilibrium with the thermal motion of surrounding materials. Therefore, in order to be classified as fissile, a material must be capable of fissioning after absorbing a thermal neutron [37]. Consequently, they impart essentially no kinetic energy to the reaction. Fission is possible in these materials with thermal neutrons, since the change in binding energy supplied by the neutron addition alone is high enough to exceed the critical energy. Some examples of fissile nuclides are uranium-235, uranium-233, and plutonium-239. Uranium as it occurs in nature contains 0.7% of the fissile isotope U-235, the rest being U-238. If bombarded with neutrons, U-238 can capture a neutron and transmute to the isotope of plutonium Pu-239, which is fissile [15]. Thus there is a possibility to create fissile material in a nuclear chain reacting system, and maybe even the opportunity to create more fissile material than is being consumed in the reactor: one can breed fissile material (e.g., Pu-239) from fertile material (e.g., U-238). The number of new neutrons released by a fissile nucleus upon absorption of a neutron is given by the parameter  $k$  which is shown in equation 3

$$k = \frac{\text{fission neutrons}}{\text{absorption in U}} = \frac{\bar{\sigma}_f U v}{\bar{\sigma}_a U} \quad (3)$$

A fissionable material is composed of nuclides for which fission with neutrons is possible. All fissile nuclides fall into this category. However, also included are those nuclides that can be fissioned only with high energy neutrons, the change in binding energy that occurs as the result of neutron absorption results in a nuclear excitation energy level that is less than the required critical energy. Therefore, the additional excitation energy must be supplied by the kinetic energy of the incident neutron. The reason for this difference between fissile and fissionable materials is the so-called odd-even effect for nuclei [15]. It has been observed that nuclei with even numbers of neutrons and/or protons are more stable than those with odd numbers. Therefore, adding a neutron to change a nucleus with an odd number of neutrons to a nucleus with an even number of neutrons produces an appreciably higher binding energy than adding a neutron to a nucleus already possessing an even number of neutrons.

Some examples of nuclides requiring high energy neutrons to cause fission are thorium-232, uranium-238, and plutonium-240. Figure 1.2 indicates the critical energy ( $E_{crit}$ ) and the binding energy change for an added neutron ( $BE_n$ ) to target nuclei of interest. For fission to be possible, the change in binding energy plus the kinetic energy must equal or exceed the critical energy ( $\Delta BE + KE > E_{crit}$ ). As the number of particles in a nucleus increases, the total binding energy also increases. The rate of increase, however, is not uniform. This lack of uniformity results in a variation in the amount of binding energy associated with each nucleon within the nucleus [15]. This variation in the binding energy per nucleon ( $BE/A$ ) is easily seen when the average  $BE/A$  is plotted versus atomic mass number ( $A$ ), as shown in Figure 1.2, illustrates that as the atomic mass number increases, the binding energy per nucleon decreases for  $A > 60$ . The  $BE/A$  curve reaches a maximum value of 8.79 MeV at  $A = 56$  and decreases to about 7.6 MeV for  $A = 238$ . The general shape of the  $BE/A$  curve can be explained using the general properties of nuclear forces. The nucleus is held together by very short-range attractive forces that exist between nucleons. On the other hand, the nucleus is being forced apart by long range repulsive electrostatic (coulomb) forces that exist between all the protons in the nucleus. As the atomic number and the atomic mass number increase, the repulsive electrostatic forces within the nucleus increase due to the greater number of

protons in the heavy elements [13]. To overcome this increased repulsion, the proportion of neutrons in the nucleus must increase to maintain stability.



(Source: nuclear Reactor physics, Raymond I. Murray)

**Figure 1.2** Binding Energy Per Nucleon Vs Binding Energy

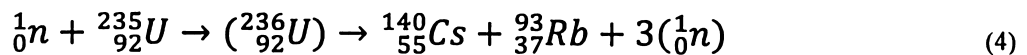
This increase in the neutron-to-proton ratio only partially compensates for the growing proton-proton repulsive force in the heavier, naturally occurring elements. Because the repulsive forces are increasing, less energy must be supplied, on the average, to remove a nucleon from the nucleus. The BE/A has decreased. The BE/A of a nucleus is an indication of its degree of stability. Generally, the more stable nuclides have higher BE/A than the less stable ones. The increase in the BE/A as the atomic mass number decreases from 260 to 60 is the primary reason for the energy liberation in the fission process [31]. In addition, the increase in the BE/A as the atomic mass number increases from 1 to 60 is the reason for the energy liberation in the fusion process, which is the opposite reaction of fission. The heaviest nuclei require only a small distortion



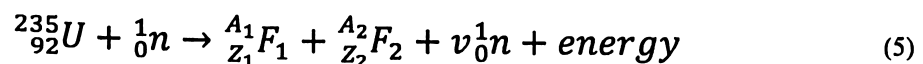
from a spherical shape (small energy addition) for the relatively large coulomb forces forcing the two halves of the nucleus apart to overcome the attractive nuclear forces holding the two halves together. Consequently, the heaviest nuclei are easily fissionable compared to lighter nuclei.

### 1.1 Nuclear Fission Reaction

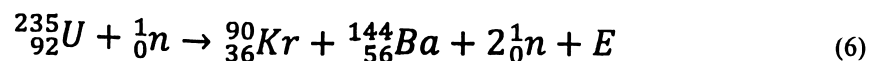
Nuclear fission results in the release of enormous quantities of energy. It is necessary to be able to calculate the amount of energy that will be produced. The logical manner in which to pursue this is to first investigate a typical fission reaction such as the one listed below in equation 4



Accompanying the fission process is the release of several neutrons, which are all-important for the practical application to a self-sustaining chain reaction. The numbers that appear  $n$  (nu) range from 1 to 7, with an average in the range 2 to 3 depending on the isotope and the bombarding neutron energy. For example, in U-235 with slow neutrons the average number  $n$  is 2.42 [38]. Most of these are released instantly, the so-called prompt neutrons, while a small percentage, 0.65% for U-235, appear later as the result of radioactive decay of certain fission fragments. These delayed neutrons provide considerable inherent safety and controllability in the operation of nuclear reactors. The nuclear reaction equation for fission resulting from neutron absorption in U-235 may be written in general form, letting the chemical symbols for the two fragments be labelled  $F_1$  and  $F_2$  to indicate many possible ways of splitting.



Thus, the appropriate mass numbers and atomic numbers are attached. One Example, in which the fission fragments are isotopes of krypton and barium, shown in the equation 6



Mass numbers ranging from 75 to 160 are observed, with the most probable at around 92 and 144 as sketched in Fig 3. The ordinate on this graph is the percentage yield of each mass number, e.g., about 6% for mass numbers 90 and 144. If the number of fissions is given, the number of atoms of those types is 0.06 as large. As a collection

of isotopes, these by products are called fission products. The isotopes have an excess of neutrons or a deficiency of protons in comparison with naturally occurring elements [38]. For example, the main isotope of barium is  ${}_{137}^{56}\text{Ba}$ , and a prominent element of mass 144 is 60. Thus there are seven extra neutrons or four too few protons in the barium

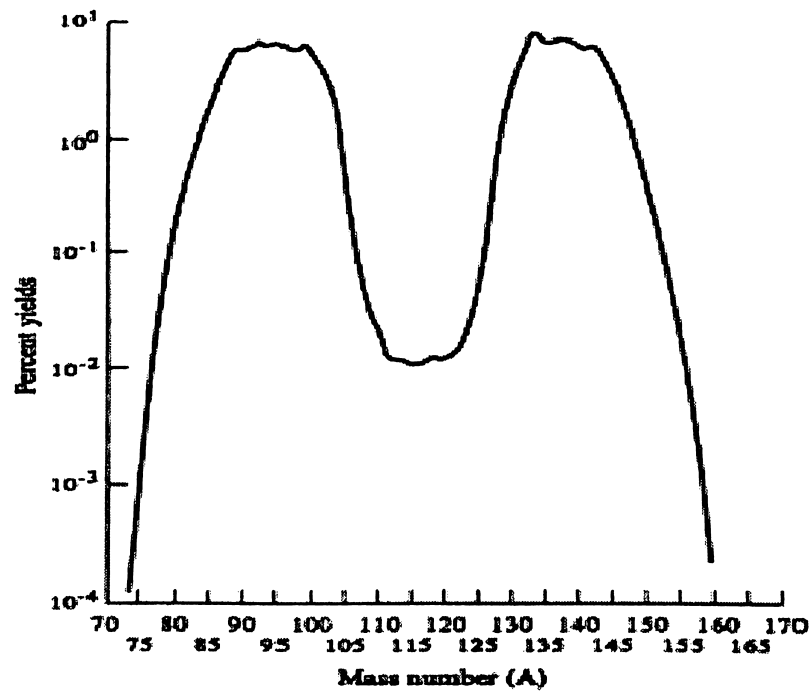


Figure 1.3 Yield of Fission Products According To The Mass Number

## 1.2 Heat Exchange In Fission Reactors

A fission reactor consists basically of a mass of fissionable material usually encased in shielding and provided with devices to regulate the rate of fission and an exchange system to extract the heat energy produced. A reactor is so constructed that fission of atomic nuclei produces a self-sustaining nuclear chain reaction, in which the neutrons produced are able to split other nuclei [38]. A chain reaction can be produced in a reactor by using uranium or plutonium in which the concentration of fissionable isotopes has been artificially increased. Even though the neutrons move at high velocities, the enriched fissionable isotope captures enough neutrons to make possible a self-sustaining chain reaction. In this type of reactor the neutrons carrying on the chain

reaction are fast neutrons. A chain reaction can also be accomplished in a reactor by employing a substance called a moderator to retard the neutrons so that they may be more easily captured by the fissionable atoms [30]. The neutrons carrying on the chain reaction in this type of reactor are slow (or thermal) neutrons. Substances that can be used as moderators include graphite, beryllium, and heavy water (deuterium oxide). The moderator surrounds or is mixed with the fissionable fuel elements in the core of the reactor. The heat energy released by fission in a reactor heats a liquid or gas coolant that circulates in and out of the reactor core, usually becoming radioactive. Outside the core, the coolant circulates through a heat exchanger where the heat is transferred to another medium [37]. This second medium, nonradioactive since it has not circulated in the reactor core, carries the heat away from the reactor. This heat energy can be dissipated or it can be used to drive conventional heat engines that generate usable power.

### 1.2.1 Thermal Utilization Factor

Once thermalized, the neutrons continue to diffuse throughout the reactor and are subject to absorption by other materials in the reactor as well as the fuel. The thermal utilization factor describes how effectively thermal neutrons are absorbed by the fuel, or how well they are utilized within the reactor [37]. The thermal utilization factor ( $f$ ) is defined as the ratio of the number of thermal neutrons absorbed in the fuel to the number of thermal neutrons absorbed in any reactor material.

This ratio is shown in equation 7 below

$$f = \frac{\text{number of thermal neutrons absorbed in the fuel}}{\text{number of thermal neutrons absorbed in all reactor materials}} \quad (7)$$

The thermal utilization factor will always be less than one because some of the thermal neutrons absorbed within the reactor will be absorbed by atoms of non-fuel materials. An equation can be developed for the thermal utilization factor in terms of reaction rates as follows

$$f = \frac{N_1(\sigma_a)_1}{N_1(\sigma_a)_1 + N_2(\sigma_a)_2 + \dots} = \frac{(\sum_a)_1}{(\sum_a)_1 + (\sum_a)_2 + \dots} \quad (8)$$

In a homogeneous reactor the neutron flux seen by the fuel, moderator, and poisons will be the same. Also, since they are spread throughout the reactor, they all occupy the same volume. Since absorption cross sections vary with temperature, it would appear that the thermal utilization factor would vary with a temperature change. But, substitution of the temperature correction formulas in the above equation will reveal that all terms change by the same amount, and the ratio remains the same.

In heterogeneous water-moderated reactors, there is another important factor. When the temperature rises, the water moderator expands, and a significant amount of it will be forced out of the reactor core. This means that  $N_2$ , the number of moderator atoms per  $\text{cm}^3$ , will be reduced, making it less likely for a neutron to be absorbed by a moderator atom [35]. This reduction in  $N_2$  results in an increase in thermal utilization as moderator temperature increases because a neutron now has a better chance of hitting a fuel atom. Because of this effect, the temperature coefficient for the thermal utilization factor is positive. The amount of enrichment of uranium-235 and the poison concentration will affect the thermal utilization factor in a similar manner as can be seen from the equation above.

### 1.2.2 Heat Flux

The rate at which heat is transferred is a measure of heat flux in a reactor represented by the symbol  $Q''$ . Sometimes it is important to determine the heat transfer rate per unit area, or heat flux[35]. The heat flux can be determined by dividing the heat transfer rate  $Q$  by the area through which the heat is being transferred.

$$Q'' = \frac{Q}{A} \quad (9)$$

### 1.2.3 Infinite Multiplication Factor (K)

The number of neutrons absorbed or leaking out of the reactor will determine the value of this multiplication factor, and will also determine whether a new generation of neutrons is larger, smaller, or the same size as the preceding generation. Any reactor of a finite size will have neutrons leak out of it. Generally, the larger the reactor, the lower the fraction of neutron leakage. For simplicity, we will first

consider a reactor that is infinitely large, and therefore has no neutron leakage. A measure of the increase or decrease in neutron flux in an infinite reactor is the infinite multiplication factor,  $k$  [35]. The infinite multiplication factor is the ratio of the neutrons produced by fission in one generation to the number of neutrons lost through absorption in the preceding generation. This can be expressed mathematically as shown in equation 10 below

$$K = \frac{\text{Neutron production from fission in one generation}}{\text{Neutron absorption in the preceding generation}} \quad (10)$$

Not all of the neutrons produced by fission will have the opportunity to cause new fissions because some neutrons will be absorbed by non-fissionable material. Some will be absorbed parasitically in fissionable material and will not cause fission, and others will leak out of the reactor. For the maintenance of a self-sustaining chain reaction, however, it is not necessary that every neutron produced in fission initiate fission [37]. The minimum condition is for each nucleus undergoing fission to produce, on the average, at least one neutron that causes fission of another nucleus. This condition is conveniently expressed in terms of a multiplication factor.

A group of fast neutrons produced by fission can enter into several reactions. Some of these reactions reduce the size of the neutron group while other reactions allow the group to increase in size or produce a second generation [30]. There are four factors that are completely independent of the size and shape of the reactor that give the inherent multiplication ability of the fuel and moderator materials without regard to leakage. This four factor formula accurately represents the infinite multiplication factor as shown in the equation 11 below

$$K^* = x p f h \quad (11)$$

Each of these four factors, which are explained in the following subsections, represents a process that adds to or subtracts from the initial neutron group produced in a generation by fission.

#### 1.2.4 Fast Fission Factor (X)

In order for a neutron to be absorbed by a fuel nucleus as a fast neutron, it must pass close enough to a fuel nucleus while it is a fast neutron. The value of  $\alpha$  will be affected by the arrangement and concentrations of the fuel and the moderator. The value of  $\alpha$  is essentially 1.00 for a homogenous reactor where the fuel atoms are surrounded by moderator atoms. However, in a heterogeneous reactor, all the fuel atoms are packed closely together in elements such as pins, rods, or pellets. Neutrons emitted from the fission of one fuel atom have a very good chance of passing near another fuel atom before slowing down significantly [37]. The arrangement of the core elements results in a value of about 1.03 for  $\alpha$  in most heterogeneous reactors. The value of  $\alpha$  is not significantly affected by variables such as temperature, pressure, enrichment, or neutron poison concentrations. Poisons are non-fuel materials that easily absorb neutrons and will be discussed in more detail later. The mathematical expression of this ratio is shown below in equation 12.

$$\alpha = \frac{\text{number of fast neutrons produced by all fissions}}{\text{number of fast neutrons produced by thermal fissions}} \quad (12)$$

The first process that the neutrons of one generation may undergo is fast fission. Fast fission is fission caused by neutrons that are in the fast energy range. Fast fission results in the net increase in the fast neutron population of the reactor core. The cross section for fast fission in uranium-235 or uranium-238 is small; therefore, only a small number of fast neutrons cause fission [38]. The fast neutron population in one generation is therefore increased by a factor called the fast fission factor. The fast fission factor is defined as the ratio of the net number of fast neutrons produced by all fissions to the number of fast neutrons produced by thermal fissions.

After increasing in number as a result of some fast fissions, the neutrons continue to diffuse through the reactor. As the neutrons move they collide with nuclei of fuel and non-fuel material and moderator in the reactor losing part of their energy in each collision and slowing down [30]. While they are slowing down through the resonance region of uranium-238, which extends from about 6 eV to 200 eV, there is a chance that some neutrons will be captured. The probability that a

neutron will not be absorbed by a resonance peak is called the resonance escape probability. The resonance escape probability ( $p$ ) is defined as the ratio of the number of neutrons that reach thermal energies to the number of fast neutrons that start to slow down. This ratio is shown below in equation 13 .

$$p = \frac{\text{number of neutrons that reach thermal energy}}{\text{number of fast neutrons that start to slow down}} \quad (13)$$

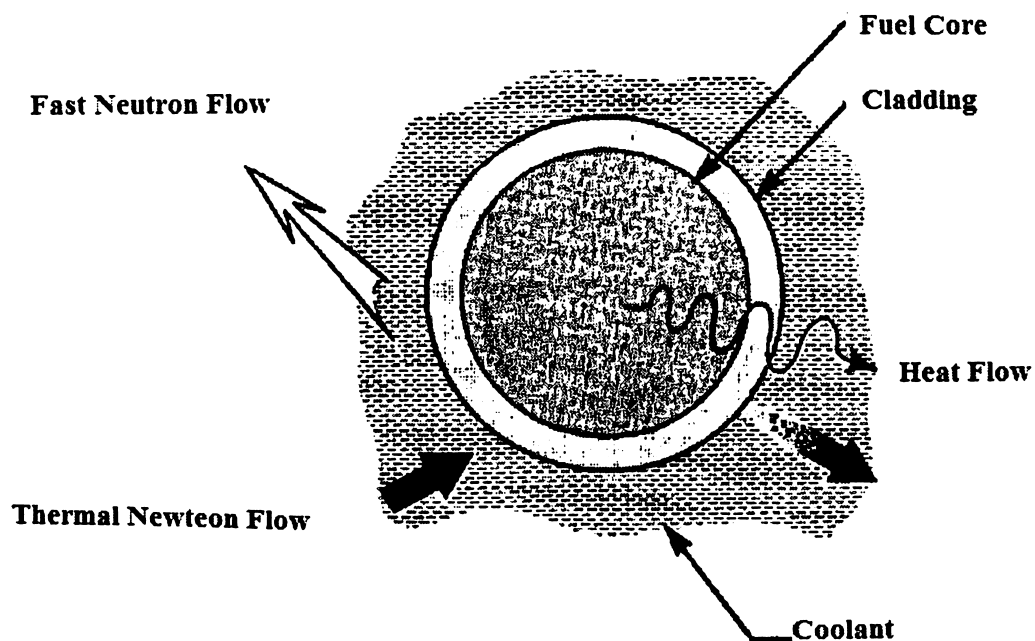
The value of the resonance escape probability is determined largely by the fuel-moderator arrangement and the amount of enrichment of uranium-235 (if any is used). To undergo resonance absorption, a neutron must pass close enough to a uranium-238 nucleus to be absorbed while slowing down. In a homogeneous reactor the neutron does its slowing down in the region of the fuel nuclei, and this condition is easily met. This means that a neutron has a high probability of being absorbed by uranium-238 while slowing down; therefore, its escape probability is lower. In a heterogeneous reactor, however, the neutron slows down in the moderator where there are no atoms of uranium-238 present [32]. Therefore, it has a low probability of undergoing resonance absorption, and its escape probability is higher.

The value of the resonance escape probability is not significantly affected by pressure or poison concentration. In water moderated, low uranium-235 enrichment reactors, raising the temperature of the fuel will raise the resonance absorption in uranium-238 due to the Doppler Effect (an apparent broadening of the normally narrow resonance peaks due to thermal motion of nuclei). The increase in resonance absorption lowers the resonance escape probability, and the fuel temperature coefficient for resonance escape is negative (explained in detail later). The temperature coefficient of resonance escape probability for the moderator temperature is also negative [22]. As water temperature increases, water density decreases. The decrease in water density allows more resonance energy neutrons to enter the fuel and be absorbed. The value of the resonance escape probability is always slightly less than one (normally 0.95 to 0.99). The product of the fast fission factor and the resonance escape probability ( $p$ ) is the ratio of the number of fast neutrons that survive slowing

down (thermalization) compared to the number of fast neutrons originally starting the generation.

### 1.3 Concept of Cooling Reactors

Heat transfer and fluid flow defines the heat exchange process in a fission reactor, because the two problems are closely integrated throughout the design of fission reaction. The fissionable material is responsible for generation of heat in a reactor where as coolant is responsible for heat transfer before its power generation. The main focus is on amount of heat removed from a heterogeneous reactor by passing a coolant through annuli about cylindrical uranium slugs or fuel pebbles [32]. Heat is generated as a source in fuel elements and it will give up to flowing fluid. We first derive a reaction between heat production and temperature distribution in the fuel elements which is shown in the figure 1.4 below.



(Source: *Design Requirements and Engineering, Banilla*)

**Figure 1.4** Heat Flow In Fuel Element

The purpose of the reactor coolant is to transport heat generated in the reactor fuel either to the turbine (direct cycle reactor) or to intermediate heat exchangers (indirect



cycle reactor). The coolants may be liquids, two-phase liquid/vapour mixtures or gases. The specific future that need to be considered while selecting coolant for the reactors are high heat capacity, good heat transfer properties, low neutron absorption, low neutron activation, low operating pressure requirement at high operating temperatures, non-corrosive to fuel cladding and coolant system and low cost. The fluids which are used in nuclear reactors as a coolants are Helium, carbon dioxide, Liquid metal, water, Heavy water and organic fluids. These coolants are compared with the properties in the table. Among these fluids the gases common in use are CO<sub>2</sub> and helium [32]. CO<sub>2</sub> has the advantages of low cost, low neutron activation (important in minimizing radiation fields from the coolant system), high allowable operating temperatures, and good neutron economy and, for gases, relatively good heat transfer properties at moderate coolant pressures [5]. At very high temperatures, it tends to be corrosive to neutron economical fuel cladding materials and also to the graphite moderator used in most gas-cooled reactors. Its chief drawback, as for all gases, is its poor heat transfer properties relative to liquids.

**TABLE 1.1 PROPERTIES OF VARIOUS COOLANTS FOR NUCLEAR REACTORS**

<b>Coolant Type</b>	<b>Neutron Economy</b>	<b>Vapour Pressure</b>	<b>Heat Capacity</b>	<b>HT Coeff</b>	<b>Activation</b>	<b>Corrosive</b>	<b>Cost</b>
He	Good	High	Low	Low	Low	Good with pure	Higher
CO <sub>2</sub>	Good	High	Low	Low	Low	Except at high T	<He
H <sub>2</sub> O	Moderate	High	High	Excellent	Low at T <sub>min</sub>	Poor	Low
D <sub>2</sub> O	Excellent	High	High	Excellent	Like H <sub>2</sub> O	Transports Corrosion	Higher
Liquid Metal	Not Great	Very Low	High	Excellent	High With T <sub>max</sub>	Yes	High
Organic	H <sub>2</sub> O <Organic <D <sub>2</sub> O	Low	High	Excellent	None	Excellent	Moderate

As a result, coolant pumping power requirements tend to be very high, particularly if high reactor power densities are to be achieved (desirable to minimize reactor capital costs). The other candidate gas, helium, possesses all of the good features of CO<sub>2</sub> and, in addition, is noncorrosive (if pure). Its chief disadvantages are higher costs, particularly operating costs, because helium is very "searching", leading to high system leakage rates unless extreme measures are taken to build and maintain a leak-proof system [9]. This has, however, been successfully done in a number of cases. Of the candidate liquid coolants, ordinary water is by far the most commonly used. It is inexpensive, has excellent heat transfer properties, and is adequately non-corrosive to zirconium alloys used for fuel cladding and reactor structural components and ferritic or austenitic steel coolant system materials [10]. Its disadvantages include only moderate neutron economy and its relatively high vapour pressure at coolant temperatures of interest. It is activated by neutrons in the reactor core but this activity dies away rapidly, permitting reasonable shutdown maintenance access to the coolant system. A further disadvantage is that water transports system corrosion products, permitting them to be activated in the reactor core.

These activated corrosion products then create shutdown radiation fields in the coolant system. The water coolant may be used as a liquid in an indirect cycle system or may be permitted to boil, producing steam in a direct cycle system. Heavy water may also be used as a coolant. Its outstanding advantage is much better neutron economy relative to ordinary water. Its primary disadvantage is its high cost. Otherwise its properties are similar to ordinary water [9]. Certain organic fluids (primarily hydrogenated polyphenyls) may also be used. They are moderate in cost, have a lower vapour pressure than water, are essentially non-corrosive, and are not significantly subject to neutron activation. Also they do not transport significant quantities of corrosion products which can become activated in the reactor core. Their chief disadvantages include higher neutron absorption than heavy water (but lower than ordinary water), in flammability, and they suffer radio-chemical damage in the reactor core which leads to a requirement for extensive purification facilities and significant coolant makeup costs. On balance, however, they may well see wider application in the

future. Certain liquid metals can be used as coolants. Of these, only sodium and a sodium/potassium eutectic called NaK have achieved significant use. Their advantages include excellent heat transfer properties and very low vapour pressures at high temperatures. Fuel cladding and coolant system materials require careful selection to avoid "corrosion". Their chief disadvantages include incomparability with water (the turbine working fluid), relatively high neutron absorption, a relatively high melting point (leading to coolant system trace heating requirements) and high coolant activation with sustained radiation fields after reactor shutdown [8]. These disadvantages have effectively precluded the use of liquid metal coolants in commercial power reactors to date with one exception and this is the fast breeder reactor which will be discussed later. In this reactor, the neutrons are "used" at relatively high energy levels where the neutron absorption of the liquid metal is much less, overcoming one of the foregoing disadvantages [14]. In addition, the economics of fast breeder reactors depend on very high core power densities where the excellent heat transfer capability of liquid metals becomes a major advantage. Furthermore, it is desirable in this type of reactor that the coolant not moderates the neutrons excessively. Liquid metals are superior to other liquids in this regard because they do not contain "light" atoms which are inherently effective moderators.

## **CHAPTER 2**

### **GAS COOLED REACTORS**

One of the major challenges of the reintroduction of nuclear energy into the world energy mix is the development of a nuclear power plant that is competitive with other energy alternatives, such as natural gas, oil or coal. The environmental imperative of nuclear energy is obvious. No greenhouse gases emitted, small amounts of fuel required and small quantities of waste to be disposed of. Unfortunately, the capital costs of new nuclear plants are quite large relative to the fossil alternatives. Despite the fact that nuclear energy's operating costs in terms of operations and maintenance and, most importantly, fuel are much lower than fossil alternatives, the barrier of high initial investment is a significant one for utilities around the world [20]. In order to deal with this challenge gas cooled reactors are going to be a good alternative. Gas cooled Reactor is a completely different design, the common aspects of gas cooled reactors under consideration are graphite cores, coated fuel particles and helium coolants. They have a higher efficiency than light water reactors because of the higher exit temperatures. The fuel used in gas reactors has a higher enrichment level, approximately 12-20% Uranium-235. They typically operate to higher burn-up levels which makes the spent fuel more proliferation proof [18]. Gas cooled reactors, because they have higher efficiencies, have lower thermal discharges to the environment. Light water reactors have a relatively inexpensive core with a high power density and a "defence in depth" type safety system. Gas cooled reactors have a more expensive core with a lower power density. The economics are potentially better because of a higher efficiency, compact balance of plant, and longer fuel life.

#### **2.1 Gas Cooled Reactor Concepts**

Potential gas coolants for reactors include hydrogen, helium, nitrogen, CO<sub>2</sub>, argon, air, and steam. A number of large gas-cooled reactors have been developed and operated worldwide. Gas-cooled reactor designs are usually moderated, and graphite is commonly selected as the moderator. However, gas-cooled reactors have been studied

and developed that employ other moderators or no moderator. A broad variety of fuel element geometries and fuel types have been used in gas-cooled reactors. The first gas-cooled reactors developed with air cooling system and employed as air cooled reactors. Later CO<sub>2</sub> coolant is considered in substituting air. Once it is tested with research reactors it was failed due to Oxidation and dissociation issues, however, have limited CO<sub>2</sub> coolant temperatures to less than 600 C [5]. Fuel element designs for these reactors included uranium metal and uranium dioxide clad in magnesium alloy and other metals. The CO<sub>2</sub>-cooled reactor approach proved successful. Nitrogen-cooled reactors were once studied for remote power sources, and hydrogen cooled reactors were developed for space applications. However, nitrogen and hydrogen cooled reactors were never developed for commercial power applications. The use of steam as a coolant/working fluid has been limited to nuclear superheat in BWR reactors.

Future work for gas coolant was lead to path way in selecting helium as an attractive coolant for gas-cooled reactors. Helium is chemically inert, exhibits good heat transfer properties among gasses, and has a very small neutron capture cross section. A small high temperature, graphite moderated, helium-cooled reactor plant was successfully operated and encouraged rest of the world for future research [8]. The Initial research reactor operated with Fuel rods are contained within the graphite blocks and helium flows through internal coolant channels in the blocks. The fuel rods consist of coated uranium carbide microspheres embedded in a graphitic binder. Maximum fuel temperatures were less than 1260 C, and the coolant outlet temperature was 785 C.

## **2.2 Gas Coolants for Reactors**

Reactor coolants and heat transport fluids should have low melting points, good heat transport properties, and low potential for chemical attack on vessels and piping. Reasonable operating pressures and compositional stability at operating temperature are also important characteristics. Other desirable properties include low toxicity and low fire and explosion hazard [12]. Reactor coolants must also possess desirable nuclear properties, such as radiation stability and low neutron activation. For thermal reactors, low parasitic capture cross sections are required. If the coolant is to serve as a

moderator, low atomic weight on statements is desirable. Property values and characteristics for potential reactor coolants are derived by gas- solid fraction coefficient which is shown in the equation 14

$$\beta = 150 \frac{\varepsilon_s^2 \mu_s}{(1-\varepsilon_s)d_s^2} + \frac{7 \varepsilon_s \rho_g |v_g - v_s|}{4 d_s}, \text{ if } \varepsilon_s > 0.225 \quad (14)$$

Increasing the flow surface area, as well as operating at high temperatures, high pressures, and high flow rates can compensate for the generally poor heat transport characteristics of gas coolants. Gas coolant operating pressures, however, are far below that for water at required cycle temperatures, and for most gas coolants, no phase change occurs for any postulated accident sequence. Most importantly, noble gases are chemically inert [13]. Gases are too diffuse to serve as effective moderators; consequently, thermal gas-cooled reactors require a separate moderator.

### 2.2.1 Reactive Gases

More importantly to this study, the corrosiveness and thermal dissociation of CO<sub>2</sub> at greater than 600 C makes this coolant option unacceptable for the proposed cycle. Limited development work has been carried out for nitrogen reactors, and chemical incompatibility of materials with high temperatures nitrogen gas is an issue. In the operated (i.e., the air coolant passing through the reactor was released directly into the atmosphere). Air-cooled reactors suffer the same limitations as CO<sub>2</sub>-cooled reactors and once-through cooling is no longer a viable approach. Although water-cooled reactors with superheated steam have been developed, nuclear superheated steam options are no longer actively pursued [18]. The high temperature oxidation of superheated steam was one of the main reasons for abandoning this approach. Furthermore, the heat transfer properties of steam are not as good as helium, and steam activation and dissociation are significant. Hydrogen-cooled reactors have been developed in the United States and Russia for nuclear rockets. Although hydrogen possesses the best heat transfer characteristics among gas coolants, the very high fire and explosion hazard of hydrogen rules out its use for terrestrial applications.

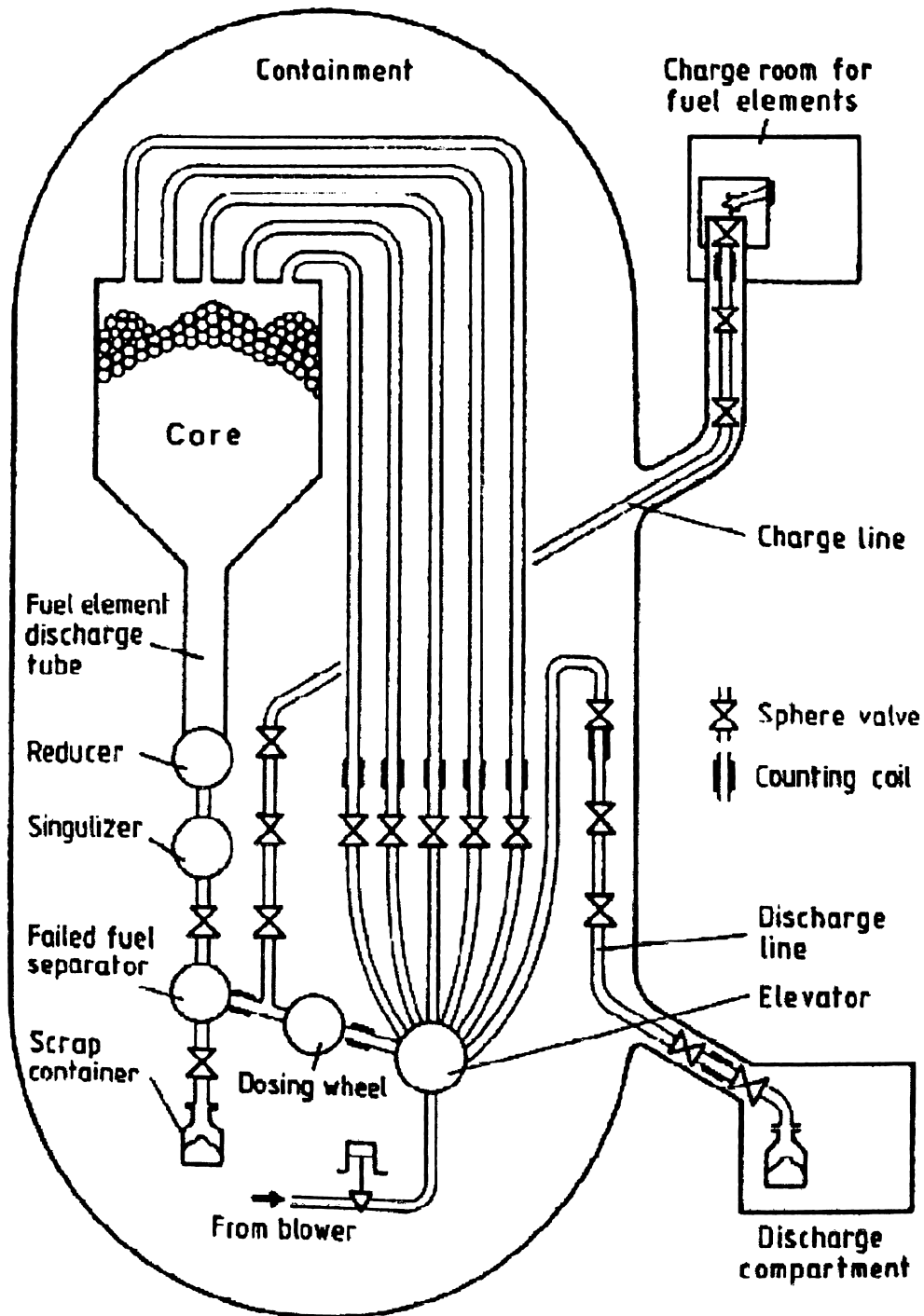
### **2.2.2 Nobel Gases**

Little development has been carried out for argon-cooled reactors. Argon is chemically inert, but heat transfer characteristics for argon are not as good as helium and neutron activation and parasitic capture are disadvantages. Significant experience has been accumulated with helium-cooled reactors. Among gasses, helium exhibits good heat transport properties [19]. Helium is neither a fire or explosion hazard, is non-toxic, is stable in radiation and high temperature environments, has a very small parasitic capture cross section, and neutron activation is extremely small. The most significant and pertinent advantage of helium is its chemical inertness. For these reasons, helium is selected as the baseline coolant for gas-cooled reactors.

### **2.3 Gas Cooled Reactor System**

Gas-cooled reactors are fairly simple systems. The working fluid in a gas-cooled reactor is a single phase gas, which flows across the reactor core. To remove the heat the gas is either run through a heat exchanger transferring the heat to some other working fluid or, as in this case, run directly through a turbine to generate power. The advantages of gas-cooled reactors are availability of inert gasses, low neutron cross section, the ability to run the reactor at high temperatures. This last factor allows high efficiency power conversion but requires exotic materials to be practical. In the reactor system consists of a container which is designed with the high temperature resistant materials which can hold high pressures. Inside the container core is arranged with three fuel loading system tubes, core will be designed in a hexagonal shape which is allowed to use fuel pebbles. The entire system mechanism is shown in the figure 2.1. With the fuel pebbles the special advantage is without obstructing the operation the fuel pebbles loading and unloading will be carried out once fuel pebbles are consumed. Change room for fuel elements and fuel elements discharge tube and discharge compartment will take care about all the process with the automatic control system [20]. Due to the high temperature and inequality in the fuel consumption some of the fuel pebbles will not be used completely, in other words failed elements will be separated through a special arrangement. In order to change the system from top to bottom in hexagonal fuel

element system will be circulated automatically with a special mechanism to interchange the rows inside core.



(Source: *Plant Design Concepts for a Gas-Cooled Fast Reactor*, C.F Henry)

**Figure 2.1** Gas Cooled Reactor Core Arrangement



### **2.3.1 Boundary Conduction/Radiation Cool Down and Thermal Inertia**

The radiation and conduction heat transfer modes are a different case from mass transfer. Pebble beds have both radiation and conduction heat transfer with radiation being the more important. The spherical form in packed beds is a good form for radiation as there are radiation pathways to the exterior boundary from within the interior of the bed. Complete shadowing is very difficult to achieve in this geometry for the range of pebble sizes of interest. But ultimately there needs to be a heat sink. In the case of the thermal gas cooled reactor, heat radiation/conduction core generated decay heat to the vessel boundary (“conduction cool down mode”) has been a major part of the safety case. This is both for the prismatic fuel design as well as for the pebble/bed fuel design. Conceptually, this is also therefore a heat sink/decay heat pathway for the pebble bed fast gas cooled reactor [24]. But as noted previously, there is a major difference between the power density of a thermal gas cooled reactor and the power density of a gas cooled fast reactor. Conduction/radiation of the core decay heat to the vessel wall boundary is a function of power density, material properties and geometry. If conduction cool down is not possible due to too large a target power density or geometrical constraints on surface-to-volume ratio, then distributed core internal heat sinks would be a potential alternative. For the pin-based reactor there is no conduction component to this pathway unless some type of a web type spacer design is envisioned but that would increase the steady-state coolant pressure drop through the core. Furthermore unless there are “few fat pins” as opposed to “many thin pins” there will be a large number of radiation interfaces between the center of the core and the vessel boundary. This could lead to large temperature drops. In the case of the block core, the radiation interfaces are the gaps between the blocks. These clearances are necessary for the mechanics of refuelling. Larger blocks could help the passive conduction of heat to the boundary but the weight would increase the requirements on the refuelling machines. Inter block gaps are a necessity. High conductivity block matrix material would be advantageous to this mode of passive decay heat removal [22]. High thermal inertia block matrix material would also be advantageous. Both these attributes would be useful for the pebble matrix material and the fuel pin pellets. Though in the case of the pellet, typically the decay heat level is low enough that it is the radiation temperature drops between the pins that

dominate. In addition to material properties, geometry matters. In particular the surface-to-volume is the important parameter. This affects the aspect ratio of the core and ultimately of the primary vessel. The PBMR and the GT-MHTGR thermal reactors are both tall thin reactors to promote the conduction of the core decay heat to the vessel boundary and thereby the conduction cool down off the vessel wall [32]. This geometry however also promotes neutron leakage from the core and impacts the neutron balance adversely. For a fast reactor where the neutron leakage is typically much larger than the thermal reactor, this would unfortunately be a large effect.

### **2.3.2 In-Core Heat Sinks with Gas Cooled Reactors**

Given the unfavourable trends it is still possible to consider conduction Cool down as a potential passive decay heat removal mechanism if the ultimate heat sink is not the vessel boundary but a series of distributed core internal heat sinks. These heat sinks could be uncooled thermal inertia sinks or cooled through secondary natural convection pathways. For the uncooled option it can be seen from Figure 2.1 and the discussion, that a significant amount of thermal capacity could be required to absorb the excess heat until the decay heat production decays to the heat removal rate possible through the vessel boundary. For the cooled options, the passive heat removal in these internal core heat sink locations could be natural convection cooled heat exchangers or special devices such as heat pipes. In all cases the cooled option requires the provision of connections through the primary system boundary to the ultimate external heat sink. There is also the use of the vessel wall as an intermediate heat sink with external cooling of the wall. However even in this case, the same difficulty exists of connecting all these internal core heat sinks to the ultimate heat sink [9]. A complex piping system for this internal heat transport problem within the vessel may have to be designed. This system would have to be accommodated by control rod drives internals and the refuelling mode of operation. Failure of this system should not depressurize the primary coolant system otherwise it would not meet the single failure criteria. The choice of coolant on the secondary side is also an important factor [29]. Moisture in the GFR core has historically been regarded as a positive reactivity effect and there are certainly combinations of fuel materials and coolant selection that should be avoided for

compatibility reasons. As far as conduction/radiation of the core generated decay heat to those in-core locations the same phenomena governing the conduction/radiation cool down to the vessel wall would govern here. The pin core with its multiple radiation interfaces would be at a disadvantage. The gaps in the block core could be minimized depending upon design [9]. The pebble bed core could have challenging temperature conditions for the heat sink boundary material as contact would be made with the pebbles.

### **2.3.3 Natural Convection in Gas Cooled Reactors**

Just a mass transfer is acknowledged as a special feature of the pebble bed fuel form and configuration; it is also acknowledged that in general the pebble bed form is not the optimum form for natural convection. The pressure drops inherent to the pebble bed configuration are not conducive for natural circulation. There is certainly more flexibility in the design of other fuel element forms to optimize for natural convection. However, even if pin based or block plate based cores are selected for the natural convection heat transfer mode, helium is a poor heat transfer medium at one atmosphere pressure. The level of the acceptable accident pressure whether a separate heavy gas injection needs to be arranged, and the means to maintaining a residual backpressure are all design questions that need to be resolved. The question of the residual back pressure required to maintain an acceptable level of natural convection to transport the decay heat away from the core is tied closely to the selection of the coolant gas. The light gas helium is acknowledged to be a natural convection medium that requires very tall chimneys and large elevation heads [10]. Heavy gases such as CO<sub>2</sub> are acknowledged to be better. A lower backpressure is required for the same heat removal rates. Conversely shorter chimneys can be used. However, since helium has been selected as the primary coolant, heavy gas injection into the primary system would be required to replace the helium with the heavy gas. The issue of mixing, bypass and timescale all need to be addressed. Furthermore fuels such as carbides are chemically reactive with gases such as CO<sub>2</sub>. The list of economic possibilities is limited. Presuming that an appropriate gas for the natural convection mode has been selected, a heat sink needs to be provided to couple to the core. Heat sinks external to the primary system would require a guaranteed

convection path through the primary boundary during depressurization accidents. Quick opening valves in the boundary would be required. This would have the drawback of being a potential system depressurization initiation. There are certainly inherent heat sinks such as shield/reflector regions, upper internals and the vessel metal, but unless provision is made for passive cooling of the vessel wall, there would be need for a dedicated emergency heat exchanger that is designed for natural convection cooling on the secondary side [3]. Credit should be taken for the inherent heat sinks, both thermal inertia and natural convection cooling off the vessel walls in the cavity/silo as the phenomena will occur. But confirmation of this type of heat loss mechanism would require substantial CFD analyses and experimental confirmation of natural convection cell patterns. Maintenance of a backup pressure during primary system break/leak induced depressurization events would require a secondary guard containment or vessel surrounding the preliminary boundary. The challenge in designing and building this guard containment would depend upon the backup pressure level selected and the layout of the primary system and balance-of-plant [15]. The questions of direct vs. indirect cycle, hydrogen production vs. electricity generation and others such as these would do have a large impact on the design of the guard containment.

## **2.4 Carbon Dioxide Cooling**

Carbon dioxide as a coolant is more suitable to the fast breeder reactors. The most common choices for gas-cooled fast reactors are helium, (supercritical) CO<sub>2</sub>, and steam. (Special mention should be made of the supercritical water-cooled reactor concept, which is proposed with thermal, epithermal, and fast neutron spectra.) The choice of coolant is dictated by the desire to introduce the smallest amount of absorption and moderation, while still being able to reliably remove the heat from this high power density configuration [16]. Commonly a liquid metal is chosen, with sodium being the most common, but a gas coolant is also possible. Even though all these coolants are composed of light isotopes, the amount of moderation is limited because of the low number density of gas coolants. Chemical compatibility with water, obviating the need of an intermediate coolant loop, and generally good chemical compatibility with

structural materials, Negligible activation of coolant, Optically transparent, simplifying fuel shuffling operations and inspection, Gas coolants cannot change phase in the core, reducing the potential of reactivity swings under accidental conditions. Reduction of the positive void effect typically associated with sodium. CO<sub>2</sub> as a coolant generally allow a harder neutron spectrum, which increases the breeding potential of the reactor. Helium is preferred to CO<sub>2</sub> as a reactor coolant due to its excellent cooling capabilities and inertness. The reactor design and development is independent of the CO<sub>2</sub> cycle development and the reactor can be used with any other indirect cycle. Small leaks of CO<sub>2</sub> into the helium side are less disturbing than a steam leak due to the similar nuclear properties of helium and CO<sub>2</sub>. The corrosion is also a smaller problem in such a case. CO<sub>2</sub> is much cheaper than helium (about 250 times per unit weight and 24 times per unit of volume) and its leakage problem in the gas turbine cycle are therefore orders of magnitude less severe than with helium. Since CO<sub>2</sub> can be stored in the liquid phase at relatively low pressures the required storage capacity is smaller than for helium. CO<sub>2</sub> gas turbine cycles achieve higher efficiencies than the helium Brayton cycles at fast breeder reactor temperatures [13]. Since the entire gas turbine plant is in the secondary loop it can be placed in the open air. The cooling system can be of the direct type because the primary coolant is not in direct contact with the cooling water. With CO<sub>2</sub> in the secondary circuit higher cycle temperatures could be used in the future. The size of the turbo machinery is smaller than for steam or helium cycles.

## **CHAPTER 3**

### **HELIUM COOLED REACTORS**

Safety is the most important criterion in evaluating the options and designing the reactors. All reactors must meet a minimum safety level described by IAEA, but those that are more inherently safe are more likely to use in the future generations. The helium cooled modular pebble bed gas cooled reactor is considered to be the safest of all designs. It's passive, inherent safety with no possibility of core melt make it the more attractive. The ability of helium cooled reactor are, they can be assembled in a factory, shipped to the construction site, and pieced together will decrease construction time.

#### **3.1 Introduction to Helium Cooled Reactor**

Helium is stable in thermal and radiation environments, entirely compatible with the intermediate loop and high temperature capability of the helium-cooled reactor can also be used to develop highly efficient systems for electrical power. The possibility of a direct Brayton cycle may result in significant efficiency improvements and reduced capital costs for the production of electricity. If the PBR is used, online refuelling, deep fuel burn, and low excess reactivity separation are feasible. Gas coolant operating pressures are high, but well within the operational envelope for gas cooled reactors. Although high pressure operation implies the possibility of rapid coolant loss, the high heat capacity of the graphite fuel elements mitigates the effects of these types of accidents [22]. Activation of He is insignificant. The high heat capacity of the core for graphite-moderated helium cooled concepts results in very gradual core heating in the event of a loss of flow accident. Furthermore, no coolant phase change occurs for any postulated accident sequence. The high fission product retention ability of the HTGR microsphere fuel provides another safety advantage. Helium is non-toxic and does not present a fire or explosion hazard. The issue has been raised concerning the possibility of rapid oxidation of the graphite fuel elements in the event of accidental air ingress into the primary system. The proponents of gas-cooled reactors argue that the high-density, high-grade graphite used for the fuel elements does not undergo rapid oxidation for

postulated loss-of-coolant accident conditions [36]. The possibility of significant water ingress seems highly improbable due to the absence of a high-pressure water interface with the primary loop which is shown in the figure 3.1.

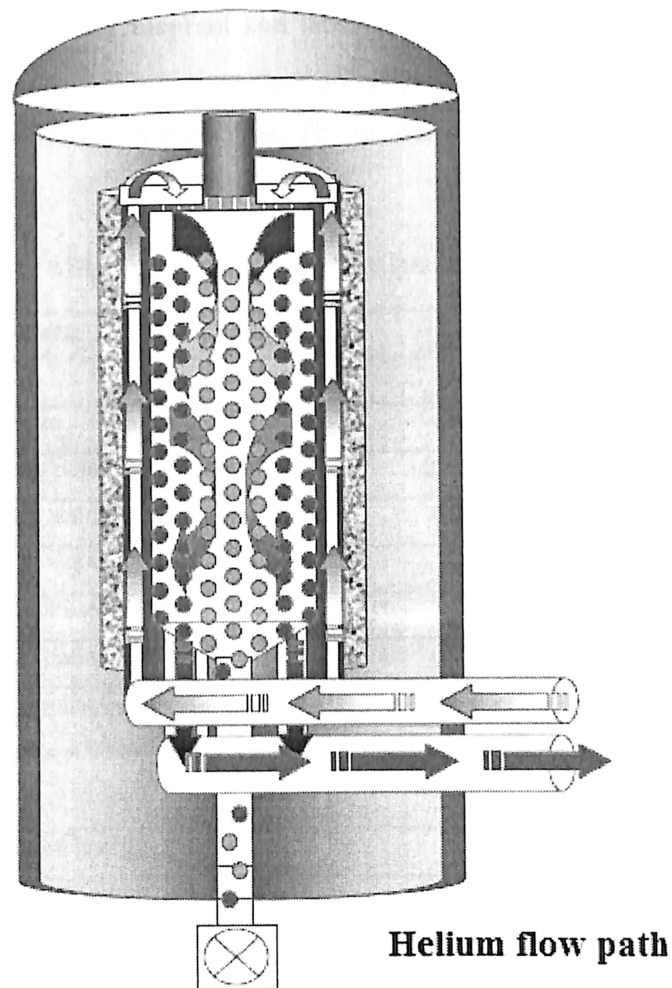


**Figure 3.1** Helium Cooled Reactor Coolant Circulating System

Gas cooled reactors, taking advantage of coated particle fuel technology, are sometimes designed without an external containment building. Here we have assumed adequate confinement by either the fuel particle coating, or by a confinement enclosure will be reflected in somewhat higher capital costs, as discussed subsequently [18]. Due to the inertness with helium gas the fuel pebbles coatings will not react with the coolant in the reactor and also the heat transfer rate will be more due to the boundary interface with the coolant. Which will indirectly increase the power density of the reactor, also reduces the reaction time inside the reactor.

### 3.2 Properties of Helium

Helium is a light, odorless, colorless, inert, monatomic gas. It can form diatomic molecules, but only weakly and at temperatures close to absolute zero [19]. Helium has the lowest melting point of any element and its boiling point is close to absolute zero. Unlike any other element, helium does not solidify but remains a liquid down to absolute zero (0 K) under ordinary pressures. The properties are tabulated below in table 3.1.

**TABLE 3.1** PROPERTIES OF NATURAL HELIUM

Property	Value
<b>States</b>	
State	Gas, (0 K) liquid
Melting point	0.95 K (-272.2 °C)
Boiling point	4.2 K (-268.9 °C)
<b>Energies</b>	
Specific heat capacity	5.193 J g <sup>-1</sup> K <sup>-1</sup>
Heat of fusion	0.0138 kJ mol <sup>-1</sup>
Heat of atomization	0 kJ mol <sup>-1</sup>
Heat of vaporization	0.0845 kJ mol <sup>-1</sup>
1 <sup>st</sup> ionization Energy	2372.3 kJ mol <sup>-1</sup>
2 <sup>nd</sup> ionization energy	5250.3 kJ mol <sup>-1</sup>
3 <sup>rd</sup> ionization energy	0 kJ mol <sup>-1</sup>
Electron affinity	0 kJ mol <sup>-1</sup>
<b>Oxidation &amp; Electronics</b>	
Shells	2
Electron Configuration	1 s <sup>2</sup>
Max. oxidation number	0
Min. Oxidation	0
Electron gravity	Pauling Scale, 0
Polarizability volume	0.198 Å <sup>3</sup>
<b>Appearance &amp; Characteristics</b>	
Structure	Hexagonal closed packed
Color	Color less
Harness	mohs
<b>Conductivity</b>	



Thermal Conductivity	0.15 W m <sup>-1</sup> K <sup>-1</sup>
Electrical Conductivity	S cm <sup>-1</sup>
<b>Radius</b>	
Atomic radius	31 ppm
Ionic Radius(1-ion):	pm
Ionic Radius(2-ion):	pm
Ionic Radius(3-ion):	pm
Ionic Radius(2-ion):	pm
Ionic Radius(1-ion):	pm
<b>Abundance &amp; Isotopes</b>	
Abundance earth's crust	8 Parts per billion by weight, 43 parts per billion by moles
Abundance solar system	23 % by Weight, 7.4% by moles

### 3.3 Why Helium -Safety Issues- Longevity

Helium is an inert gas and, in its pure state, should be ideal for operation at the required temperature of 900 C. Although materials effects can result from impurities in the coolant, operational experience showed no significant materials issues related to impurities in the coolant. . The helium cooled reactor operated in the past include a high temperature around 950 C. Consequently, gas-cooled reactors have been successfully operated in the desired 40 optimal temperature ranges. The best example in front of us is Japanese prismatic fuel HTTR will also operate at coolant temperatures greater than 900 C. It describes the benefits, as well as experience on the engineering prospective. The GT-MHR is meltdown-proof and passively safe. The GT-MHR safety is achieved through a combination of inherent safety characteristics and design selections that take maximum advantage of the inherent characteristics [20]. These characteristics and design selections include. Helium coolant, which is single phase, inert, and has no reactivity effects, graphite core, which provides high heat capacity and slow thermal response, and structural stability at very high temperatures, refractory (TRISO) coated particle fuel, which retains fission products at temperatures much higher than normal operation and postulated accident conditions, negative temperature coefficient of reactivity, which inherently shuts down the core above normal operating temperatures

without the need for operator action and an annular, low power density core in an un insulated steel reactor vessel surrounded by a natural circulation reactor cavity cooling system (RCCS).

### **3.3.1 Proliferation/Terrorist Resistance**

The GT-MHR has very high proliferation/terrorist resistance. Both GT-MHR fresh fuel and spent fuel have higher resistance to diversion, proliferation and potential terrorist opportunities than other nuclear reactor options. GT-MHR fresh fuel has high proliferation/terrorist resistance because the fuel is much diluted by the fuel element graphite (low fuel volume fraction) and because of the technical difficulty to retrieve materials from within the refractory fuel coatings. GT-MHR spent fuel has these same characteristics plus self-protecting high radiation fields [18]. Furthermore, the low volume fraction and low quality (high degradation due to high burn up) of plutonium in GT-MHR spent fuel make it particularly suitable for gas turbine modular helium cooled reactors.

### **3.3.2 Spent Fuel Management**

GT-MHR spent fuel is ideally suited for both long term storage and permanent disposal in a repository. The TRISO fuel particle coating system, which provides containment of fission products under reactor operating conditions, also provides an excellent barrier for containment of the radio nuclides for storage and geologic disposal of spent fuel [17]. Experimental studies have shown the corrosion rates of the fuel particle TRISO coatings are very low under both dry and wet conditions. Measured corrosion rates indicate the TRISO coating system should maintain its integrity for a million years or more in a geologic repository environment.

### **3.3.3 Low Environmental Impact**

The high thermal efficiency and high burn up capability of the GT-MHR results in reduced environmental impacts relative to other reactor options. The thermal discharge (waste heat) from the GT-MHR is one-half that for light water reactors per unit of electricity produced because the GT-MHR's thermal efficiency is 50% greater than that

of light water reactors [10]. The detailed explanation on safety and efficiency point of view figure 3.2 signifies specific characteristics. Also, because of its high efficiency and high fuel burn up, the GT-MHR produces significantly less heavy metal radioactive waste than conventional nuclear power plants per unit of electricity produced.

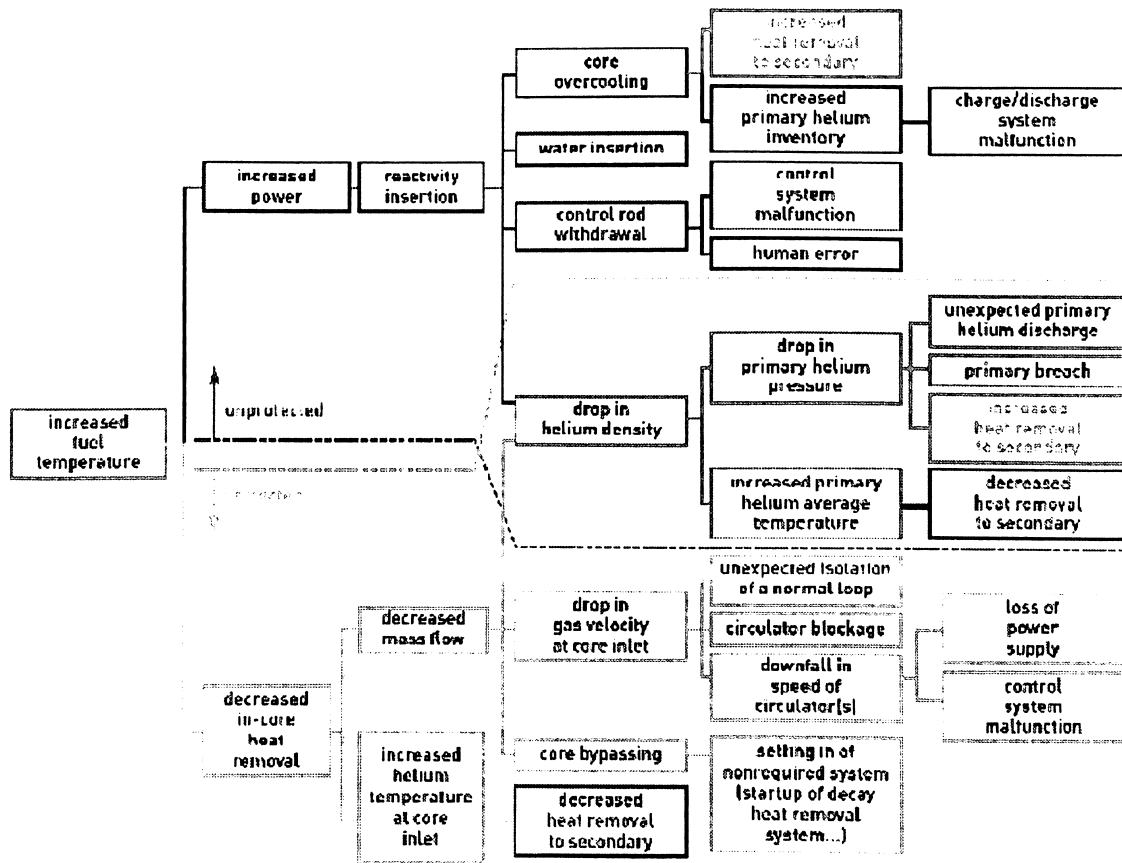
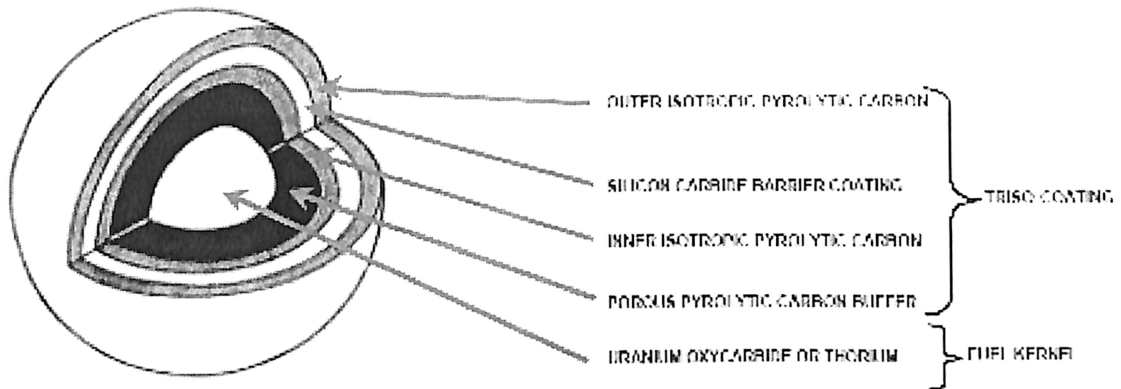


Figure 3.2 Helium Cooled Reactor Fuel Temperature Effect

### 3.4 Nuclear Fuels for Helium Cooled Reactors

In helium cooled reactors Tesco coated fuel pebble bed of spherical fuel particles, such as the fuel pebble shown in figure 8. Approximately 380,000 spheres are loaded in the core. Each fuel sphere contains the uranium oxycarbide or thorium core, a porous pyrolytic carbon buffer, an inner isotropic pyrolytic carbon layer, a silicon carbide barrier coating, and an outer isotropic pyrolytic carbon layer; the total sphere is approximately the size of a racquet ball. The inner part of the core is called fuel kernel which takes major part in fusion reaction [8]. The outer core is a sequence of coatings

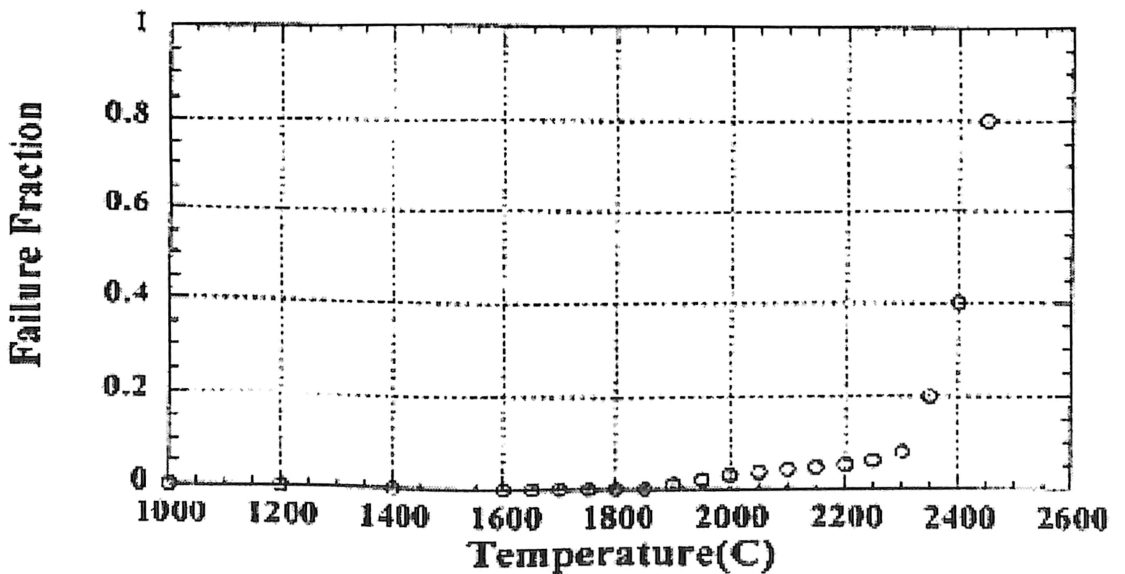
used for the protection and heat transfer enhancement between the fuel elements to the coolant.



(Source: *Plant Design Concepts for a Gas-Cooled Fast Reactor*, Argonne National Laboratory)

**Figure 3.3** TRISO Coated Fuel Pebbles

The inherent safety is derived from the sphere because it takes temperatures of approximately 2000 °C in order for the ball to begin to break down. Figure 3.4 shows the fuel failure fraction as a function of fuel temperature. Based on these design parameters, the highest temperature the fuel would achieve is approximately 1600 °C and it would take approximately 3 days to reach that peak fuel temperature before the fuel starts to naturally cool [40]. Cooling to the core with a complete loss of coolant is achieved via natural conduction from the core to the surroundings.



(Source: *Massachusetts Institute of Technology: Independent Activities*)

**Figure 3.4** Maximum Temperature Selection For Trisco Coated Fuel Pebbles

Not only does the fuel offer a "naturally-safe" feature, but also easily facilitates online fueling. The fuel pebbles can be cycled through the core as necessary and discharged when fully burned out. Another advantage of having the fuel in pebble form is waste removal and storage [43]. The spent fuel is inherently contained by the carbon material; therefore no spent fuel pool is needed and the storage facilities can be a lot less complex.

### **3.4.1 Parameters Fuel Pebbles Helium Cooled Reactors**

Several "old" concepts have been revisited, and one of them is based on the concept of fuel fluidization. This fluidized bed nuclear reactor consists of a graphite-walled tube partially filled with TRISO-coated fuel particles. In contrast with other GT-MHR where the TRISO particles are encased within a graphite pebble or rods, the particles are laid in the bottom part of the cavity of the tube, forming a packed bed. Helium is used as a coolant that flows from bottom to top through the tube, thereby fluidizing the particle bed [42]. During the fluidization process, the bed of solid particles is transformed into something closely resembling a liquid. When the flow is absent or at low rate, the bed remains packed. When the flow rate is increased, the bed expands and forms a fluidized state. Only when the coolant flow is large enough does the reactor become critical because of the surrounding graphite that moderates and reflects the neutrons.

### **3.4.2 Kernel-Coating Mechanical Interaction (KCMI)**

At sufficiently high burn-up values, it is inevitable that all gas gaps between the kernel and coatings will close, thereby resulting in a mechanical interaction between the two (KCMI). This is because the kernel will swell inexorably during the course of the irradiation. Modelling studies predict that the SiC layer will fail shortly after the onset of KCMI. To date, this failure mechanism has not been reported experimentally[]. Possibly this is because even if, at the end of the irradiation, KCMI occurs, a gas gap will always

be created as the particle cools to room temperature owing to the kernel's comparatively higher thermal expansion coefficient. Perhaps this fact was overlooked in some PIE investigations. But clearly this failure mechanism could be of increasing importance as attempts are made to achieve higher.

### **3.4.3 Solubility Of Fission Products In UO<sub>2</sub> Fuel**

From atomic-scale calculations, it is also possible to derive estimates of fission product solubilities in irradiated UO<sub>2</sub> to be compared to the values obtained from experiments [20]. It is well acknowledged that noble gases exhibit almost total insolubility. Iodine, Br and Te are also highly insoluble whereas Cs and Ba exhibit only low solubility in the case of hyper stoichiometric fuel. Then the solubility increases from Zr (depending on temperature) to Sr, reaching very high solubilities for the rare earth elements, namely Ce, which is extremely soluble.

### **3.4.4 Behaviour of Gaseous Fission Products (Xe And Kr) In UO<sub>2</sub> Fuel**

Fission products in the fuel lattice can diffuse out of the UO<sub>2+x</sub> to grain boundaries. The diffusion mechanism depends on the nature of the fission product trap sites and on the fission product intrinsic characteristics like size and charge [21]. Irradiation effects can greatly enhance or reduce this diffusion by trapping mechanisms on extended defects (dislocations, for example). The behavior of fission-gases is unique because of their very low solubility and high volatility. The gases precipitate primarily as intragranular bubbles. These bubbles can grow by gas-atom and vacancy absorption [25]. Generally speaking, bubble mobility is limited (defects and impurities created by irradiation limit bubble diffusivity) [23]; nevertheless, because of high fuel temperatures, some bubble coalescence cannot be excluded. Additional mechanisms for bubble growth are associated with interactions with dislocations, essentially at high burnup, that can induce high local stresses increasing bubble diffusivity, bubble trapping and the possibility of bubble growth by dislocation-loop punching (mainly during transients). The thermodynamic state in the bubbles depends greatly on the interaction with defects, mainly vacancies. Bubble relaxation is a function of the local vacancy concentration, and in the case of limited vacancy concentration, highly-over pressurized

bubbles can be observed. For the  $\text{UO}_2$  kernel in TRISO fuel particles, both fission-rate and temperature help to strongly limit bubble size and maintain a substantial fission-gas atom population in the fuel lattice by re-resolution of gas from bubbles. Fission gases can migrate to grain boundaries by atomic or bubble diffusion to form inter granular bubbles (porosities) where they can grow by addition of gas and vacancies (thermally produced at grain boundaries). Like intragranular bubbles, high levels of irradiation induced re-resolution significantly limits this growth (and bubble-induced swelling of the kernel) while stresses in the particle may also limit the equilibrium bubble size. Once inter granular-bubble growth becomes significant causing interconnection of porosity, a path from within the kernel to the buffer is created leading to fission-gas release by a percolation mechanism.

### **3.4.5 Behaviour of Chemically Active Fission Products In Fuel**

For the behaviour of solid fission products one must consider solubility, possible oxidation and diffusion. For oxygen potentials expected in HTGR fuel particles, the Rare Earths (RE) are highly soluble being incorporated in the fuel lattice as oxides ( $\text{REO}_2$  or  $\text{RE}_2\text{O}_3$ ) where they remain stable with the possible exception of Ce seen to be significantly released at around 1743 K for 4% enriched fuel. With respect to UCO fuel, we note that as the  $\text{UC}_2/\text{UO}_2$  ratio increases then so do the motilities of the REs since their “trapping” in the kernel in oxide form is lessened. Zirconium, Nb and Sr have significant solubility in  $\text{UO}_2$  (more at high temperature for Zr) and are easy to oxidize ( $\text{ZrO}_2$ ,  $\text{Nb}_2\text{O}_3$  and  $\text{SrO}$ ). Barium is in the form of low-solubility  $\text{BaO}$  and can migrate to grain boundaries forming separate complex ternary compounds with Sr, Zr, REs (and small amounts of Cs and Mo, see below) of perovskite structure. This complex phase can only be observed at high temperature and high burn up (it was not observed at 4% even at high temperature; furthermore, significant Ba release out of the kernel was measured) [26]. Tellurium is also of low solubility and is difficult to oxidize; at grain boundaries it forms inter-metallic compounds (e.g., with Pd) and  $\text{Cs}_2\text{Te}$  (rarely observed) and is significantly released from the kernel. Many of the other metallic elements also have rather low solubility and are difficult to oxidize except at high oxygen potentials and, after segregation at grain boundaries, form metallic inclusions.

Noble metals (Mo, Ru, Rh, Tc and Pd) constitute the main type of inclusion. Other inclusions of Te, Sn or Pd, Ag, Cd are also observed. The size of inclusions is very temperature dependent. Pd and Ag have high volatility and are significantly released out of the fuel kernel. Molybdenum has a complex behaviour because its oxidation potential is close to the value corresponding to stoichiometric fuel and a significant amount can be oxidized to  $\text{MoO}_2$  (limiting increase of fuel stoichiometric), a low solubility oxide. At high temperature Mo can form molybdate compounds with Cs or Ba but even at high temperature greater than 1673K these were not observed in Caesium also has low solubility and might be oxidized to  $\text{Cs}_2\text{O}$  depending on the fuel temperature and oxygen potential. This oxide also has low solubility. Once again, formation of complex ternary phases could be foreseen at high temperature and high burn up but were not observed in where significant release of Cs from the kernel was observed.

#### **3.4.6 Urania ( $\text{UO}_2$ ) Kernel Oxygen Potential**

Uranium-atom fissions (i.e., burn up) deplete the uranium content replacing each uranium atom with two fission products that, overall, have a slightly lower affinity for the oxygen of the urania (in particular, a large fraction of the noble gas xenon (~28%) is produced. Thus, the fuel oxygen potential increases during irradiation and the fuel becomes slightly hyper stoichiometric (excess oxygen), a trend tempered by some of this oxygen reacting with the carbon buffer layer [26]. Different approaches can be used to determine the oxygen potential in TRISO particles. Fission yields can be used to determine the amount of each fission product element and then calculate the oxygen requirements as metal monoxide ( $\text{BaO}$ , etc.), sesquioxide ( $\text{La}_2\text{O}_3$ , etc.) and dioxide ( $\text{ZrO}_2$ , etc.);

#### **3.4.7 Silicon Carbide Corrosion By Fission Products**

In the typical HTGR TRISO coating design, the silicon carbide layer serves as a critical fission product barrier. Nevertheless, it has been shown experimentally that the silicon carbide layer can be corroded by metallic fission products; in particular, palladium. It was additionally found that silver could be transported through intact SiC layers [35]. These processes tend to limit the fuel life time, especially at high



temperature. For this reason, considerable literature exists on the experimental study of interface reactions between metallic fission products and SiC. For Pd, the reaction with SiC can be qualitatively explained by phase-diagram arguments (the Si-C-Pd system was experimentally investigated and recently modelled by. To prevent corrosion by Pd, new combinations of coating layers were proposed. The idea was to introduce a sacrificial layer inside the SiC coating able to retain the offending fission products. An alternative approach consists of replacing the SiC coating by a ZrC layer. Review and evaluation of the ZrC coating for HTGR fuel particles has been performed. In particular, experimental observations showed neither Pd attack nor thermal degradation of ZrC up to 1600°C. Zirconium carbide was also shown to have a high capacity to retain caesium. However, Ru retention was not as good as for SiC. At higher temperatures, the deterioration of the ZrC particle is caused by failure of the IPyC. The development of TRISO-coated particles with a ZrC-coating must be viewed as at an early stage compared to the development of the SiC-coated design for which many experiments have been performed. Silver release has been observed from undamaged particles suggesting that Ag migrates through intact SiC layers at temperatures >1100°C. Today, the Ag migration mechanism remains not fully understood. A review of the possible explanations for this process is available. In many situations of the past, Ag release was modelled as a diffusive mechanism since measurements of silver release exhibited temperature dependence. It seems that recent experimental results do not support this mechanism. It was shown that, if grain-boundary diffusion is assumed, the expected value of the diffusion coefficient in SiC is inconsistent with the value derived from Ag release measurements. It is speculated that Ag migration is due to the presence of free silicon at the grain boundaries. Recent experimental studies indicate that Ag migration by diffusion (intragranular or intragranular) does not occur up to 1300°C and alternative explanations are proposed [17]. Once caesium has migrated into the buffer, it can react with carbon. The question of the stability of the CnCs compounds at temperatures higher than 1100 K is an important concern. At nominal temperatures, caesium may be released and associated with carbon of the buffer layer to form compounds. These compounds if they are not stable with increasing temperatures, may become a potential source of caesium release. The thermodynamic properties of these compounds, CnCs (n=8, 10, 24, 36, 48,

60), can be derived from vapour pressures measured in the temperature range between 670 and 1070 K. There are no data at higher temperatures as mentioned in different reviews, It was only shown that caesium-graphite compounds are not stable at 923 K under vacuum and decompose to give caesium vapour and graphite. A method was developed for estimating the conditions under which graphite reacts with caesium in HTGR conditions (high temperatures and low caesium pressures) to form compounds.

### 3.4.8 Fission Product Release

The transport of fission metals through the fuel constituent materials is modelled as a transient diffusion process. The transient diffusion equation is typically solved numerically with appropriate boundary and interface conditions. The transport of mobile fission metals, including Cs, Ag, Sr and Eu isotopes, is undoubtedly much more complicated than classical Fickian diffusion. These apparent migration coefficients are generally structure sensitive which indicates that their transport process is not a simple diffusion process but likely a combination of lattice diffusion, grain boundary diffusion, pore diffusion, etc., complicated further by effects like irradiation-enhanced trapping and adsorption. Consequently, any quoted diffusion coefficients should be called “effective” diffusion coefficients [18]. The fission product speciation in the kernel changes with burnup, especially with UCO kernels as the oxygen potential changes, and these changes in chemistry could affect the mobility of oxide-forming species, including Cs and Sr. The probable exception is silver which appears to remain in elemental form for all kernel compositions and burn up of interest. Atoms and molecules have the spontaneous tendency to disperse as a consequence of the second law of thermodynamics. The rate of migration of an atom through a medium is measured by its mass flux  $J$  is expressed as atoms  $m^{-2} s^{-1}$ . Atoms migrate down a concentration gradient as described in equation 15.

$$J_x = -D \frac{\partial c}{\partial x} \text{ or, more general, } \mathbf{j} = -D \cdot \nabla c \quad (15)$$

With  $c$  atoms. $m^{-3}$  being the concentration as a function of time and space coordinates. The flux of atoms diffusing through a medium is proportional to the concentration gradient. Which give us the balance equation in the absence of source and decay terms,

$$\frac{\partial c}{\partial t} = -\frac{\partial J}{\partial x} \text{ or } \iiint_V \frac{\partial c}{\partial t} dV = -\oint_S j \cdot \vec{dS} \quad (16)$$

Where V and S are volume and surface under consideration, inserting the diffusion flux J in the balance equation gives us Fick's second law. Fick's second law of diffusion describes in equation 17 the time dependent diffusion process.

$$\frac{\partial c}{\partial t} = \nabla(D\nabla c) \text{ and this is } \frac{\partial c}{\partial t} = \frac{D}{r} \frac{\partial^2 (rc)}{\partial r^2} \text{ in spherical coordinates and constant D} \quad (17)$$

Where by r(m) is the radial position in a kernel, in a particle or in a spherical fuel elements. This is known as the diffusion equation, and mathematically, it is a partial differential equation of parabolic type. In a fuel element is a source S of atoms production from nuclear fission and a removal term  $\lambda_c$  radio active decay so that the diffusion equation shown in equation 18.

$$\frac{\partial c}{\partial t} = D \left( \frac{\partial^2 c}{\partial r^2} + \frac{1}{r} \frac{\partial c}{\partial r} \right) - \lambda c + S \quad (18)$$

With the following boundary conditions

For reasons of symmetry, the concentration gradient is at r=0.

$$\frac{\partial c}{\partial r} = 0 \text{ at } r=0 \quad (19)$$

Continuity of concentration and flux at the interface between two adjacent materials with diffusion constant  $D_1$  and  $D_2$

$$C_L = C_R \text{ and } -D_1 \frac{\partial c}{\partial r} \Big|_L = -D_2 \frac{\partial c}{\partial r} \Big|_R \quad (20)$$

Mass transfer at the fuel surface

$$-D \frac{\partial c}{\partial r} \Big|_{r=r_c} = \beta (\alpha c_z - c_s) \quad (21)$$

### 3.4.9 Fission Product Release From Fuel Materials

In the equivalent sphere model, the primary fission product retaining object is a  $UO_2$  or  $(Th.U)O_2$  grain that is modeled as a sphere with radius a. With the initial and boundary conditions

$$c(0 \leq r \leq a, t = 0) = 0, \frac{\partial c(r=0, \forall t)}{\partial r} = 0, c(r = a, \forall t) = 0 \quad (22)$$

Solving the diffusion equation

$$\frac{\partial c}{\partial t} = D \left( \frac{\partial^2 c}{\partial r^2} + \frac{1}{r} \frac{\partial c}{\partial r} \right) - \lambda c + S \quad (23)$$

For concentration  $c$  as a function of radius  $r$  and time  $t$  reveals

$$c(r, t) = \frac{S}{\lambda} \left[ 1 - \frac{\sinh \rho \sqrt{\frac{\lambda}{D'}}}{\rho \sinh \sqrt{\frac{\lambda}{D'}}} - \left[ \frac{2 S}{\pi D'} \frac{e^{-\lambda t}}{\rho} \sum_{n=1}^{\infty} (-1)^{n+1} \frac{e^{-n^2 \pi^2 D' t}}{n(n^2 \pi^2 + \frac{\lambda}{D'})} \sin n \pi \rho \right] \right] \quad (24)$$

With reduced radius  $\rho = \frac{r}{a}$  and reduced diffusion coefficient  $D' = \frac{D}{a^2}$

For short lived fission gases,  $\lambda \geq 10^{-6}$  s, and, only the steady state first term of equation 24 needs to be used then the moderated equation is

$$\frac{R}{B} = 3 \sqrt{\frac{D'}{\lambda}} \left( \coth \sqrt{\frac{\lambda}{D'}} - \sqrt{\frac{D'}{\lambda}} \right) = 3 \sqrt{\frac{D'}{\lambda}} \propto \sqrt{\tau} \quad (25)$$

Where  $R/B$  is the ratio of release-rate( $R$ ) over birth-rate( $B$ ) is approximately proportional to the square root of the half life.  $\square^{1/2}$  The diffusion coefficient used here is given by

$$D = D_0' e^{\frac{Q}{RT}} \quad \text{with} \quad (26)$$

$$D_0' = 2.1 \times 10^{-5} \text{ s}^{-1}, \quad Q = 126 \text{ kJ/mol activation energy}$$

Fluidized beds have several features that are advantageous for a nuclear reactor, such as a uniform temperature distribution due to rapid particle mixing and a high transfer rate between particles and fluid. The high heat transfer rate between particles and fluid yields a high temperature of fluid without leading to an excessive fuel temperature [13]. This offers the advantages of a high core outlet temperature and the use of a highly efficient direct-cycle gas turbine. The excellent mixing properties guarantee a uniform power distribution and consequently a uniform fuel burn up. Another possible advantage of using a fluidized bed for nuclear reactors is that the bed height increases when the gas flow increases. The change in geometry of the bed affects

the neutronic of the reactor and consequently the power produced will change as well. In this manner the power generation can be controlled by altering the inlet flow rate, thus reducing dependencies on control rod mechanisms which is shown in the figure 3.5.

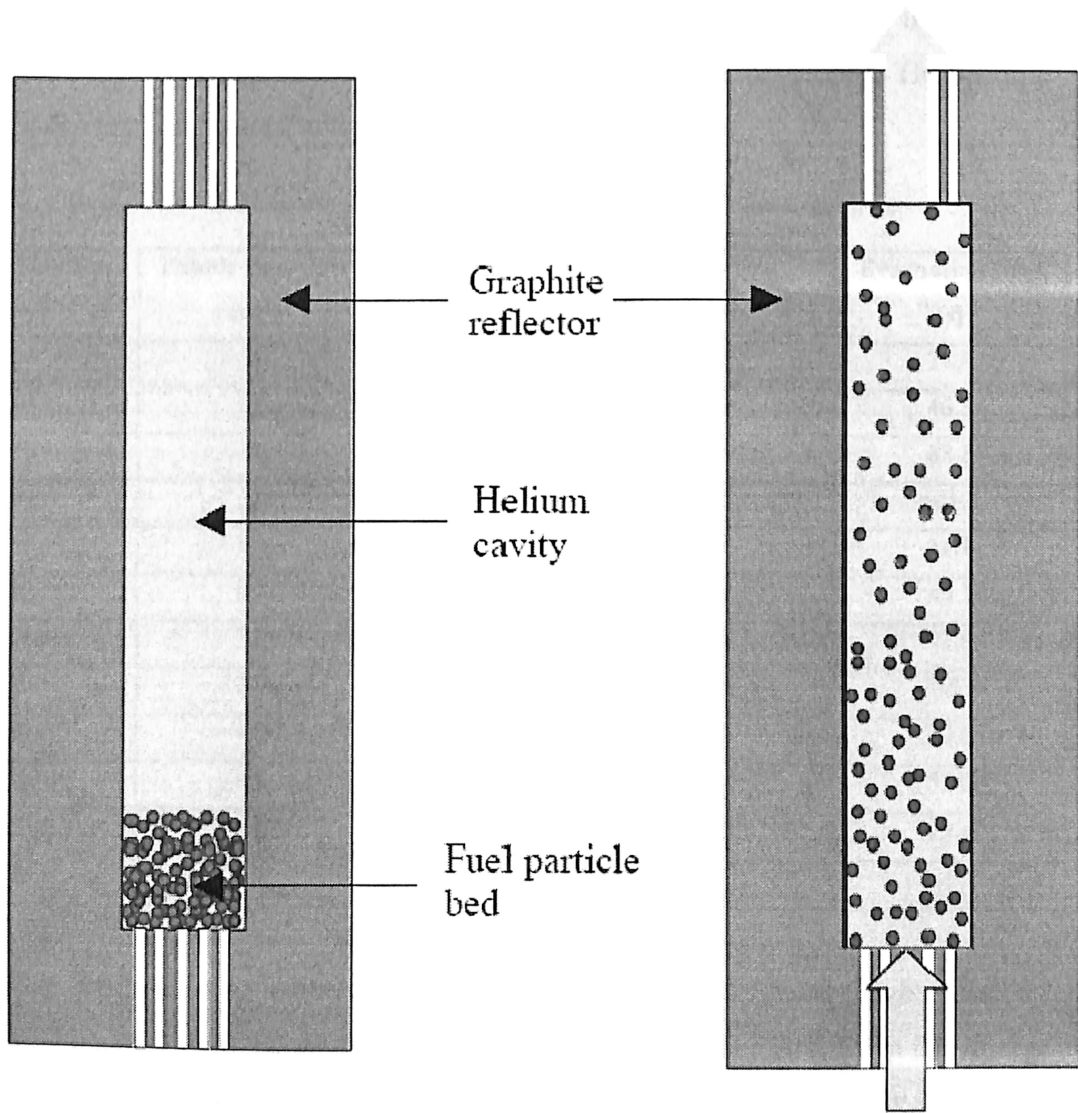


**Figure 3.5** Helium Cooled Reactor Fuel Partical Bed Arrangement

Pebble bed concept long-term decay heat removal In view of the above conclusions this work has concentrated on ultimate safe storage configurations of the pebbles, which have to satisfy the following two requirements like The configuration must be sub-critical assuming fresh fuel (presumably the most reactive) [10]. A value of the multiplication factor of 0.95 will be assumed to be sufficiently sub-critical. The decay

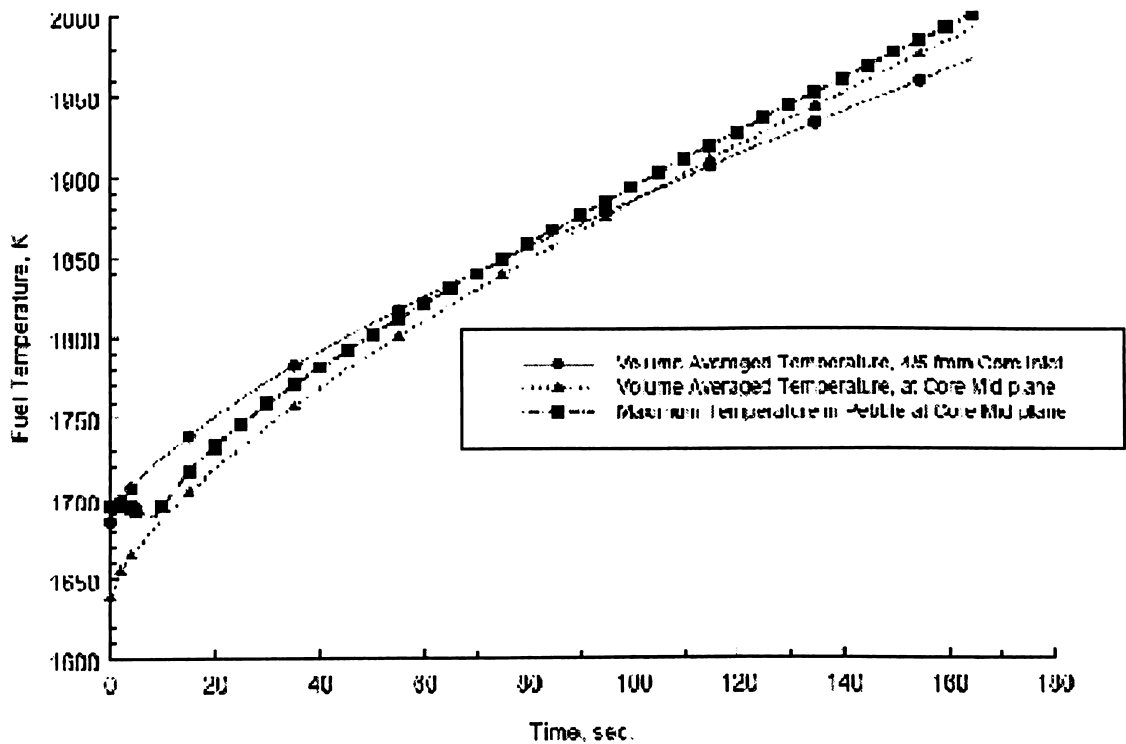
heat remaining in the fuel pebbles must be conducted out of the storage configuration and into a long-term heat removal system. The maximum temperature of the pebbles must be below the maximum allowed accident temperature ( $\sim 1600^\circ\text{C}$ ) both the above two requirements are more difficult to meet for gas cooled fast reactor fuel than for the gas cooled thermal reactor concept for which this concept was developed. The specific size with density is tabulated with different sizes in table 3.2.

**TABLE 3.2 CORE EVACUATION TIME FOR REPRESENTATIVE PEBBLE DENSITIES**

<b>Orifice diameter (cm)</b>	<b>Pebble Diameter (cm)</b>	<b>Pebble Density (gm/cc)</b>	<b>D/d</b>	<b>Evacuation time (s)</b>
60	3	6.5	20	27.6
50	3	6.5	17	46.5
40	3	6.5	13	88.2
20	3	6.5	6.5	681.2
60	3.5	6.8	17	29.1
50	3.5	6.8	14	49.1
40	3.5	6.8	11	93.8
20	3.5	6.8	5.5	735.5
60	4.0	7.1	15	30.6
50	4.0	7.1	12.5	51.8
40	4.0	7.1	10	99.2
20	4.0	7.1	5	817.0

The pebble fissile loading in the case of the fast reactor is significantly higher than for the thermal reactor, and thus the possibility of creating a critical assembly in the storage bins is a lot higher for the fast reactor fuel. Since the operating power density in the case of the fast reactor is much higher than in the thermal reactor concept, the decay heat is proportionately higher and thus the long term heat removal by conduction through the pebble bed and natural convection using air is not practical [8]. The pebble temperature as a function of time following the start of the accident is shown in the figure 3.6. It is seen that initially the temperature drops to a minimum of  $\sim 670^\circ\text{C}$  after  $\sim 200\text{ s}$ , and then increases adiabatically for  $\sim 1000\text{ s}$  before it reaches the unacceptable limit. Thus, it is necessary that any self-sustaining scheme for removing the decay heat start up and

reach steady state operation in 1000 s. In the current case this implies that the core evacuation and transition to long-term heat removal take place in this time frame. The core evacuation will take place in 90 s – 120 s, thus ~ 800 s are available to transition to steady state heat removal.



(Source: *Fuel Element Experience in Nuclear Power Reactors*, Gordon and Breach Science Publ.)

**Figure 3.6 Helium Cooled Reactor Fuel Temperature Limits**

In view of the above heat removal limitations, a scheme is proposed in which the eventual configuration of the pebbles consists of a randomly packed bed infiltrated by a suitable eutectic [4]. The eutectic must have a density below that of the pebbles (in order that the pebbles sink into the molten eutectic), a sufficiently high thermal conductivity to remove the decay heat to the container surface, a melting point temperature well below the unacceptable limit, and a boiling point above the unacceptable temperature limit. Several candidate eutectics exist that satisfy at least two of the above criteria, but only an aluminium-magnesium (Al-Mg) alloy (equally mixed) satisfies all the conditions. It

has a density of  $\sim 2.7$  gm/cc (well below the pebble density), melting point ( $\sim 450^\circ\text{C}$ ), a boiling point above  $2000^\circ\text{C}$ , and high conductivity ( $\sim 100$  W/m-K). Assuming that the initial pebble temperature contacting the surface of the eutectic is  $670^\circ\text{C}$ , and progressively higher temperatures, it was assumed that the process at the interface between the particles and the solid eutectic is similar to that of ablation, in that the melt phase is removed from the surface as it forms. In the ablation case this process is clear, and in the current case the molten material is assumed to infiltrates into the spaces between the pebbles behind the layer in contact with the solid eutectic. Thus fresh eutectic is continually melted and flows up into the pebble bed. The molten eutectic is the primary heat removal medium to the container walls. It can be shown that the rate of melt front progression is proportional to the heat flux, and inversely proportional to the density, heat of fusion, and the heat required to raise the solid eutectic to the melt temperature. Preliminary estimates of the melt front progresses at  $1.0$  mm/s –  $2.5$  mm/s, depending on assumptions made regarding the initial eutectic temperature, and the heat flux [12]. At this rate a column of pebbles  $50$  cm high would sink into the eutectic in  $\sim 500$  s or less. This value is well within the time limit discussed above, and should ensure that it is possible to cover the pebbles with an appropriate molten eutectic before the unacceptably high temperatures are reached. Assuming that the columns are  $50$  cm high and have a radius of  $20$  cm, it would be necessary to divide the initial core volume into  $96$  cylindrical containers. These containers are arranged in a hexagonal lattice with a pitch of  $45$  cm. The containers are made of borated stainless steel with a wall thickness of  $0.5$  cm. The spaces between the containers are assumed to be filled with light water, which is assumed to be boiling in the steady state long-term heat removal phase. Thus boron was added to the stainless steel wall to de-couple the water from the fissile material in the pebbles [17]. The boron was assumed to be natural boron, and  $\sim 8000$  ppm are necessary to ensure that the multiplication factor is below the target value of  $0.95$ . Finally, assuming that the heat transfer at the container surface is by boiling then the maximum center line temperature of the pebble-eutectic mixture is  $\sim 800^\circ\text{C}$ , and the inner surface temperature of the container is  $\sim 350^\circ\text{C}$ . This is a modest operating temperature for stainless steel, and it should be able to withstand any imposed mechanical and pressure induced loads. These total fuel material selection is done, to



force the heat transfer under the forced turbulence conditions and proper steam flow occurs inside the reactor.

### 3.5 Conduction/Radiation Cool Down To Boundary And Thermal Inertia

The major design parameter for accommodating decay heat passively for all three fuel types is core fuel power density. Certainly major fuel power de rating from the traditional GCFR values. This is still a major reduction from the historical range. With core fuel power density of 70-100 w/c<sup>3</sup>, the thermal gas reactor “conduction cool down” mode of passive heat transfer of core generated heat through conduction and/or radiation inter and intra fuel elements to the vessel boundary is not possible for the GFR. This is regard less of fuel form, Block or plate, pin or pebble. With the limited conductivity of the potential core fuel and structural materials, even 1 to 2% decay heat would lead to core disruption conditions. With the high temperature requirements of the Gen IV GFR (~850, coolant outlet) and the fuel flux/fluence conditions the set of potential materials is small [35]. However, even if graphite with its neutron spectrum softening disadvantage, utilized in the thermal gas reactor cores was used, success would not be attained. The crux of the matter is the low (~ 5w/cc) power density of the thermal gas reactor. To lower the density of the fuel by adding diluents, equation (27) shows that it could lower the power density and still retain the high specific power requirements. This would also be attractive from the viewpoint of adding thermal inertia. However a fast reactor core requires significantly higher fuel densities/loading to maintain criticality over a high burnup fuel cycle (~ 30% volume function of 10 gm/cc ceramic fuel with 20% fissile). Moreover the thermal properties of potential diluents are in the same range of the fuel. Adding diluents is not a potential solution for the GFR given the state of future core material development work. Adding thermal inertia to absorb decay power in sensible heat until ~0.1% decay power is reached, is not feasible.

$$\eta = \frac{P}{kl\Delta T} = f\left(\frac{D}{l}\right) \quad (27)$$

But conduction alone is not the sole mechanism for transporting core decay heat to the wall boundary through the fuel elements. For fuel forms such as the pin or the

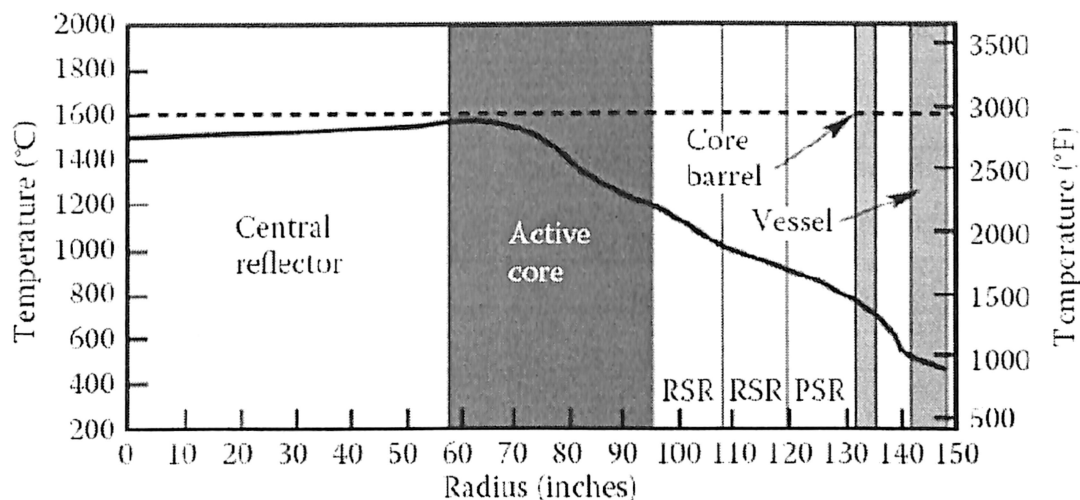
pebble, as opposed to monolithic blocks, radiation heat transfer is a major component of the fuel element-to-fuel element heat transfer. To compare the relative effectiveness of conductivity relative to radiation in transferring heat from fuel element to fuel element to the vessel wall boundary.

**TABLE 3.3 THERMAL PROPERTIES OF PEBBLE MATERIAL**

<b>Material</b>	<b>Thermal Conductivity (1000 °C) W/m-K</b>	<b>Density, Kg/m<sup>3</sup> ρ</b>	<b>Specific heat capacity (1500 °C) J/kg-K (C<sub>p</sub>)</b>	<b>Product of ρ × C<sub>p</sub> J/m<sup>3</sup>-k x 10<sup>-6</sup></b>	<b>Melting point/ Dissociation Temperature, °C</b>
Silicon Carbide	35.7	3160	1336	4.22	2000
Titanium Nitride	22	6400	595	3.18	3230
Zirconium Carbide	22	6510	250	1.63	3530
Uranium Oxide	3.6/3.2	10960/9660	339	3.72/3.27	2730
Uranium Carbide	20/17.5	136030/12970	272	3.71/3.53	2400
Uranium Nitride	24.6	14320/13510	272	3.90/3.97	2600
Graphite	30	1700	2000	3.4	3650

The Tables 3.3 and Figures 3.7 show the temperature rise from the boundary to the pin for a solid opaque cylinder (conduction) and for a transparent material with zero conductivity (radiation). Clearly materials with the conductivity of copper are far superior, but even with the conductivity of steel it is not until the temperature range is between 1000 - 1200 °C that radiation heat transfer becomes better than conduction heat transfer. Furthermore, in the case of radiation heat transfer, the central fuel pins are shadowed from the vessel wall boundary by many other rows of fuel pins. It can be seen that ten rows of pins with the corresponding radiation interfaces is very challenging for radiative heat transfer. Even if the hex assemblies were made of solid block fuel there would still be radiation interfaces due to the clearances gaps between the blocks

designed for refuelling This translates to 13 rows of 469 block-type fuel assemblies radiating heat through the gaps between the blocks made with infinite conductivity material to the vessel, which is held at 316°C. This shows that even with perfectly conducting block fuel, the fuel clearance gaps will make it very difficult to conduct/radiate decay heat through the fuel elements to the vessel wall boundary without damaging the fuel.



(Source: Nuclear Engineering Hand Book, Kenneth D. Kok)

Figure 3.7 GT-MHR Radial Temperature Gradient During After-Heat Rejection maximum

As discussed previously, the possibility exists to absorb excess decay heat by increasing the core thermal inertia, stretch out the time scale and reach a lower decay heat level before the conduction cool down phase with boundary heat losses is required. Table 3.3 shows the thermal properties of candidate GFR core material being considered. It can be seen that the volumetric heat capacity, which is important to the thermal criteria, is largely in the range of 3-4 j/m<sup>3</sup>-K. While there are variations, there is no quantum improvement [32]. However, even in the case of the thermal conductivity the value is principally in the range 20-30 w/m<sup>2</sup>°K, with the exception of uranium oxide fuel, replacing fuel with matrix material can lead to improvements but it is not a quantum one. Table 3.4 shows the results for a series of one-dimensional transient conduction calculations performed for the one-dimensional slice through a reactor. The pebble design is a two region pebble when the inner region is an unfueled region. This decreases the temperature peaking in the pebble and leads to the Possibility of using

different thermal inertia material in the center of the pebble and perhaps also taking credit for the latent heat of the inner region [28]. For the results presented in Table 3.4, both inner and outer region material utilizes the properties of steel. Furthermore, in another effort to boost heat capacity, a number of the calculation in Table 3.5 is for an annular core design where the central core region is filled with unfueled pebbles. This once again is an effort to increase the thermal inertia. The reactor vessel boundary condition is both radiation and convection to an environment at 149°C (300°F).

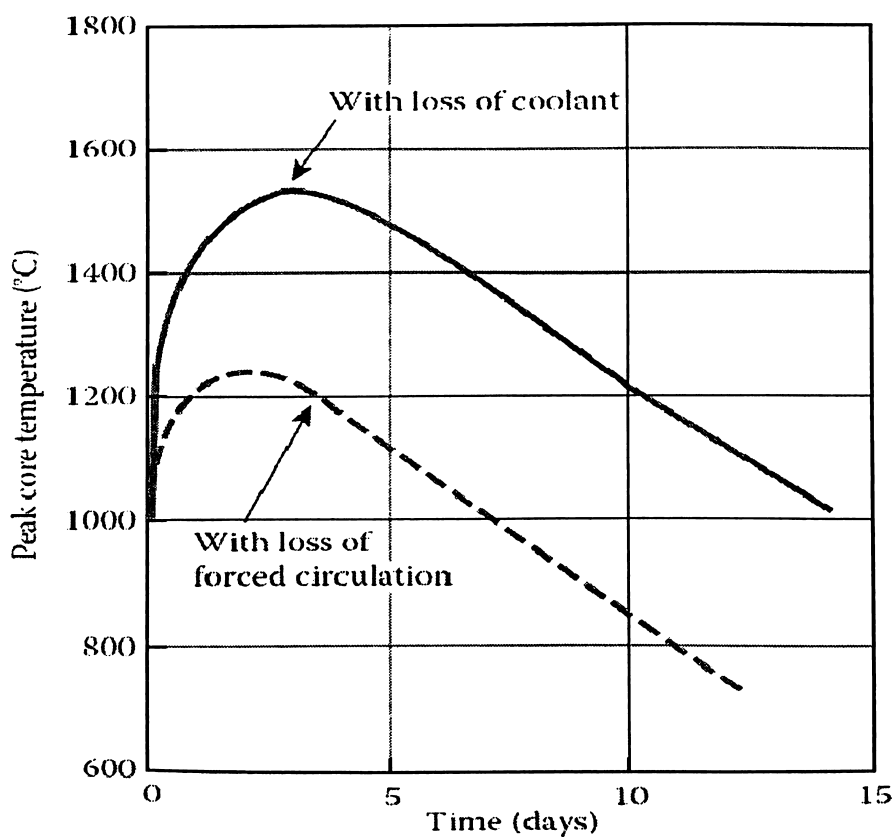
**TABLE 3.4 VESSEL CONDUCTION DECAY HEAT REMOVAL**

Pebble Type	Core Maximum Temperature, C	Vessel Maximum Temperature, °C
Steel with Latent Heat	1575	521
Steel Without Latent Heat	1628	532
Silicon Carbide	1661	540
Zirconium Carbide	1774	564
Tungsten	1682	561

### 3.5.1 Core Heat Sinks

Inertia is insufficient and for the passive heat transfer option to be successful, there is the possibility of heat sinks internal to the core. Fuel forms would make a difference here. Pin-based and plate-based cores can be ruled out, as there are too many radiation interfaces. Block cores would be the optimum if no inter block gaps was required. However for defueling this is not an option so pebble bed cores can be equally considered from the viewpoint of heat transfer. Furthermore transport of the decay heat from the heat pipe to the ultimate heat sink requires another fluid transport system, whereas for the cold finger a pressurized all-CO<sub>2</sub> system has been proposed. But with both concepts, refuelling for the block core has to be bottom entry. For a passive system the heated coolant in the heat pipes and the cold fingers rise to the top of the reactor core [25]. All the piping connections are made at the top, which makes top refuelling for the block-based core very challenging. However this is not the case for the pebble bed core. Conceptually the pebble can be rolled in from the top of the reactor in to the lattice of

heat pipes/cold fingers. Moreover, the short term decay heat transient from ~6% to 3% power may require additional passive heat removal systems. . If these phenomena are insufficient there may be the need for accumulators, which then leads to the discussion later on the balance between active and passive systems. Core control rods have to be provided cooling regardless of design, so the concept encloses the control rod with its thimble in a separate pressure tube housing isolated from the main primary system core coolant flow.



(Source: Nuclear Engineering Hand Book, Kenneth D. Kok)

**Figure 3.8** GT-MHR Coolant Flow Variation In Reactor Core

Within the pressure tube there is an insulator tube that surrounds the thimble and provides the means for the control rod coolant flow with a  $U_{turn}$  at the bottom. The redirected upward flow then cools the pressure tube from the inside [28]. During the accident sequence the core decay heat would be conducted/radiated through the fuel elements towards the internal core heat sinks, the cold fingers, instead of only toward

the vessel wall boundary. By design, the cold fingers would be inserted at the traditional control rod locations and connected to a natural convection pressurized CO<sub>2</sub> system. The ultimate heat sink would ultimately have to be a fully passive dry cooling power for example. Table 3.4 shows design results for two types of pebble design, a 50/50 metallic pebble and a solid graphite pebble. The metallic designation is merely to indicate that the thermal properties used are largely typical of metals whereas the solid graphite pebble, which has no unfueled region, has thermal properties typical of graphite and the family of silicon carbides.

**TABLE 3.4 FULE PEBBLES DESIGN PARAMETERS FOR HELIUM COOLED REACTORS**

<b>Parameter</b>	<b>Fissile Particle</b>	<b>Fertile Particle</b>
Composition	UC <sub>0.5</sub> O <sub>1.5</sub>	UC <sub>0.5</sub> O <sub>1.5</sub>
Uranium enrichment, %	19.8	0.7 (Natural Uranium)
<b>Dimensions (μm)</b>		
Kernel diameter	350	500
Buffer thickness	100	65
IPyC thickness	35	35
SiC thickness	35	35
OPyC thickness	40	40
Particle diameter	770	850
<b>Material Densities (g/cm<sup>3</sup>)</b>		
Kernel	10.5	10.5
Buffer	1.0	1.0
IPyC	1.87	1.87
SiC	3.2	3.2
OPyC	1.83	1.83
<b>Elemental Content Per Particle (μg)</b>		
Carbon	305.7	379.9
Oxygen	25.7	61.6
Silicon	104.5	133.2
Uranium	254.1	610.2
Total particle mass (μg)	690.0	1184.9
Design burn up (% FIMA) <sup>a</sup>	26	7

The thermal discharge (waste heat) from the GT-MHR is significantly less than the PWR plant because of its greater thermal efficiency. If this waste heat is discharged using conventional power plant water heat rejection systems, the GT-MHR requires <60% of the water coolant per unit of electricity produced. Alternatively, because of its significantly lesser waste heat, the GT-MHR waste heat can be rejected directly to the atmosphere using air-cooled heat rejection systems such that no water coolant resources are needed. Because of this capability, the use of the GT-MHR in arid regions is possible [18]. The GT-MHR produces less heavy metal radioactive waste per unit energy produced because of the plant's high thermal efficiency and high fuel burn up. Similarly, The GT-MHR produces less total plutonium and Pu239 (materials of proliferation concern) per unit of energy produced. The deep-burn capability and high radionuclide containment integrity of TRISO particles offer potential for improvements in nuclear spent fuel management. A high degree of degradation of plutonium and other long-life fissile actinides can be achieved by the deep burn capability.

### **3.5.2 Reactor Control**

In the pebble bed reactor core, there are usually two reactivity control systems. The control rod system and the small absorber ball system, the control rod system consists of several control rods and the same number of drive mechanisms. It is usually utilized as the power regulating and control system and the first shutdown system as well. The control rod drive mechanism inserts the control rod into the side reflector and removes it out. For a large pebble bed reactor, the control rods can, in principle, be inserted into the reactor core. However, the disadvantages are that the rod insertion will interfere with the pebble fuel elements and may damage them [4]. The small absorber ball system is the second shutdown system. If emergency shutdown is required and the control rod system cannot be assured to work, boronated (boron carbide) balls are dropped by gravity into side channels to shut down the system. In order to restart the system, the small absorber ball system provides means to remove the absorber balls from the channels and to put them back into the ball storage vessels. In the indirect cycle design, the circulator provides the pressure head for the helium to overcome the pressure losses through primary system. The mass flow rate in the primary system is proportional

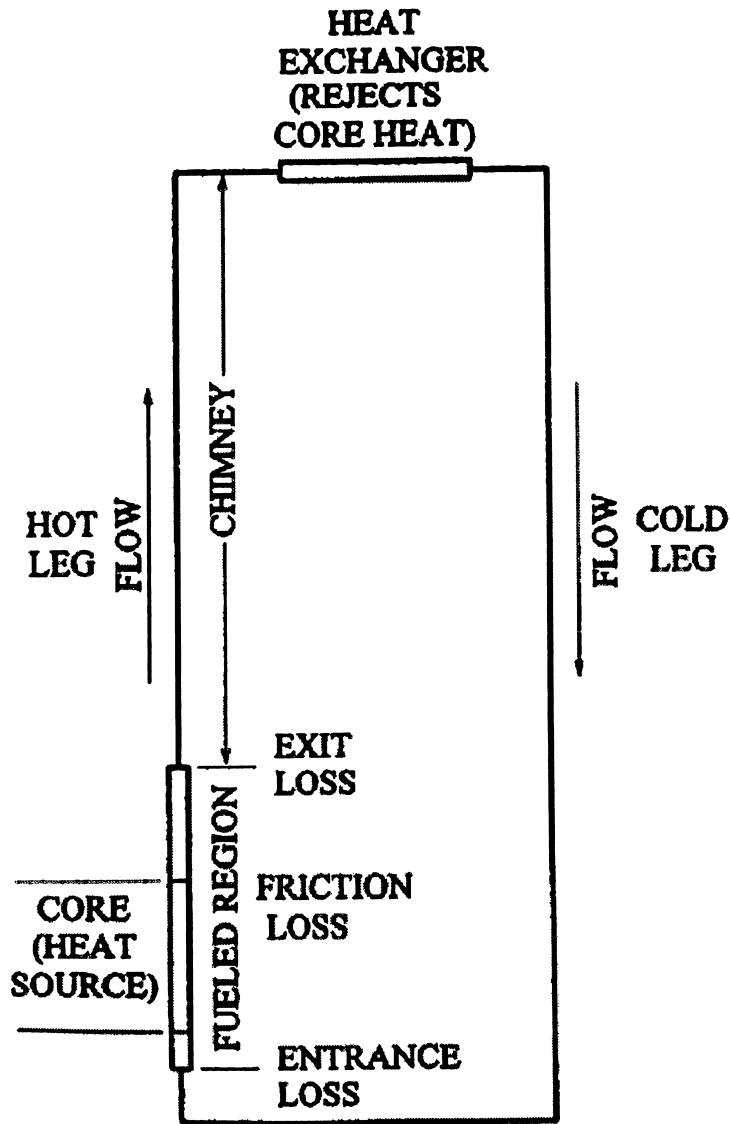
to the circulator speed. If the circulator speed is adjusted, the mass flow rate is changed correspondingly. Therefore, the mass flow rate in the primary system can be manipulated by adjusting the circulator speed. In the AVR and THTR, mass flow control in the primary system was achieved by varying the circulator speed [1].

### **3.5.3 Natural Convection**

Conduction and radiation aside, the third possible heat transfer mode is convection which in the passive form is natural convection. It has historically been known that gas coolant provides a poor heat transfer medium with low thermal inertia at low pressure ~ 1 atmosphere, but historically it has been shown by design calculation that even for the historical high power density cores (~250w/cc) natural convection can successfully remove core decay heat at pressurized conditions (70 bar) for acceptable primary system elevation differences. Even the short-term decay transient from 6% - 3% power can be accommodated. The pebble-bed fuel form would be the most challenging form for this option. Pebble beds have inherently high resistance to core flow, which are difficult to overcome through design. It is best to focus on block/plate and pin cores for the natural convection option [10]. For this option to work, a guard confinement or double containment/vessel would be required. The approach is to only permit depressurization of the primary system through design means for a secondary backup pressure. The choice of the backup pressure is a major design choice. The lower the pressure the worse the natural convection heat removal capability but the less challenging the design and construction issues for the guard containment. The current optimum choice would be a block core design with a guard containment sized for 20 bar accident pressure. Show the effects of primary system coolant choice, core outlet temperatures and decay power level on the primary coolant pressure required to maintain the steady state core heat removal capability. The block coolant channel sizes have been optimized for fabrication specifications. Any larger coolant volume fractions would probably lead to a plate-type core instead of a block-type core. As with the block core it has been optimized for both the 100% steady conditions and the natural convection accident conditions. The resulting guard containment pressure required for the natural convection removal of the



decay heat is quite comparable between the two core designs [9]. The natural convection loop is shown in the figure 3.9, on the top due to less density heat rejection takes place. The clod lag is from the down loop on the other side of the reactor core.



(Source: Nuclear Engineering Hand Book, Kenneth D. Kok)

Figure 3.9 Natural Convection Loop In Side The Reactor

## CHAPTER 4

### CFD ANALYSIS OF HEAT TRANSFER IN THE NUCLEAR CORE

Nuclear reactor concepts based on helium cooling with fine uranium fuel pellets have attracted considerable attention over the years. Reasons behind this interest lie in their excellent heat transfer capabilities. The latter unifies the temperature of the pebbles, and increases the active surface area from which heat transfer occurs. In addition, the constant mixing of the pebble potentially leads to a uniform burn up of the uranium particles. A self-controlling feature is also present in that as the pebbles are fluidized and the gas flow increases the power achieves a maximum at a particular structure height. At this height, the power will be that at which heat production is balanced by heat losses. The primary energy source for a nuclear reactor is the core. To model the energy generation in the core, volumetric heat sources are placed into appropriate heat structures [10]. Heat structures represent the selected, solid portions of the thermal-hydrodynamic system. Being solid, there is no flow, but the total system response depends on heat transferred between the structures and the fluid, and the temperature distributions in the structures are often important requirements of the simulation.

#### 4.1 Initial and Boundary Conditions

The initial conditions are a set of the dependent variables of the problem. The hydrodynamic model requires four thermodynamic state variables in each volume and the velocities at each junction. Heat structures require the initial temperature at each node, control systems require the initial value of all control variables, and kinetics calculations require initial power and reactivity. Boundary conditions may be required for hydrodynamic models, heat structures, or control components if these parameters are governed by conditions outside of the problem boundaries [12]. The hydrodynamic boundaries of a system are usually modeled using time-dependent volumes and junctions. Examples of these could be mass and energy inflows or an externally

specified control parameter. Obtaining a desired simulation is very dependent upon proper specification of initial and boundary conditions.

#### **4.1.1 Steady-State Initialization**

The fundamental concept of steady-state is that the state of a reactor system being modeled does not change with respect to time. In the hydrodynamic solution scheme, three terms can be monitored whose variation in time include the variation of all of the other terms [2]. These three terms are the thermodynamic density, internal energy, and pressure. Furthermore, these three terms can be combined into a single-term, enthalpy. Hence, monitoring the time variation of enthalpy is equivalent to monitoring the time variation of all of the other variables in the solution scheme [5]. The method used to solve the transient hydrodynamic, kinetics, and control system algorithms and a modified heat structure thermal transient algorithm to converge to a steady-state. The differences between the steady-state and transient options are that a lowered heat structure thermal inertia is used to accelerate the response of the thermal transient, and a testing scheme is used to check if steady-state has been achieved. Also, in case of steady-state calculations, the desired core power and other initial conditions are specified through the input table without kinetics package activation [43]. When steady-state is achieved, the run is terminated, thus saving computer time. The results of the steady-state calculation are saved so that a restart can be made in the transient mode. In this case, all initial conditions for the transient are supplied from the steady-state calculation.

#### **4.2 Fuel Elements Arrangement in a Core**

In standard water cooled reactors, it is customary to use fuel rods and then to circulate the water around these fuel rods to cool them down and to exchange the heat into a usable work. Hence, a more heterogeneous reactor design is used causing a lot of safety and design concerns to take place within the reactor. However, when helium is used as a coolant, you are not bounded by these constraints and you can use a more homogeneous design in the reactor core.

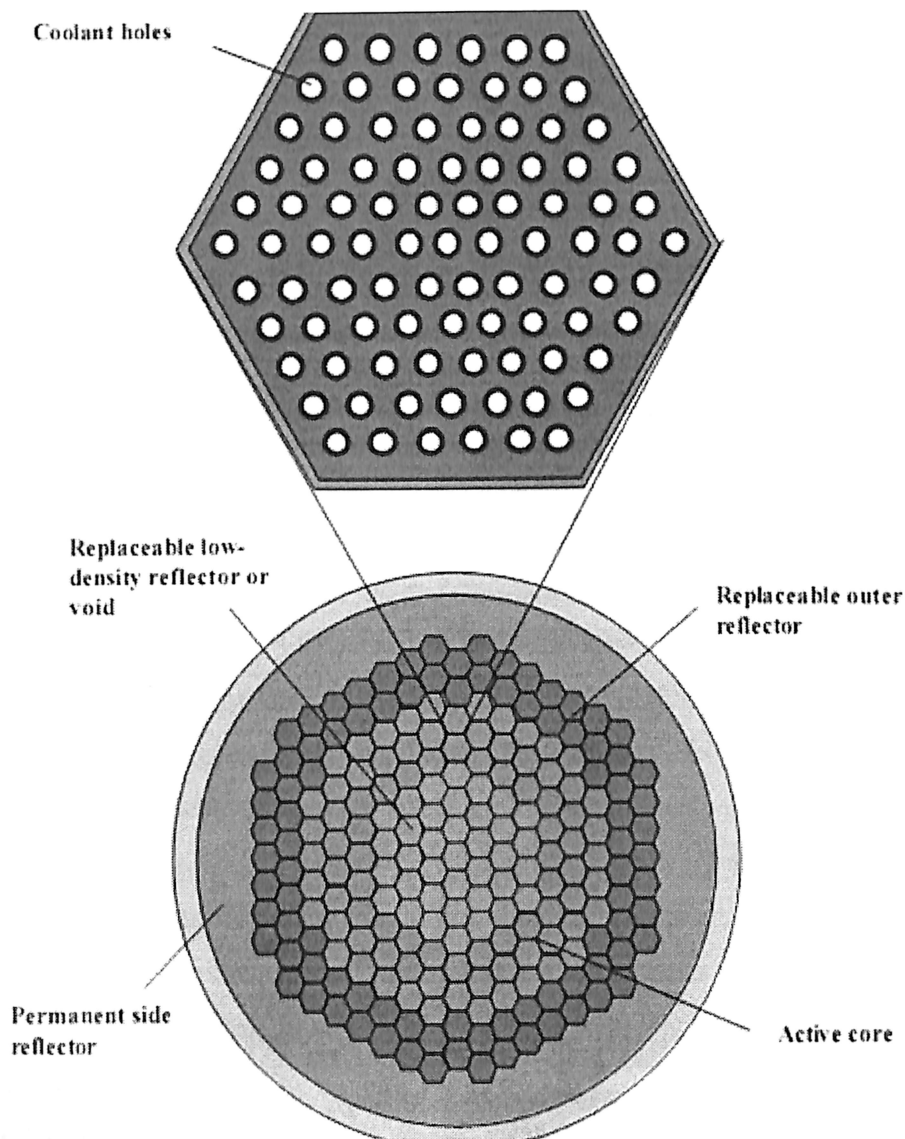
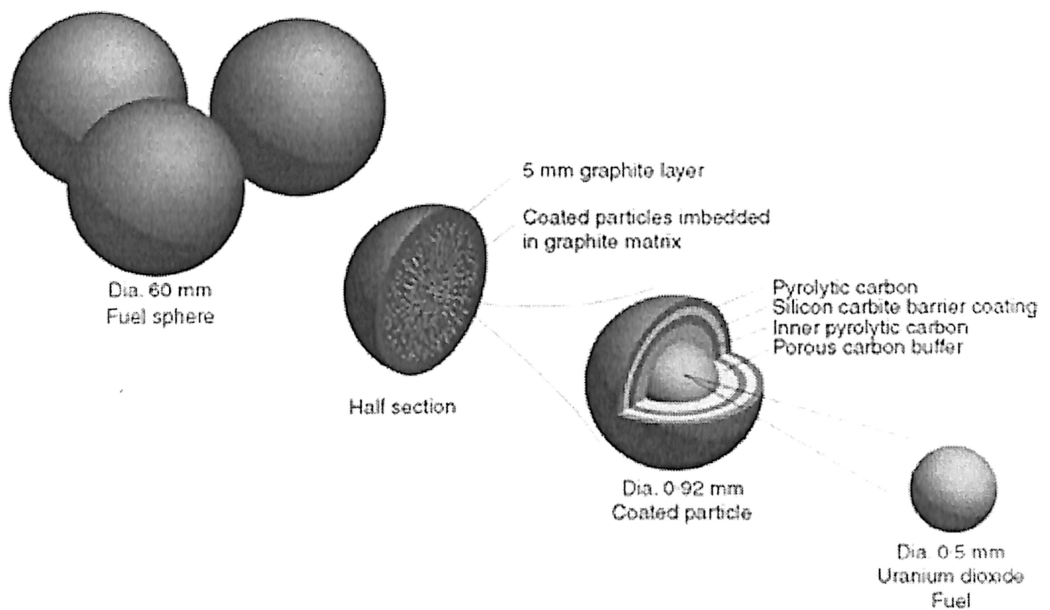


**Figure 4.1** Fuel Pebbles Arrangement In Side The Nucler Core

When dealing with helium as a coolant, it is essential to choose a proper geometric configuration that allows for maximum efficiency in the convection and conduction process. The convective heat transfer coefficient of helium is already high, but with a more conductive fuel element, this can be greatly enhanced. In addition, the geometry of the fuel elements must be conducive to turbulent flow that may occur around the fuel elements as the coolant passes through them the arrangement is shown in figure 4.1.



(Source: Pebble bed modular reactor, the first Generation IV reactor to be constructed, S.Ion)

**Figure 4.2** Fuel Pebbel Structure

There are two types of fuel elements possible for helium cooled reactors. Either prismatic modular fuel elements or spherical fuel elements can be used with ease in a HCNR. One of the best designs in terms of simplicity and efficiency is definitely spherical fuel elements, shown in the figure 4.2. From a purely geometric point of view, these types of elements allow for maximum absorption of heat when a gas is passed through them as a coolant. Hence, their shape allows for a higher thermodynamic efficiency and criticality can be achieved by piling them on top of each other using a geometrically unique shape. The coolant is allowed to pass through them radially, as the helium is fed through the outer lateral surface of the reactor core. At the same time, the spherical shape of the fuel elements allow the heated helium to be removed from the inner perforated wall of the nuclear reactor [22]. Due to the geometric nature described above, spherical fuel elements will need to incorporate the nuclear fissile material itself as well as the moderator and even the reflector to some extent in it. Moderator is usually graphite. The main part of the fuel element has miniature microspheres or microelements containing uranium oxide ( $U^{235}$ ) as the fissile fuel. Hence, fuels are in the form of TRISO particles and the diameter of the fuel pellets are about a millimeter. Here, the fuel particles are enriched around 15 to 20 percent of  $U^{235}$ . The encasing can be ceramic in nature or carbides can also be used. Recent data suggests that usage of

ceramic fuel elements may be more efficient as compared to carbides and other forms. As a moderator<sup>2</sup>, pyrolytic graphite is used. The best design characteristics suggest that the fissile material needs to be placed in the middle and then covered with pyrolytic graphite<sup>2</sup> and then encased in composite ceramic elements such as SiC [13]. The overall size of the spherical fuel element can be compared to a billiard ball or to a tennis ball. These single fuel elements can have a diameter ranging from 15 mm to 60 mm with corresponding heat transfer characteristics. In this study, the optimal single fuel element diameter is found to be 20 mm. Uranium oxide concentration in the fuel elements is recommended as 10.8 g/cm<sup>3</sup> in this analysis.

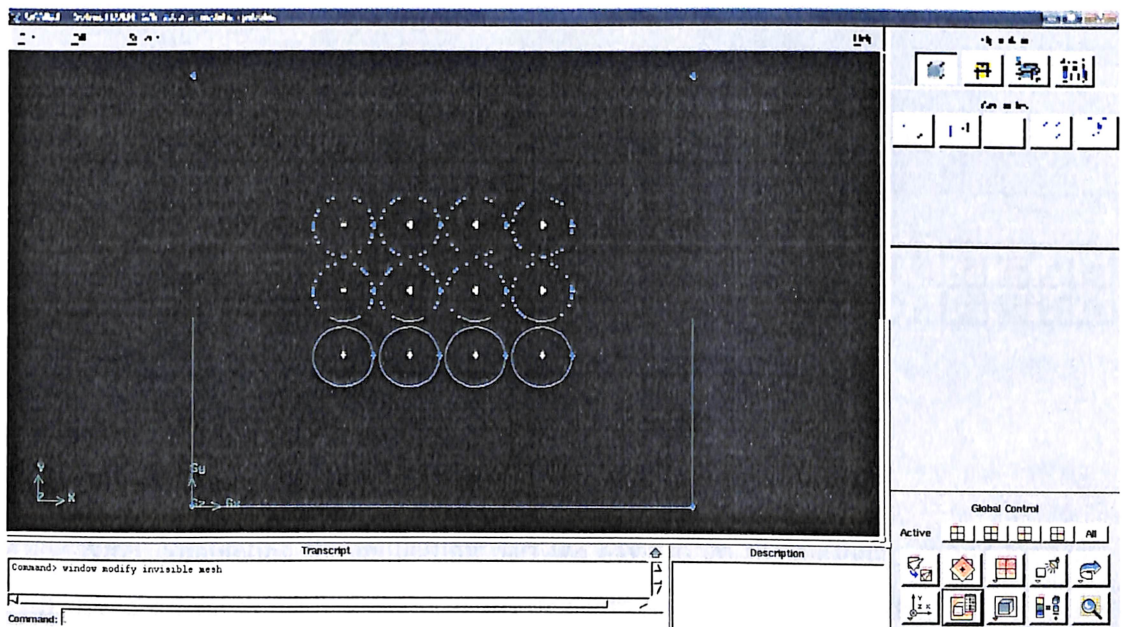


**Figure 4.3** 2D Modelling Of Fuel Pebbles In GAMBIT.

In a gambit model Initially it is scaled for the operating window and then creation of vertex will be done with help of coordinates, visible in the figure 4.3 . All the vertex are located for the out casing and fuel pebbles inside the boundaries. With the help of vertex edges will be created according to the selection of vertex. For creating the fuel pebbles inside the reactor a pebbles is created with a rifference vertex upon which a edge is created then it is moved to the all the specified positions inside the core. Once all the edges are created then creation of faces will be done with help of specified edges in a

operations window. For creating the faces for all the fuel pebbles we have to select the center and two more reference points on the circumference. After repeating the same procedure for all the 12 pebbles we have to subtract the faces from the core, retaining the fuel pebbles needs to be done.

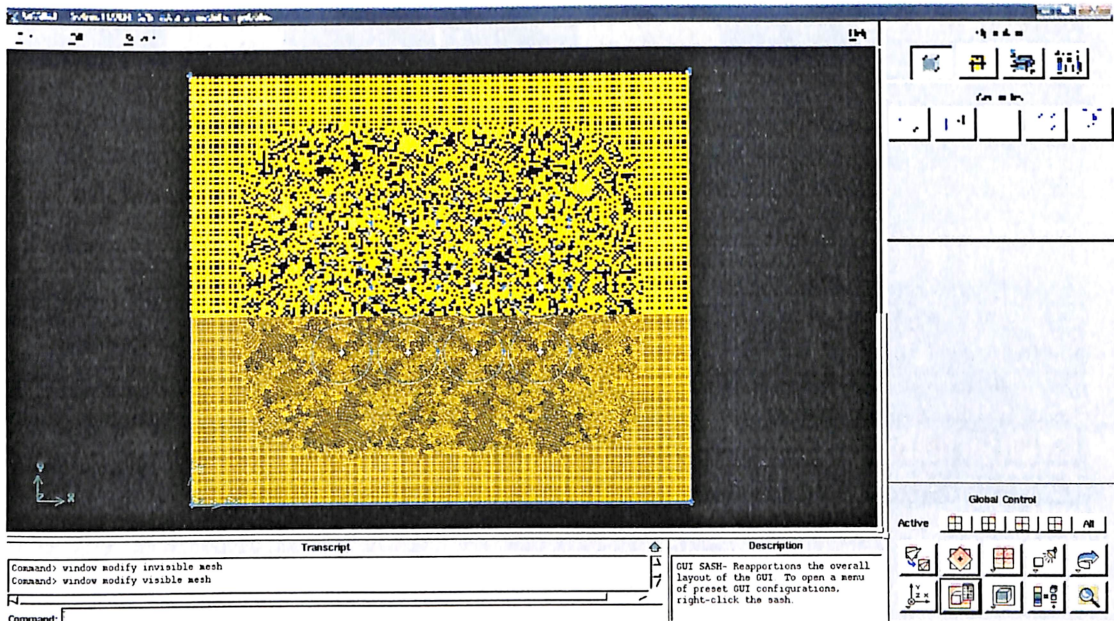
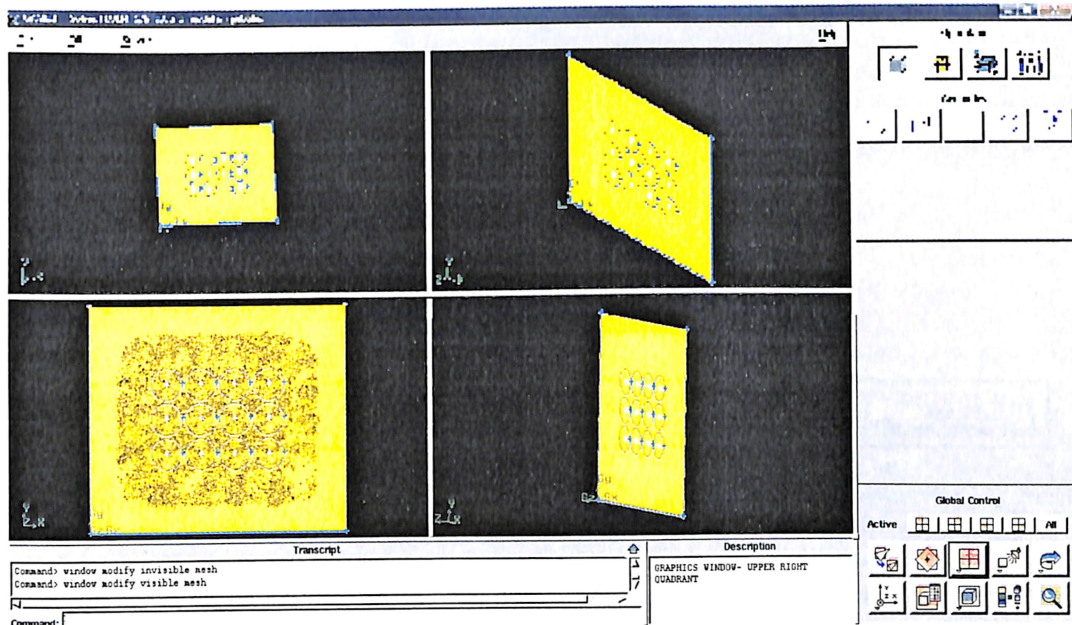


Figure 4.4 Mesh Generation On 2D Model

After completing the modelling part we have to go for meshing. In meshing we will use quad mesh with finer structure for the better analysis results. Since we are considering the core as a rectangle and pebbles are considered as a flow obstacles inside the reactor. The model is designed from the core of the reactor pebble arrangement and inside the core at the center crust is under consideration. Each fuel pebble is of size 20 mm diameter, the far field is modelled twice the distance that maintained in the two pebbles and in between the fuel pebbles 2 mm of distance is maintained. The meshing is shown in the figure 4.4 clearly. The fuel pebbles are considered for the pave meshing since these are in circular shape, to understand more accurate deflections in the model simulation an initial step is done for face edge meshing and then it will be converted into

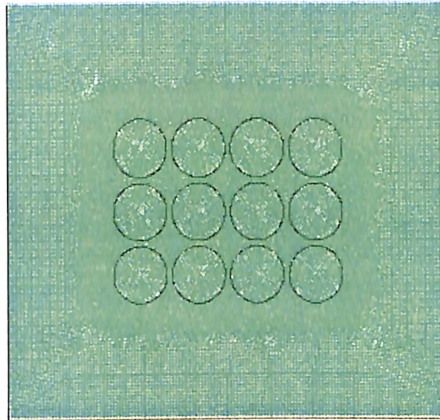
face mesh with a default value of size function. The pebbles meshing from all the directions are shown in the figure 4.5.



**Figure 4.5** Mesh Generation On Fuel Pebbles

Once the meshing is successful with all the trails, specifying the boundary conditions are done in the gambit. The upper edge is defined as a velocity inlet and the bottom edge is defined as a pressure outlet. The other two edges are defined as a walls, fuel pebbles are defined as a walls and treated as a obstruction and will be defined as a heat source in fluent. Once all the steps are successful then these things will be imported in the form of msh file and saved with the specified name. The msh file can be uploaded to fluent, since the solver selected is fluent 5/6. The fluent window shows the menu bar, from the menu bar select the case and read the msh file and check for the model and display the grid. The displayed grid for the model which is solved in the project is displayed below in the figure 4.5. If the model is not prepared properly then while checking the model in fluent it will show the errors then we need to re model or if instructions are clear then we have to solve for the error rectification in the gambit. In grid display we have to look for all the zones that are specified in gambit are exactly matching are not, if it is then only model import is correct.





Grtd Apr 10, 2011  
FLUENT 6.3 (2d. dp. pbne. lam)

**Figure 4.6** Grid Displayed In Fluent 2D Model

Once the model import is successful we have to specify the boundary conditions inside the fluent interface. Since the strategy of CFD is to replace the continuous problem domain with a discrete domain using a grid. In the continuous domain, each flow variable is defined at every point in the domain. For this analysis all the boundary conditions applied are tabulated the Appendix D to I. In the discrete domain each flow variable is defined only at the grid points. In a CFD solution one would directly solve for the relevant flow variables only at the grid points. The governing partial differential equations and boundary conditions are defined in terms of the continuous variables. The discrete system is a large set of coupled, algebraic equations in the discrete variables. Setting up the discrete system and solving it involves a very large number of repetitive calculations a task with the fluent. The method of deriving the discrete equations using Taylor's series is called the truncation error, since the truncation error above is zero; this discrete equation is a first order accurate. This method is deriving the discrete equation using the Taylor's series expansion is called the finite difference method. This code is solved in fluent; this is solved under the finite volume method. The problem defines in fluent is useful to solve for the conservation of momentum and energy for the cells. Similarly, depending upon the solution it also can be solved for the 2D or 3D cells will be taken into consideration.

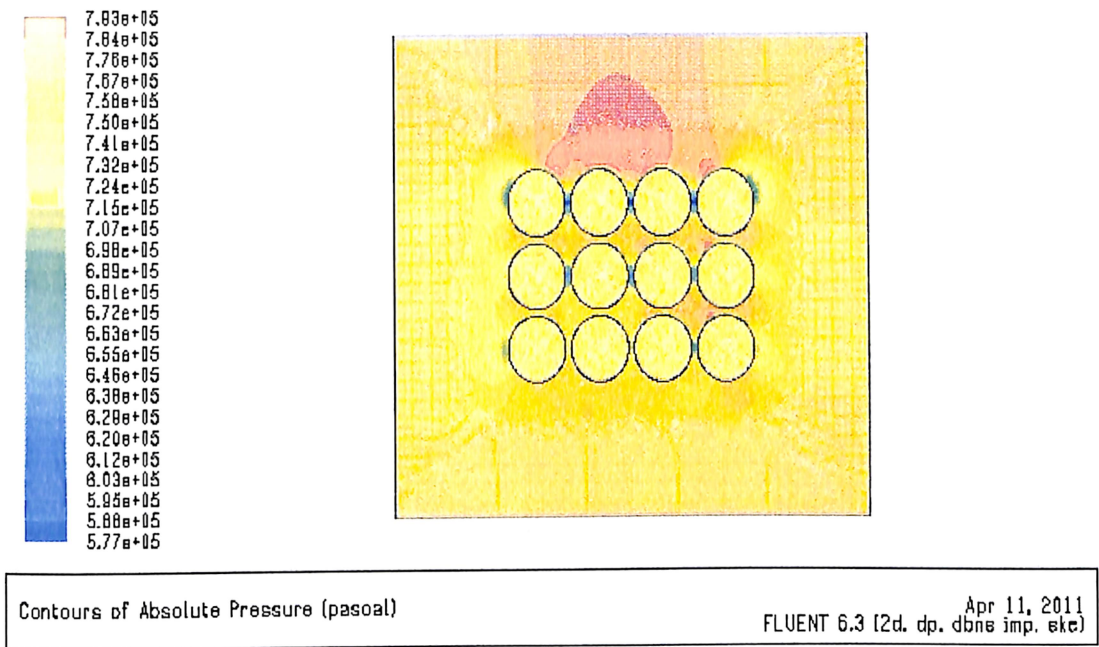
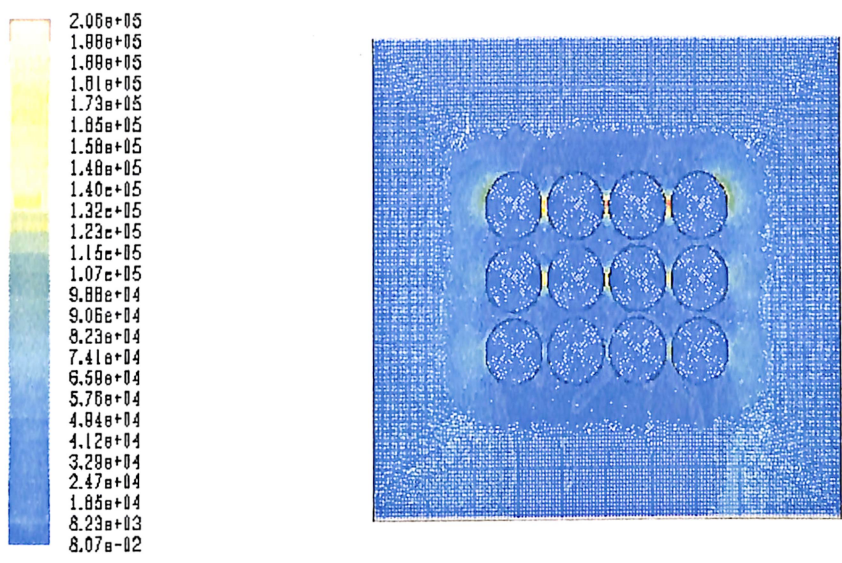


**Figure 4.7** Absolute Pressure Contours Of 2D Model

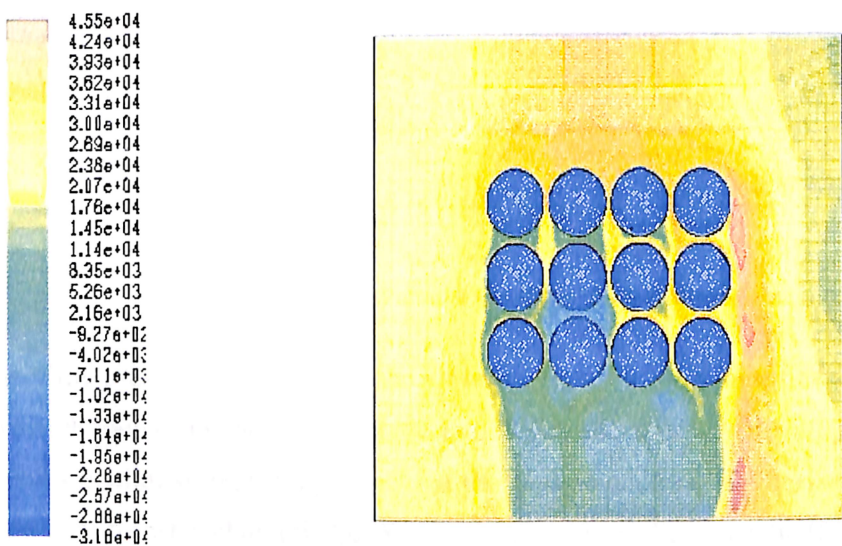
In the model used for sloving in fluent which is having an operating pressure of 7.42 Mpa, which is considered in the model due to which the pressure variations athat are showing in the figue 4.7 on absalute pressure contous are reaching the hight value of pressure at the first layer of the fuel pebbles since these pebbles are acting as a walls and also acting as aheat source so the temperature at the outer layer of the fuel pebbles is so high for this reation the pressure beteen the fuel pebbles the reasion shown in the red colour specifies the highest pressure regions in the model. The dynamic pressure contours are showun in the figure 4.8, the inlet of the coolent where velocity is high, the pressure at the inlet in the dynamic pressure countours is low. Due to the less gap between the fuel pebbles that is specified in the modelling as a 2 mm. Since the high velocity fluid hits the pebbles and converts the kinetic energy into pressure energy. Due to this reason in between the fuel pebbles the development of dyanamic pressure is taking place. In case of relative total pressure at the intial condition so fthe model is maintaing the safe pressure and due to which the pebbles act as a wall, and obstructs the flow. Due to this reasion revers flow takes place and the end of the pebble channel the development of the pressure we can see from the figure 4.9 below.



Contours of Dynamic Pressure (pasal)

Apr 11, 2011  
FLUENT 6.3 (2d. dp. dbne imp. etc)

Figure 4.8 Dynamic Pressure Contours of 2D modell



Contours of Relative Total Pressure (pasal)

Apr 11, 2011  
FLUENT 6.3 (2d. dp. dbne imp. etc)

Figure 4.9 Relative Total Pressure Inside the Reactor

The pressure effect on the flow can be described by the pressure coefficient contours, which is shown in the figure 4.10 below. The high velocity fluid which is having higher kinetic energy will be entered into the flow field and it will flow towards the pressure out let. Due to the walls as a pebbles it will diverts the flow direction as well as these fuel pebbles acting as a heat source due to which the reat portion is the highest pressure coefficient at the inet of the pebble system in the reactor core.

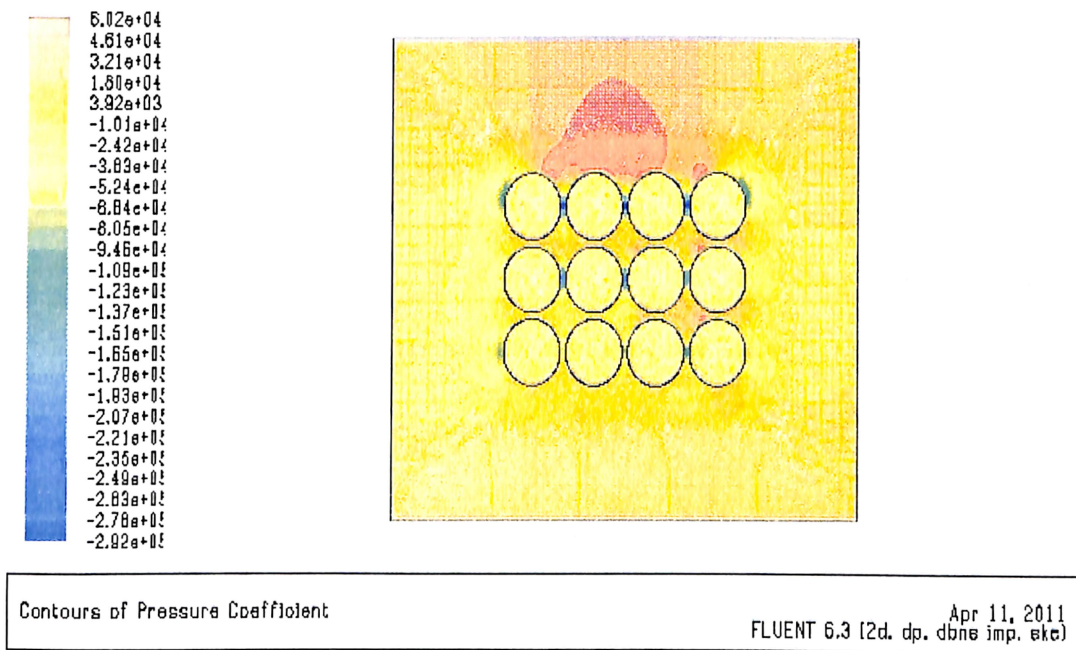
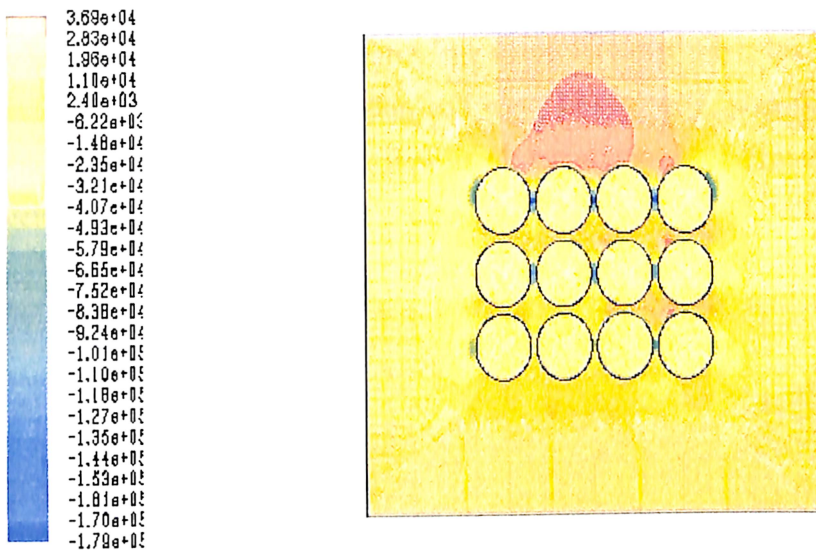


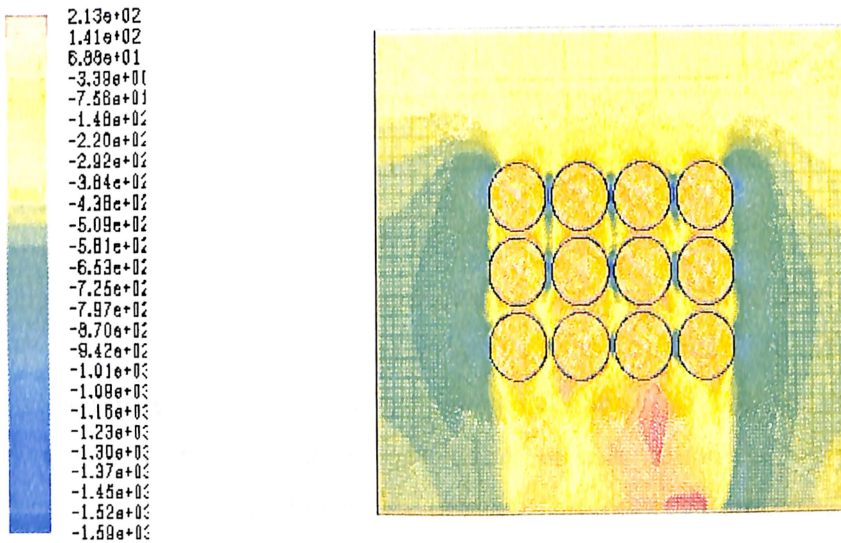
**Figure 4.10** Pressure Coefficient for a Pebbles system

The static pressure contours are shown in the figure 4.11, it signifies the same effect as a pressure coefficient, but under static conditions the pressure development between the pebbles is high so that it signifies that the flow is acquiring the desired turbulence and a good heat transfer characteristics we can expect from these results. If we look at relative velocity contours the flow is becoming more turbulence at the pressure out let, since the fluid entering the reactor is at higher pressure and it will be added a relative amount of heat to the fluid. Due to this more pressure in the out flow and also it is shown in the red portion in the out let of the reactor model. The pebbles also started deforming due to the flow velocity, high temperature.



Contours of Static Pressure (pasca) Apr 11, 2011  
FLUENT 6.3 (2d. dp. dbns imp. etc)

**Figure 4.11** Static Pressure in side the Reactor



Contours of Relative Y Velocity (m/s) Apr 11, 2011  
FLUENT 6.3 (2d. dp. dbns imp. etc)

**Figure 4.12** Relative Y Velocity In Side The Reactor

The contours of x define the flow conditions due to the higher value of velocity than the y direction contours. It describes from the figure 4.13 that due to the back flow the effect of velocity is more on x- direction and it is showing critical at the right edge of the pebble. The point at which the flow is diverging there the highest value of relative velocity i.e. shown in the scale is occurring.

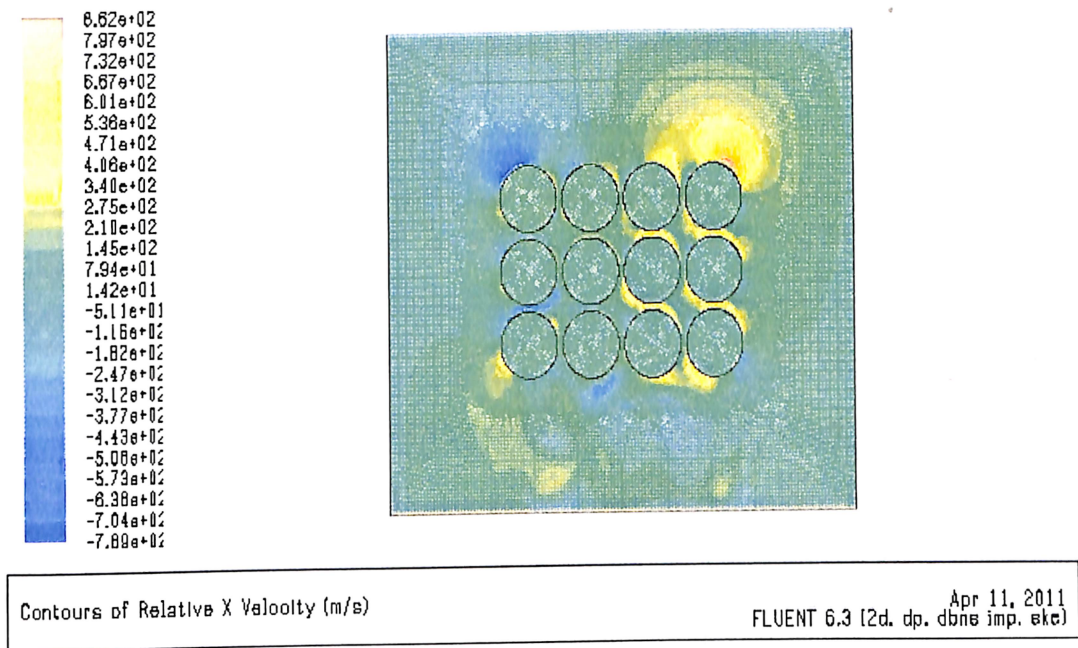
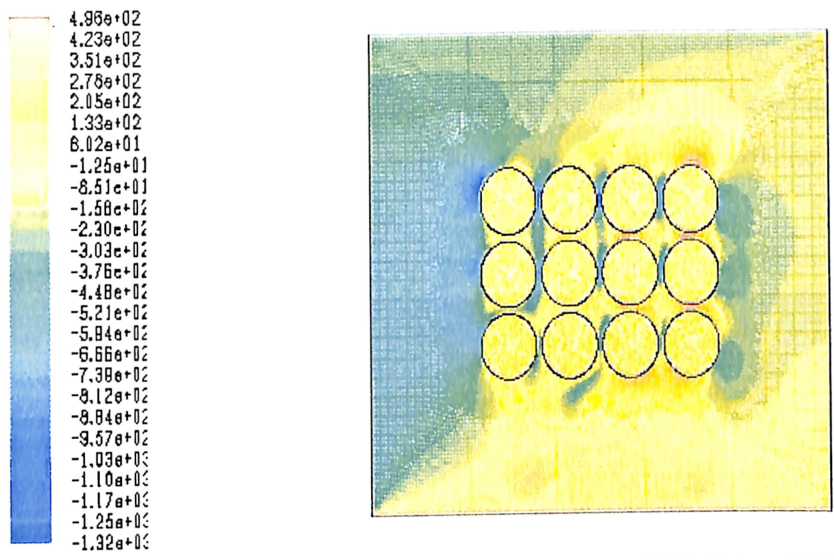


**Figure 4.13** Relative X Velocity In Side The Reactor

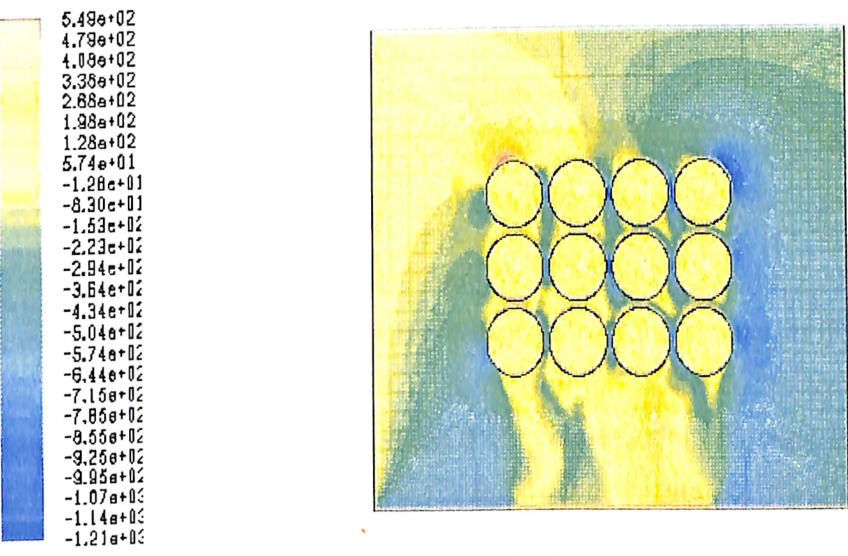
In the radial Velocity contours shown in the figure 4.14 specifies the flow direction after hitting the fuel pebbles. The flow reversail is occuring from left side of the model to the right side of the total fuel arrangement. Since these results are for the 2D model, the flow is not accurately visible in the radial direction. The trends shows that it is converging towards the accurate solution. In case of tangential velocity the flow is critical in the front just hitting the pebbles. The results of tangential velocity is visible form the figure 4.15. The maximum value point of view the tangential velocity is obtaining the value at 5.96 an were as the radial velocity poin of view it is bit low due to the stagnation at the flow reversial poin and crwating more wall shear stress between the fuel pebbles and the coolant.



Contours of Radial Velocity (m/s)

Apr 11, 2011  
FLUENT 6.3 (2d. dp. dbns imp. etc)

Figure 4.14 Radial Velocity Contours In Side The Reactor

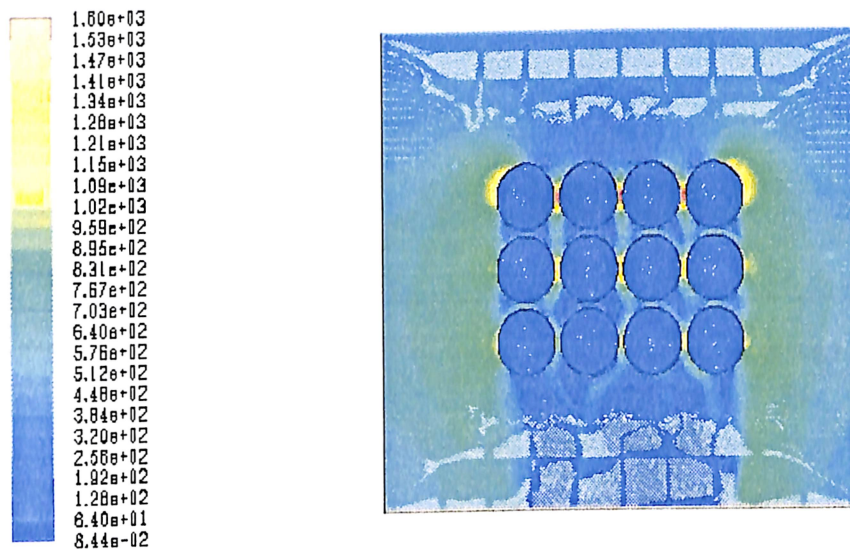


Contours of Tangential Velocity (m/s)

Apr 11, 2011  
FLUENT 6.3 (2d. dp. dbns imp. etc)

Figure 4.15 Tangential velocity Contours In Side The Reactor

Velocity vectors colored by the relative velocity magnitude shown in the figure 4.16 defines the flow field. Due to the condition at which the coolant enters the fuel pebbles the distance between the pebbles is low and the velocity of the coolant is high and due to high temperature the turbulence will be created and which will help in increasing the heat transfer to the coolant.



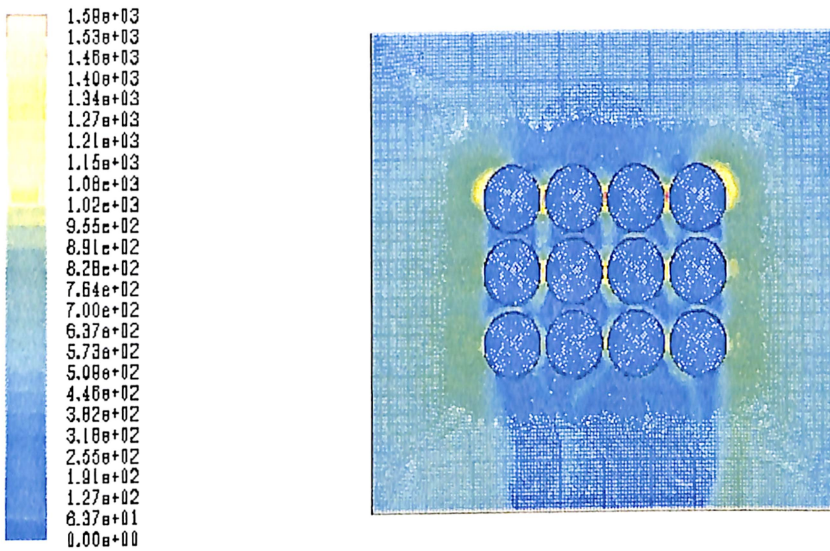
Velocity Vectors Colored By Relative Velocity Magnitude (m/s)

Apr 11, 2011  
FLUENT 6.3 (2d, dp, dbns imp, etc)

**Figure 4.16** Velocity Vectors colored by Relative Velocity Magnitude

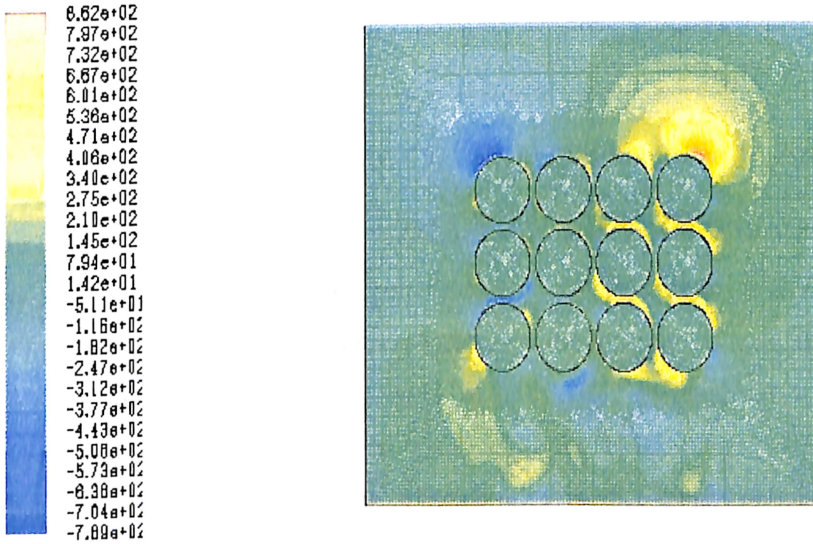
The relative velocity magnitude and the X-Velocity contour inside the reactor are shown in the figures 4.17 and 4.18. Which defines the change in it's relative velocity with respect to the fluid flow and to the transfer rate. X- velocity explains the change in magnitude in the flow from the inlet to the pressure outlet. The regions where the flow is maximum it indicates that flow is diverging and reaching to a super sonic level. For maximum benefit, the reactor geometry is taken as a cylinder. This way, the spherical fuel elements are placed on top of each other, while they are stacked in a radial fashion around the core. This allows for ample space for the helium to circulate around the fuel pebbles and the amount of wake crated in the downstream of the flow is minimized to some extent.





Contours of Relative Velocity Magnitude (m/s) Apr 11, 2011  
FLUENT 6.3 (2d. dp. dbns imp. etc)

**Figure 4.17** Relative velocity Magnitude



Contours of X Velocity (m/s) Apr 11, 2011  
FLUENT 6.3 (2d. dp. dbns imp. etc)

**Figure 4.18** X- Velocity Contours In Side The Reactor

The Y velocity specifies the sudden increase in velocity at the outlet due to the turbulence that was created in the model and which is causing a pull in the flow. The heat transfer capabilities will be increased because the time at which generated heat is carries away from the source will be the interst of doing this work. In figure 4.19 shows that it will be entering at higher velocities which is due to the flow rate provided at 320 m/s. The range in Y velocity transulation is from  $-1.59 \times 10^2$  to  $2.13 \times 10^2$ .

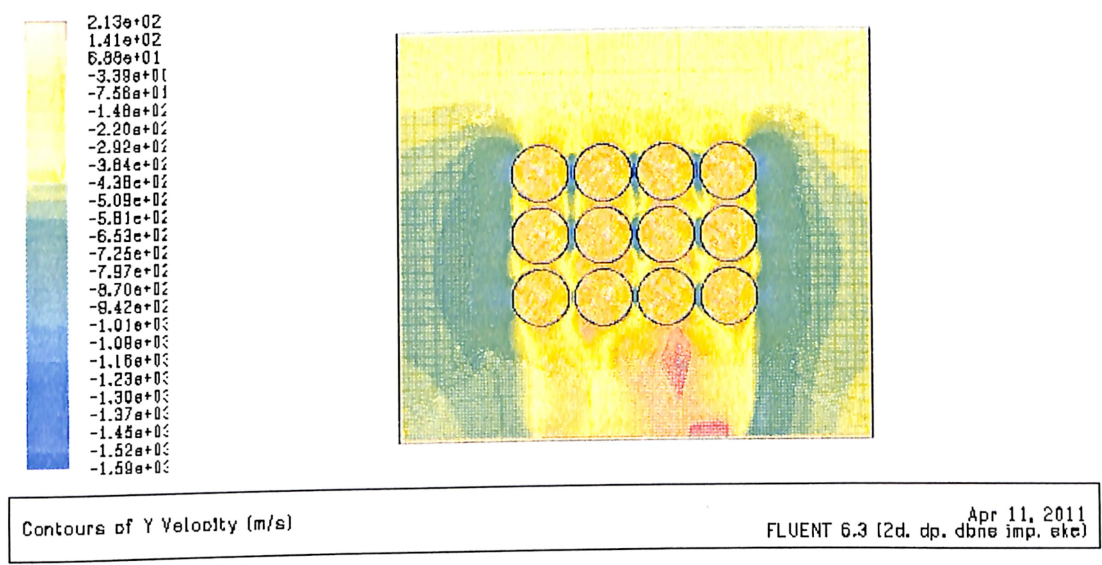
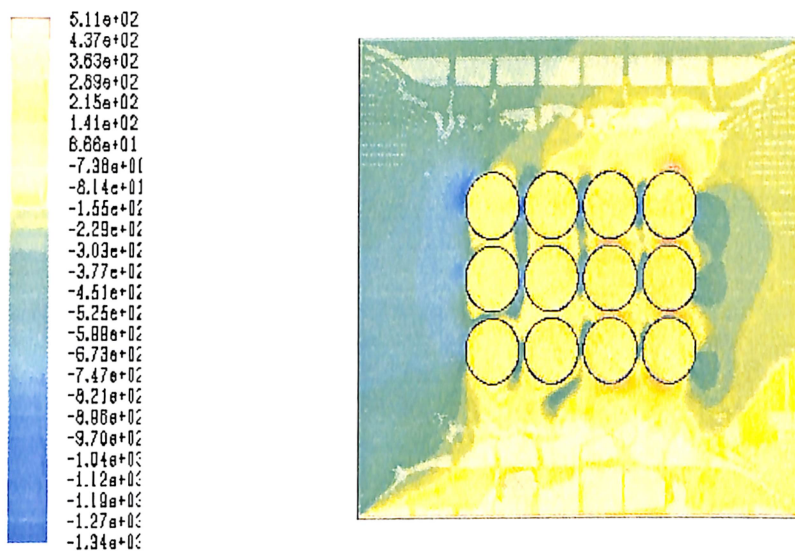


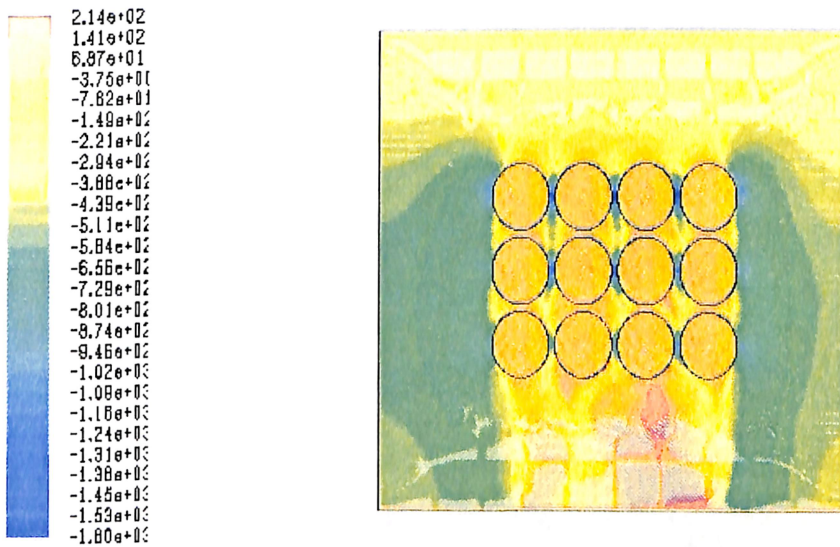
**Figure 4.19** Y- Velocity Contours In Side The Reactor

In case of vectors the plots of radial velocity and Y- velocity are shown in the figure 4.20 , 4.21. Which indicate the appropriate velocity that model is exhibiting is  $-7.38 \times 10^2$ . But in between the fuel pebbles the velocity development is indicating the flow is more active in those regions. This will help in interacting the coolant with the pebbles. The outer region of the fuel pebbles are around the temperature 1173 k and the core is maintained at the 1600 k. The effectiveness of the heat transfer takes place when interaction of the coolant with the core temperature. The region which is showing in the y- direction it more effective in between the flow and the fuel pebbles. Due to the density of the coolant the flow is more effective in reaching more reactor power density. Radial Velocity is at higher is around  $5.11 \times 10^2$ .



Velocity Vectors Colored By Radial Velocity (m/s) Apr 11, 2011  
FLUENT 6.3 (2d. dp. dbns imp. etc)

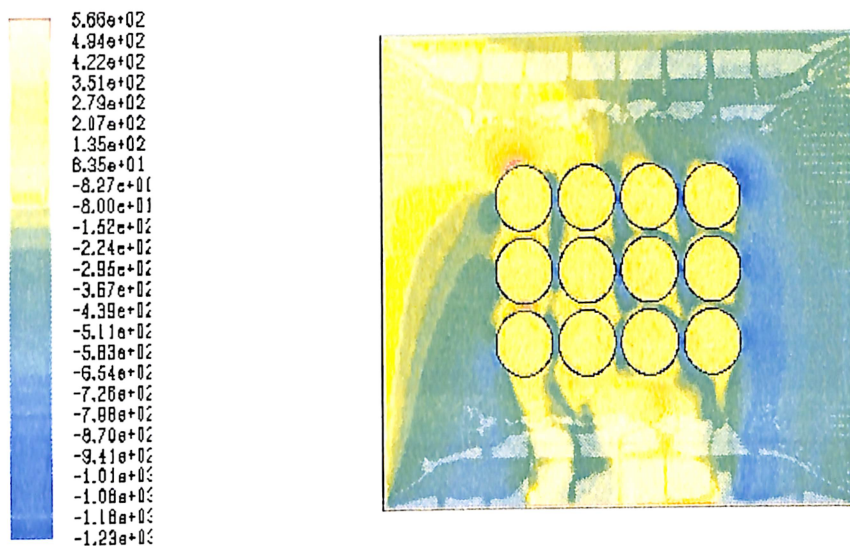
**Figure 4.20** Vector colored by Radial Velocity



Velocity Vectors Colored By Y Velocity (m/s) Apr 11, 2011  
FLUENT 6.3 (2d. dp. dbns imp. etc)

**Figure 4.21** Velocity Vector colored by Y Velocity

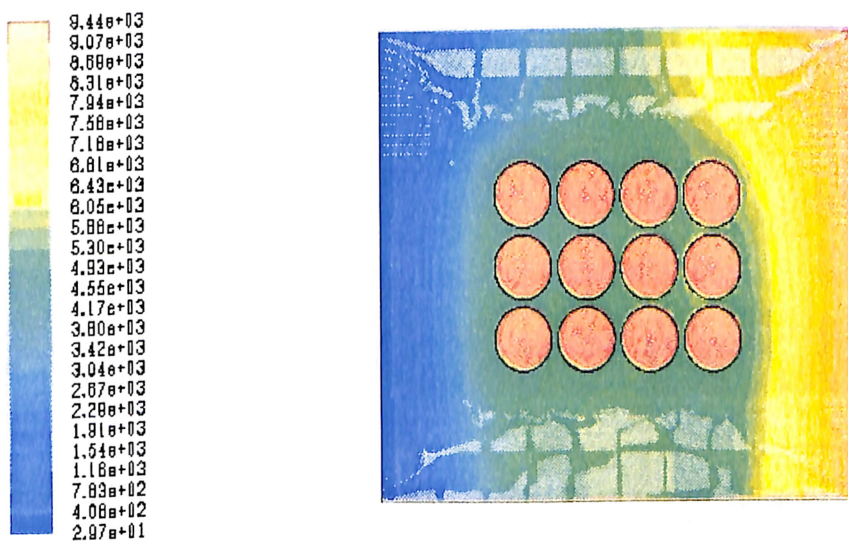
In case of tangential velocity the same trends are showing like as radial velocity and y-velocity plots. The difference is these results which are there in the figure 4.22 is showing a critical zones at the edge of the pebble model.



Velocity Vectors Colored By Tangential Velocity (m/s)

Apr 11, 2011  
FLUENT 6.3 (2d, dp, done imp, etc)

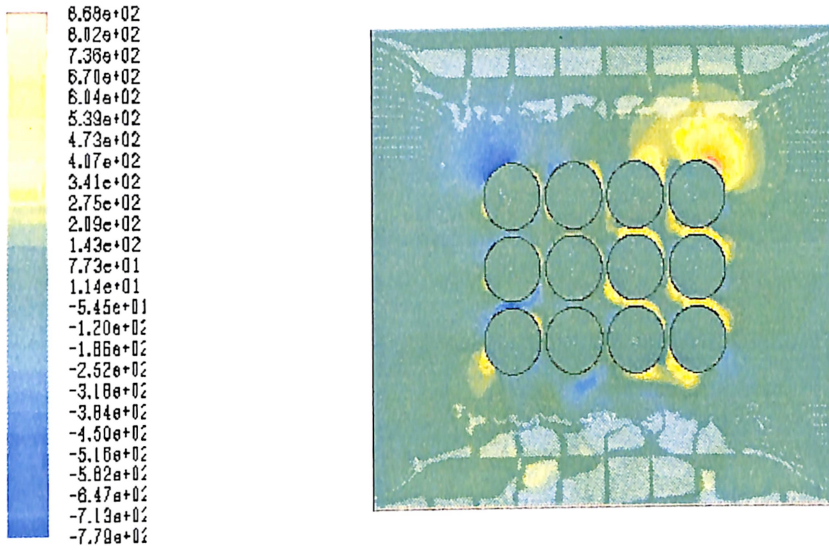
Figure 4.22 Velocity Vector Colored By tangential Velocity



Velocity Vectors Colored By Stream Function (kg/s)

Apr 11, 2011  
FLUENT 6.3 (2d, dp, done imp, etc)

Figure 4.23 Velocity vectors Colored by Steam Function Side The Reactor



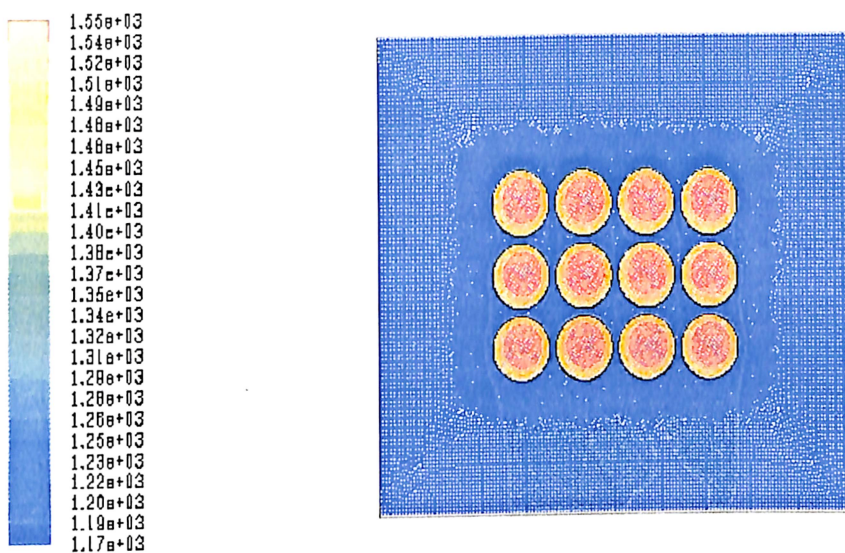
Velocity Vectors Colored By X Velocity (m/s) Apr 11, 2011  
FLUENT 6.3 (2d. dp. dbns imp. etc)

Figure 4.24 Velocity Vectors Colored by X Velocity



Contours of Static Temperature (k) Apr 11, 2011  
FLUENT 6.3 (2d. dp. dbns imp. etc)

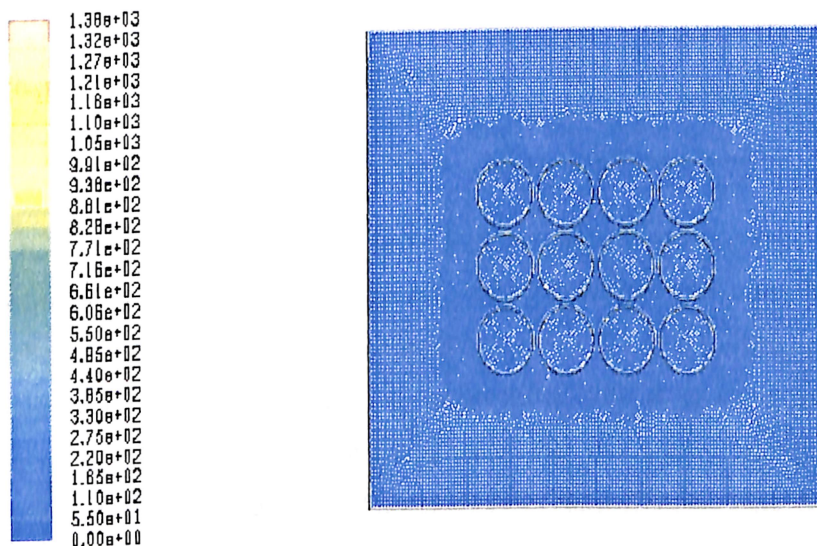
Figure 4.25 Static Temperature Contours



Contours of Relative Total Temperature (k)

Apr 11, 2011  
FLUENT 6.3 (2d. dp. dbns imp. etc)

Figure 4.26 Relative Total Temperature



Contours of Wall Temperature (Outer Surface) (k)

Apr 11, 2011  
FLUENT 6.3 (2d. dp. dbns imp. etc)

Figure 4.27 Outer surface wall Temperature

While defining the boundary conditions with the fluent, the model is solved on the basis of convective heat transfer and radiation is not considered due to the limitations in the solution. The boundary conditions defined for the model is tabulated in the appendix H. The actual temperature range inside the core is considered as 1173 K and the free stream temperature is taken in convection as 550 K.

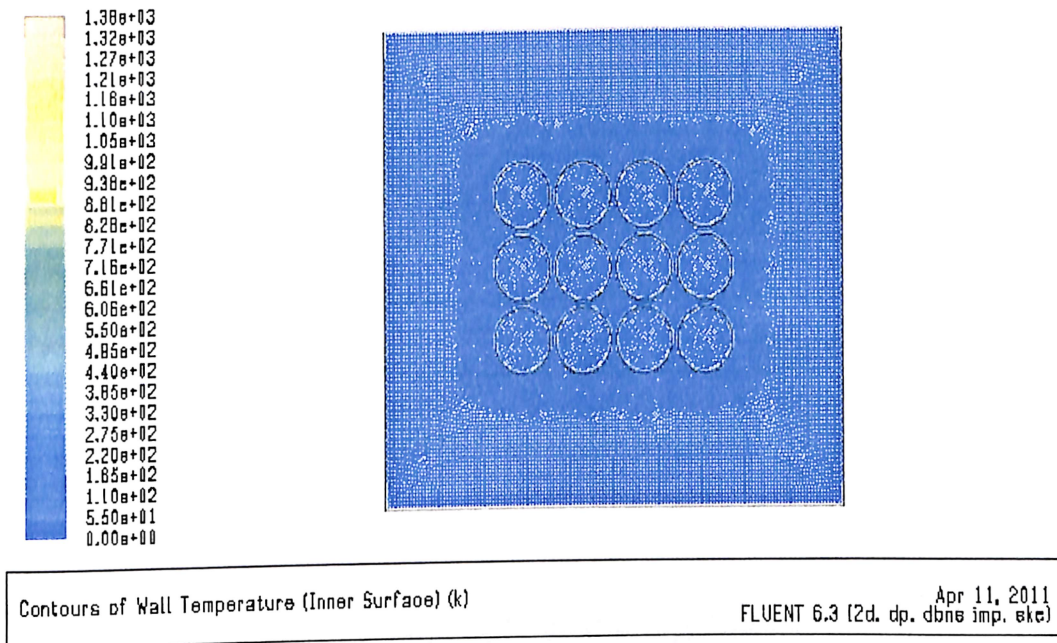
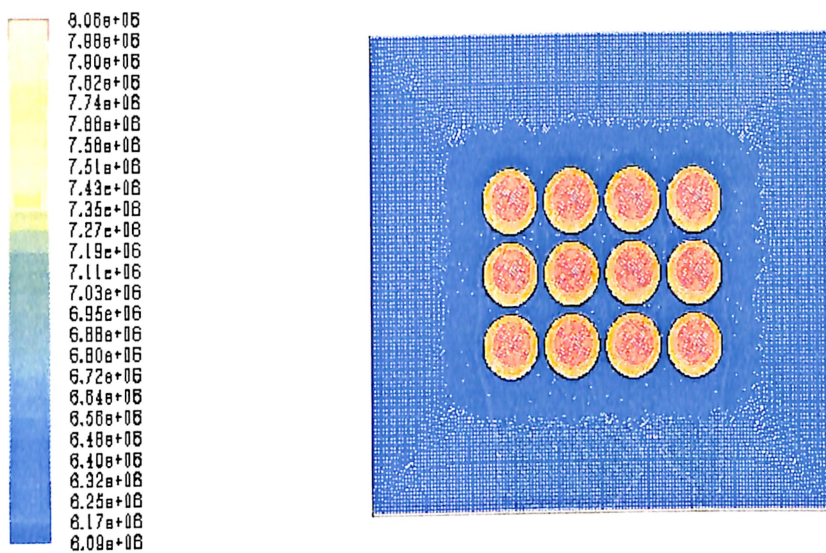


**Figure 4.28** Inner Surface wall Temperature

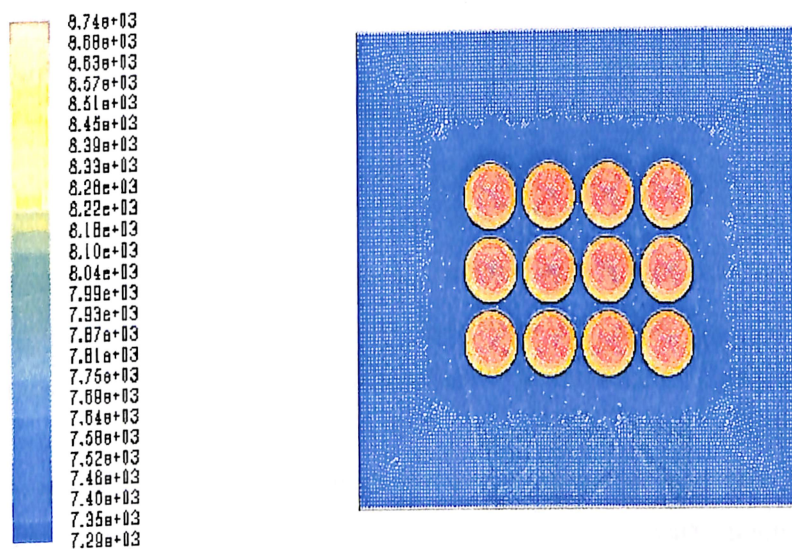
The temperature models shown in the figure 4.28 is specifying the outer core of the fuel pebbles are at 1380k. The total temperature contours are explaining from the figure 4.26 which specifies the reactor core temperature as 1127 as a minimum value and the fuel pebbles core as a maximum temperature as a 1556 K is showing in the result. The theoretical calculations are showing that the maximum temperature that will be maintained at the core of the fuel pebbles is a round 1600 K. This specifies the design is accurate and within the designed parameters the reactor operation is going to takes place with these parameters. Due to the turbulence created inside the reactor the coolant is achieving these properties. Also due to this temperature range the coolant circulation ratio is high, but ultimately this will result in increasing the enthalpy of the reactor.



Contours of Internal Energy (J/kg)

Apr 11, 2011  
FLUENT 6.3 (2d. dp. dbne imp. etc)

Figure 4.29 Contours of Internal Energy

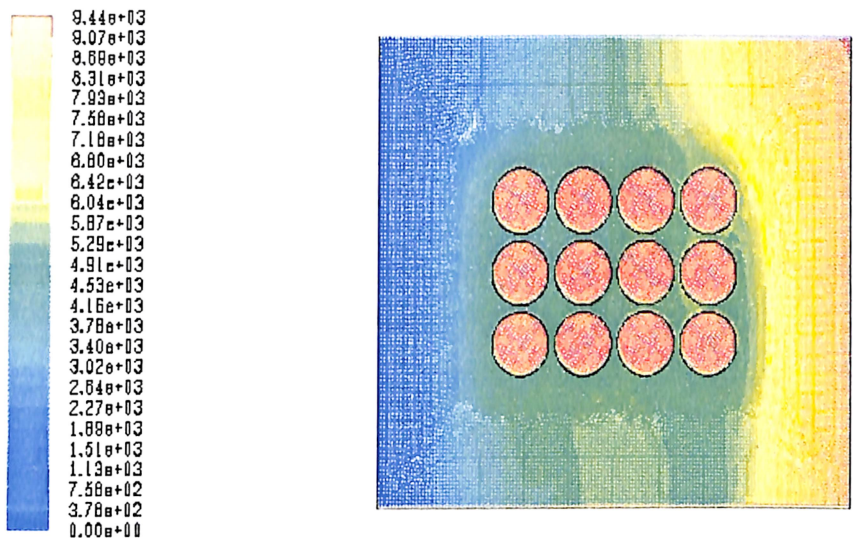


Contours of Entropy

Apr 11, 2011  
FLUENT 6.3 (2d. dp. dbne imp. etc)

Figure 4.30 Contours Of Entropy

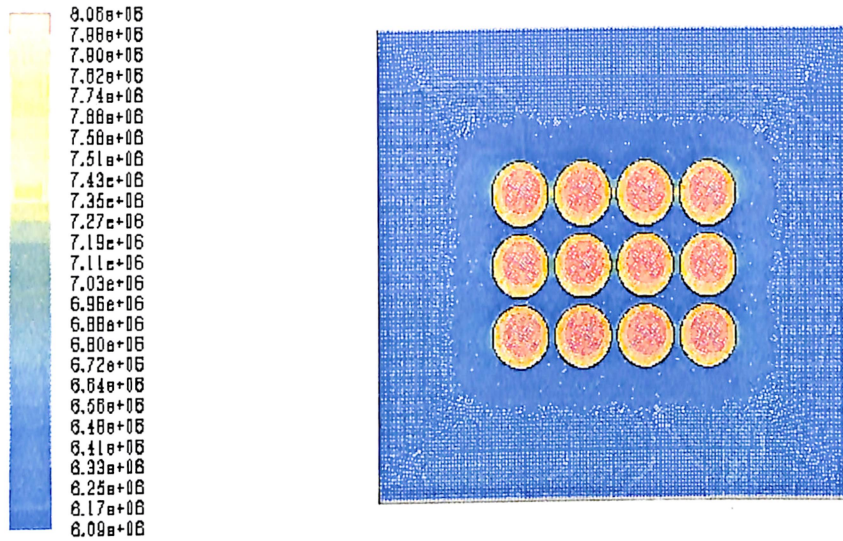




Contours of Stream Function (kg/s) FLUENT 6.3 (2d, dp, dbns imp, etc) Apr 11, 2011

**Figure 4.31** Stream Function

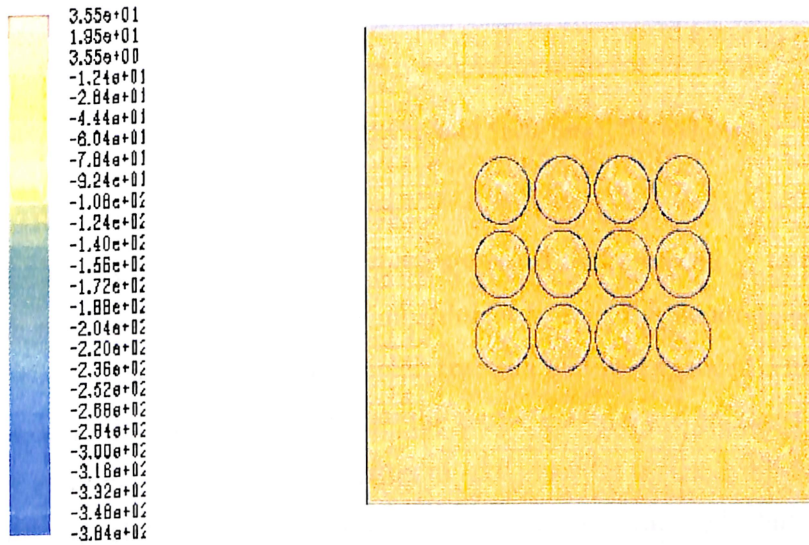
The concept of increasing the operating pressure has its merits, but there are limitations to how much pressure can be raised. Various considerations of the materials involved in the construction of the reactor core will affect the maximum operable pressure within the system. It is a well documented fact that high operable pressures will lower the operational lifetime of the components that are exposed to these pressures. In addition, the maximum operable pressure will also be dependent upon the thermodynamic gas cooling cycle that will exit the nuclear reactor core. Thus, for the two reasons stated above, the ability to increase the pressure is only applicable to a certain extent. The wall shear stress showed in the figure 4.33 and the 4.34 shows that the transfer of energy and due to which the development of wall shear stress is visible between the pebbles. In the figure 4.32 the energy levels at the core of the fuel pebbles are high due to the maximum temperature which is showing from the total temperature contours, which is coming around 1550 °C, which is very much close to the design temperature at 1600 °C. The total energy levels are changing from 6.09 to 8.05 and these shows the energy transfer is more progressive. This result shows the power density of the reactor is closer to the calculated value.



Contours of Total Energy (J/kg)

FLUENT 6.3 (2d. dp. dbns imp. etc) Apr 11, 2011

Figure 4.32 Total Energy Contours



Contours of Y-Wall Shear Stress (pasool)

FLUENT 6.3 (2d. dp. dbns imp. etc) Apr 11, 2011

Figure 4.33 Y-Wall shear Stress

The wall shear stress which is in Y- wall shear stress is more when compared to the X- wall shear stress, The X- direction the value is changing from -1.24 to 1.50 due to the pressure rise in side the reactor when heat is added to the coolant. In case of Y direction the shear stress is varying from -3.84 to 3.55, which says that the development in y direction is more because the flow is occurring in the same direction.

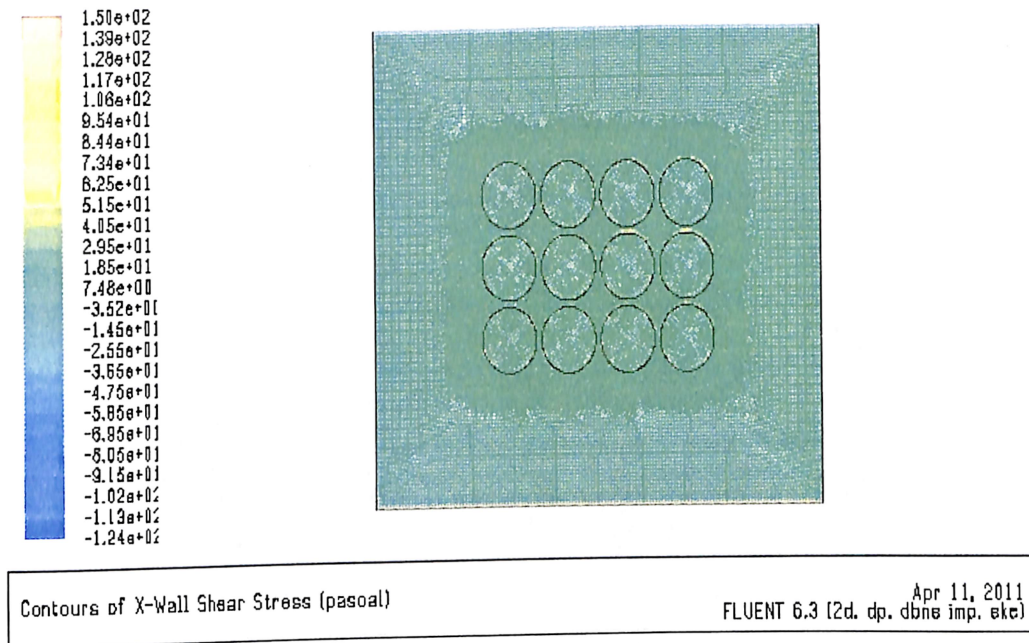


Figure 4.34 X-Wall Shear Stress Development

### 4.3 3D Modeling on Fuel Pebbles

The best configuration of these spherical fuel elements is to place them on top of each other. Once the neutron bombardment begins, the neutrons will scatter across the reactor core assembly and the fission reaction will be enhanced within the spherical fuel elements. Since the moderator and the fissile material are enclosed together, this causes a much more homogeneous reaction to take place. In essence, this reduces the poisoning of the fuel elements since they are not configured as fuel rods, but rather as fuel pellets. The spherical elements are configured, so that helium passes through them unimpeded. Hence, the homogeneity described above is accentuated and this causes more homogenized neutron profiles to be formed within the reactor. This is an added advantage as the criticality of the reactor can be controlled more easily. The biggest

advantage of helium cooled reactors is the passive safety systems that are embedded in the criticality of the core itself.

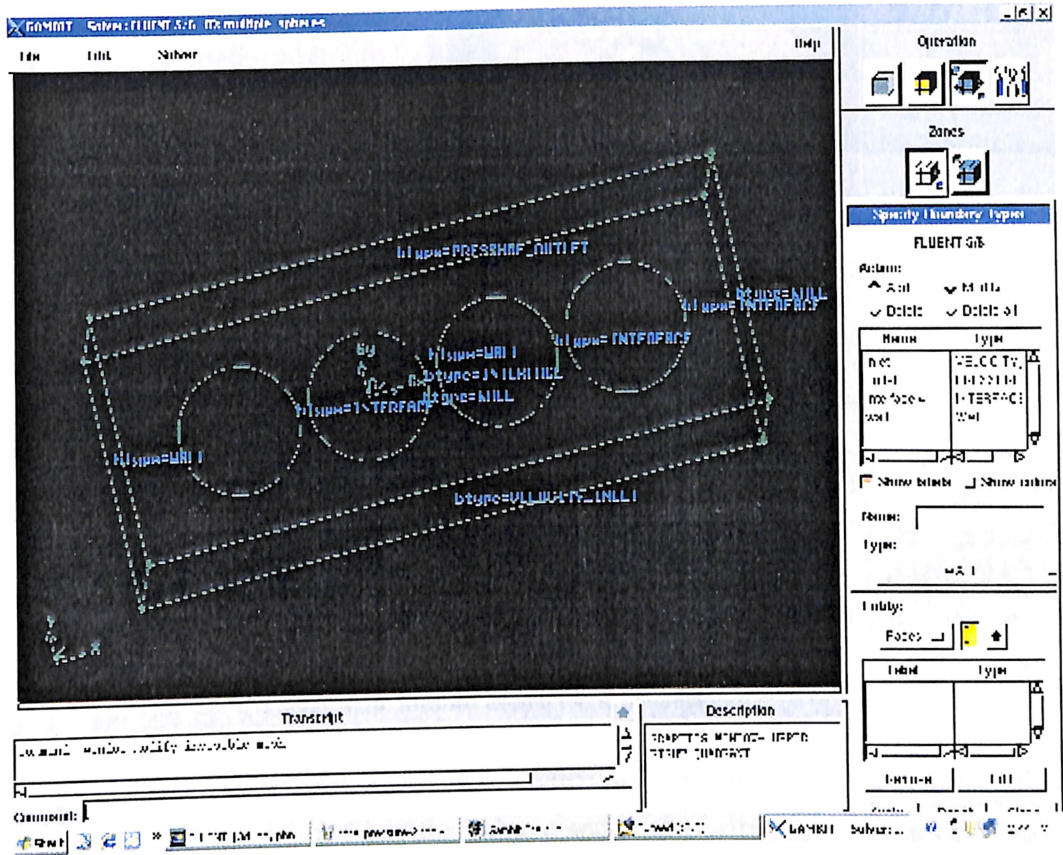


Figure 4.35 Gambit Modelling based on 3D

Due to more homogenized neutron profiles, the need for advanced control rods is greatly decreased. As the temperature profile increases, the amount of neutrons circulating decreases due to the natural processes inherent in the system. This is a very important self control feature that helps to limit a runaway reaction probability. The power levels of the reactor as well as the criticality can be changed easily by changing the coolant flow rate as well as the density and the viscosity of the coolant. Hence, in this particular design, the need for control rods is minimized and they can be exchanged with scram rods which are only to be used in case of extreme emergency. So, as the temperature levels rise, the core starts to generate less power.

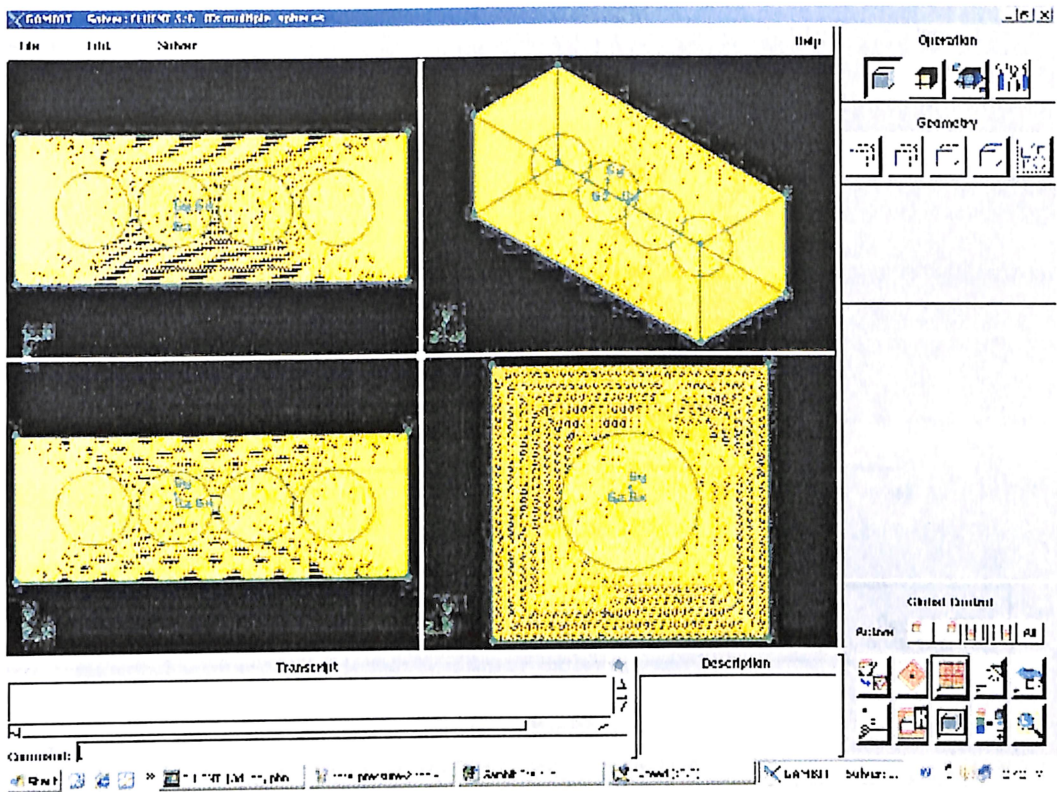
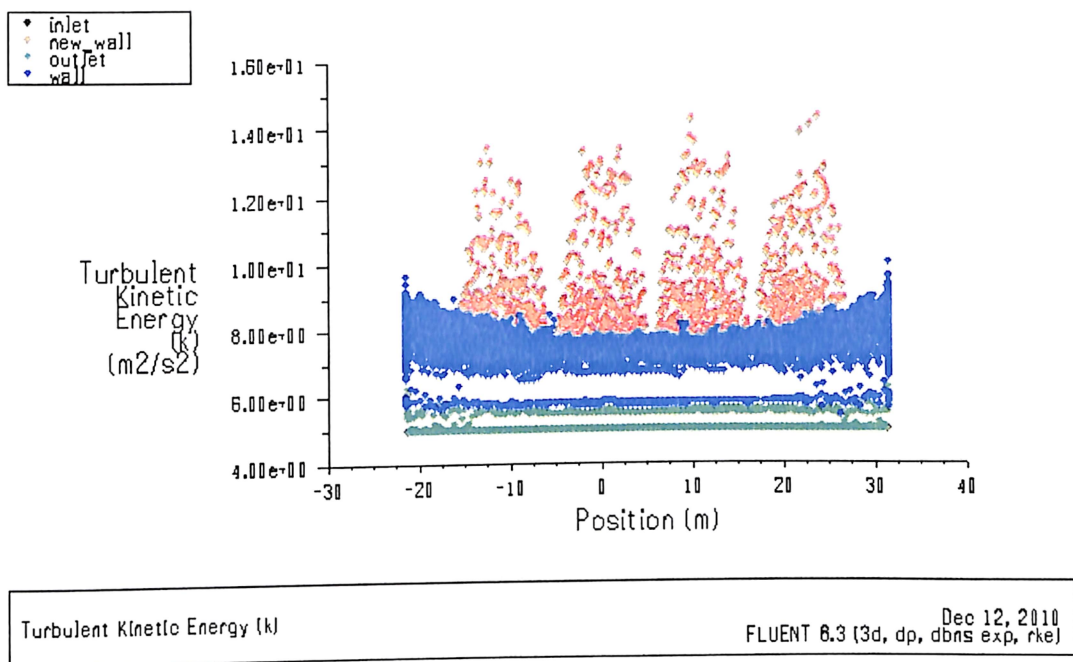


Figure 4.36 Meshed Model for 3D Simulation

The 3d model is developed in gambit in terms of vertex and modeling is done with the face and it can be converted into the volume and it will be meshed first in faces and total model will be meshed with volume. An important point that needs to be considered is the heat transfer characteristics of the fuel elements used in the nuclear reactor. As stated in the above sections of this paper, it is essential to create the maximum heat transfer that is possible within the limitations imposed by the nuclear reactor design concept. The main limits on the thermal design of the nuclear reactor can be described as the allowable temperature values for the coolant, as well as the allowable temperatures for the nuclear fuel elements and the structural materials. In effect, a properly prescribed temperature envelope can be defined clearly, as well as a criterion for the design temperature. Hence, in order to achieve this, it is essential to increase the amount of heat that is safely reached inside the fuel element and it is also essential to increase the amount of heat transfer from the fuel element into the cooling medium, namely Helium.



**Figure 4.37** Turbulance Kinetic Energy

Various studies conducted with the South African Pebble Bed Reactor show that the maximum temperature reached in the fuel elements is around 1250 degrees Celsius. In emergency conditions, it is supposed that the fuel elements will reach around 1600 degrees Celsius, which can be troublesome for the heat containment. However, even under a high temperature profile, the passive safety aspects of the helium cooled pebble bed reactor still stands creating an important advantage for this particular design. Helium as a coolant is one of the more important points in the design of this reactor. It is essential for the heat transfer to be as maximal as possible for better efficiency in the overall design. In this aspect, Helium is the proper choice of a coolant as it has one of the highest heat transfer areas per unit area. Hence, although carbon dioxide as well as Hydrogen has better heat transfer characteristics, all of them require great areas if the pumping power, temperature, pressure and flow areas are kept as fixed. Moreover, the presence of translational, rotational, vibration degrees of freedom allows Helium to have a higher molar specific heat. Thus, the selection of Helium seems to be the best choice for a reactor under similar constraints. In addition, turbulent flow<sup>3</sup> characteristics of Helium also allow it to be a good choice. The formation of a boundary layer using Helium

creates much less turbulence and rotational flow in the far field of the localized flow region. This is a very important concept, as creating too much turbulent flow can also cause the other fuel elements to have a lesser heat transfer characteristics due to the internal energy that is dissipated in the heat transfer process. Hence, a contained turbulent flow field is designed near the fuel elements, in order to minimize their negative impact on surrounding fuel elements.

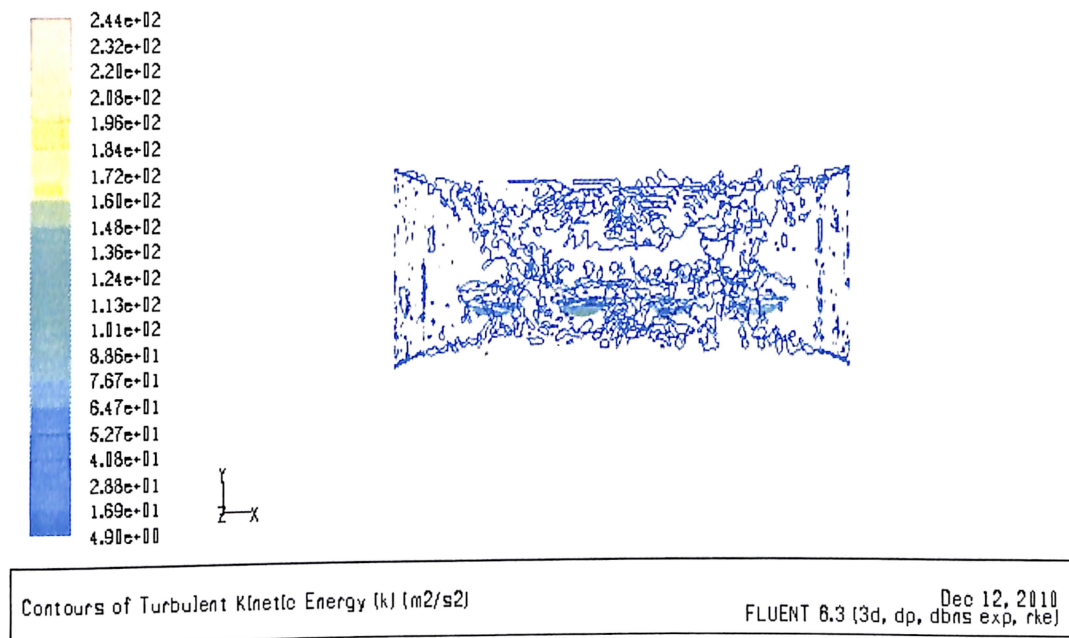


**Figure 4.38** Turbulence Kinetic Energy

Naturally, the roughening process can be done in various stages. It can be possible to put dimples on the spherical fuel elements which can significantly increase the amount of surface area that is exposed to the Helium gas acting as a coolant. However, the concept of putting dimples on the spherical fuel elements would create configuration problems. The dimples on the surface of the spherical fuel elements would create shear stress when they are placed on top of each other and cause failure in the long run. Moreover, due to the laws of fluid dynamics, this would cause a heavy turbulent flow to be formed in the coolant circulating around the fuel elements. Naturally, a heavy turbulent flow is something that needs to be avoided for better operational stability. However, at the same time, some degree of turbulent flow would also help transfer the

heat through the coolant toward the pressure outlet of the reactor core at the bottom as seen in Figure 4.39.

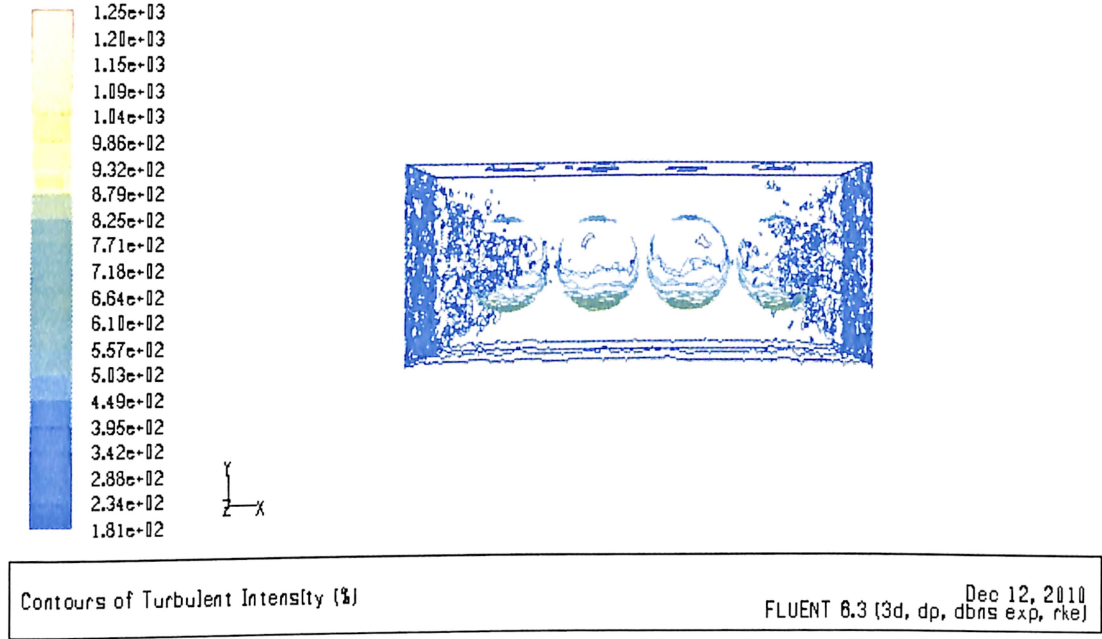


Figure 4.39 Turbulent Intensity

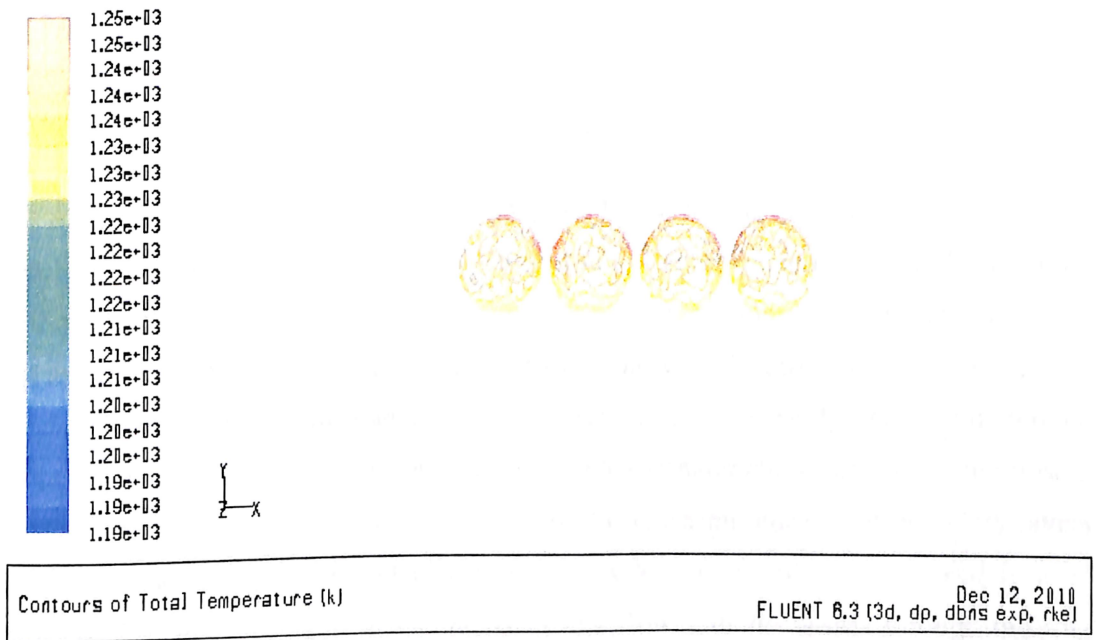
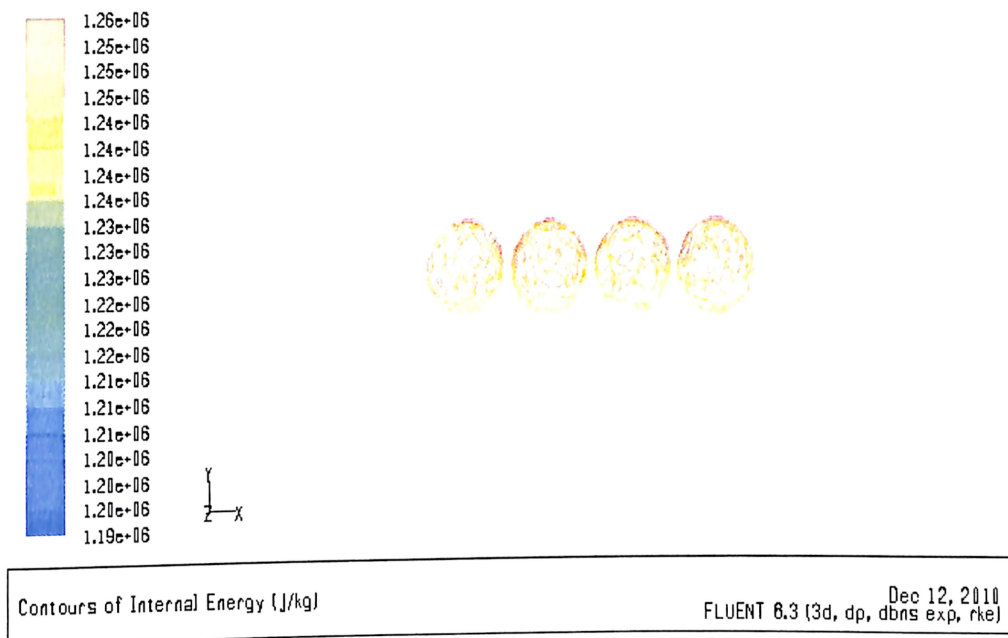


Figure 4.40 Total Temperature Between Fuel Pebbles



The second scheme that is possible with increasing the surface roughness of the fuel elements would be to use transverse roughing. In this scheme<sup>3</sup>, the fuel element surface would be dimpled inward and this would help increase the heat transfer as well as to decrease the amount of turbulent flow that would be formed over the fuel elements. Of course, it is essential to keep the transverse roughing within certain parameters to help preserve the structural integrity inside the fuel element.



**Figure 4.41** Internal Energy Development in Between Pebbles

As stated above, the dominant flow over the fuel elements in the nuclear reactor core would be turbulent and viscous flow. The amount of compressibility would be around 1 to 2 percent, so the flow can be calculated as incompressible flow without loss of too much accuracy. Hence, the main characteristics that would need to be examined would be the viscous flow and turbulent flow characteristics. In this study, the helium coolant flow rate is taken as 320 kg/sec and the heat – mass transfer characteristics of the flow is analyzed using Fluent 6.3. Due to the viscous flow, certain amount of boundary layers will be formed around the fuel elements as they are subjected to high speed flow of Helium. The flow is radial in nature, since the flow radially passes through the ring shaped layer, as it comes in contact with the fuel elements. The recommended mass

transfer rate of Helium is 320 kg / sec and this can cause an effective boundary layer to be formed on the fuel elements.

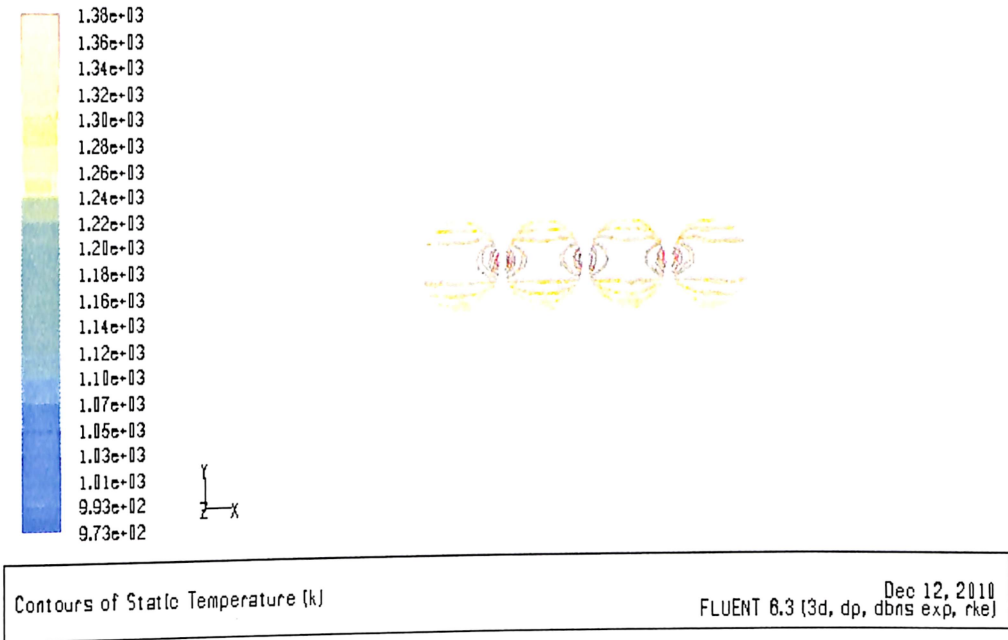


Figure 4.42 Static Temperature in Between Pebbles

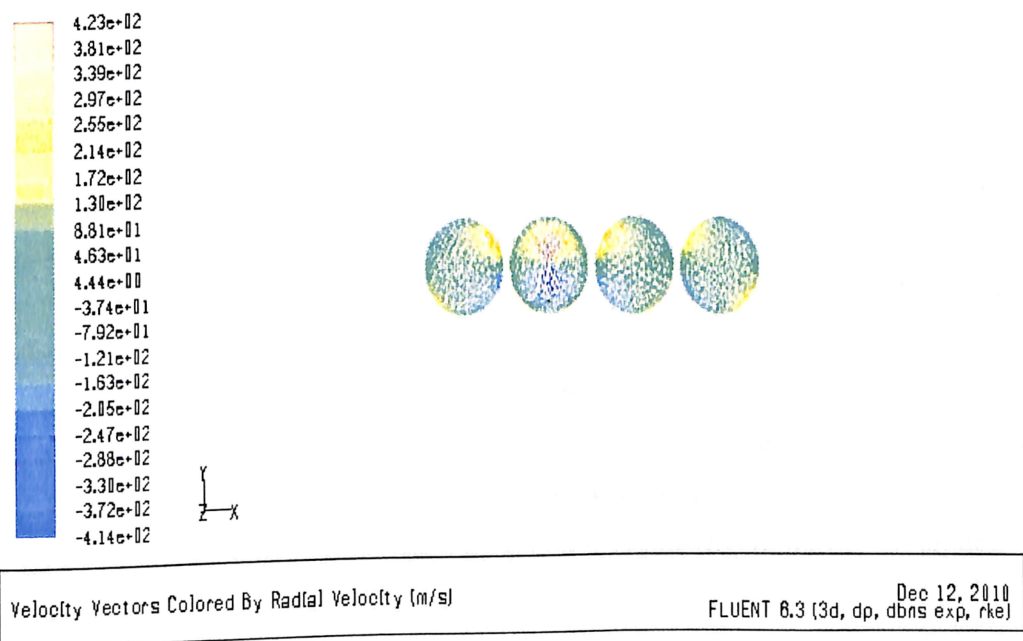


Figure 4.43 Velocity Vector Colored By Radial Velocity

The boundary layer would create no slip condition on the surface of the element and would adjust the flow to outside of the momentum boundary layer. As compared to air, the boundary layers would have less thickness, but they would affect the flow nonetheless with the formation of eddies.

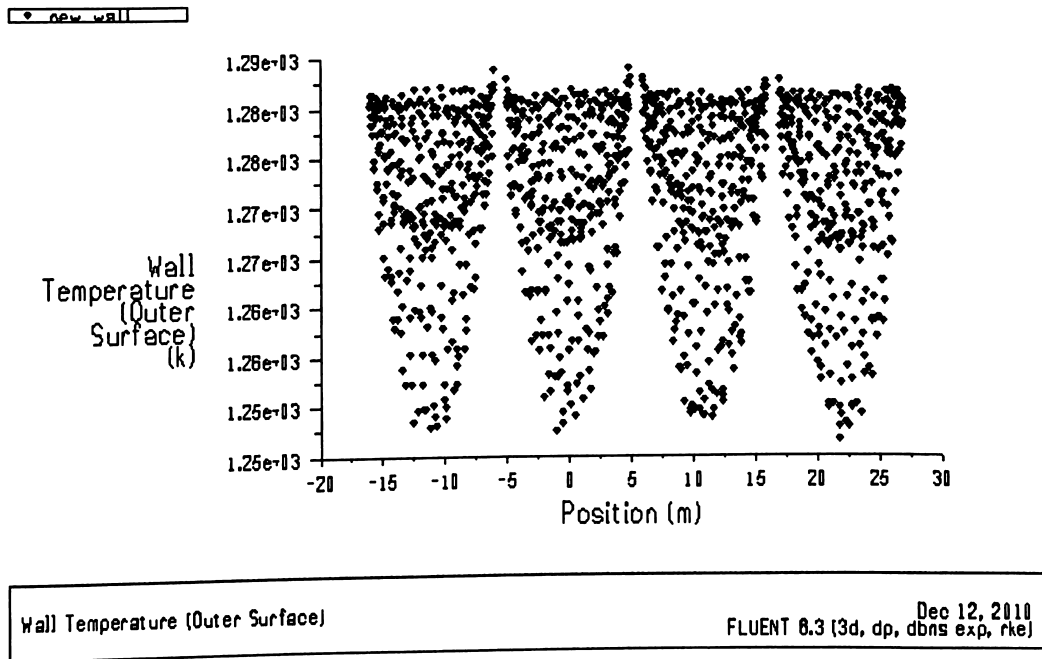


Figure 4.44 Wall Temperature Effect on Pebbles

The turbulent flow characteristics also need to be considered, as significant amounts of momentum and energy transfer would take place within the flow. Up to some extent, this can improve the heat transfer characteristics between the helium molecules, but it would cause wakes to be formed which would be counterproductive in the long run. Hence, the right answer would be to reduce the turbulent flow characteristics and to have the boundary layers as thin as possible on the spherical fuel elements as seen in Figure 4.45. The turbulent intensity is being dissipated evenly throughout the fuel elements as well as the surrounding coolant flow. It is possible to analyze the flow using the Baldwin Lomax model up to some extent, since compressibility can be omitted and thus the flow can be handled as a subsonic flow.

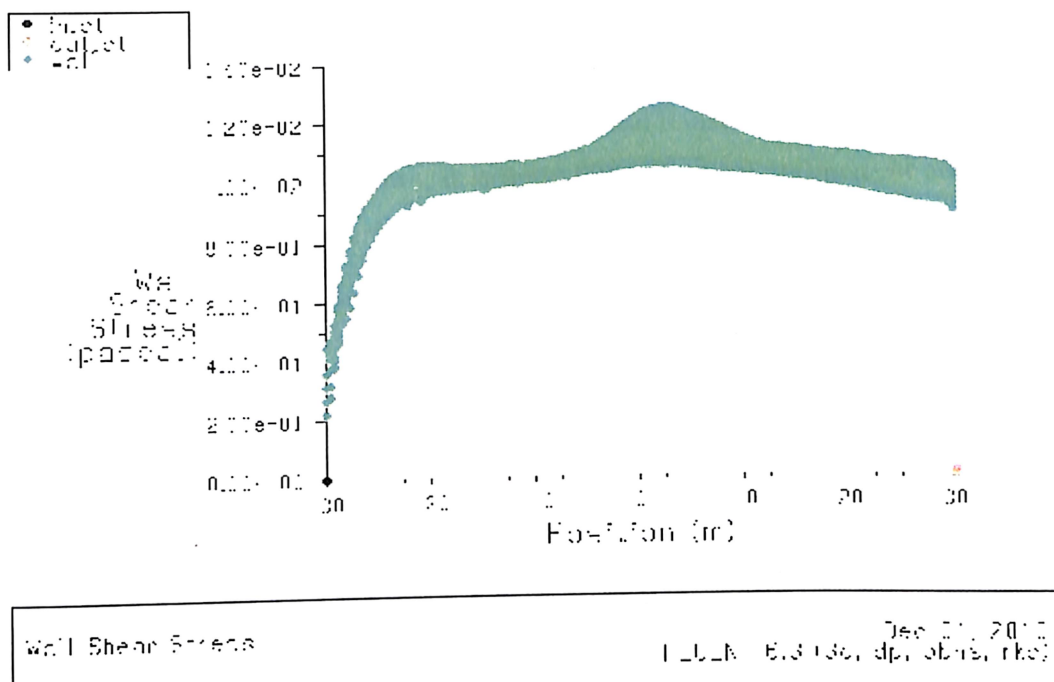


Figure 4.45 Wall Shear Stress Development

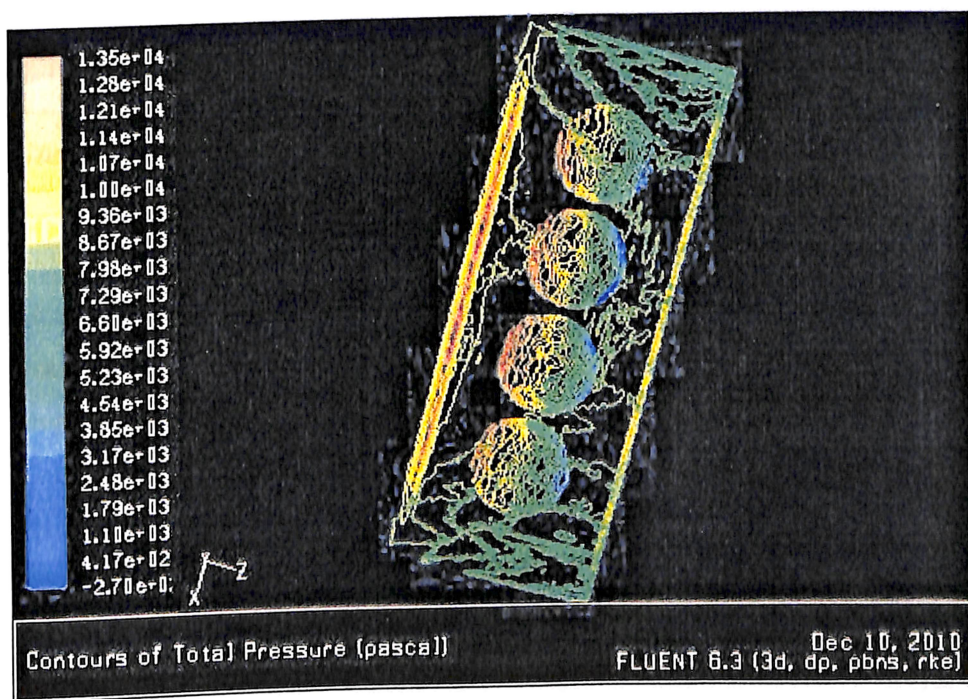
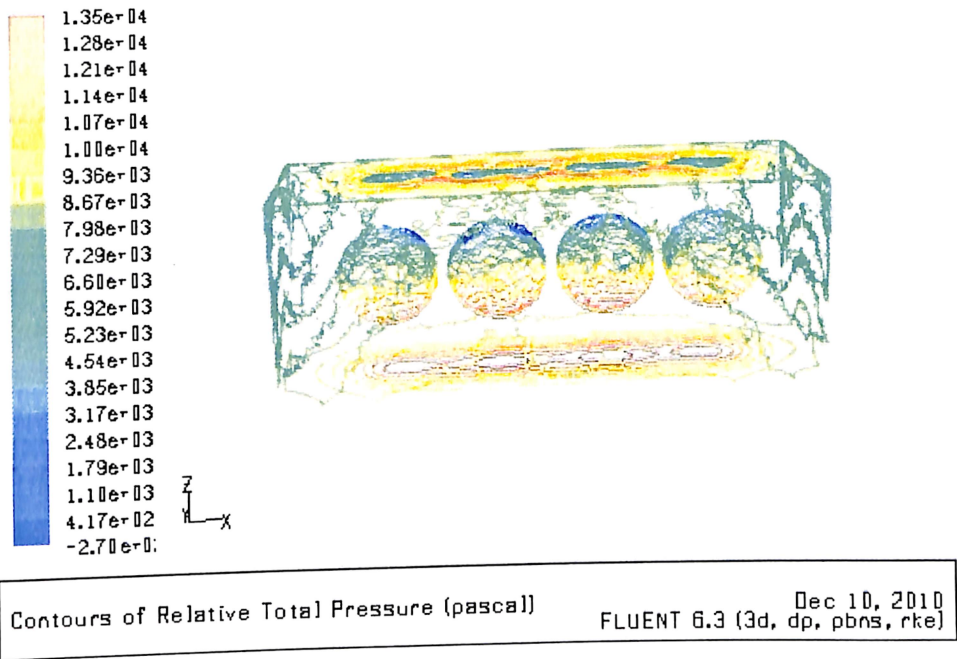


Figure 4.46 Total Pressure Development in side the 3D Model

As it can be seen in Figure , which is depicting a CFD analysis of sample fuel elements in turbulent kinetic flow of Helium as a coolant; if boundary layers are kept as thin as possible, the flow is actually helping out with the heat transfer process to the coolant. Of course, as with all turbulent flows, it is quite difficult to get 100 percent accuracy by using eddy momentum transfers



**Figure 4.47** Relative Total Pressures

As it can be seen in Figure 4.48, which is depicting a CFD analysis of sample fuel elements in turbulent kinetic flow of Helium as a coolant; if boundary layers are kept as thin as possible, the flow is actually helping out with the heat transfer process to the coolant. Of course, as with all turbulent flows, it is quite difficult to get 100 percent accuracy by using eddy momentum transfers. However, as it is seen in Figure 9, the dynamic pressure of the flow itself is high, but well within manageable levels, which allow some control of the conditions of the turbulent flow. Both in Figures 4.48 and 4.49, black and white pictures have been used for clarity. In Figure 4.49, the axes have been reversed to allow for clear representation of the inlet where the flow is entering the system in order to interact with the fuel pellets.

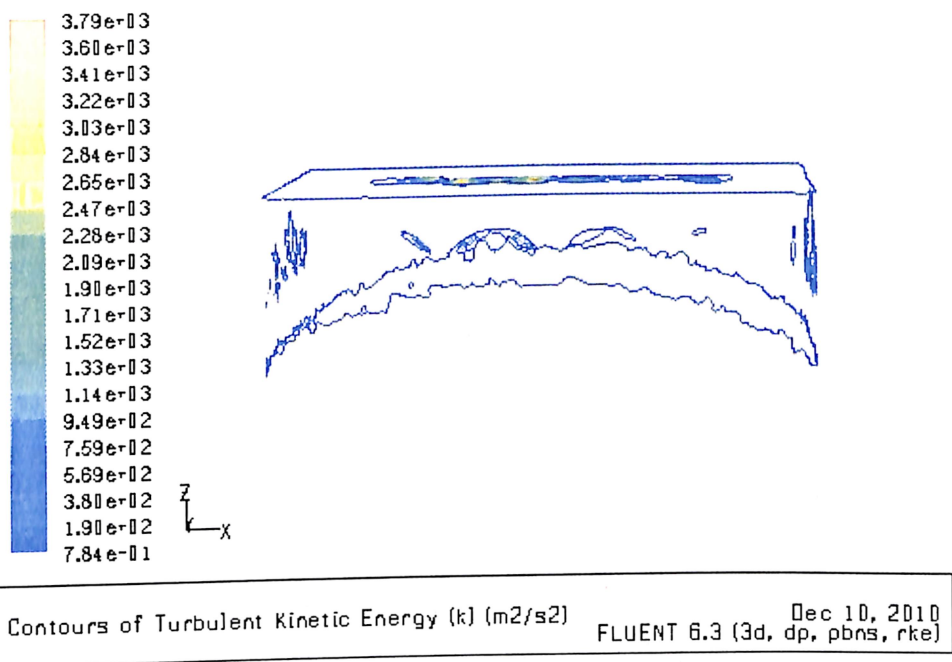


**Figure 4.48** Total Turbulence Kinetic Energy

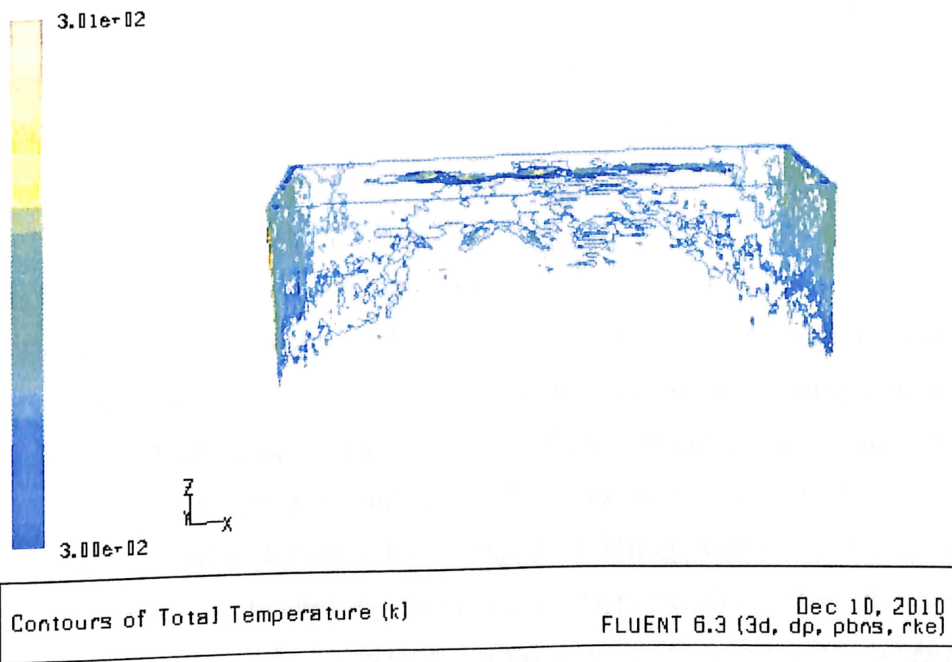


**Figure 4.49** Total Temperature Contours

## CHAPTER 5

### THERMODYNAMIC ANALYSIS OF GT-MHR

In a thermodynamic point of view Gas turbine Modular Helium reactor cycle design is carried out in this chapter along with computing the solution to the energy balance around a gas turbine in order to calculate the intake mass flow and the turbine inlet temperature. This chapter offers a new approach to compute the energy balance around a gas turbine. The energy balance requires that all energy flows going into and out of the control volume be accounted for. The difficulty of the energy balance equation around a gas turbine lies in the fact that the exhaust gas composition is unknown as long as the intake flow is unknown. Thus, a composition needs to be assumed when computing the exhaust gas enthalpy. This allows the calculation of the intake flow, which in turn provides a new exhaust gas composition, and so forth; by viewing the exhaust gas as a flow consisting of ambient air and combusted fuel. Based on the thermal design, structural design, neutronic and metallurgy will be future designed. The main emphasis will be on fuel elements in relation to reactors for electrical power generation. If the restriction is only on core thermal design was to limit certain temperature and also with this heat transfer problems also greatly simplified.

#### **5.1 Gas Turbine Power Conversion System**

The size of gas turbines must be increased with respect to conventional designs for that a specific approach is followed, to accommodate the heat energy transformation proposed for a HTGR module. The technology for an effective compact heat exchanger must be available for hydrogen production. The feasibility of a large magnetic bearing must be demonstrated with current technology [17]. Using magnetic bearings instead of oil-lubricated bearings obviates the oil-ingress problem which contaminates the helium coolant. The gas turbine HTGR plant holds the promise for electricity generation with high efficiency. Reported expected efficiencies of 43% to 48% have been calculated. Rankine cycle nuclear plants, such as the PWR and BWR, usually provide an efficiency of around 33% for electricity generation. Both the conceptual designs of the GT-MHR and PBMR adopt a direct closed gas turbine cycle for the power conversion system. The

power conversion unit of the GT-MHR utilizes a single-shaft arrangement consisting of a turbine, an electric generator, and two gas compressors on a common, vertically oriented shaft supported by magnetic bearings. The power cycle unit also includes a recuperator, pre cooler and intercooler. In the power cycle unit of the GT-MHR, there are three vertically oriented shafts shown in the figure 5.1. The high-pressure turbine drives the high-pressure compressor while the low-pressure turbine drives the low-pressure compressor. The power turbine drives the electric generator. Also, a recuperator, pre cooler and intercooler are used in the GT-MHR. However, implementing the gas turbine nuclear plant depends on the technical feasibility of helium gas turbo machines and the compact heat exchanger. The following describes the technologies for helium gas turbo machines and compact heat exchanger.

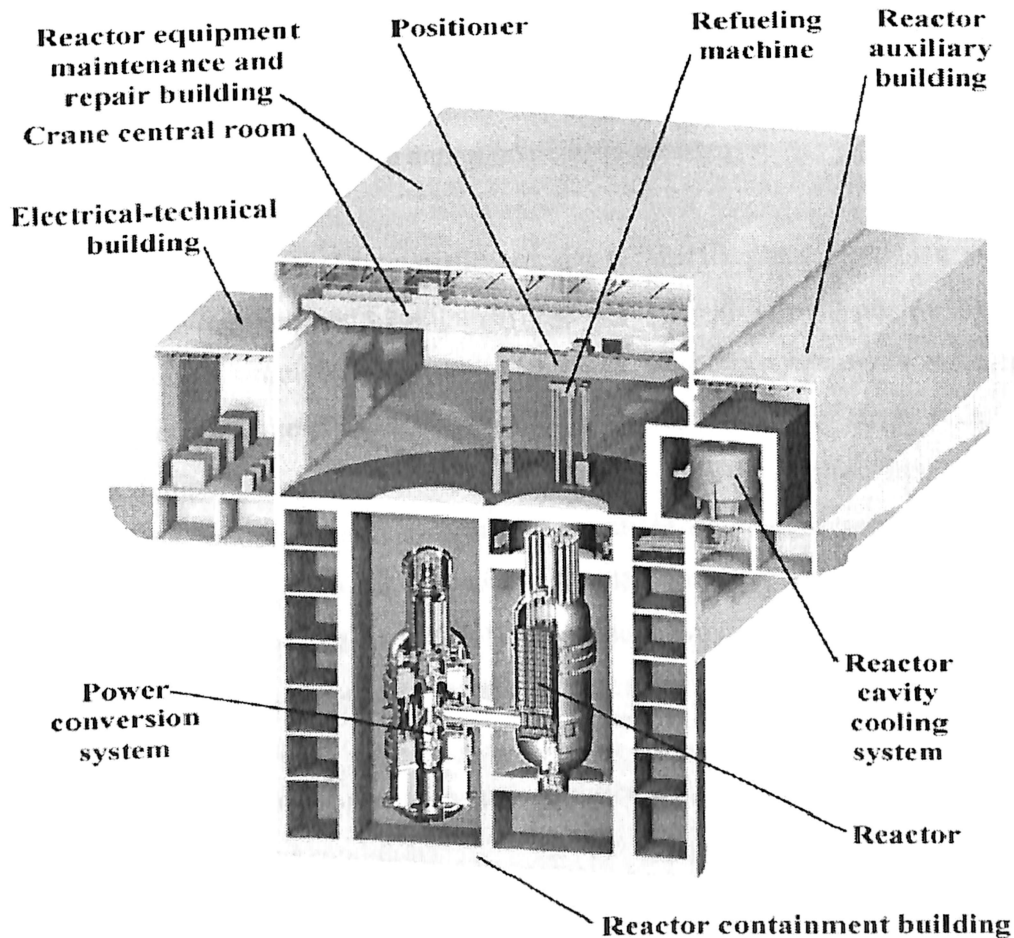


**Figure 5.1** GT-MHR Power Conversion Unit



## 5.2 Thermal Design of GT-MHR

The GT-MHR is a prismatic core type high temperature gas cooled reactor (HTGR). It operates at a thermal power level of 850 MWth corresponding to compressor power input. The power density is 32 MW/m<sup>3</sup>. The reactor system is located below grade and operates at elevated temperatures with a helium outlet temperature comprise between 850°C (electricity production) and 460 °C (hydrogen production) which leads to high plant thermal efficiency. The reactor's layout is presented on Figure 65. The GT-MHR utilizes uranium oxy-carbide fuel with TRISO coating as fuel particles. The GT-MHR features a good conversion ratio and superior fuel economics in comparison with other types of reactors. This is the consequence of a good neutron economy which is obtained from two factors which are Nuclear grade graphite constitutes most of the MHR structures (fuel particle coating, core structural material, and moderator and coolant channel walls) and helium is an inert coolant. As a result the GT-MHR experiences low parasitic capture and good neutron economy.

The basic design characteristics of the GT-MHR plant provide a significant reduction in the required plant equipment if compared with current nuclear plants. The GT-MHR features simplified and reduced number of safety systems. In the electricity production version, the GT-MHR allows the removal of the large steam power conversion equipment. The plant simplification, the reduction in required systems and equipment, the modularization and the reduction in equipment requiring regulatory oversight, all contribute to an increased capacity factor relatively to other nuclear concepts [8]. Because of the GT-MHR innovative elements, higher operating temperatures and helium coolant, specific technical issues and information needs must be addressed. Extended studies and appropriate development activities have to be pursued in fuel design confirmation and qualification, as well as passive decay heat removal under abnormal conditions.

A big part of the design was motivated by safety issues. In the design of the GT-MHR, the desirable inherent characteristics of the inert helium coolant, graphite core, and coated fuel particles are supplemented with specific design features to ensure

passive safety. The release of large quantities of radio-nuclides is precluded by the fuel particle ceramic coatings, which are designed to remain intact during normal operation and off normal events. The integrity of the particles coatings as a barrier is maintained by limiting heat generation, assuring means of heat removal and by limiting the potential effect of air and water ingress on the particles under accident conditions. For this design, the possibility of a core meltdown is precluded through the use of refractory, coated-particle fuel and nuclear-grade graphite fuel elements with high thermal capacity and conductivity, combined with operation at a relatively low power density with an annular-core arrangement [12]. For instance, during a loss-of-coolant accident, decay heat is removed from the core by convection and radiation, both natural heat transfer mechanisms, to the Reactor Cavity Cooling System (RCCS). The GT-MHR fuel is considered to be proliferation resistant and storage proof. Not only the fuel particle coating acts as fission fragments barrier but it is also a highly resistant barrier for ground water during spent fuel storage. It is so resistant that, as of today, no technology exists to retrieve the fuel from the particles. It is anticipated that the spent fuel would contain 30 times less amounts of plutonium than typical light water reactors thanks to higher burnup achievement in GT-MHR.

### **5.3 Helium Gas Turbo machines**

Gas turbines have been used throughout the world for marine/aviation propulsion and power generation in land based power plants for many years. Large scale gas turbine output power can be over 200 MW for a land based power plant. However, its working fluid is combustion gases (from the mixture of air and fuel, such as natural gas or oil). For the GT- MHR there are special designs to install higher capacities more than 850 MW power turbines are under design for this as experience china is constructing a power plant with this capacity at present. The past experience with design and operation of closed cycle helium turbo-machinery has been finite but limited [13]. Two large-scale helium facilities for testing closed cycle helium turbo-machinery have been operated in Germany. The first facility is tested with 50MW (e) in Oberhausen helium turbine plant, and the second one is high temperature helium test plant (HHV). The design of the test plant was for an electrical power of 50 MW and heating (district heat) power 53.5 MW.

The thermal heat source for the closed helium cycle was a fossil-fired heater. The basic flow scheme and design parameters are considered for the present design. A two-shaft arrangement was selected for the turbo machinery.

The high-pressure (HP) turbine drives the low-pressure (LP) compressor and HP compressor on the first shaft with a rotational speed of 5,500rpm and the LP turbine drives the generator synchronizing with the grid (rotational speed 3,000rpm) on a separated shaft. Both shafts are interconnected by a gear. Since the power generated from the HP turbine is consumed by the compressors, there is not much power to transfer from the HP turbine to the generator through the gear. As shown in Figure 65, the HP turbine inlet temperature and pressure were 835°C and 7.42 MPa, respectively. Helium mass flow rate for the cycle was 320 g/s. The power regulation of the test plant uses the same principle adopted for closed cycle air turbine plants. Both inventory control and bypass valve control, which will be described in the next section, are used. The HP turbine has 18 stages with 50% reaction. The turbine rotor disc and the blade feet are cooled by extracting a helium stream from the HP compressor outlet. The LP turbine has 11 stages. The HP compressor and LP compressor have 15 stages and 10 stages, respectively, both with 100% reaction. Oil lubricated labyrinth seals are used for sealing. The housing and nozzles are also cooled. The blade feet, rotor and housing are cooled by means of a cooling gas system or a sealing gas system. For the cooling gas system, radial-type compressors circulate the cooling helium of 56.8 kg/s at an inlet temperature of 236°C and inlet pressure of 4.9MPa and an outlet pressure of 5.35MPa at 258°C. The radial-type compressors are driven by a 6.5MW electric motor. The plant over all layout is shown in the figure 5.2, the stage one is the reactor output where the helium is at high temperature and at higher pressure, it is connected to the high pressure turbine at a stage of two and later the output of the high pressure turbine will be allowed to expand in a low pressure turbine so that it will be bought at a temperature range of 480°C and will be allowed to enter into the inter mediate heat exchanger which is connected to the steam generating unit to perform steam reforming process for hydrogen production. The processing is designed separately with the hydrogen production plant. The out let of the heat exchanger is connected to the recuperater.

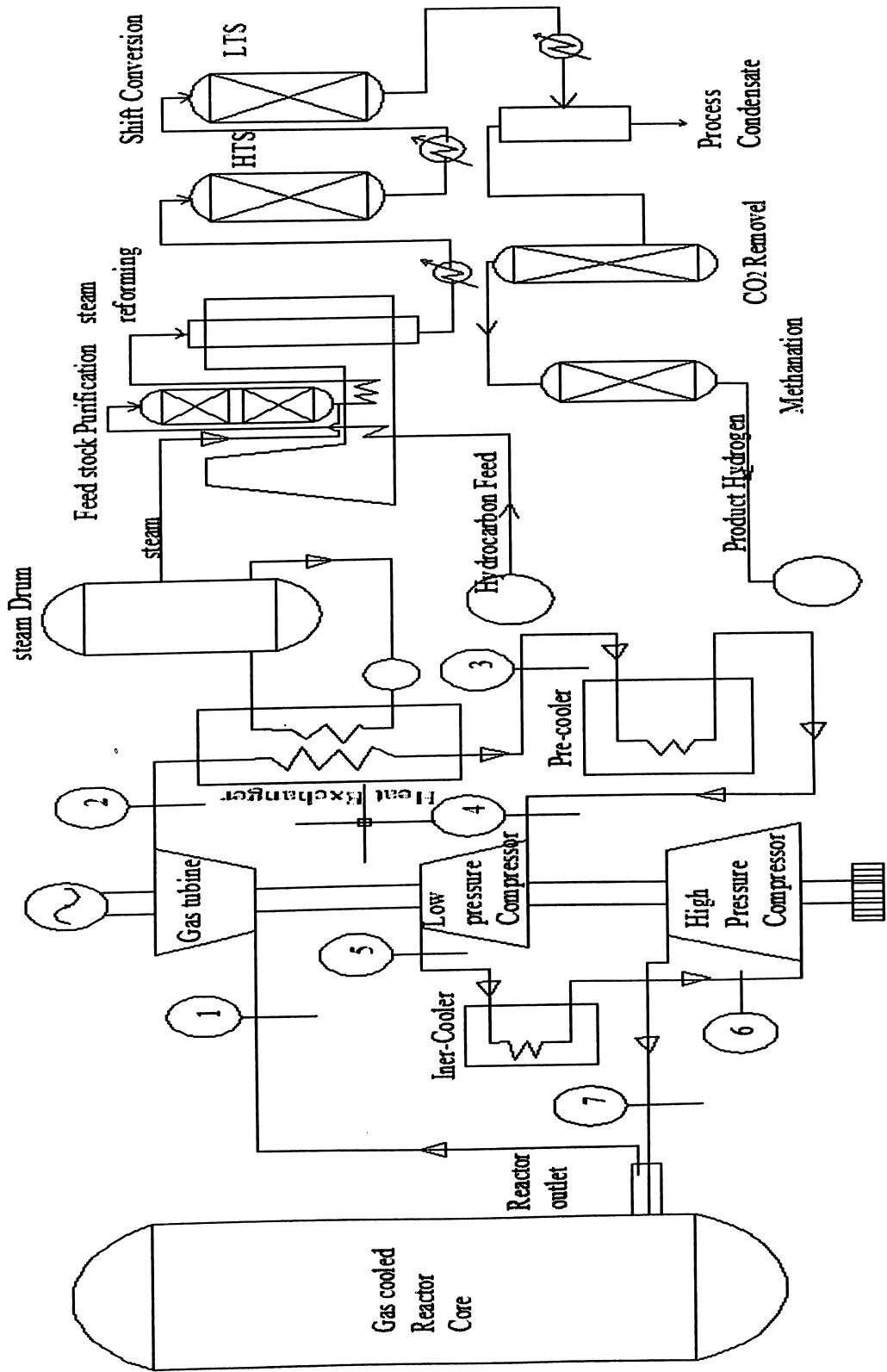


Figure 5.2 GT-MHR Thermodynamic Cycle Design

**TABLE 5.1 THERMAL REACTOR DESIGN PERMETERS**

<b>Name of parameter</b>	<b>Value</b>
Coolant Temperature	950 °C
Fuel Temperature	1600 °C
Helium Flow Rate	320 Kg/s
Thermal Power	850 MW(t)
Core Height	700 Cm
Efficiency Rate	48 %
Uranium Enrichment	20%
Core Avg. Heat Density	32 MW/m <sup>3</sup>
Diameter of fuel Elements	20 mm

The outlet of the heat exchanger is connected to the pre cooler and the temperature is will be bring down to 65° C and it will be allowed to enter the low pressure compressor and its pressure will be brings to 4.20 MPa and the temperature will increase to 80 °C and it will be connected to a inter cooler to bring down the temperature to 45 °C and will be allowed to enter the high pressure compressor, so that the work input required to drive the compressor will be reduced and the out let of the compressor pressure will be at 7.48 MPa. This is the pressure required at the inlet of the reactor. The stage analysis of the thermodynamic cycle details is listed in the table VIII. The total power required raising run low pressure compressor and high pressure compressor will be calculated with the following pressures. That power required will be 44.1 Mw, The selection of the compressors is done in equal configuration at 26.1 Mw low pressure compressor and 26.1 Mw high pressure compressors are selected for the flowing conditions.

**TABLE 5.2 THERMAL CYCLE DESIGN PERMETERS**

<b>Stage</b>	<b>Temperature(° C)</b>	<b>Pressure (MPa)</b>	<b>Enthalpy(KJ/Kg)</b>
Stage 1	900	7.45	4933.35
Stage 2	480	2.80	2492.64
Stage 3	115	2.41	597.195
Stage 4	65	2.38	337.545
Stage 5	80	4.20	415.44
Stage 6	45	4.15	233.685
Stage 7	135	7.48	701.055

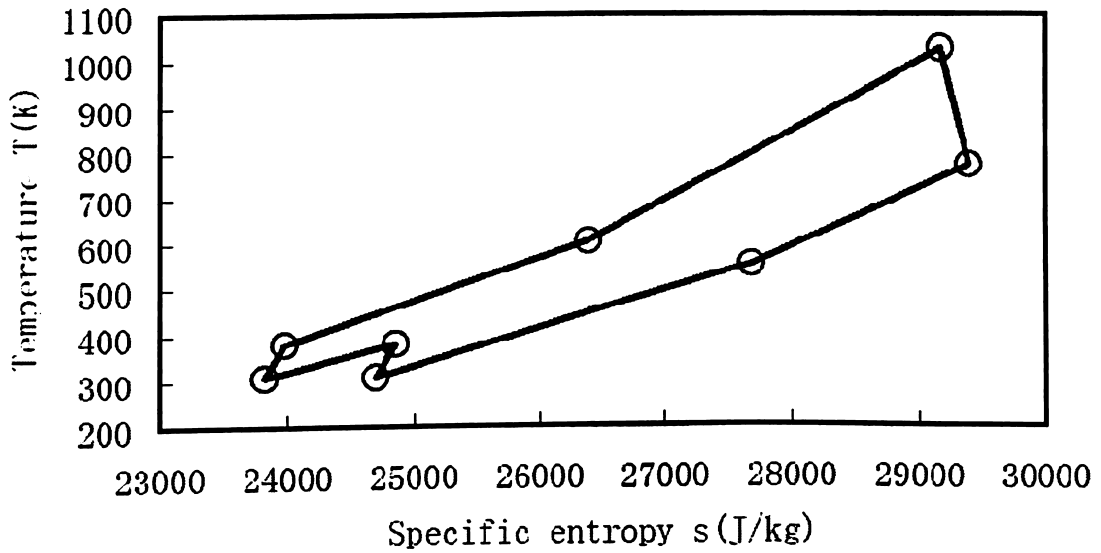


Figure 5.3 T-S Diagram for GT-MHR Cycle

From the cycle analysis data P-V and T-S diagrams are drawn for future analysis from the thermodynamic point of view. The figure 5.3 shows T-S diagram, which is explaining about the heat addition and power convection, heat addition process along with the inter cooling. The pressure and specific volume change according to the cycle is shown in the figure 5.4.

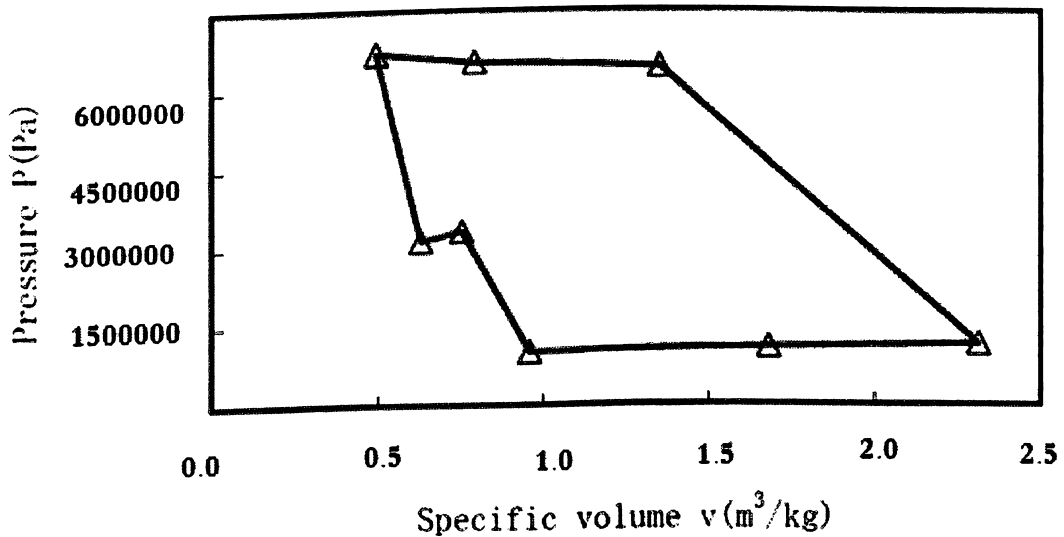


Figure 5.4 P-V Diagram for GT-MHR Cycle

**TABLE 5.3 HELIUM PROPERTIES FOR THERMAL CYCLE DESIGN PERMETERS**

Properties	Molar weight (g/mol)	Specific Gravity	Density Kg/m <sup>3</sup>	K W/m <sup>0</sup> C	Tmin K	T Max K	Melting Point <sup>0</sup> C	Boiling point
He	4.00	0.1368	3.8	0.29	1.76	5.2	<-272.2	-268.9

The Helium properties used in performing stage analyses are shown in the table IX. The helium cooled reactor is designed with helium as a circulating fluid and expands in a turbine and re circulates through cycle. The Cycle Design is on the basis of direct Brayton cycle and overall efficiency of the cycle is accounted in this for this cycle. The important property of the circulating fluid is heat carrying capacity an overall heat transfer coefficient of the helium based on different advantages it is selected. From the stage 1 high temperature and high pressure helium enters into the turbine and expands isentropic ally [8]. Ideally the process is considered as isentropic process without accounting the pressure losses in the turbine, later part of the work it is accounted and a practicable cycle is drawn. From the stage 2 we have low pressure and exhaust temperature of the turbine is available and which will undergo heat extraction process in a heat- exchanger for thermal heat applications, ideally heat-exchange process is also considered as isentropic exposition. The total heat output in the cycle is a combination MWe and MW th are accounted separately. In order to make cycle more efficient a thermal heat application is introduced. From the stage 3 we have low temperature and low pressure helium is available it is allowed cool in a pre cooler in order to reduce work of compression in the first stage. After the stage 5 there is a change in pressure in temperature, in order to bring temperature and pressure up to the designed level to the reactor inlet a high pressure compression process is in interpreted with the help of a inter cooling to reduce high pressure compressor [19]. According to the thermodynamic design the reactor basic structural design parameters are designed, which are shown in the diagram 68 and the GT- MHR or this having two stares of total height 80 m and the actual reactor vessel system is about 45 m height. The reactor vessel system constructs in underground in terms of width 32 m of total area will be considered for installation. The total area require to install these systems are 2560 m<sup>2</sup> of floor are required for the reactor systems. For the auxiliary systems according to the plant layout additional area is required for future installations.

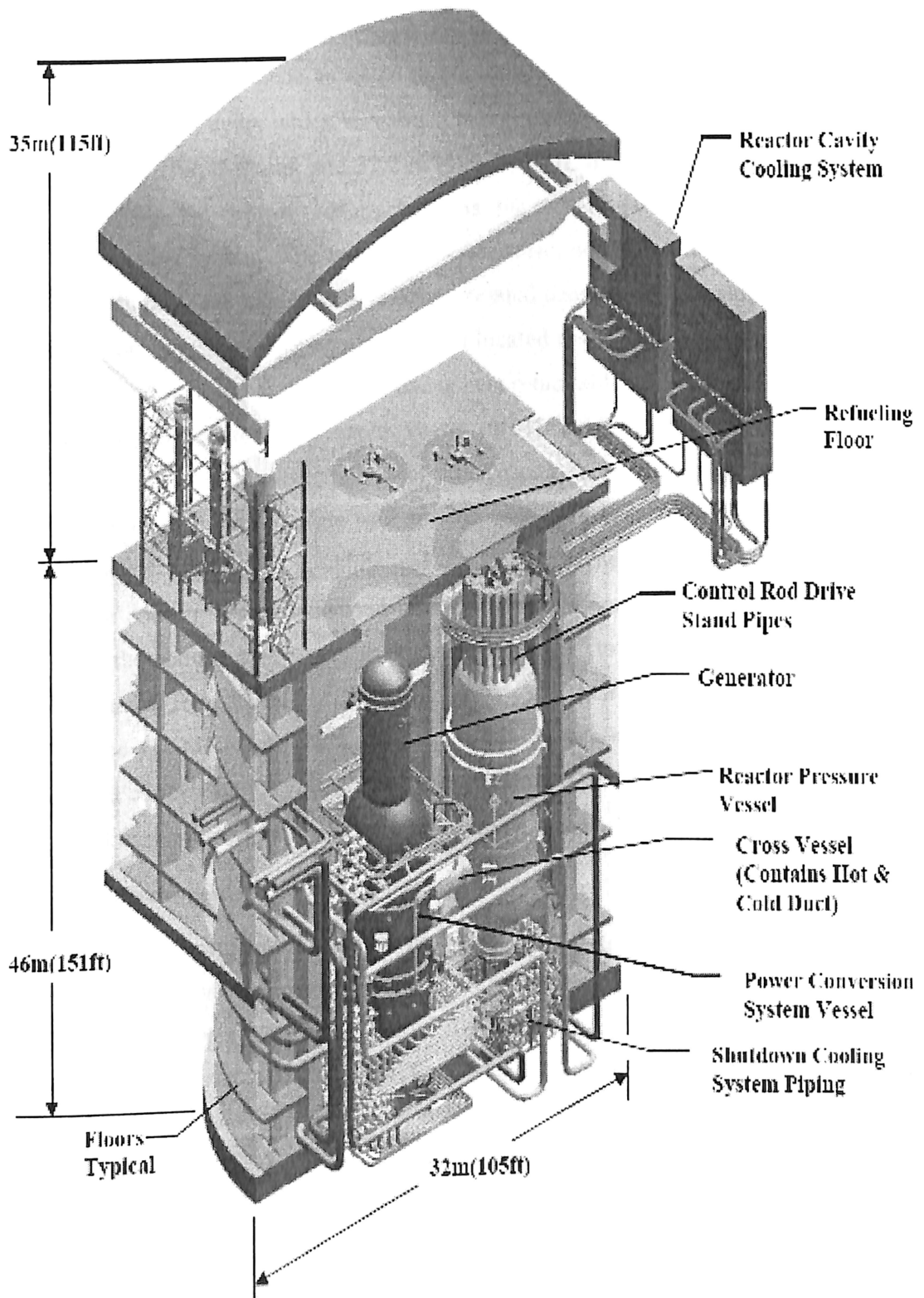


Figure 5.5 GT-MHR Model Design



## 5.4 Reactor Vessel

The primary components of the MHR are contained within a steel vessel system. The module is located inside an underground concrete silo 25.9 m (85 ft) in diameter and 42.7 m (140 ft) deep, which serves as the containment structure. The reactor vessel is 8.4 m (27.5 ft) in diameter and 31.2 m (102 ft) high. It contains the reactor core, the reactor internals, the control rods mechanisms, the refueling access penetration and the shutdown cooling system. The reactor vessel is surrounded by a reactor cavity cooling system which provides totally passive safety-related decay heat removal by natural draft air circulation. The shutdown cooling system located at the bottom of the reactor vessel provides forced helium circulation for decay heat removal for refueling and maintenance activities. Figure 5.5 shows the reactor vessel. (491°C/915°F) enters the reactor through the outer annulus within the cross vessel, flows up the core inlet riser channels located between the reactor vessel inside wall and the core lateral restrain and enters the upper plenum located above the graphite core [18]. Then the coolant flows downwards through the cooling channels located in the active core parts and the reflector parts. A fraction of the coolant by-passes the channels holes and flows into gaps between blocks and into control rods channels (approximately 3%). This fraction is comprised between 10% for the H2-MHR and 20% for the GT-MHR. When leaving the core, the high temperature coolant (900°C/1562°F) is collected in the lower plenum and then exits the core vessel through the inner annulus within the cross vessel.

### 5.4.1 Core Arrangement

The core arrangement is illustrated on Figure 5.5. The reactor is made of an assembly of hexagonal graphite fuel and reflector elements, also called blocks, arranged into an annular disposition. The active fuel region of the core consists of 102-fuel columns, each made of 10 blocks high. Each block contains blind holes housing the fuel, and full length channels for the helium coolant flow [18]. The columns are arranged in three annular rings. The active core is surrounded with reflector elements. The inner and outer reflectors are made of respectively 61 and 156 columns. The reflectors above and below the core are composed of two layers. During normal operations, the core reactivity is controlled with 48 control rods. 36 of them, the operating control rods, are located in the inner annulus of the outer reflector.

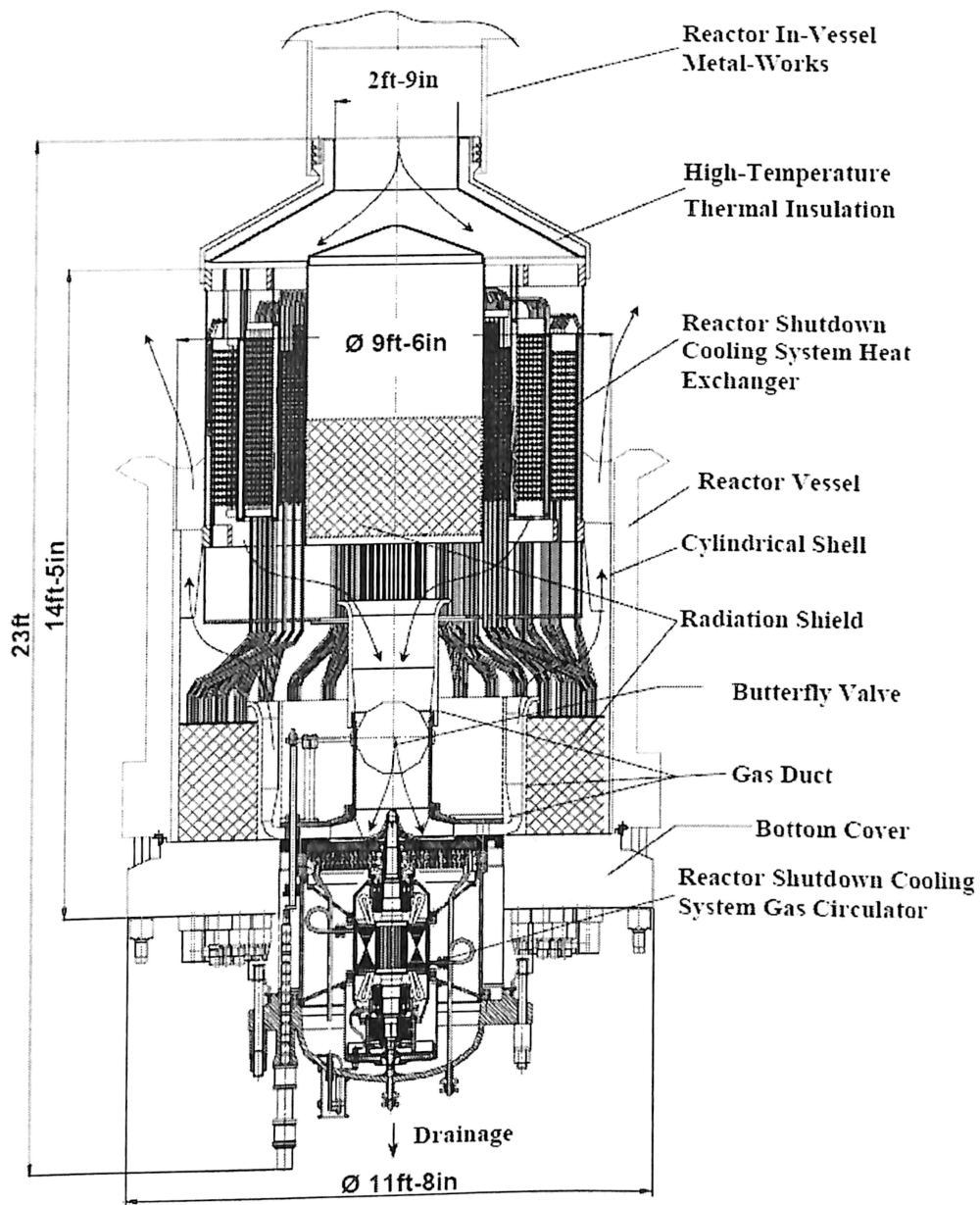


**Figure 5.6** Reactor Core Design for GT-MHR Plant

The 12 remaining control rods, the start-up one, are located in the inner radius of the active core. The startup control rods are fully withdrawn during normal operation of the reactor. They are only inserted during startup/shutdown and refueling operating modes. Only the control rods located outside of the active core are used during reactor operations [20]. For abnormal situations, eighteen columns in the active core also contain channels for reserve shutdown material. The reserve shutdown material consists

of boronated pellets stored above the core. The pellets are released in the active core if reactor scram is required. The core is designed to preclude exceeding the maximum stress design limits of graphite and metal in the core. The annular core concept associated with low-power density and length to diameter ratio around 2 was chosen because it is able to reject the passive heat passively as RSR stands for replaceable side reflector; PSR stands for permanent side reflector.

### **5.5 Compact Heat Exchanger**

The heat exchangers incorporated in the power conversion system of the HTGR, the recuperator need to have a high effectiveness, and superior mechanical characteristics as they operate under conditions of high pressure and high temperature. Furthermore, they are required to be as compact as possible to limit their size to enhance the plant layout. Many ways are used to classify heat exchangers [17]. For example, the fluid types (gas-gas, gas liquid, liquid-liquid), the flow arrangement (counter-flow, cross-flow), surface compactness, the construction type and industry are used. In a heat exchanger, the heat-exchanger surface (or matrix) is the structure in which heat transfer takes place from one fluid to another fluid. One of the fundamental characteristics of a heat exchanger surface is the surface area per unit of volume occupied by the surface. A “compact heat-exchanger surface” is defined as a surface configuration or matrix having a “large” surface area per unit of volume [10]. Usually, any matrix with an area density greater than  $328 \text{ m}^2/\text{m}^3$  is defined as compact matrix or compact surface. A compact heat exchanger is constructed from compact surfaces. a shell-and-tube type heat exchanger is too large to be economic without an extensive materials qualification for HTGR application. Therefore, in this work, the non-tubular compact heat exchanger will be considered as the base design for the recuperator [9]. Many current technologies of compact heat exchangers are available including plate fin, spiral, micro channels, and plate. Plate fin heat exchangers (PFHE) have been extensively used in applications such as industrial, natural gas liquefaction, air separation and hydrocarbon separation. The fins are brazed to the parting sheets and then the parting sheets are assembled to form a single block. The blocks are stacked and then the inlet and outlet headers are welded to

the blocks to construct a heat exchanger. Numerous fin configurations such as straight fin, straight perforated fin and serrated fin have been developed. Spiral heat exchangers (SHE) are often used in applications where a phase change occurs. In the SHE, the fundamental part is two metal plates welded together and rolled to form the flow passages [12]. Micro channel heat exchangers are heat exchangers in which the flow channels are around or less than 1 mm in diameter. The small channels are manufactured on flat plates by means of technologies such as chemical etching, micromachining or electron discharge machining. In the printed circuit heat exchanger, the plates are stacked and then diffusion bonded. Compared to other type heat exchangers, the micro channel heat exchanger is heavier if the sizes are the same. Plate heat exchangers (PHE) have been widely used in the applications of chemical, petrochemical, district heating and power industries. A PHE is constructed by the stacking of corrugated plates [8]. Different materials such as aluminum or stainless steel are used for different operating conditions and three technologies such as gaskets, welding and brazing can be used to ensure tightness. The applicable limits for different types of compact heat exchangers are shown in Table X. Note that the maximum pressure and maximum temperature cannot be reached simultaneously. Under HTGR conditions, a high pressure difference is imposed on the recuperator (>4MPa) and high temperature operation (no lower than 850°C) is required for the IHX. Thus, only welded, brazed or diffusion bonded heat exchangers can be used, as shown in Table 5.4.

**TABLE 5.4 OPERATING CONDITIONS FOR COMPACT HEAT EXCHANGERS**

<b>Technology</b>	<b>Max. Pressure (MPa)</b>	<b>Max. Temperature (°C)</b>	<b>Fouling</b>
Stainless steel plate fin heat Exchanger	8	650	No
Aluminum plate fin Heat exchanger	8-12	70-200	No
Ceramic plate fin heat exchange	0.4	1300	No
Spiral heat Exchanger	3	400	Yes
Diffusion bonded heat exchanger	50	800-1000	No
Brazed plate heat exchanger	3	200	No
Welded plate heat exchanger	3-4	300-400	Yes/No
Gasketed plate heat exchanger	2-2.5	160-200	yes

The thermal Effectiveness for a heat exchanger is defined by equation

$$E = \frac{T_4 - T_3}{T_1 - T_3} \quad (28)$$

Pressure drop in a heat exchanger is defined by

$$dP = \left[ \frac{DP_1}{P_1} + \frac{DP_2}{P_2} \right] \times 100 \quad (29)$$

Where DP equals inlet pressure minus outlet pressure

$$(P_2 - P_1) \times \text{safety margin} \quad (30)$$

Assuming the safety margin is about 10 %, a cold side design pressure in the range of 5.0 MPa to 6.6 MPa is anticipated. On the hot side the design pressure needs to be little more than the steam pressure drop. Based on normal operation design temperatures on both the hot and cold sides will be in the range of 550°C. Consideration must also be given to non design conditions, such as total unexpected loss of load on the power generator [4]. Brief temperature excursions perhaps as high as 800°C may occur, under these non-design conditions. Under these transient conditions as the temperature increases, so the differential pressure falls. The increasing temperature and consequent reduction in design stress is offset by the fall in pressure. It therefore seems reasonable to assume that an austenitic stainless steel such as SS316 will satisfy the design criteria for the direct cycle recuperator. Pressure vessel design codes such as ASME VIII Division 1 already allow the use of austenitic stainless steels such as SS316 to 815°C (1500°F) [25]. Although the majority of nuclear codes have not qualified austenitic stainless steels beyond the temperature requirements of Light Water Reactors. Material and mechanical considerations therefore restrict exchanger selection to those types that can be fabricated in austenitic stainless steel or equivalent and withstand pressures of up to 6.6 MPa. This almost certainly prohibits the use of those plate type exchangers where support is only provided at the edge of the plate. Use of those plate type exchangers will help in providing support is only provided at the edge of the plate. Design temperatures and pressures must be restricted such that the allowable design stress at temperature is at least twice the design pressure. The temperature limitations are shown in the figure 5.7 below.

### Alloy 800 HT

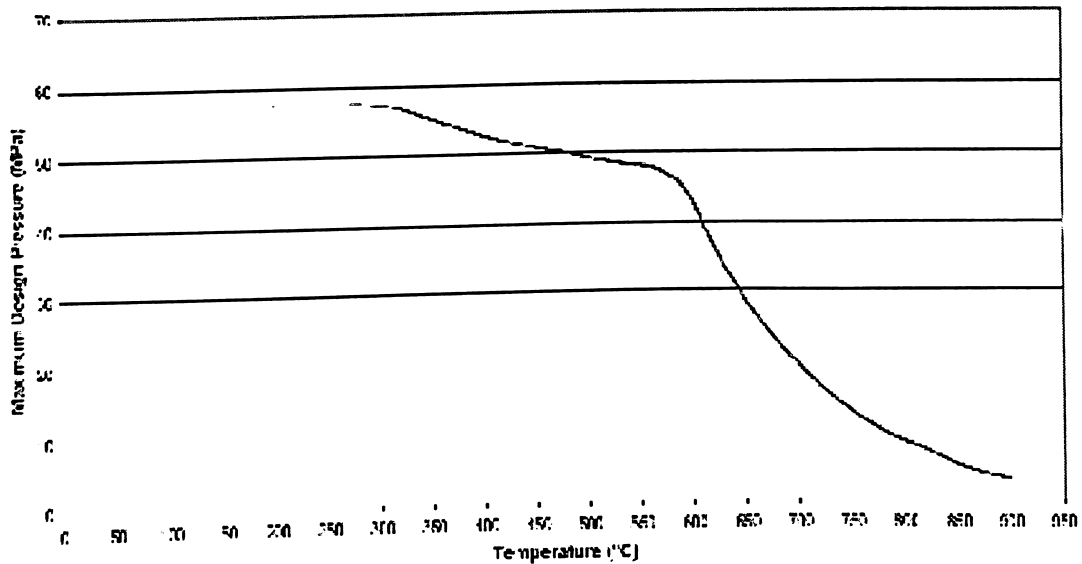


**Figure 5.7** Uranium Enrichment with respect to its work requirement

Consideration must also be given to differential pressure design, if the operating conditions are not to be limited to more moderate temperature and pressure combinations. As the fluids are independent, precautions will be necessary to maintain the correct pressure differential in the event of unscheduled upset. Whereas an upset in the direct cycle gives rise to thermal transient considerations, an upset in the indirect cycle will also result in pressure transient considerations [8]. What becomes apparent is that given the material and allowable stress considerations, only an exchanger type where all joints have parent (or near parent) properties should be considered. Brazed structures would almost certainly not be fit for purpose if proper consideration is given to mechanical and design life considerations.

#### 5.5.1 Thermal and Hydraulic Considerations

For both the direct and indirect cycles, the exchanger specifications require a thermal effectiveness of 95% or more; typically between 10 and 20 NTUs. Further, allowable pressure drops are low. This is particularly true for the direct cycle recuperator. Hence, irrespective of exchanger type, the hot and cold fluid contact arrangement will need to be predominantly counter current. Further, the flow length will almost certainly be

limited by pressure drop. As discussed in section 5.5, non compact heat exchangers for this type of duty will be excessively large 135 tonne per 10MW, implying a 11,475 tonne recuperator for a 850 MW (thermal) reactor. The majority of compact heat exchangers tend to be plate type, or plate variant [26]. Therefore we can conclude that the heat exchanger will be a plate type exchanger with counter current contact arrangement. However, no plate type exchanger can be truly counter current, as the plate must have width as well as length and the fluid must be introduced across the full width of the plate. Therefore every plate exchanger must have some cross flow component. Fluid introduction and the cross flow component can be handled in several ways. With conventional plate fin type exchangers a distributor is used on one or both of the streams.

## **5.6 Turbine - Compressor Analysis**

A key virtue of the gas turbine is very high power output relative to its size. Existing technologies applied to air-breathing gas turbines can be basically employed for closed cycle helium turbo machinery. Helium gas has been regarded as a proper choice for the GT-MHR gas turbine due to its radioactive stability and high thermal capacity. Although the helium gas turbine design follows the existing design practice for combustion gas turbines, there are obvious differences because of the physical properties of helium and the pressure condition in the nuclear application. The unique characteristics of the helium gas turbine are a shorter blade height and a larger number of stages compared with the air gas turbine. The shorter blade height leads to an increase in the leakage flow through the blade tip clearance, resulting in a higher loss in the efficiency [33]. A longer flow passage from a larger number of stages causes end-wall boundary layer growth and secondary flow, also resulting in a higher loss in the efficiency. As the hub-to-tip ratios of the helium compressor are high, around 0.9 throughout all the stages, consideration of secondary flow loss in the blading design is crucial for attaining better efficiency and a higher stall margin. Also, advanced blading techniques are needed to eliminate flow separation and a blade over chamber is required to compensate for flow distortion near the end-wall. The seal mechanism for helium is

also much more complex than that for air or steam. However, the helium gas turbine also offers important advantages; including a lower Mach number and a higher Reynolds number than the air-breathing gas turbine. As the flow in a compressor decelerates, the losses due to the tip clearance and secondary flow through the compressor can be more substantial than in the turbine. While the estimation of the losses in the air compressors is sufficiently accurate because of extensive related design and operating experiences, very limited experiences have been obtained with axial helium gas compressors. The present study focuses on helium gas turbines from a thermodynamic point of view [27]. Detailed discussion of the stress and vibration analysis or the design of magnetic bearings is beyond the scope of this thesis. In the present developed technology high-temperature gas-cooled reactors (HTGRs) are designed to work with closed Brayton cycle with helium gas as the working fluid. Thermodynamic performance of the axial-flow helium gas turbines is of critical concern as it considerably affects the overall cycle efficiency. Helium gas turbines pose some design challenges compared to steam or air turbo machinery because of the physical properties of helium and the uniqueness of the operating conditions at high pressure with low pressure ratio. We have developed a new through flow calculation code to calculate the design-point performance of helium gas turbines. Use of the method has been illustrated by applying it to the coolant flow in the turbine, which is developed in C++, for the code refer appendix J.

**Table 5.5** Design parameter of compressors

Unit	Air Breathing Compressors			Helium Compressors ( GT-MHR)		
	C135	C141	NACA	GT-HTR 300	LP	HP
Number of Stages	2	4	8	20	14	19
Design Pressure ratio	1.88	2.95	10.26	2.00	1.70	1.70
Inlet hub-tip Ratio	0.38	0.69	0.48	0.88	0.87	0.90
Exit Hub- to tip Ratio	0.57	0.81	0.90	0.91	0.88	0.90
Mass Flow/ Unit Annulus area (Kg/s-m <sup>2</sup> )	207	189	189	447	591	1141
Blade tip Speed (l", m/s)	423.0	362.0	356.0	321.0	301.7	245.8

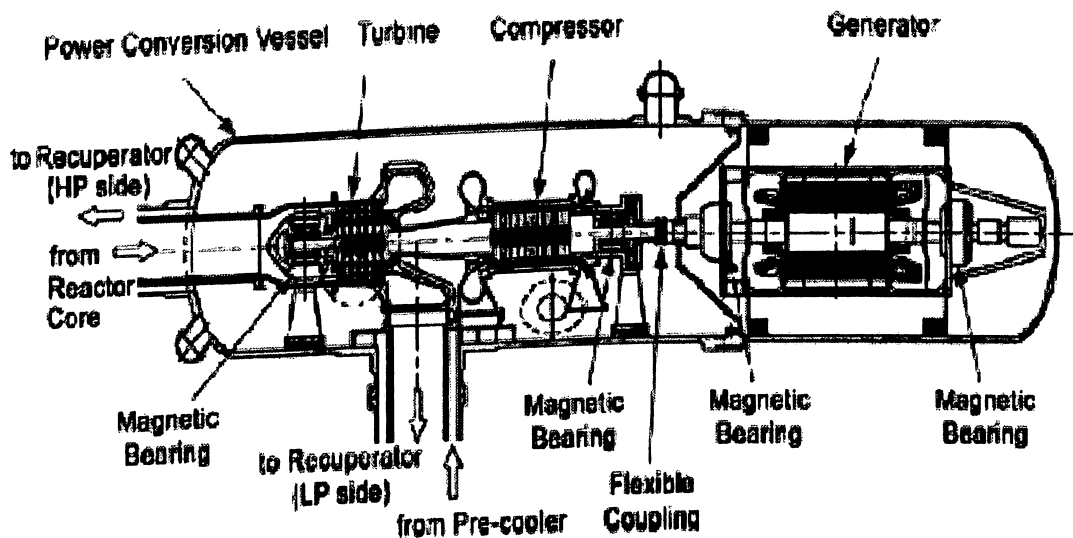


In this regard, helium gas turbines have been extensively investigated for reactor applications, particularly with respect to achieving high efficiency in electricity generation based on a closed Brayton cycle as a replacement for the conventional steam Rankine cycle. The Pebble Bed Modular Reactor (PBMR), the Gas Turbine Modular High Temperature Reactor (GT-MHR), and the Gas Turbine High Temperature Reactor of 850 MWe nominal capacities (GT-MHR 850) are representative programs employing the helium gas turbine cycle. A key virtue of the gas turbine is very high power output relative to its size [3]. Accordingly, gas turbines have been used for jet propulsion in aircrafts and power generation in power plants for many years, and considerable experience related to open cycle air-breathing gas turbines has been accumulated. Existing technologies applied to air-breathing gas turbines can be basically employed for closed cycle helium turbo machinery. Helium gas has been regarded as a proper choice for the HTGR gas turbine due to its radioactive stability and high thermal capacity [26]. Although the helium gas turbine design follows the existing design practice for combustion gas turbines, there are obvious differences because of the physical properties of helium and the pressure condition in the nuclear application. The unique characteristics of the helium gas turbine are a shorter blade height and a larger number of stages compared with the air gas turbine. The shorter blade height leads to an increase in the leakage flow through the blade tip clearance, resulting in a higher loss in the efficiency. A longer flow passage from a larger number of stages causes end-wall boundary layer growth and secondary flow, also resulting in a higher loss in the efficiency. As the hub-to-tip ratios of the helium compressor are high, around 0.9 throughout all the stages, consideration of secondary flow loss in the blading design is crucial for attaining better efficiency and a higher stall margin. Also, advanced blading techniques are needed to eliminate flow separation and a blade over camber is required to compensate for flow distortion near the end-wall [27]. The seal mechanism for helium is also much more complex than that for air or steam. However, the helium gas turbine also offers important advantages; including a lower Mach number and a higher Reynolds number than the air-breathing gas turbine. As the flow in a compressor decelerates, the losses due to the tip clearance and secondary flow through the

compressor can be more substantial than in the turbine. While the estimation of the losses in the air compressors is sufficiently accurate because of extensive related design and operating experiences, very limited experiences have been obtained with axial helium gas compressors

### 5.6.1 GT-MHR Helium Gas Turbines

For closed cycle gas turbines, helium is considered a promising working fluid because it has many favorable aspects for GT-MHR application. Helium is an inert gas that is non-corrosive and does not become radioactive. The cycle efficiency has a theoretical advantage owing to the high specific heat ratio of helium. The choice of working fluid significantly influences not only the cycle efficiency but also the system compactness [13]. Additionally, the heat exchanger design also is advantageous because the thermal conductivity and heat transfer coefficient for helium are higher than those for air. On the other hand, helium leakage could easily occur due to its low molecular weight and thus reliable sealing of the system is imperative. As outlined above, HTGR helium gas turbines differ from other gas turbines using air or combustion gases. The arrangement of turbo machinery is shown in the figure 5.8.



(Source: Gas Turbines Text book, V Ganesan)

Figure 5.8 Turbine and Compressor Arrangement on shaft

### **5.6.2 General Features of Helium Gas Turbines**

The fluid properties of helium strongly influence the size, geometries, and performance of gas turbine. High pressure operation is needed to achieve a compact power conversion system in the GT-MHR. The helium gas turbines have high hub-to-tip ratios throughout the machine because the rotational speed is restricted to the synchronous speed when the turbo machines are directly connected to the generator. A comparison of the design parameters between air breathing compressors and HTGR helium compressors is given in Table below. Although helium compressors are operating at a low pressure ratio, the specific heat and specific heat ratio are high, and consequently the compressor needs a large number of stages to achieve the required pressure ratio [20]. These design features unfavorably affect the aerodynamic performance. A low blade aspect ratio tends to increase the secondary flow and tip leakage flow, and many stages tend to increase the end-wall boundary layer growth and secondary flow. On the other hand, it is possible to provide higher circumferential speeds without approaching the sonic range due to the high sonic velocity of helium. In addition, shock loss also can be neglected in the design point operation.

### **5.6.3 PBMR Turbo Machinery**

The design of the power conversion unit (PCU) of the PBMR has been modified several times. In the original design, the PBMR power conversion unit has a 3-shaft vertical arrangement including a LP turbo-unit, HP turbo unit, and a power turbine with a generator, as shown in Fig 5.9. Each rotor is housed in each vessel [24]. This necessitates smaller capacity of the axial magnetic bearing and its associated catcher bearing, small temperature and pressure variations, and shorter rotor length due to multi-rotors. This type of system is shown in the figure 5.9. The issues raised in the vertical multi-shaft configuration are cost problems, an over speed problem in the case of load rejection, and pressure seal and reliability in the structural design because of complicated flow pass. A single shaft horizontal arrangement is adopted the low cycle pressure ratio simplifies the gas turbine mechanical design with optimum cycle without an intercooler.

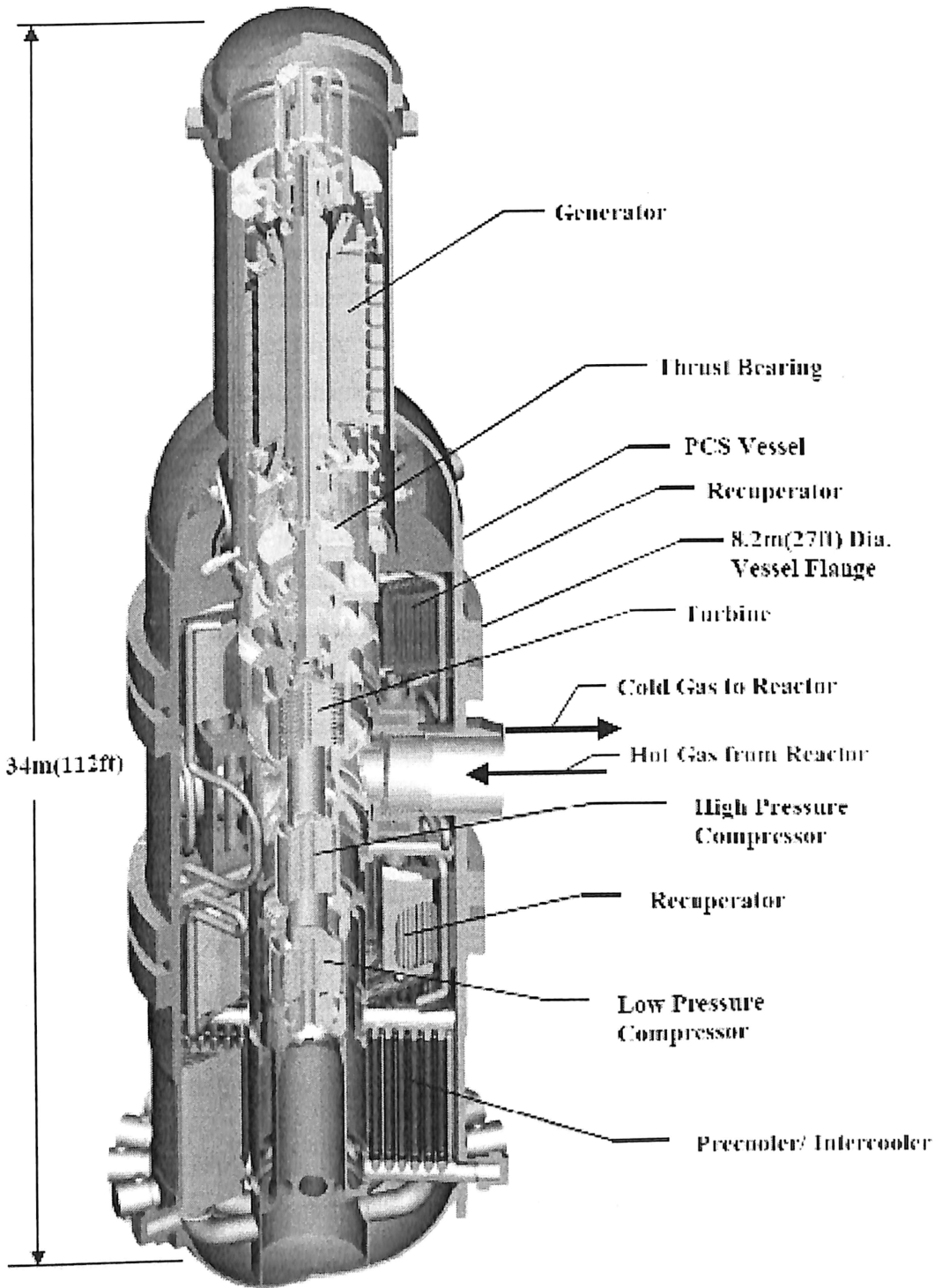


**Figure 5.9** BMR Power Conversion System

## CHAPTER 6

### MATERIAL ANALYSIS FOR HELIUM COOLED REACTORS

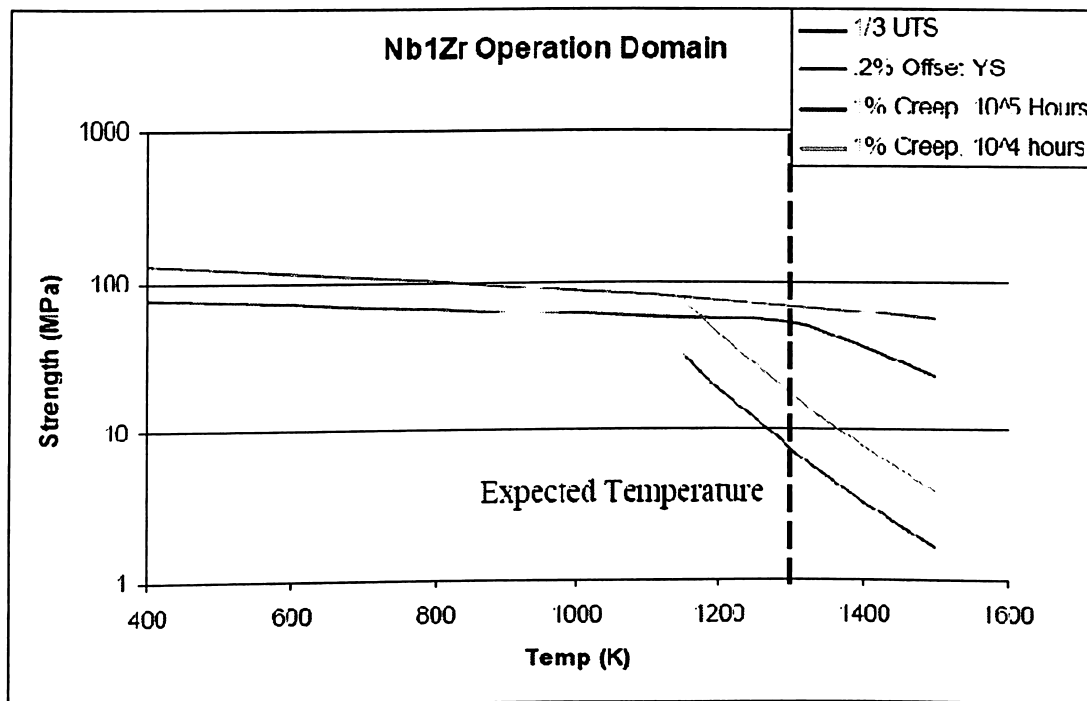
In gas cooled reactors selection materials plays an important role in terms of its core selection and radiation shielding, biological shielding. Material properties selection and design is based on international nuclear safety center data base from experimental data of words commercial reactors. In material selection point of view from different sources the focus is more on Light water reactors and initial emphasis on high priority properties of materials. In this chapter we have taken a special approach in analyzing the special properties required for the helium cooled reactors. A list of properties for each material and the phases to be considered are determined based on a needs assessment. The longer-term goal is to include data that will meet future needs such as materials used in evolutionary reactor designs, properties of extended burn up fuel, and possibly properties of mixed oxide fuels. A variety of relevant properties at the estimated temperatures for the given material will also be examined. There are three general classes of materials in the reactor: Metals, Ceramics, and Gasses.

#### 6.1 Niobium 1% Zirconium

Niobium 1% zirconium is an alloy of 99% niobium and 1% zirconium with a melting point of Nb1Zr is 2673 K and a density of 8.64 g/cc at room temperature Nb1Zr is a robust alloy that retains its strength up to high temperatures. The nominal temperature limit for the alloy is 1350 K. The expected peak temperature for Nb1Zr as a cladding is 1300 K, below its nominal limit [1].

##### 6.1.1 Mechanical Properties

Figure 6.1 shows the operational domain of Nb1Zr with vertical line showing the expected operating temperature 1300 K. This chart represents minimum values expected for Nb1Zr. Several other sources listed higher values for both the yield strength and tensile strength [15]. This plot shows that at the expected temperatures, the maximum yield strength is roughly 68 MPa and the 1/3 tensile strength limit is 52 MPa.



(Source: Nuclear Materials Handbook, IAEA publication, may 2008)

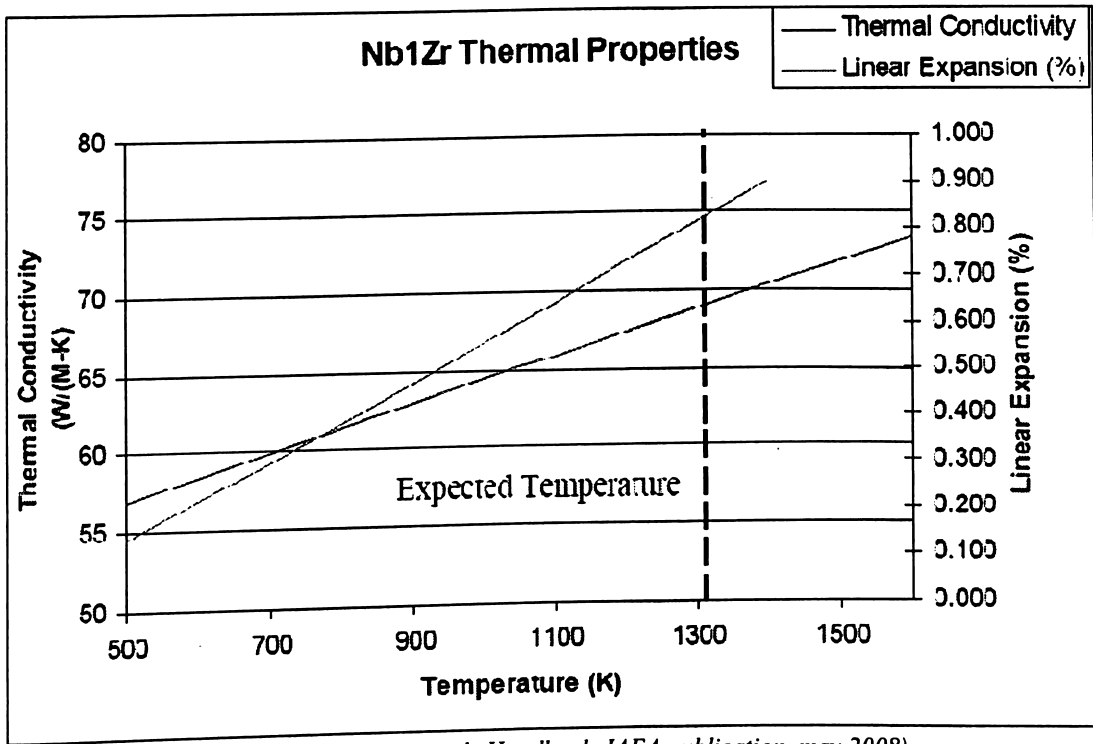
**Figure 6.1** Niobium 1 % Zirconium Mechanical Properties

In any event, at the desired temperatures, neither of these properties is the limiting factor; creep strength is. The 1% creep strengths of Nb1Zr in a liquid lithium environment are also shown in Figure (x). While the Nb1Zr will be in a He environment, it was the best data available. The 1% creep limit at 105 hours shows the stress limit on the niobium 1% zirconium is about 7.38 MPa [15]. Of the possible limiting stresses for the metal this is the lowest at 1300 K and thus becomes the limiting property for Niobium 1% Zirconium.

### 6.1.2 Thermal Properties

The thermal conductivity of Nb1Zr at 1300 K is 69 W/m-K. The linear expansion of Nb1Zr at 1300 K is 1% . Figure 6.2 shows linear expansion and thermal conductivity as a function of temperature. There are some limitations to Nb1Zr based alloys. At high temperatures Niobium oxidizes rapidly in atmospheres containing oxygen, resulting in significant embrittlement this restricts the use of Nb1Zr when in contact with most atmospheres [19]. These limitations preclude the use of Nb1Zr on the outside surfaces of

the reactor. The strength of Nb1Zr is also limited. There has been little indication that such a breakthrough has been made to date.



(Source: Nuclear Materials Handbook, IAEA publication, may 2008)

Figure 6.2 Niobium 1 % Zirconium Thermal Properties

There is a slight variant called PWC-11 that introduces 0.1% carbon into the Nb1Zr alloy. This increases the creep strength properties by 30-40% while not changing the thermal properties [9]. It would probably merit further investigation as a material choice.

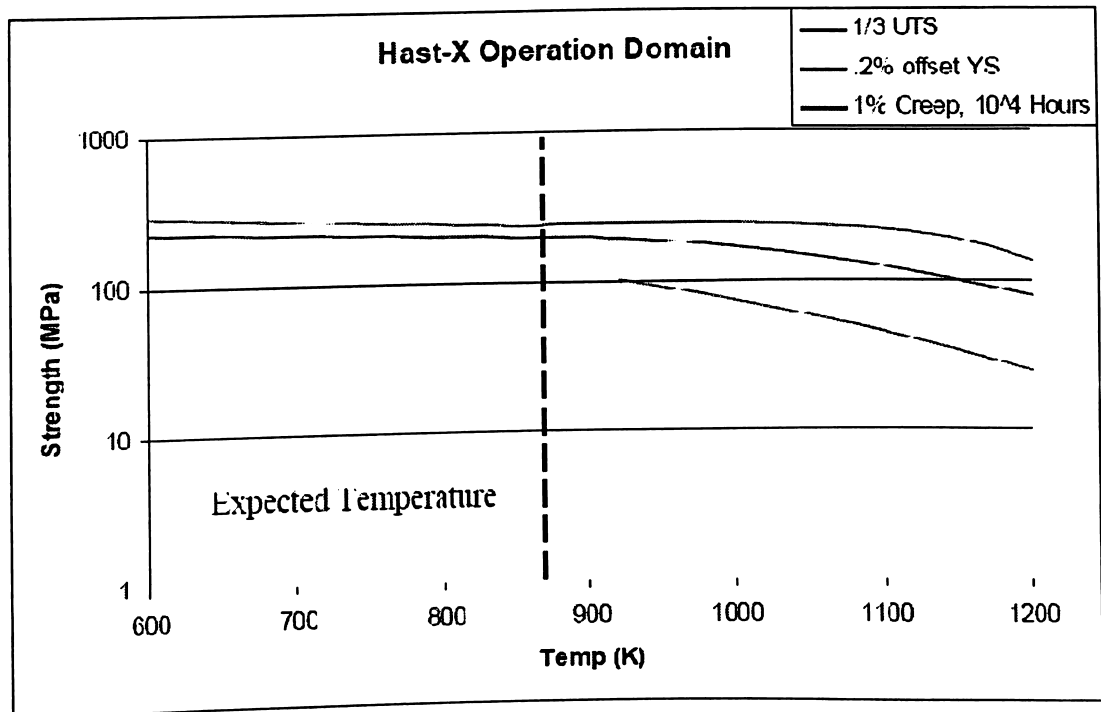
## 6.2 Hastelloy X

Hastelloy X (HastX) is a nickel-based super alloy used in a variety of applications. Its composition is 49% nickel, 22% chromium, 18% iron, 9% molybdenum, 1.5% cobalt and 0.5% tungsten. The melting point of HastX is about 1530 K, and it has a density of 8.22 g/cc. This material has been suggested as a possible reactor material for a variety of reasons. HastX is a material with decent high temperature characteristics [19]. Hastelloy is also noted for excellent corrosion, oxidation and carburization resistance at the desired temperatures. Finally, Hastelloy-X is a commonly used metal whose properties

are well understood. The expected peak temperature of Hastelloy-X is roughly 875 K when used for the pressure vessel of the reactor.

### 6.2.1 Mechanical Properties

Figure x shows the Yield Strength, 1/3 UTS, and 1% creep at 10000 hours (Approximately 1 year).



(Source: Nuclear Materials Handbook, IAEA publication, may 2008)

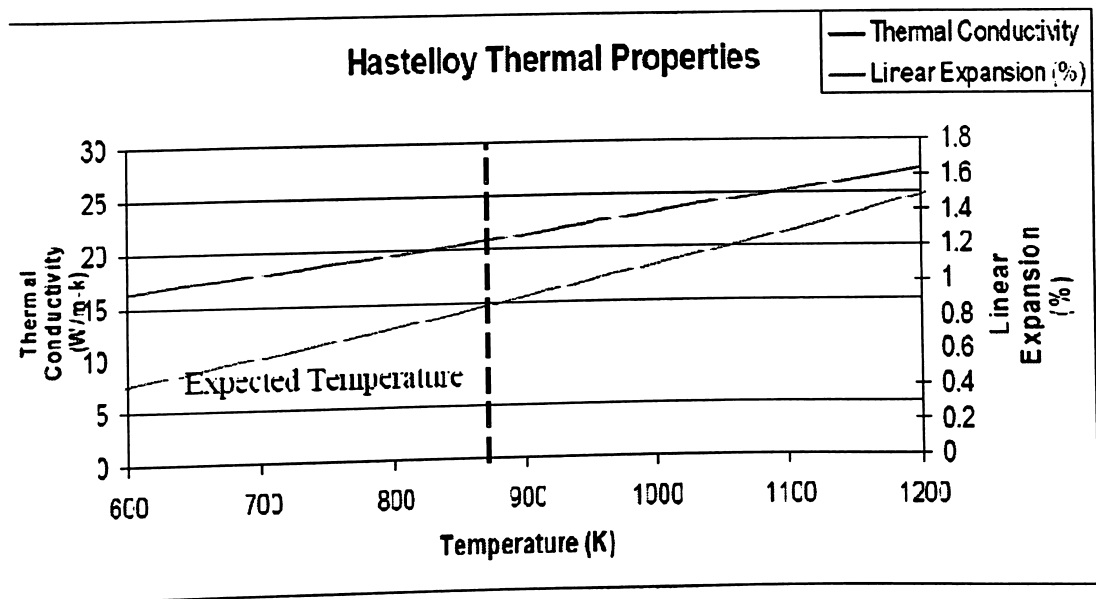
Figure 6.3 Hast-X Mechanical Properties

There are some notable limitations to this data. The 1% creep data for 10<sup>5</sup> hours was not available. The 10<sup>4</sup> hours creep data did not extend to the desired temperatures. The 1/3 UTS is roughly 195 MPa and the 0.2% offset yield strength was 245 MPa at 860 K [8]. In all likelihood, all three limits are close to the same value at the expected operation temperature. The creep strength is constraint most likely to be exceeded.

### 6.2.2 Thermal Properties

The thermal conductivity of HastX is 20.8 W/m-K at 860K and the linear expansion is 0.8%, as shown in Figure 6.4.





(Source: Nuclear Materials Handbook, IAEA publication, may 2008)

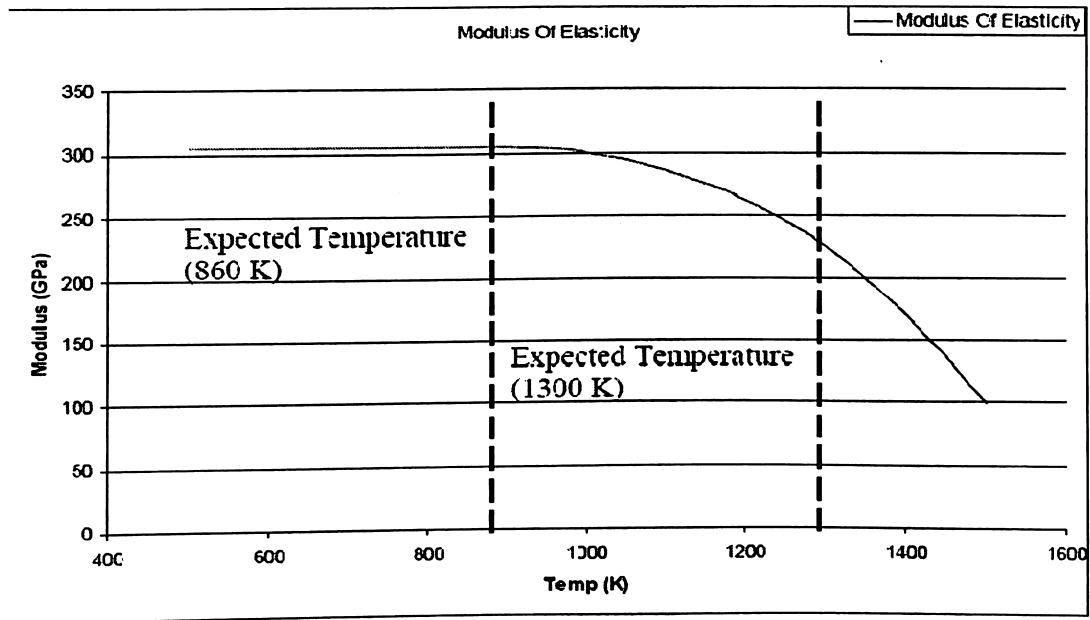
Figure 6.4 Hast-X Thermal Properties

### 6.3 Beryllium Oxide

BeO is a ceramic with a 1-to-1 atom ratio of beryllium to oxygen. It is primarily used in the nuclear field as a neutron reflector. The oxygen component results in BeO being an extremely good scattering material as it has a very high scattering to absorption cross section ratio. In addition to being a reflector, there is an n-2n reaction in beryllium that increases neutron numbers, increasing this material's attractiveness [6]. BeO will be located in two different regions of the core with drastically different temperatures. In the individual fuel pins, axial reflectors of 5 cm BeO at the pin ends will be at around 1300 K. The radial reflectors will be at some temperature between 860 K and the environmental temperature.

#### 6.3.1 Mechanical Properties

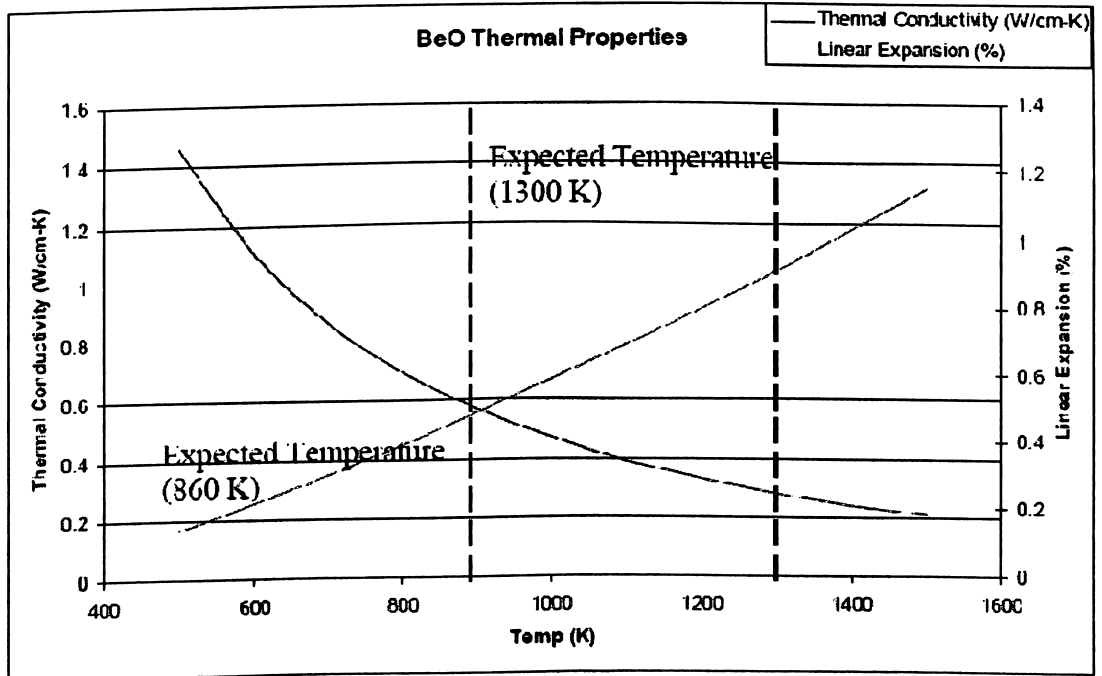
For the material beryllium oxide the modulus of elasticity in the operating range of 860 K is 300 Gpa, when in the higher temperature range at 1300 k is will be 225 Gpa. In the extreme condition it will still fall below 100 Gpa at near to the 1600 k temperatures. For the good results the operating range is between 860k to 1300 k.



(Source: Nuclear Materials Handbook, IAEA publication, may 2008)

Figure 6.5 BeO Mechanical Properties

### 6.3.2 Thermal Properties



(Source: Nuclear Materials Handbook, IAEA publication, may 2008)

Figure 6.6 BeO Thermal Properties

BeO has a thermal conductivity of 0.635 W/cm-K at 860 K and 0.28 W/cm-K at 1300 K. The linear expansion is 0.45% at 860 K and 0.912% at 1300 K.

## 6.4 Rhenium

Rhenium is a super dense refractory metal that will be used in a non-structural capacity in the reactor. Its melting point is 3459 K, and its density is 21 g/cc. There are a variety of characteristics of rhenium that make its use a challenge. There seems to be a great deal of variability in the mechanical properties of rhenium, depending greatly on the methods used to prepare the sample. All of these things complicate any attempt to use it in the reactor, but the amount of rhenium in the core is limited and not used in a structural capacity. Rhenium is used as a liner 0.062 cm thick between the cladding and the fuel [4]. Thermally speaking, there is an almost negligible drop of temperature across the liner. Rhenium is not used as a structural material so its mechanical properties are not that important. The thickness of the rhenium layer is so thin that its thermal properties have a minimal impact on the core.

### 6.4.1 Attractive Features

One of its attractive features of rhenium is that it is a spectral shift absorber (SSA), which means that it has a low relative absorption cross section for fast neutrons; while in the thermal spectrum its absorption cross section increases dramatically. This has safety applications for the reactor design in accident scenarios. Rhenium has an absorption cross section of in the fast spectrum, however the magnitude of the difference between the absorption cross section and the fast fission cross section of  $^{235}\text{U}$  is low compared to the difference at a thermal spectrum. It also provides a barrier that protects Niobium 1% Zirconium from nitrogen attack and damage caused by other fission products that outgas from the fuel [3]. Most of the other SSA materials have a relatively low melting point, making them less attractive. So not only high-temperature, high fast-flux resistant materials will have to be utilized but also with high mechanical impingement structural resistance. However the refractory metals have poor neutronic properties. In summary, the current design results show that while cold fingers are an option, it would be difficult

to reach the power density range of 100 w/cc without additional passive safety mechanisms and there will be a challenging materials development effort.

## 6.5 Crystal Structures

Metallic materials exhibit a crystal structure they are formed by an elementary unit, periodically repeating across space, known as a unit cell, consisting of atoms, in precise, definite numbers and positions. Repetition of such structures endows them with specific properties. Three of these structures, defining the position of the atoms, are of importance. The body centred cubic structure (that found in iron at ambient room temperature, chromium, vanadium); such materials as a rule exhibit a ductile–brittle behaviour transition, depending on temperature. The face centred cubic structure (nickel, aluminium, copper, and iron at high temperature). The hexagonal structure (that of zirconium, or titanium). Depending on temperature and composition, the metal will structure itself into elementary crystals, the grains, exhibiting a variety of microstructures, or phases. The way these arrange themselves has a major influence of the properties exhibited by metals, steels in particular [23]. The ferrite of pure iron, with a body centred cubic structure, turns into austenite; a face centred cubic structure, above 910 °C. Martensite is a particular structure, obtained through tempering, which hardens it, followed by annealing, making it less brittle. Bainite is a structure intermediate between ferrite and martensite, likewise obtained through tempering followed by annealing. Among metals, high-chromium-content (more than 13%) stainless steels, exhibiting as they do a corrosion and oxidation resistance that is due to the formation of a film of chromium oxide on their surface, take the lion's share [8]. If the criterion for stainless ability (rust proof ness) is taken to be chromium content, which should be higher than 13%, such steels fall into three main categories: ferritic steels, austenitic steels, and austenitic–ferritic steels.

### 6.5.1 Steel Families

Ferritic steels, exhibiting a body-centred cubic structure (e.g. F17), are characterized by a low carbon concentration (0.08–0.20%), and high chromium content. As a rule containing no nickel, these are iron–chromium, or iron–chromium–

molybdenum alloys, with a chromium content ranging from 10.5% to 28%: they exhibit no appreciable hardening when tempered, only hardening as a result of work hardening. They exhibit a small expansion coefficient, are highly oxidation resistant, and prove suitable for high temperatures. In the nuclear industry, 16MND5 bainitic steel, a low-carbon, low-alloy (1.5% manganese, 1% nickel, 0.5% molybdenum) steel, takes pride of place, providing as it does the vessel material for French-built PWRs, having been selected for the qualities it exhibits at 290 °C, when subjected to a fluence of  $3 \cdot 10^{19} \text{ n cm}^{-2}$ , for neutrons of energies higher than 1 MeV [44].

### 6.5.2 Martensitic Steels

Martensitic exhibiting a body-centered cubic structure, are ferritic steels containing less than 13% chromium (9–12% as a rule), and a maximum 0.15% carbon, (1) Ceramics are used on their own, or incorporated into composites, which may be of the cercer (a ceramic held in a matrix that is also a ceramic) or cermet (a ceramic material embedded in a metallic matrix) types. With regard to nuclear fuel, this takes the form of a closely mixed composite of metallic products, and refractory compounds, the fissile elements being held in one phase only, or in both. Which have been subjected to annealing, they become Martensitic when quenched, in air or a liquid, after being heated to reach the austenitic domain [39]. They subsequently undergo softening, by means of a heat treatment. They may contain nickel, molybdenum, along with further addition elements. These steels are magnetic, and exhibit high stiffness and strength, however they may prove brittle under impact, particularly at low temperatures. They have gained widespread use in the nuclear industry (fastenings, valves and fittings...), owing to their good corrosion resistance, combined with impressive mechanical characteristics [40].

### 6.5.3 Austenitic Steels

Austenitic steel characterized by a face centred cubic structure, contain some 17–18% chromium, 8–12% nickel (this enhancing corrosion resistance: the greater part, by far, of stainless steels are austenitic steels), little carbon, possibly some molybdenum, titanium, or niobium, and, mainly, iron (the remainder) [6]. They exhibit remarkable ductility, and toughness, a high expansion coefficient, and a lower heat conductivity

coefficient than found in ferritic– martensitic steels. Of the main grades (coming under US references AISI(2) 301 to 303, 304, 308, 316, 316L, 316LN, 316Ti, 316Cb, 318, 321, 330, 347), 304 and 316 steels proved particularly important for the nuclear industry, before being abandoned owing to their excessive swelling under irradiation. Some derivatives (e.g. 304L, used for internal structures and fuel assembly end-caps, in PWRs; or 316Ti, employed for claddings) stand as reference materials [18]. In fast reactors, they are employed, in particular, for the fabrication of hexagonal tubes (characteristic of reactors of the Phoenix type) (316L[N] steel), while 15/15Ti austenitic steel has been optimized for fuel pins for this reactor line, providing the new cladding reference for fast reactors.

#### **6.5.4 Austenitic–Ferritic Steels**

Austenitic ferritic steels, containing 0%, 8%, 20%, 32%, or even 50% ferrite, exhibit good corrosion resistance, and satisfactory weldability, resulting in their employment, in molded form, for the ducts connecting vessels and steam generators. One class of alloys that is of particular importance for the nuclear industry is that of nickel alloys, these exhibiting an austenitic structure. Alloy 600 (Inconel 600, made by INCO), a nickel (72%), chromium (16%), and iron (8%) alloy, further containing cobalt and carbon, which was employed for PWR steam generators (along with alloy 620) and vessel head penetrations, was substituted, owing to its poor corrosion resistance under stress, by alloy 690, with a higher chromium content (30%). For certain components, Inconel 706, Inconel 718 (for PWR fuel assembly grids), and Inconel X750 with titanium and aluminium additions have been selected, in view of their swelling resistance, and very high mechanical strength [43]. For steam generators in fast reactors such as Phoenix, alloy 800 (35% nickel, 20% chromium, slightly less than 50% iron) was favoured. Alloy 617 (Ni–Cr–Co–Mo), and alloy 230 (Ni–Cr–W), widely employed as they are in the chemical industry, are being evaluated for gas-cooled VHTRs.

#### **6.5.5 Ferritic–Martensitic Steels (F–M Steels)**

Ferritic–Martensitic steels (F–M steels) exhibit a body-centred cubic structure. In effect, this category subsumes the Martensitic steel and ferritic steel families. These steels combine a low thermal expansion coefficient with high heat conductivity.

Martensitic or ferritic steels with chromium contents in the 9–18% range see restricted employment, owing to their lower creep resistance than that of austenitic steels. Fe–9/12Cr Martensitic steels (i.e. steels containing 9–12% chromium by mass) may however withstand high temperatures, and are being optimized with respect to creep [4]. For instance, Fe–9Cr 1Mo molybdenum steel might prove suitable for the hexagonal tube in SFR fuel assemblies. Under the general designation of AFMSs (advanced ferritic–martensitic steels), they are being more particularly investigated for use in gas-cooled fast reactors.

#### **6.5.6 Oxide-Dispersion-Strengthened (ODS) Ferritic and Martensitic Steels**

Oxide-dispersion strengthened (ODS) ferritic and Martensitic steels were developed to combine the swelling resistance exhibited by ferritic steels, with a creep resistance in hot conditions at least equal to that of austenitic steels. They currently provide the reference solution for fuel cladding, for future sodium-cooled reactors. The cladding material in light-water reactors, for which stainless steel had been used initially, nowadays consists of a zirconium alloy, selected for its “transparency” to neutrons, which exhibits a compact hexagonal crystal structure at low temperature, a face-centered cubic structure at high temperature [8]. The most widely used zirconium–iron–chromium alloys are tin-containing Zircalloys (Zircaloy-4 in PWRs, Zircaloy-2 in BWRs, ZrNb – containing niobium – in the Russian VVER line), owing to their outstanding behavior under radiation, and capacity with respect to creep in hot conditions. After bringing down tin content, in order to improve corrosion resistance, a zirconium–niobium alloy is presently being deployed for such cladding. Among nuclear energy materials, graphite calls for particular mention: along with heavy water, it is associated with reactors that must operate on natural uranium; it proves advantageous as a moderator, as being a low neutron absorber [42]. For GFRs, novel ceramics, and new alloys must be developed, to the margins of high fluences. Researchers are storing high hopes on refractory materials containing no metals. In particle fuels, uranium and plutonium oxides are coated with several layers of insulating pyrocarbons, and/or silicon carbide (SiC), possibly in fibrous form (SiCf). These are known as coated particles (CPs). While SiC-coated UO<sub>2</sub>, or MOX balls stand as the reference, ZrC coatings might

afford an alternative. At the same time, conventional sintered uranium oxide (and plutonium oxide, in MOX) pellets might be supplanted by advanced fuels, whether featuring chromium additions or otherwise, with the aim of seeking to overcome the issues raised by pellet cladding interaction, linked as this is to the ceramic fuel pellet's tendency to swell under irradiation. Oxides might be supplanted by nitrides (compatible with the Purex reprocessing process), or carbides, in the form e.g. of uranium–plutonium alloys containing 10% zirconium [44].

## 6.6 Fuel Materials

The specific conditions attributable to radiation conditions prevailing inside nuclear reactors mean it is imperative to look to materials exhibiting special characteristics, which may be grouped under two main categories: cladding and structural materials, on the one hand, and fuel materials, on the other [41]. The characteristics, in terms of resistance to temperature, pressure, fatigue, heat, corrosion, often under stress, that should be exhibited, as a general rule, by materials involved in any industrial process must, in the nuclear energy context, be virtually fully sustained, notwithstanding the effects of irradiation, due in particular to the neutron flux. Indeed, irradiation speeds up, or amplifies processes such as creep (irradiation creep), or causes other ones, such as swelling, or growth, i.e. an anisotropic deformation occurring under the action of a neutron flux, in the absence of any other stress [39]. Structural materials in the reactor itself are subject, in particular, to the process of activation by neutron bombardment, or bombardment by other particles (photons, electrons). Materials employed for fuel structures (assemblies, claddings, plates, and so on) are further subjected to yet other stresses. Finally, the fuel itself is a material, taking the form, in current light-water reactors, for instance, of sintered uranium and/or plutonium ceramics, in the form of pellets.

A fissile material is composed of nuclides for which fission is possible with neutrons of any energy level. What is especially significant about these nuclides is their ability to be fissioned with zero kinetic energy neutrons (thermal neutrons). Thermal



neutrons have very low kinetic energy levels (essentially zero) because they are roughly in equilibrium with the thermal motion of surrounding materials. Therefore, in order to be classified as fissile, a material must be capable of fissioning after absorbing a thermal neutron. Consequently, they impart essentially no kinetic energy to the reaction. Fission is possible in these materials with thermal neutrons, since the change in binding energy supplied by the neutron addition alone is high enough to exceed the critical energy [6]. Some examples of fissile nuclides are uranium-235, uranium-233, and plutonium-239. A fissionable material is composed of nuclides for which fission with neutrons is possible. All fissile nuclides fall into this category. However, also included are those nuclides that can be fissioned only with high energy neutrons. The change in binding energy that occurs as the result of neutron absorption results in a nuclear excitation energy level that is less than the required critical energy [18]. Therefore, the additional excitation energy must be supplied by the kinetic energy of the incident neutron. The reason for this difference between fissile and fissionable materials is the so-called odd-even effect for nuclei. It has been observed that nuclei with even numbers of neutrons and/or protons are more stable than those with odd numbers. Therefore, adding a neutron to change a nucleus with an odd number of neutrons to a nucleus with an even number of neutrons produces an appreciably higher binding energy than adding a neutron to a nucleus already possessing an even number of neutrons. Some examples of nuclides requiring high energy neutrons to cause fission are thorium-232, uranium-238, and plutonium-240. Table indicates the critical energy ( $E_{crit}$ ) and the binding energy change for an added neutron ( $\Delta BE_n$ ) to critical target nuclei of interest [4]. For fission to be possible, the change in binding energy plus the kinetic energy must equal or exceed the critical energy

$$\Delta BE + KE \geq E_{crit} \quad (31)$$

Uranium-235 fissions with thermal neutrons because the binding energy released by the absorption of a neutron is greater than the critical energy for fission; therefore uranium-235 is a fissile material [8]. The binding energy released by uranium-238 absorbing a thermal neutron is less than the critical energy, so additional energy must be possessed by the neutron for fission to be possible. Consequently, uranium-238 is a fissionable material.

**TABLE 6.1 CRITICAL ENERGIES COMPARED TO BINDING ENERGY OF LAST NEUTRON**

Target Nucleus	Critical Energy $E_{\text{crit}}$	Binding Energy of last Neutron $BE_n$	$BE_n - E_{\text{crit}}$
${}^{232}_{90}\text{U}$	7.5 MeV	5.4 MeV	-2.1 MeV
${}^{238}_{92}\text{U}$	7.0 MeV	5.5 MeV	-1.5 MeV
${}^{235}_{92}\text{U}$	6.5 MeV	6.8 MeV	+0.3 MeV
${}^{233}_{92}\text{U}$	6.0 MeV	7.0 MeV	+1.0 MeV
${}^{239}_{94}\text{Pu}$	5.0 MeV	6.6 MeV	+1.6 MeV

In Helium cooled reactors uranium with high percentage of enrichment will give better result in fission reaction point of view. Uranium found in nature consists largely of two isotopes, U-235 and U-238. The production of energy in nuclear reactors is from the 'fission' or splitting of the U-235 atoms, a process which releases energy in the form of heat. U-235 is the main fissile isotope of uranium [3]. Natural uranium contains 0.7% of the U-235 isotope. The remaining 99.3% is mostly the U-238 isotope which does not contribute directly to the fission process. Uranium-235 and U-238 are chemically identical, but differ in their physical properties, notably their mass. The nucleus of the U-235 atom contains 92 protons and 143 neutrons, giving an atomic mass of 235 units. The U-238 nucleus also has 92 protons but has 146 neutrons - three more than U-235, and therefore has a mass of 238 units. The difference in mass between U-235 and U-238 allows the isotopes to be separated and makes it possible to increase or "enrich" the percentage of U-235 [9]. All present enrichment processes, directly or indirectly, make use of this small mass difference. Uranium is a metal of high density (18.9 g/cm<sup>3</sup>). The earth's crust contains an average of about 3 ppm (= 3 g/t) uranium and seawater approximately 3 ppb (=3mg/t). Naturally occurring uranium consists of three isotopes, all of which are radioactive: U-238, U-235, and U-234. U-238 and U-235 are the parent nuclides of two independent decay series, while U-234 is a decay product of the U-238 series. The critical energy for these materials are tabulated in the table 6.1 among them

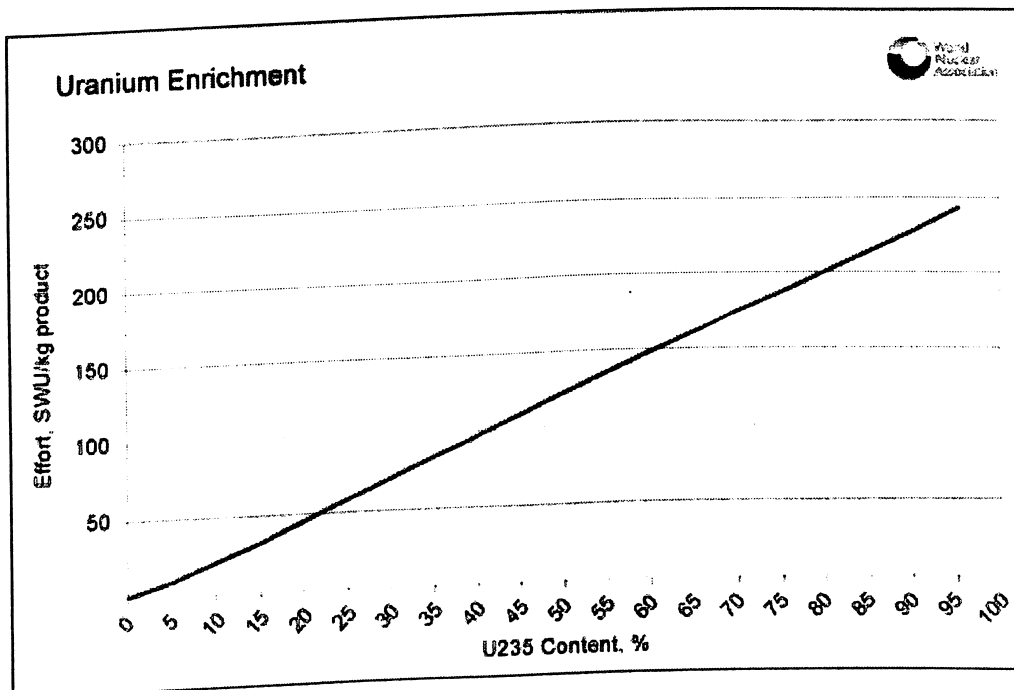
U-232. The last neutrons binding energy is more for the Pu-239 and their difference is also more for the same compound.

**TABLE 6.2 PROPERTIES OF DIFFERENT URANIUM ISOTOPES**

Parameters	U-234	U-235	U-238
Half-Life	244,500 years	$703.8 \times 10^6$ years	$4.468 \times 10^9$ years
Specific Activity	231.3 MBq/g	80,011 Bq/g	12445 Bq/g
Atom %	0.0054%	0.72%	99.275%
Weight%	0.0053%	0.711%	99.284%
Activity %	48.9%	2.2 %	48.9%
Activity 1 g $U_{nat}$	12,356 Bq	568 Bq	12356 Bq

### 6.6.1 Uranium Enrichment

Uranium enrichment is a process of improving the quality of the fuel for better performance. Uranium which exists in nature consists of 0.72 percent. There are two approaches for more isolation of separation of  $U^{235}$  and  $U^{238}$  by a gaseous diffusion process or production of pu-239 from  $U^{238}$  by breeding [11]. But in order to enrich fuel there are also efforts required in terms of input energy the graph shown in the figure 76.

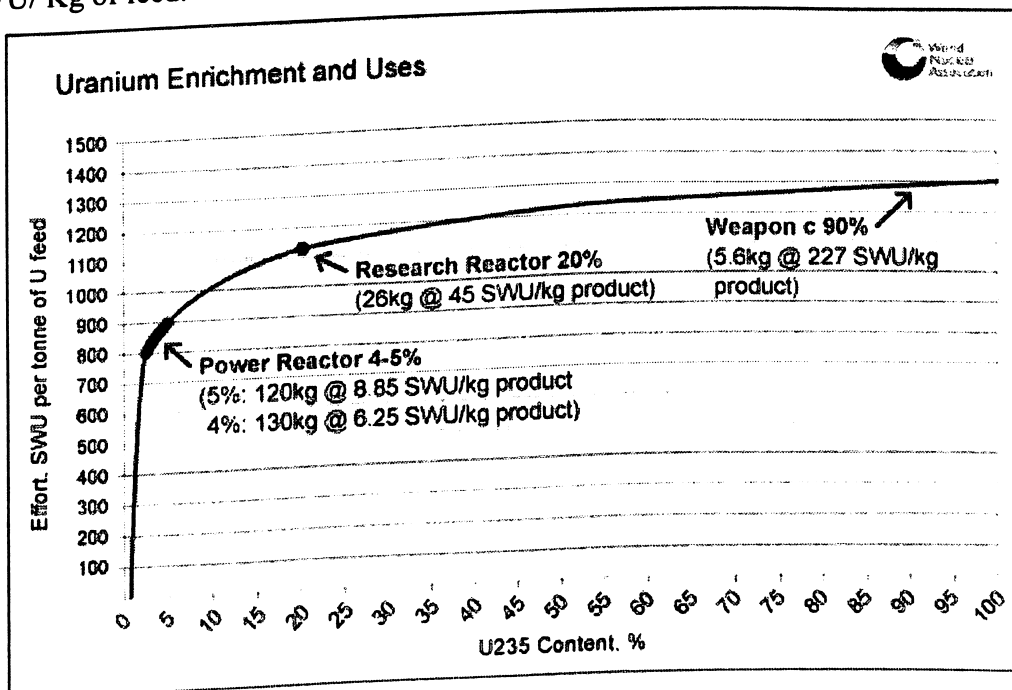


(Source: WNA, Nuclear Energy Fuel Enrichment data2011)

Figure 6.7 Uranium Enrichment with respect to its work requirement

### 6.6.2 Enrichment for Helium Cooled Reactors

According to the application of the nuclear fuel the enrichment level and the method also will change. Due to its higher cost in enrichment process it is limited depending upon the primary quality and the major issues related with the process will be taken into consideration in percentage of enrichment selection. The detailed analysis is shown in the figure 6.7, for the power reactors the enrichment levels are from 4-5 % maximum at 5% of enrichment for a 120 kg of uranium will take the energy approximately 8.85 SWU/Kg/. For a 4 percent of enrichment, power reactor of 130 kg fuel quantity processing required 6.25 SWU/Kg of feed [12]. In terms of research reactors more than 20 % enrichment is suggested due to which its performance is uncertain and according to the prototypes reaction it will be taken into the consideration for the main reactors. For a research reactor with 20 % enrichment in order to use a fuel of 26 kg, it is required 45 SWU/kg of feed. In the case of weapons it is requires more than 90 % of enrichment, because the fission reaction takes place is continuous and it has to be self sustain. For a weapon of c 90%, 5.6 Kg of fuel processing required 227 SWU/ Kg of feed.



(Source: WNA, Nuclear Energy Fuel Enrichment selection data2011)

**Figure 6.8** Uranium Enrichment with respect to its work requirement

For the helium cooled reactor, with gas turbine modular helium cooling system the fuel enrichment levels are shown in the table below, which says the best combination is  $14 \text{ }^{235}\text{U} + 86 \text{ }^{238}\text{U}$  which result in enrichment with respect to  $14 \text{ }^{235}\text{U}$  and converts like a fissile material [13]. For the same composition mass fraction breed for the materials are shown approximately  $86 \text{ }^{238}\text{U}$ .

**TABLE 6.3** TYPES AND COMPOSITION OF FUEL IN THE GT-MHR

Variant	Fuel	Fuel Composition %	Enrichment w.r.t fissile uranium	Mass fraction of breeding Materials
1	Enriched Uranium	$14 \text{ }^{235}\text{U} + 86 \text{ }^{238}\text{U}$	$14 \text{ }^{235}\text{U}$	$\sim 86 \text{ }^{238}\text{U}$
2	Weapons Grade Uranium + thorium	$15\text{U} + 85\text{Th}$	$14 \text{ }^{235}\text{U}$	$\sim 85 \text{ Th.} \sim 1 \text{ }^{238}\text{U}$
3	Weapons grade Thorium	$91.7 \text{ }^{239}\text{Pu} + 6.6 \text{ }^{240}\text{Pu} + 1.2 \text{ }^{241}\text{Pu} + 0.4 \text{ }^{242}\text{Pu} + 0.1 \text{ }^{238}\text{Pu}$	$\sim 93 \text{ Pu fissile}$	$7 \text{ }^{240}\text{Pu}, \text{ }^{242}\text{Pu}$
4	Power Grade Plutonium	$59 \text{ }^{239}\text{Pu} + 24 \text{ }^{240}\text{Pu} + 11 \text{ }^{241}\text{Pu} + 5 \text{ }^{242}\text{Pu} + 1 \text{ }^{238}\text{Pu}$	Same, 70	$30 \text{ }^{240}\text{Pu}, \text{ }^{242}\text{Pu}$
5	Mixed Uranium-Plutonium	$15 \text{ Weapons-grade} + 15 \text{ U natural} + 40 \text{ ZrO}_2 + 30 \text{ Ce}_2\text{O}_3$	Same, 46	$\sim 50 \text{ U natural} + 3.5 \text{ }^{240}\text{Pu}, \text{ }^{242}\text{Pu}$
6	Weapons-grade plutonium+Am, Cm*	$70 \text{ Pu} + 22 \text{ Am.Cm}$	Same, 73	$\sim 5 \text{ }^{240}\text{Pu}, \text{ }^{242}\text{Pu}$
7	Power-Grade plutonium+Am.Cm*	$90\text{Pu} + 10 \text{ Am.Cm}$	Same, 64	$26 \text{ }^{240}\text{Pu}, \text{ }^{242}\text{Pu}$

In the case of fuel pebbles in the modular gas turbine helium cooled reactors TRISO coated pebbles are designed with the uranium oxide, porous carbon buffer and pyc coating, Sic coating and outer Pyc coating is employed in a specific composition. Apart of enrichment this is a special method for the helium cooled reactors [44]. The CFD analysis results shows that the effective ness of these materials usage in the system will improve reactor performance and it will also solve many material related issues. The

primary kernel is a uranium composition and which will be inserted as small balls inside the pebbles and these can be designed based on its density.

**TABLE 6.4 MATERIAL COMPOSITION OF TRISO FUEL PARTICLE**

Material	Density (g cm <sup>-3</sup> )	Outer diameter (mm)
UO <sub>2</sub>	10.88	0.26
Porus Carbon Buffer	1.1	0.77
PyC Coated	1.9	0.85
SiC Coating	3.2	0.92
PyC Coating	1.9	1.00

### 6.7 Reactor Shielding Analysis

Neutron irradiation can cause a major alteration in the properties exhibited by the materials employed in the various components of a reactor. In metals, and metal alloys, but equally in other solid materials, such as ceramics, such alterations are related to the evolution of the point defects generated by this irradiation, and to the extraneous atoms generated by nuclear reactions, substituting for one of the atoms in the crystal lattice. The nature, and number of such defects depends both on the neutron flux, and neutron energies, however the neutrons that cause appreciable structural evolutions are, in thermal-neutron reactors as in fast-neutron reactors (fast reactors), the fast neutrons. A crystal invariably exhibits some defects, and irradiation may generate further defects. Point defects fall under two types: vacancies (one atom being expelled from its location in the crystal), and interstitials (one extra atom positioning itself at a supernumerary site, between the planes of the crystal lattice) [18]. Dislocations, marking out a region where the crystal stack is disturbed by local slipping, affecting a single atomic plane, in turn act as sources, or sinks of point defects. Vacancies may come together to form vacancy clusters, loops, or cavities, while interstitials may form interstitial clusters, or dislocation loops. At the same time, copper, manganese, and nickel atoms, e.g. in a vessel steel alloy, tend to draw together, to form clusters, resulting in hardening of the steel. Finally, grain boundaries are defects bounding two crystals exhibiting different orientations, and thus act as potential factors of embrittlement. Many of the metal's properties are subject

to alteration at these boundaries. The damage occasioned to such materials is expressed in terms of displacements per atom (dpa), with  $n$  dpa implying that every atom in the material has been displaced  $n$  times, on average, during irradiation [21].

### **6.8 Material Selection of Helium-Cooled Fusion Power Plant Designs**

Helium-coolant has been used for different fusion power plant designs, cooling the first wall, blanket, shield and divertor components. A variety of structural materials were selected for these designs. The BCSS designs employed martensitic steel as the structural material, and solid ceramic like Li<sub>2</sub>O, Li<sub>2</sub>SiO<sub>4</sub> or LiAlO<sub>2</sub>, as the tritium breeder. Similarly the recent European designs used martensitic steel as the structural material, and solid breeder, LiAlO<sub>2</sub> or Li<sub>2</sub>ZrO<sub>3</sub> and liquid breeder, Pb-17Li as tritium breeding materials. ARIES helium-cooled designs used Sic-composite as the structural material and solid ceramic, Li<sub>2</sub>O or Li<sub>2</sub>ZrO<sub>3</sub> as the breeder. The first one uses vanadium alloy (V-alloy) as the structural material and the second one uses Sic-composite as the structural material [26]. These helium-cooled design options can have the coolant routing arranged in the poloidal or toroidal direction. The coolant can enter the blanket in the poloidal direction at the back plenum of the blanket and then distribute through the radially oriented pipes and flow toroidally cooling the first wall and blanket before returning to the back plenum of the blanket module. This configuration can be applied to metallic alloy and ceramic composite structural material design options. The innovation for the V-alloy helium cooled design is the use of a mixed tritium breeders of Li<sub>2</sub>O and Li. This Li<sub>2</sub>O/Li mixture can potentially control the problem of compatibility between V-alloy and the impurities of oxygen and hydrogen in the helium coolant. Instead of forming V-hydride and V-oxide which can weaken the structural material, the presence of lithium would lead to the formation of more stable lithium hydride and Li<sub>2</sub>O. Other advantages of this design option are the possibility of breeding adequate tritium without the use of Be neutron multiplier, and the elimination of the problem of contact resistance between solid breeder and structural wall [28]. The helium coolant outlet temperature for this option is limited by the V-alloy which has a maximum temperature limit of 7000 °C, due to helium embrittlement. Therefore the thermal efficiency is limited to the steam Rankine cycle system which may have a gross thermal efficiency of 40% to 45%.By

changing the structural material from V-alloy to a Sic-composite which has a higher temperature limit in the range of 1000°C to 1200 °C, the coolant outlet temperature can be operated in the range of 850 to 1000°C, which allows the use of a closed cycle helium gas turbine Brayton cycle with a gross efficiency of 57 ~ 55%. It should be noted that the mixed Li<sub>2</sub>O/Li breeder approach will not be applicable for the Sic-composite material, due to the incompatibility of Sic and lithium at the temperature range of 900-1200°C [33] .

### **6.8.1 Sic-Composite Material**

Sic-composite is a low activation material with minimal heat flux, with the heat transfer it will be induced radio activity. Compared to Martensitic steel and V-alloy, Sic-composite is in the early stages of development as a structural material for fusion. Martensitic steel as a class is a mature structural material that has been used for many industrial components like steam generators [23]. Relatively, the application of V-alloy is limited. There is essentially no industrial experience in the design and fabrication of significant structures from any V-alloy but fabrication tests have demonstrated that V-alloy exhibits fabrication properties similar to the stainless steels. If this fact is substantial by further test the capability of fabricating large structural components is available. For the Sic-composite material, it is being developed for different applications as rocket nozzles and advanced heat exchangers [28]. However, the development of fusion relevant, high performance, helium-cooled Sic-composite components is in its infancy. Some of the critical issues of irradiation properties and life time, leak tightness, brazing and joining of composite parts, large components design and fabrication will need to be addressed.

### **6.8.2 Helium Cooling For High Heat Flux Components**

A key concern in the use of helium as the coolant is its capability of removing high surface heat fluxes; this is especially true for the cooling of divertors at a maximum surface loading Copper alloy was used in these systems [35]. For the case of removing the surface heat flux of 8 MW/m<sup>2</sup>, the test module consisted of a heated length of 80



mm and a width of 25 mm, fin height of 5 mm, fin pitch of 1 mm and a fin thickness of 0.4 mm. The corresponding pumping power fraction was only 0.8% of the removed thermal power. For the case of removing surface loading 16 MW/m<sup>2</sup>, with a heat removal area of 1 cm<sup>2</sup>, a porous medium configuration was used instead of the fin configuration. Similar demonstration components will need to be developed for Sic-composite material [40].

### 6.8.3 Materials for Fusion Reactors

The design goal for high operating temperatures (~1000 °C) for the structure in the high power density He-cooled concept severely limits the structural materials that can be considered. Pure tungsten or tungsten alloyed with ~5%Re (to improve fabricability) appear to be suitable candidates [41]. The un irradiated mechanical properties of tungsten are strongly dependent on thermo mechanical processing conditions. The best tensile and fracture toughness properties are obtained in stress-relieved material. In order to be conservative, since data are not available on the possibility of radiation-enhanced recrystallization of W, and also to account for the presence of welds in the structure, the preliminary design is based on re crystallized mechanical properties. There are no known mechanical properties data on tungsten or tungsten alloys at irradiation and test temperatures above ~800 °C. There are no known fracture toughness impact data on tungsten irradiated at any temperature [43]. Pronounced radiation hardening is observed in W and W-Re alloys irradiated at temperatures of 300-500 °C to doses of ~1-2 dpa, which produces significant embrittlement in tensile tested specimens (~0% total elongation). Simple scaling from existing data on irradiated Mo alloys suggests that the operating temperature for W should be maintained above ~800<sup>0</sup>-900 °C in order to avoid a significant increase in the ductile to brittle transition temperature (DBTT). The upper operating temperature limit for tungsten will be determined by thermal creep, helium embrittlement, or oxide formation issues. The thermal creep of W becomes significant at temperatures above ~1400 °C. Helium embrittlement data are not available for tungsten; however, based on results obtained on other alloys, helium embrittlement would be expected to become significant at temperatures above ~1600 °C (~0.5 melting temperature, TM). The

formation of volatile oxides is another potential problem in tungsten at temperatures above  $\sim 800$  °C, especially during an up-to-air event. However, if the oxygen partial pressure in the helium coolant can be maintained at or below 1 appm, then the rate of corrosion is calculated to be less than 2 m/year for temperatures up to  $\sim 1400$  °C. In summary, the selected upper temperature limit for tungsten in the structure of the preliminary design He-cooled system is  $1400^{\circ}\text{C}$ , depending on the applied stress.

### **6.9 Mechanical Design and Reliability**

The mechanical design of the helium cooled refractory blanket concept must satisfy the basic design goals. These goals include minimum requirements on heat removal, shielding, tritium breeding, and availability as well as provisions for heating and diagnostic penetrations, vacuum pumping, and plasma exhaust (divertor). Several first wall and blanket system configurations were evaluated. The helium cooled refractory alloy design includes a high temperature helium-cooled first wall and a lithium bath that is also cooled with high temperature helium [ 8]. The first wall is made up of separate units, which in this case are connected to separate cooling manifolds at the back of each module. The first wall units consist of multiple parallel passages connected through an integral manifold to round inlet and outlet connections. The large modules contain the lithium in a single volume, with pure lithium in the breeding zone and a combination of lithium and steel balls in the shielding zone. The temperature is relatively uniform, although there will be some gradients, albeit transient, between the front and back structural walls. There are two inboard and three outboard modules to each of the 16 sectors arranged in the toroidal direction [46]. The piping is routed in two circuits. The first circuit includes the first wall and part of the interior heat exchange tubing. Helium at  $800^{\circ}\text{C}$  enters the first wall through the supply manifold and exits into the first wall outlet manifold at  $950^{\circ}\text{C}$ . The helium is then routed inside the lithium can to the first supply manifold for the heat exchange tubes. The first tube circuit exits into a return manifold at  $1100^{\circ}\text{C}$ . The second tube circuit is fed at  $800^{\circ}\text{C}$  and exits at  $1100^{\circ}\text{C}$ . The structural design parameters are shown in the figure below. One of the primary goals of the system design is to increase the availability of fusion reactors by increasing the mean time between failures and by decreasing the mean time to repair. To this end,

we recommended the approach of sector maintenance, modular maintenance for everything and pre-tested modules for all components.

**TABLE 6.5 KEY DESIGN PARAMETERS FOR DIFFERENT STRUCTUREAL MATERIALS**

<b>Properties</b>	<b>Ferritic steel</b>	<b>V-alloy</b>	<b>SiC/SiC Composite</b>
Material $T_{max}$ , °C	550	700	$\geq 1000$
Coolant/ $T_{out}$ , °C	He/520 (Rankine Cycle)	Li/600 (Rankine Cycle1)	He/650-750 Rankine Cycle
Coolant/ $T_{out}$ , °C	LiPb/425 (Rankine Cycle)	He/550	He/ $\geq 850$ (Bryton cyle)
Industrial maturity	High	Low	Very Low

## CHAPTER 7

### USAGE OF HELIUM COOLED REACTORS IN VARIOUS APPLICATIONS

Nuclear fusion reactors, if they can be made to work, promise virtually unlimited power for the indefinite future. This is because the fuel, isotopes of hydrogen, is essentially unlimited on Earth. Nuclear fusion is the source of energy in the sun and stars where high temperatures and densities allow the positively-charged nuclei to get close enough to each other for the (attractive) nuclear force to overcome the (repulsive) electrical force and allow fusion to occur. Helium cooled reactors are used for many other applications including power generation. Nuclear space propulsion is one new concept which is gaining a lot of attention due to future space journeys, which are attached with huge distances like inter stellar travel, Vehicles for Mars and other longer distanced. The other areas are hydrogen production, even this we can use as a thermal energy generation source.

#### 7.1 Space Power Applications

The vast distances in the solar system make travelling a very difficult prospect for the astronauts involved in such a mission. With today's standards, even a simple mission to far planets such as Jupiter, Saturn or even a nearby planet like Mars would take a long time. Even in the case of Mars, you would need to commit more than one year for such a mission. In the case of Jupiter or other far away planets in our Solar System, the travelling times can be more than a decade. Hence, this would make it most difficult to find suitable candidates to undertake such a mission [42]. However, if you consider out of solar system destinations such as Proxima Centauri, you would need to travel for hundreds of years just to reach there. So, as a result, a more advanced means of travel is required for deep space missions. Luckily, the option of nuclear energy provides a way to obtain such a way since the specific impulse of a rocket can be raised by several magnitudes as it will be demonstrated in this chapter.

**TABLE 7.1 DISTANCES IN OUR SOLAR SYSTEM**

<b>Astronomical Body</b>	<b>Distance from Earth</b>
VENUS	37.92 million km
MARS	57.6 million km
MERCURY	76.8 million km
JUPITER	1542.4 million km
URANUS	4.112 billion km
PLUTO	4.2 billion km
NEPTUNE	4.4 billion km
SUN	148.8 million km

Moreover, besides the space propulsion applications, it is also imperative to understand that continuous power will need to be provided to the astronauts involved in such a mission. For example, if you were to provide continuous power for 3 astronauts who are involved in a 3 year mission, you would have to consider their life support requirements, as well as the operational power for the onboard systems such as navigation, communications as well as various other systems which require electric power. This would accumulate tremendously over time and it could not be met by conventional chemical batteries or even by Nuclear Isotope Thermal Generators. You would need a full scale nuclear reactor in order to function [39]. Thus, whether you are aiming for space propulsion or whether you are aiming for long term space power applications doesn't matter as you would need to make sure that you use some sort of a solution that uses a nuclear reactor to generate the required power. In this chapter, the principles required for both space propulsion as well as space based power systems is considered, so that its importance as well as its primary principles can be understood.

### **7.1.1 Space Propulsion**

When in space, the purpose of a propulsion system is to change the velocity, or  $v$ , of a spacecraft. Since this is more difficult for more massive spacecraft, designers generally discuss momentum,  $mv$ . The amount of change in momentum is called impulse [5]. So the goal of a propulsion method in space is to create an impulse. When launching a spacecraft from the Earth, a propulsion method must overcome a higher gravitational pull to provide a net positive acceleration. In orbit, any additional impulse will result in a

change in the orbit path. In order for a rocket to work, it needs two things: reaction mass and energy. The impulse provided by launching a particle of reaction mass having mass  $m$  at velocity  $v$  is  $mv$ . But this particle also has kinetic energy  $mv^2/2$ , which must come from somewhere. In a conventional solid, liquid, or hybrid rocket the fuel is burned, providing the energy, and the reaction products are allowed to flow out the back, providing the reaction mass.

The efficiency of a propulsion system depends on the reaction mass. Reaction mass must be carried along with the rocket and is irretrievably consumed when used. One way of measuring the amount of impulse that can be obtained from a fixed amount of reaction mass is the specific impulse, the impulse per unit weight-on-Earth (typically designated by  $I_{sp}$ ). The unit for this value is seconds. Since the weight on Earth of the reaction mass is often unimportant when discussing vehicles in space, specific impulse can also be discussed in terms of impulse per unit mass. This alternate form of specific impulse uses the same units as velocity (e.g. m/s), and in fact it is equal to the effective exhaust velocity of the engine (typically designated  $v_e$ ). Confusingly, both values are sometimes called specific impulse. The two values differ by a factor of  $g_n$ , the standard acceleration due to gravity  $9.80665 \text{ m/s}^2$ . A rocket with a high exhaust velocity can achieve the same impulse with less reaction mass.

$$v_g = I_{sp}g_n \quad (32)$$

However, the energy required for that impulse is proportional to the square of the exhaust velocity, so that more mass-efficient engines require much more energy, and are typically less energy efficient. This is a problem if the engine is to provide a large amount of thrust. To generate a large amount of impulse per second, it must use a large amount of energy per second. So highly (mass) efficient engines require enormous amounts of energy per second to produce high thrusts. As a result, most high-efficiency engine designs also provide very low thrust. Some typical specific impulses for various type of rockets can be seen in Table 7.2 .

**TABLE 7.2 SPECIFIC IMPULSE FOR 10,000 KG SPACE PROBE**

Engine	Effective Exhaust Velocity (Km/s)	Specific Impulse (s)	Fuel Mass (Kg)	Energy Required (GJ)
Solid Rocket	1	100	190000	95
Bipropellant Rocket	5	500	820	103
Ion Thruster	50	5000	620	775
Advanced Electrically powered Drive	1000	10000	30	15000

### 7.1.2 Nuclear Rocket

Nuclear rocket systems include thermal propulsion (“NTP”) systems, nuclear electric propulsion (“NEP”) systems, hybrid NTP/NEP concepts, and nuclear pulse rockets that are propelled by the force of nuclear explosions. Nuclear thermal propulsion systems provide thrust through the heating of liquid hydrogen propellant by nuclear fission. There are several designs for nuclear thermal rockets, including solid, liquid, and gas core nuclear rockets. Solid core nuclear rockets, a relatively mature propulsion technology, operate by pumping the liquid hydrogen propellant through narrow channels in a solid nuclear reactor. As liquid hydrogen moves through the channels, it is heated by the reactor into a high temperature gas, and then ejected from the exhaust nozzle of the rocket at high speeds. Liquid and gas core nuclear rockets operate according to a similar principle, but, instead of using a solid fuel core to heat the hydrogen propellant, they use a liquid or gaseous nuclear fuel, respectively. Solid, liquid, and gas core nuclear propulsion systems have never been developed into an operational rocket. However, they offer two potential major advantages over traditional chemical propulsion: a substantially larger specific impulse and a propellant with extremely low molecular weight. First, a large specific impulse translates into faster travel and the possibility of carrying heavier, more complex, and more experiment-laden Payloads into space. Second, propellants with low molecular weight increase the propulsive force per unit of propellant flow, allowing for an increased proportion of a mission’s total weight to be composed of payload rather than propellant. Nuclear electric propulsion systems,

already employed on a number of orbital missions, use superconducting magnetic cells to ionize gas and a nuclear reactor to heat the gas to high temperatures. The gas is expelled at very high velocities to provide thrust. Although the total thrust of nuclear electric propulsion is less than that of nuclear thermal propulsion, an electrical engine can provide sufficient thrust over long periods of time to propel an unmanned spacecraft to the outer edges of the Solar System.

A different type of nuclear electric propulsion, an electro bombardment ion engine uses electrical energy, rather than heat energy, to accelerate the exhaust gas to provide thrust. Energy from the nuclear reactor is converted into electricity and then channelled through an electrostatic grid to accelerate the ionized gas. Ion engines are considered particularly promising; they combine high levels of conversion of electric power into thrust with much higher exhaust velocities than chemical rockets and an extremely long operational lifetime. Perhaps the most futuristic and controversial of the nuclear propulsion concepts is a nuclear pulse rocket propelled by actual nuclear explosions. The nuclear pulse rocket operates by ejecting specially-constructed low-yield nuclear bombs, which explode some distance behind a large ablative "pusher plate" at the rear of the spacecraft. The blast from each explosion bounces off the pusher plate, which thrusts the vehicle forward through a system of special hydraulic shock absorbers. Although such a vehicle has never been tested, it is one of the more intriguing options for advanced space travel. It offers an even better utilization of the energy yield from the fission reaction than a nuclear thermal rocket.

### **7.1.3 Space Power Concepts**

In space, whether you have a space based station or whether you have a ground based installation; you will need to have extensive support to create the necessary power for the various requirements such as the life support, communications, waste removal, etc. Thus, functional power sources are needed that can function in the long term. Due to its basic properties, chemical or thermal means of generating electricity would be quite difficult in microgravity conditions. Moreover, it would create several control and stability issues as well too. However, with the availability of a nuclear reactor, all of the



power requirements in a space based station with microgravity or reduced gravity conditions can be met for several years without any difficulty.

Nuclear reactor power systems can support human exploration at surface outposts as well as onboard spacecraft. A nuclear reactor on the surface of the Moon or Mars can be a source of reliable power to provide life support, to replenish fuel cells for mobile systems, and to supply the large power demands of facilities processing materials. A continuous source of power is needed for life support onboard a spacecraft. Power levels for surface and shipboard life support systems are approximately equivalent. However, the environments in the two applications can vary dramatically. Shipboard systems will need to radiate all waste heat to the vacuum and will need to have a low specific mass (i.e., kg/kW), which calls for operation at higher temperatures and the use of more exotic materials. Specific mass is typically less important for surface systems as opposed to actual mass, which must be minimized for ease of transportation and so more common materials can be used, and it will be easier to address radiation shielding.

#### **7.1.4 Space Nuclear Reactors**

A nuclear reactor operates by converting heat generated by the controlled fission of heavy atoms into electricity. In a traditional uranium reactor, a neutron strikes the nucleus of a uranium-235 atom, which splits into lighter atoms, releasing energy and emitting other neutrons. In an operational reactor, a neutron ejected from fission of uranium-235 atom causes fission to occur. When this process occurs as continuous, controlled chain reaction, it produces useful amounts of energy. Space nuclear reactors operate according to the same process as nuclear reactors in terrestrial nuclear power plants. To produce usable power, “the heat generated by the controlled Fission is transferred by a heat-exchange coolant to either a static or dynamic conversion system, which transforms it into electricity. The system releases waste heat through a radiator. The amount of fissile material in the reactor depends on the duration and power requirements of the mission. Nuclear reactors offer major advantages over solar and chemical power sources in terms of mass, efficiency, durability, and longevity. Like RTGs, nuclear reactors are capable of producing a reliable stream of electrical power

over long periods of time. Unlike RTGs, however, nuclear reactors are capable of producing extremely high power levels. “The energy available from a unit mass of fissionable material is approximately [100 million] times larger than that available from the most energetic chemical reactions.” According to one estimate, a five thousand kilogram nuclear reactor operating over a seven-year lifespan is the equivalent of a 750 square-meter solar array or a six million kilogram chemical power source. These numbers illustrate that nuclear reactors are virtually the only viable power source for space missions requiring high power levels over long time periods.

### **7.1.5 Gas Core Reactors for Space Applications**

The main problem with using nuclear reactors in space applications is with control issues in microgravity conditions as well as with the high temperatures that are required to be reached in high speed applications. Due to this, standard solid core nuclear reactors are usually not preferred in space based applications. One of the more popular modes of reactors is gas core reactors for both rocket applications as well as for powering space stations. In a gaseous core nuclear fuel is usually Uranium Hexafluoride or uranium Tetra fluoride, which is basically fissile Uranium 235 in gaseous form. With this type of a nuclear reactor, no solid core or no solid fuel rods as well as control rods are needed as the whole concept is based on a gaseous design. For instance, when the fissile reactivity of the core needs to be increased, the pressure of the fissile fuel Uranium Hexafluoride is increased. Thus, in nuclear rockets, the specific impulse of the rocket can easily be controlled in direct relation to the pressure of the gaseous core nuclear reactor. Moreover, in space station applications, the pressure of the gaseous core can determine the overall power output of the system.

Various options for high temperature fuel elements are possible. These differ from each other mainly in terms of heat flow and transfer through the fuel element. One of the most promising layouts of the gas core nuclear reactor incorporates a fuel element that has a stagnant zone of fissile material. In this fuel element the fissile uranium plasma is located in the centre of a cavity enclosed by the neutron moderator reflector. The working gas flows close to the cavity walls and is heated by high temperature plasma

radiation. The process governed by permitting an initial build-up of the reaction to some predetermined level is then maintaining the reaction at this level when each fissioned nucleus produces on the average one neutron which goes to fission another nucleus. If the neutron production is at higher level the reaction would get out of hand, if it is at lower level the reaction would die.

### 7.1.6 Heat Transfer Characteristics in a Gas Core Reactor

The problem of heat-exchanger stability is one which is extremely important in nuclear reactor rockets. This stems from the desirability for high power density, which, if coupled with flow or heat removal instabilities could result in hot spots and reactor-core failure. Typically, stability criteria are difficult to establish, since most analytical treatments require many limiting assumptions. For overcoming this problem physical model investigation will answer some of the aspects. This is completed by duplicating the fission power distribution within the model. In general best approach is to go for simplified models analysis the results can be applied to actual case.

For gaseous nuclear core reactors in space applications, it is preferred to have laminar flow over the reactor core. This is essential for the purposes of controlling reactivity in the core itself. Moreover, it is essential to realize that in microgravity conditions, turbulent flow inside the reactor core can be quite unpredictable and may cause fluctuations in the neutron flux inside the core. Thus, both from the point of view of neutron dynamics as well as from the point of fluid dynamics, the reaction kinetics will become unpredictable. Hence, below the case of laminar flow in a capillary is given as an example of the use of a simplified model. If the velocity of flow is constant and neglecting heat conduction in the direction of flow, the equations describing the system, in non dimensional form are

$$w(t) = -\frac{1}{T^{n+1}} \frac{\partial p(x,t)}{\partial x} \quad (33)$$

Equation (2) is a form of the Hagen-Poiseuille equation for laminar flow in a pipe.

$$q_o = \frac{\partial T(x,t)}{\partial t} + w(t) \frac{\partial T}{\partial x} \quad (34)$$

Equation (34) is the heat conduction equation of a flowing gas

$$\mu = T^n \quad (35)$$

To examine the stability of a system of two or more capillaries in parallel, considering first steady state solutions. If all the quantities are independent of time, and are so designated by the subscript zero,

$$T_0 = 1 + \frac{x}{w_0} \quad (36)$$

$$\Delta p_0 = - \int_0^1 \frac{\partial p_0}{\partial x} dx = w_0 \int_0^1 \left(1 + \frac{x}{w_0}\right)^{n+1} dx \quad (37)$$

The exponent of the temperature in the viscosity- Temperature relationship is greater than zero. The requirements of the coolant material to be selected should have good thermal properties, like high specific heat, thermal conductivity, low power requirements for pumping high boiling point and low melting point, stability to heat and to radiation, Non-corrosive characteristics, Small cross section for neutron capture, Non-hazardous including low induced radioactivity and low cost.

TABLE 7.3 PHYSICAL PROPERTIES OF COOLANT MATERIALS

Coolants	Temp °C	Density g/cm <sup>3</sup>	Specific Heat Cal/g	Thermal Conductivity Cal/sec cm <sup>2</sup> -°C/cm	σ <sub>a</sub> barns/nucleus
H <sub>2</sub>	100	6.6×10 <sup>-5</sup>	3.43	5.33×10 <sup>-4</sup>	0.33
	300	4.3×10 <sup>-5</sup>	3.50	7.36×10 <sup>-4</sup>	
He	0	1.8×10 <sup>-4</sup>	1.25	3.3×10 <sup>-4</sup>	0
	100	1.4×10 <sup>-4</sup>	1.25	4.0×10 <sup>-4</sup>	
CO <sub>2</sub>	100	1.5×10 <sup>-3</sup>	0.218	5.0×10 <sup>-5</sup>	0.003
	300	9.5×10 <sup>-4</sup>	0.231	9.0×10 <sup>-5</sup>	
lead	200	10.46	0.035	0.023	0.1
	600	9.91	0.035	0.035	
lithium	200	0.507	1.0	0.09	0.033
	600	0.474	1.0		

### 7.17 Thermodynamics of a Gas Core Reactor

The Thermodynamic design conditions of a gas core reactor are a reflector moderated cavity containing fissile plasma that is isolated from the cavity walls by hydrodynamic forces of an inert buffer gas. The removal of heat is by photo flux through an optically transparent port like heat pipe etc in the form of radiant energy. The MHD generator was modeled as an isentropic turbine with an operating efficiency ranging between 95-97 %. For He compression an isentropic compression process is carried out at operating efficiency ranging from 85-88 % an initial pressure ratio of 1.73 is maintained. Work done by the compressor for He circulation is calculated by

$$W_s = \frac{n\gamma RT_{mi}}{\eta_c(\gamma-1)} \left[ \left( \frac{P_2}{P_1} \right)^\gamma - 1 \right] \quad (38)$$

Mixing of Helium and Uranium Tetra fluoride is done in a nozzle; normally the composition percentage is in between 10-60 % of UF<sub>4</sub> is employed for the better power density. A gas core reactor with BeO reflector shielding are employed to maintain fission reaction self sustained. A purification unit after the reaction cycle is present for separating actinide waste in a propellant and waste will be deposited in a dump tank. In thermodynamics of the gas core reactors, the microgravity affects needs to be considered as well. The reason for this stems from the fact that the thermodynamic extraction of work would be greatly hampered by microgravity conditions as extra work may be required to reach the necessary efficiencies. However, in gas core reactor, these issues are minimized more as compared to other types of reactors.

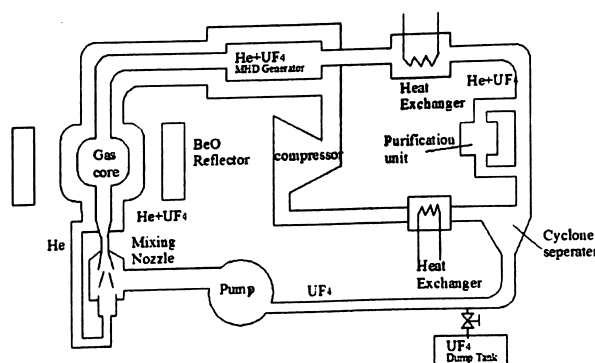
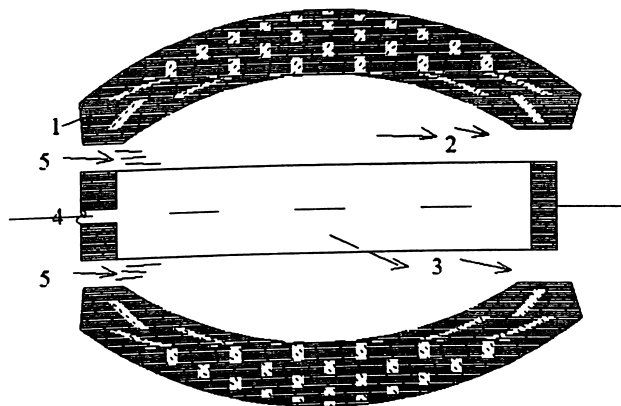


Figure 7.1 Gas Core Reactor Cycle

## 7.18 Gravity effect on a reactor

The nuclear reaction under microgravity conditions is possible under special design conditions. Since fission reaction is more to do with nucleus and with the neutrons; in order to self sustain any fission reaction, sufficient amount of energy is required. The main problem with the nuclear reactors under microgravity conditions is the controlling of the flow, which is a big challenge. In order to keep reaction self sustained, a special chamber design needs to be introduced to keep flow inside the core as a laminar flow, so that enough amounts of energy levels are maintained. Under turbulent flow conditions, due to the randomness of the molecules, it is difficult to keep flow within specified boundaries. Hence, low Reynolds number flows are preferred under microgravity conditions.



**Figure 7.2** Cavitated Gas Core Nuclear Reactor Fuel Elements

1. Reflector moderator, 2. Gaseous fissile material zone, 3. Working medium flow zone 4. fissile material diminution replenishment, 5. Working medium inlet.

If it is not under the specified boundaries, then the chain reaction time will increase. Due to uncontrolled conditions in the reactor core, heat distribution is not proper and some parts of the reactor core will be exposed to lower melting range. Due to this effect, in the reactor hot spots. will be formed. In order to overcome this problem, a special core design shown in the figure 7.2 is introduced to sustain fission reaction under control. Various options for the high temperature fuel elements are possible with this design. These differ from each other mainly in terms of heat flow and transfer

though the fuel elements. This design incorporates a fuel element that has a stagnant zone of fissile material. The fissile material i.e. uranium plasma will be located in the center of a cavity enclosed by the neutron moderator reflector. The working gas flow is close to the cavity walls and it is heated by the high temperature plasma radiation which causes the fission reaction to be self sustained under microgravity conditions.

## 7.2 Hydrogen Production

Fuel cells are introduced for vehicular applications, hydrogen might become an energy carrier for transport applications. Manufacture via steam-reforming of natural gas is a low- cost option for hydrogen production. When hydrogen is produced from natural gas, a concentrated stream of CO<sub>2</sub> is generated as a by-product. This work also deals with the feasibility of combining the production of hydrogen from natural gas with CO<sub>2</sub> removal.

TABLE 7.4 SOURCES FOR HYDROGEN PRODUCTION

Composition	Coal-Gas	Bio-Gas	Nat.Gas
Hydrogen (H <sub>2</sub> )	14.0%	18.0%	-----
Carbon Monoxide (CO)	27.0 %	24.0%	-----
Carbon Dioxide (CO <sub>2</sub> )	4.5 %	6.0 %	-----
Oxygen (O <sub>2</sub> )	0.6 %	0.4 %	-----
Methane (CH <sub>4</sub> )	3.0 %	3.0 %	90.0 %
Nitrogen (N <sub>2</sub> )	50.9 %	48.6 %	5.0 %
Ethane ( C <sub>2</sub> H <sub>6</sub> )	-----	-----	5.0 %
HHV ( Btu/ scf)	163	135	1,002

The first step in the conventional manufacture of hydrogen from natural gas involves reforming the natural gas feedstock with steam at high temperature, to produce a gaseous mixture consisting mainly of carbon monoxide and hydrogen. Subsequently the gaseous product of the reformer is processed in shift reactors operated at much lower temperatures. In these reactors, the carbon monoxide reacts with steam to produce hydrogen plus CO<sub>2</sub>. Subsequently, the hydrogen and CO<sub>2</sub> are separated using pressure swing adsorption (PSA) units, the CO<sub>2</sub> is vented to the atmosphere, and the purified hydrogen (up to 99.999% pure) is compressed (e.g. to 75 bar as an input pressure for a

long-distance transmission line). Carbon dioxide leaves the hydrogen production plant in two streams: in a diluted stream as a component of the reformer stack gases (about 30% of the total CO<sub>2</sub>) and in a concentrated stream that is separated from the hydrogen in the PSA unit (about 70% of the total).

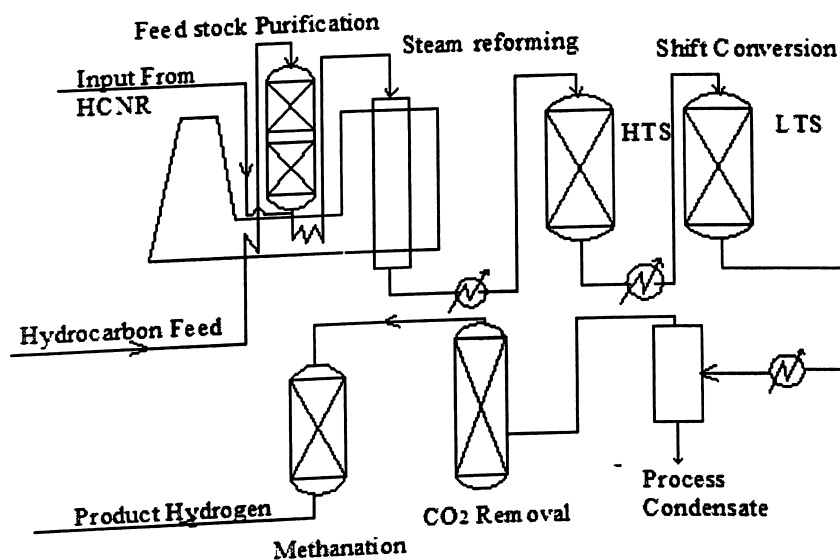
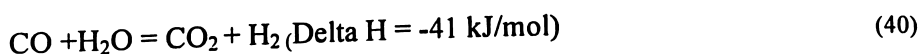
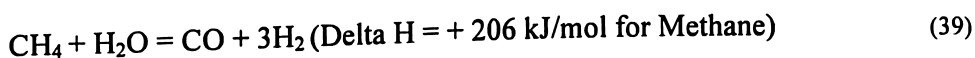


Figure 7.3 Hydrogen Production Cycle With Steam Reforming

### 7.2.1 Reformation of Natural Gas

The first step of the SMR process involves methane reacting with steam at 750-800°C (1380-1470°F) to produce a synthesis gas (syngas), a mixture primarily made up of hydrogen (H<sub>2</sub>) and carbon monoxide (CO).

### 7.2.2 Shift Reaction

In the second step, known as a water gas shift (WGS) reaction, the carbon monoxide produced in the first reaction is reacted with steam over a catalyst to form hydrogen and carbon dioxide (CO<sub>2</sub>). This process occurs in two stages, consisting of a high temperature shift (HTS) at 350°C (662°F) and a low temperature shift (LTS) at



190-210°C (374-410°F). Hydrogen produced from the SMR process includes small quantities of carbon monoxide, carbon dioxide, and hydrogen sulphide as impurities and, depending on use, may require further purification.

### **7.2.3 Feedstock Purification**

This process removes poisons, including sulfur (S) and chloride (Cl), to increase the life of the downstream steam reforming and other catalysts.

### **7.2.4 Product Purification**

In a liquid absorption system, CO<sub>2</sub> is removed. The product gas undergoes a methanation step to remove residual traces of carbon oxides. Newer SMR plants utilize a pressure swing absorption (PSA) unit instead, producing 99.99% pure product hydrogen. High to ultra-high purity hydrogen may be needed for the durable and efficient operation of fuel cells. Impurities are believed to cause various problems in the current state-of-the-art fuel cell designs, including catalyst poisoning and membrane failure. As such, additional process steps may be required to purify the hydrogen to meet industry quality standards. Additional steps could also be needed if carbon capture and sequestration technologies are developed and utilized as part of this method of hydrogen production.

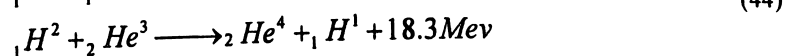
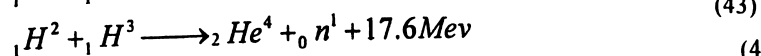
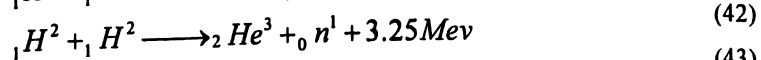
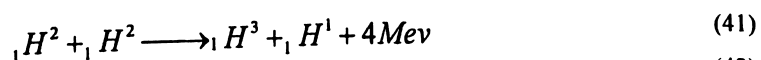
## **7.3 Helium Cooling For Fusion Reactor**

Helium cooling has been successfully used for fission reactors in the past. Helium is an attractive coolant for fusion reactors because it is chemically and neurotically inert and can be used directly for power conversion in gas turbine cycle. In addition, as was shown during ITER evaluation, it is very attractive from safety considerations. On the other hand, it is thought that use of helium cooling requires high pressure, large pumping power and larger manifold sizes due its low density at atmospheric pressure. It is shown that use of heat transfer enhancement techniques reduces the flow, pumping power and pressure requirements. A number of proven heat transfer enhancement

techniques such as extended surfaces, swirl tape, roughening, porous media heat exchanger and particulate addition are reviewed. Recent experiments with some of these methods have shown that expected heat fluxes of 5 to 10 MW/m<sup>2</sup> in fusion reactors can be removed by helium cooling at a modest pressure of 4 Mpa. It is concluded that a number of these techniques are practical for fusion reactor application. The problem of controlled fusion is difficult ones. But against the possibility that fusion reactors may never work, there is the fact that one that does work will use cheap fuel, operate without a critical mass, produce no significant wastes, and by-pass the heat cycle. The fusion reaction is not a chain reaction in the sense that reaction products must be fed back into the flame to keep it going. Thus the critical –mass concepts does not apply. Since one can dispense with critical mass, one need not face many of the problems of fission reactors- principally those of over cautious control and safety.

### 7.3.1 Nuclear Fusion Reactions

Nuclear fusion reaction will release energy when two atoms join together to form one. Two hydrogen atoms come together and they will form helium atom, neutrons and vast amount of energy. There are several types of fusion reactions. Most involve the isotopes of hydrogen called deuterium and tritium. Proton- proton chain reaction which is normally takes place in stars; sun is the best example of this kind. Two pairs of protons of protons to make two deuterium atoms each deuterium atom combines with a proton to form a helium-3 atom, two helium-3 atoms combine to form beryllium-6, which is unstable, Beryllium-6 decays into two helium-4 atoms. These reactions produce high energy particles like protons, electrons, neutrinos, positrons an radiation in the form of light,  $\gamma$ -rays. In deuterium- deuterium reaction they will combine to form a helium-3 and neutron, if it is between deuterium- tritium reactions one atom of deuterium and one atom of tritium will combine to form Helium-4 and neutron with huge amount of energy in the form of high energy neutron.

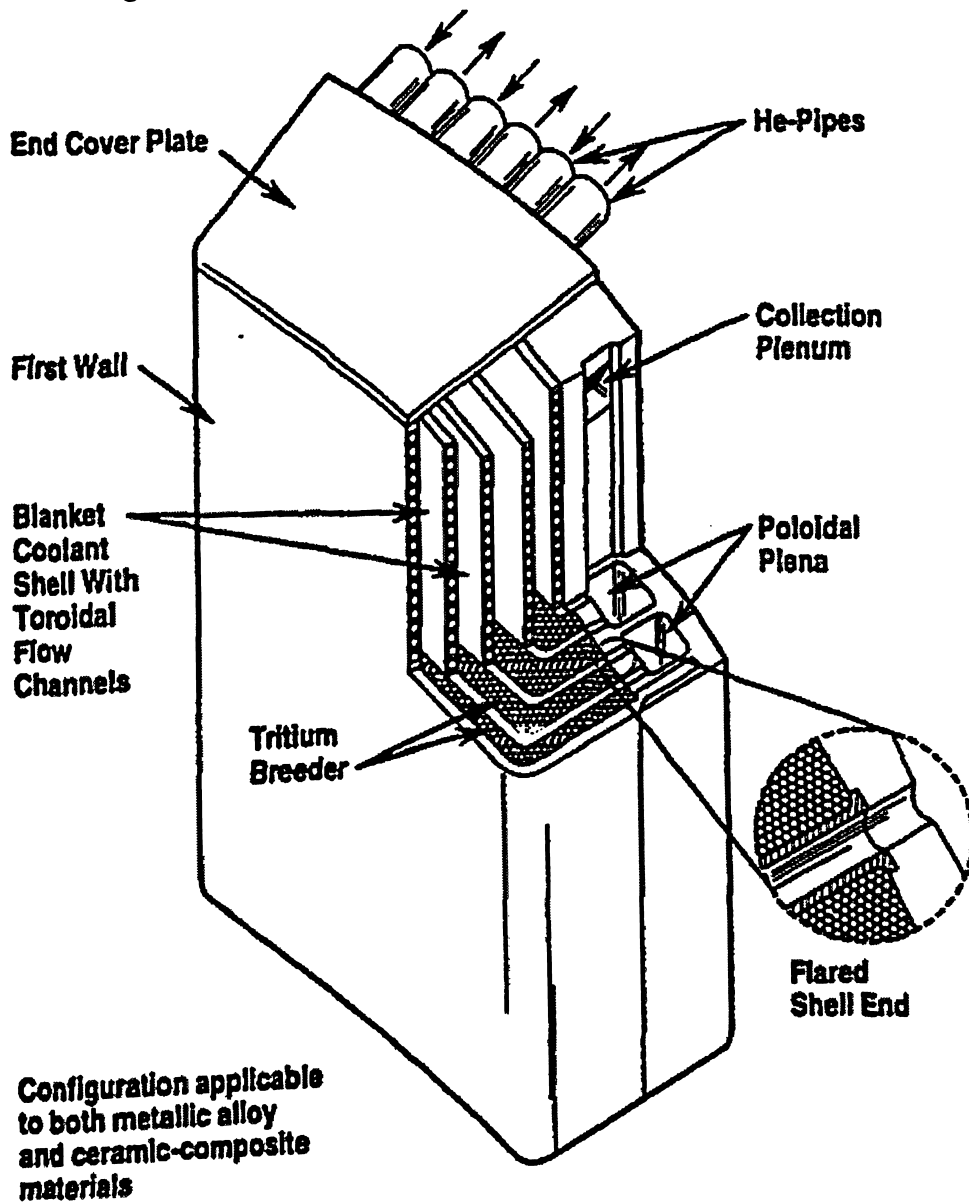


When hydrogen atoms fuse, the nuclei must come together. However, the protons in each nucleus will tend to repel each other because they have the same charge (positive). To achieve fusion, you need to create special conditions to overcome this tendency. The conditions required to achieve fusion reaction inside the reactor are the higher pressure and high temperature, some time higher pressure is the best for the different compounds in the equations above will describe its required limit depending upon the energy release.

### **7.3.2 Helium Cooled Fusion Reactors for Power Generation**

Fusion reactors have been getting a lot of press recently because they offer some major advantages over other power sources. They will use abundant sources of fuel, they will not leak radiation above normal background levels and they will produce less radioactive waste than current fission reactors. Fusion power has the potential to be a safe and environmentally acceptable power source in the future. To realize this potential, fusion power plants must be economically competitive and environmentally attractive by controlling capital cost, achieving high reliability and minimizing the amount of generated radioactive waste and radioactive sources potentially available for release during normal and abnormal events. A way to reach high thermal efficiency is to operate the working fluid at high exit temperature. Compared to coolants like water and liquid lithium, helium has the potential to meet these economic and environmental attractiveness requirements. For fusion application, advantages of helium-coolant for fusion application include its chemical inertness, its transparency to neutrons, and its stable heat transfer regime. Depending on the blanket coolant exit temperature, helium is applicable to either the Rankine or Brayton cycle power conversion system. The disadvantages of helium are its low density and correspondingly low volumetric specific heat. These characteristics lead to very low shielding effectiveness, modest heat transfer coefficient, and the requirement of relatively high pumping power. To alleviate these problems high coolant pressure designs in the range of 5-18 MPa. In fusion reactors Very high ignition temperatures are one of the main problems in advanced fuel fusion targets. These limits were derived from the projection of radiation damage of structure materials operated under the fusion neutron flux and fluence conditions. These radiation

damages can be caused by displacement of atoms and/or by the generation of helium. The latter can lead to swelling and or embrittlement of the material followed by the loss of structural integrity, highest cooling outlet temperature for fusion power plant, mainly due to the higher temperature capability of Sic-composite.



(Source: *Introduction to nuclear Energy*, Raymond L. Murry)  
**Figure 7.4** Fusion Blanket Used In Helium Cooled Reactor

As the turbine inlet temperature increases, higher thermal efficiency can also be reached. Correspondingly, Fig. X shows the gross plant efficiency as a function of direct

cycle gas turbine inlet temperature, which is the same as the blanket coolant outlet temperature. Based on the desire of maximizing the turbine inlet temperature, only the helium-cooled, Sic-composite combination has the potential to compete economically with advanced fission power plant. As indicated in Fig. X a blanket model which is having the Helium-cooled, Sic-composite option also has the best potential to achieve the goal of inherent safety and the ease of waste disposal for fusion power plant. The common comparison is between three coolants namely liquid metal, helium and water is consider for fusion reactors. With the help of basic conditions inside the reactor core with fusion environment it is compared. From safety considerations helium is the best coolant due to its chemical and neutronic inertness. Hence a study was undertaken to investigate the feasibility of helium cooling for fusion divertors. Volumetric flow rate and pumping power are the two important parameters which determine the feasibility and practicability of using helium. The volumetric flow rate determines the size of manifolds required, and pumping power impacts the efficiency. The volumetric flow of helium required to remove Q Watts of power from a divertor L m long, with an inlet temperature of  $T_{in}$  and maximum heat sink temperature of  $T_{max}$

$$V = \frac{Q}{c_p \rho (T_{max} - T_{in} - \frac{\delta q_{max}}{k} - \frac{q_{max}}{h})} \quad (45)$$

On heat transfer coolant circulation had a specific effect; Pumping power W is a function of key parameters as follows:

$$W = F\{L^{n1}, q_{max}^{n2}, Q, \frac{f}{h^3}, \frac{1}{\rho^2}\} \quad (46)$$

Volumetric flow rate and pumping power can be reduced by obtaining a large heat transfer coefficient. In order to increase the heat transfer coefficient, the friction factor is also increased; however the net effect is to decrease the pumping power. In practice, it is not necessary to increase the heat transfer coefficient (and thus friction factor) on the entire cooled surface but only in areas with large heat fluxes. In fusion machines, this area is less than 50% of the divertor surface there are two reasons for this. Firstly, the coolant temperature rise is negligible and secondly the conduction spreads the heat flux, thereby reducing the effective heat flux at the coolant interface.

## **CHAPTER 8**

### **RESULTS AND DISCUSSIONS**

A nuclear power plant with a modular helium cooled reactor using spherical fuel elements promises a great potential for the future. The thermodynamic efficiency of such a reactor is around 48 percent and that is minimum ten points higher than a standard pressurized light water reactor. Thus, from an electrical production point of view, the increase in efficiency alone is a good reason to use this type of a nuclear power plant.

In addition, the presence of added safety measures through a negative coefficient of reactivity, as well as the online loading capability of the spherical fuel elements causes the system to be economically efficient as well, too. The reactor's maintenance is also simplified as the usage of helium as a coolant reduces the corrosiveness of the reactor core elements and reduces the process of aging in the reactor core's critical components. The amount of radioactive waste material that is produced as result of fission is also contained within the fuel elements as they are not excreted into the coolant cycle. Hence, for long term nuclear power plant operation, helium cooled reactors offer a great deal of interest.

The CFD analysis performed on fuel pebbles with the configuration of 2D model and 3D model has described a good experience in understanding the effect of turbulence on the heat transfer between Helium and the fuel pebbles. Also it has described with the small size compared to the larger pebbles, the effectiveness of the heat transfer will increase there by over all power density of the reactor is increasing greatly. The overall thermodynamic efficiency is calculated with the experience of the power density based on the reactor output. The thermodynamic balance is based on standard turbo machinery systems and efficiency is considered based on the conventional power plant standards.

For the better results with the 3D model, more computational results are required for future more accurate analysis. This thesis is specifically considered in understanding the pebbles behavior and its heat transfer characteristics and based on that thermodynamics analysis is conducted. In solving the 2D model there are 12 pebble

considered in analyses, the results are explaining how the boundary is developing between each of the pebble and how it is effecting the heat transfer. Wall shear stress is more at the center pebbles as it shows that the core is contains the higher temperature. In case of 3D model analysis is performed for the four fuel pebbles, due to the limitations of computational power, future more analysis need to be carried out for reaching best conclusions, the results which are obtained from the 3D model is explaining the trends and it was giving an idea how each parameter effected the design. With these results, it is difficult to reach a specific conclusion, but it will be a good path way for solving the problem for future work.

The possibility of combining a hydrogen production cycle with an intermediate heat exchanger increases the economic feasibility of such a reactor, so that it can be considered as one of the best Generation IV Reactor designs. Perhaps in the future, combined modular nuclear power plants with helium cooling cycle along with hydrogen producing chemical reactors can become the standard for production of energy. Thus, this thesis has been prepared in hopes of highlighting the importance of studying such a design for creating even more amicable solutions for the future.

## References

1. A.C. Kadak, R.G. Ballinger, T. Alvey, C.W. Kang, P. Owen, A. Smith, M. Wright and X. Yao," Nuclear power plant design project" Massachusetts Institute of Technology, Independent Activities Period January 1998.
2. Angelo, J. A., Jr., and D. Buden, Space Nuclear Power, Orbit Book Company, Inc., Malabar, FA, 1985.
3. Anghaie, S., Pickard, P., Lewis, D. (unknown date). Gas Core & Vapor Core Reactors- Concept Summary
4. Brown, L.C. (2001). Direct Energy Conversion Fission Reactor: Annual Report For The Period August 15, 2000 Through September 30, 2001.
5. Brown, Nicholas, Gas-Cooled Reactor Vessel Design and Optimization with COSMOS FloWorks, American Nuclear Society Student Conference, Rensselaer Polytechnic Institute, NY, March 31, 2006.
6. Bussard & Delauer, "Fundamentals of Nuclear Flight ,Mcgraw-Hill,1965.
7. Bussard & Delauer, Nuclear Rocket Propulsion,Mcgraw-Hill,1958
8. Barbry, F., 1987. Fissile solution criticality accidents-review of pressure wave measurements experiments in the SILENE reactor. Institut de Protection et de Surete Nucleaire, Technical note SRSC No. 87.96.
9. BAXI, C., "Helium-Cooled High Surface Heat Flux Experiment," 18<sup>th</sup> Symposium on Fusion Technology, August 22-26,1994, Karlsruhe, Germany.
10. Bankston, C. A., Fluid friction, heat transfer, turbulence and interchannel flow stability in the transition from turbulent to laminar flow in tubes. M.Sc.D. Thesis, U.S.A.,New Mexico, 1965.
11. C. Rubbia: Fission fragments heating for space propulsion, CERN SL-Note 2000-036 EET (2000).
12. C. Forsberg and P. Pickard, Advanced High-Temperature Reactor for Hydrgen and Electricity Production, Oak Ridge National Laboratory view graph presentation, May, 2001.



13. C. S.Handwerk,M. J. Driscoll, and P. Hejzlar, "Optimized core design of a supercritical carbon dioxide-cooled fast reactor,"*Nuclear Technology*, vol. 164, no. 3, pp. 320–336, 2008.
14. C. W. Forsberg, "The Advanced High-Temperature Reactor for Production of Hydrogen or Electricity," *Nuclear News*, Feb. 2003, p.30.
15. Charles F. Bonilla, "Nuclear Engineering", McGraw-Hill Book Company, ISBN-56-8167, pp. 360-675, 1957.
16. Drachlis, Dave. "NASA calls on industry, academia for in-space propulsion innovations", NASA, October 24, 2002. Retrieved on 2007-07-26.
17. D.F. DA CRUZ, J.B.M. DE HAAS and A.I. VAN HEEK ," A small scale nuclear power plant for new markets" NRG, P.O. Box 25, NL-1755 ZG Petten, The Netherlands.
18. E. E. Feldman and T. Y. C. Wei, "Plant Design Concepts for a Gas-Cooled Fast Reactor," Argonne National Laboratory NERI Project #01-022 Topical Report, February, 2002
19. E. E. Feldman and T. Y. C. Wei, "Design Approach for a Small Modular Pebble Bed Gas-Cooled Fast Reactor Optimized for Decay Heat Removal," Argonne National Laboratory NERI Project #01-022, August, 2003.
20. Feng K M, et al. Design Description Document for the Chinese Helium Cooled Solid Breeder ( CH HC SB ) Test Blanket Module (Version II) , 2005.
21. G.M. Gryaznov, "Nuclear Power for Space Vechiles: A new Division in the Energy Technology of the future," *Lzvestiya Akademii Nauk SSSR. Energetika i transport* , UDC 620.92;629.786, vol .29. No 6, pp. 24–33, 1991.
22. G. Melese, R. Katz, Thermal and Flow Design of Helium Cooled Reactors, American Nuclear Society, 1984
23. Hess, M.; Martin, K. K.; Rachul, L. J.. "Thrusters Precisely Guide EO-1 Satellite in Space First", NASA, February 7, 2002. Retrieved on 2007-07-30.
24. INTERNATIONAL ATOMIC ENRGY AGENCY, Current status and future development of modular high temperature gas reactor technology, IAEA-TECDOC (new), Vienna, (2000).

25. INTERNATIONAL ATOMIC ENERGY AGENCY, Design and development of gas cooled reactors with closed cycle gas turbines, IAEA-TECDOC 899, Vienna, (1996).
26. Johnson, C. E., Thermophysical and Mechanical Properties of Advanced Carbide and Nitride Fuels., ANL-AFP-26., June 1976.
27. J. Dunham and P.M. Came, "Improvements to the Ainley-Mathieson Method of Turbine Performance Prediction," Journal of Engineering for Power, Transactions of the ASME, pp. 252-256, 1970.
28. J. Schlosser, et al., "Technology Developments for the ITER Divertor," Proc. 17<sup>th</sup> Symposium on Fusion Technology, (1993) 367.
29. L. C. Brown, High efficiency Generation of Hydrogen Fuels Using Nuclear Power,NERI Proposal, January 29 1999.
30. Manson Benedict, Thomas H. Pigford, " Nuclear Chemical Engineering", McGRAW-HILL book company, ISBN-56-12523, pp. 254-358, 1957.
31. M. W. Thring, "Nuclear Propulsion ", Butter Worths, Landon 1960.
32. M. Simnad, Fuel Element Experience in Nuclear Power Reactors, Gordon and Breach Science Publ., NY, 1971.
33. McDonald, C.F., "The Nuclear Gas Turbine-Towards Realization After Half a Century of Evolution, International Gas turbine and Aeroengine Congress and Exposition, Houston, TX, June 5-8, 1995.
34. M. S. sEl-Genk, A Critical Review of Space Nuclear Power and Propulsion 1984-1993, American Institute of Physics, NY, 1994.
35. Raymond L. Murray, "Introduction to Nuclear Engineering", Second edition, Printice- Hall, Inc, ISBN-61-10793,pp. 159-260, 1961.
36. Robert Rosen and A.Dan Schnyer, "Civilian Usage of nuclear reactor in space", Volume I, pp.147-164, Science & Global security , 1989.
37. R.Hobar Ellis, " Nuclear Technology for Engineers", McGRAW-HILL book company, ISBN-59-13201, pp. 196-277, 1959.
38. Raymond L. Murray, "Nuclear Reactor Physics", Second edition, Printice- Hall, Inc, ISBN-57-8234 ,pp. 210-290, 1961.

39. P. Norajitra et al., "The European Development of He-cooled Divertors for FusionPower Plants," Proceedings of the 20th IAEA Fusion Energy Conference, Portugal, 2004.
40. Touloukian, Y. S., et al, Vol. 1 Thermal Conductivity Metallic Elements and Alloys, Thermophysical Properties Research Center, Purdue University. IFI/Plenum, New York, 1970.
41. U.S. DOE Nuclear Energy Research Advisory Committee and The Generation IV International Forum, "A technology roadmap for Generation IV nuclear energy systems," December 2002, <http://gif.inel.gov/roadmap>. [Ref.Date: 19-12-2010].
42. W. F. G. van Rooijen, Improving fuel cycle design and safety characteristics of a as cooled fast reactor, Ph.D. thesis, Delft University of Technology, Delft, The Netherlands, 2006, <http://repository.tudelft.nl>. [ref.Date:2-02-2011].
43. WONG, C.P.C., et al., "A Robust Helium-Cooled Shield blanket Design For ITER," proceeding of 15th IEEE/NPS Symposium on Engineering, Hyannis, Ma., October 11-15, 1993.
44. Y. Kato, T. Nitawaki, and Y. Muto, "Medium temperature carbon dioxide gas turbine reactor," Nuclear Engineering and Design, vol. 230, no. 1-3, pp. 195-207, 2004.

## APPENDIX

### A. Physical Properties Of The Fluids

Individual Gas Constants-R			
Gas	Imperial Units (ft lb/slug °R)	SI Unit (J/Kg K)	Molecular Weight (g/mole)
Argon, Ar	---	208	39.94
Carbon Dioxide, CO <sub>2</sub>	1130	188.9	44.01
Carbon Monoxide, CO	---	297	28.01
Helium, He	12,420	2,077	4.003
Hydrogen, H <sub>2</sub>	24,660	4,124	2.016
Methane-natural gas, CH <sub>4</sub>	3,099	518.3	16.04
Nitrogen, N <sub>2</sub>	1775	296.8	28.02
Oxygen, O <sub>2</sub>	1554	259.8	32
Propane, C <sub>3</sub> H <sub>8</sub>	--	189	44.09
Sulfur dioxide, SO <sub>2</sub>	--	130	64.07
Air	1716	286.9	28.97
Water vapor	2760	461.5	18.02

### B. Thermodynamic Properties Of The Fluids

Gas or Vapor	Formula	Specific Heat Capacity				Ratio of Specific Heats C <sub>p</sub> /C <sub>v</sub>	Individual Gas Constant R	
		C <sub>p</sub> kJ/kgK	C <sub>v</sub> kJ/kgK	C <sub>p</sub> Btu/lb <sub>m</sub> °F	C <sub>v</sub> Btu/lb <sub>m</sub> °F		C <sub>p</sub> ·C <sub>v</sub> kJ/kgK	Btu/ lb <sub>m</sub> °F
Acetone	---	1.47	1.32	0.35	0.32	1.11	0.15	---
Acetylene	C <sub>2</sub> H <sub>2</sub>	1.69	1.37	0.35	0.27	1.232	0.319	59.34
Air	--	1.01	0.718	0.24	0.17	1.40	0.287	53.34
Alcohol	C <sub>2</sub> H <sub>5</sub>	1.88	1.67	0.45	0.4	1.13	0.22	--

	<i>OH</i>							
Alcohol	$CH_3$ <i>OH</i>	1.93	1.53	0.46	0.37	1.26	0.39	--
Ammonia	$NH_3$	2.19	1.66	0.52	0.4	1.31	0.53	96.5
Argon	<i>Ar</i>	0.520	0.312	0.12	0.07	1.667	0.208	
Benzene	$C_6H_6$	1.09	0.99	0.26	0.24	1.12	0.1	--
Blast furnace gas	--	1.03	0.73	0.25	0.17	1.41	0.3	55.05
Bromine	--	0.25	0.2	0.06	0.05	1.28	0.05	--
Butadiene	--	--	---	---	--	1.12	--	--
Butane	$C_4H_{10}$	1.67	1.53	0.395	0.356	1.094	0.143	26.5
Carbon dioxide	$CO_2$	0.844	0.655	0.21	0.16	1.289	0.189	38.86
Carbon Monoxide	$CO$	1.02	0.72	0.24	0.17	1.40	0.297	55.14
Carbon disulphide	---	0.67	0.55	0.16	0.13	1.21	0.12	--
Chlorine	$Cl_2$	0.48	0.36	0.12	0.09	1.34	0.12	--
Chlorofo rm	--	0.63	0.55	0.15	0.13	1.15	0.08	
Combustio n Products	--	1	---	0.24	---	---	----	--
Ethane	$C_2H_6$	1.75	1.48	0.39	0.32	1.187	0.276	51.5
Ether	--	2.01	1.95	0.48	0.47	1.03	0.06	--
Ethylene	$C_2H_4$	1.53	1.23	0.4	0.33	1.240	0.296	55.08
Freon 22	--	---	---	---	--	1.18	---	--
Helium	<i>He</i>	5.19	3.12	1.25	0.75	1.667	2.08	386.3
Hexane	--	--	--	--	--	1.06	--	--
Hydrogen	$H_2$	14.32	10.16	3.42	2.43	1.405	4.12	765.9
Hydrogen Chloride	$HCl$	0.8	0.57	0.191	0.135	1.41	0.23	42.4
Hydrogen Sulfide	$H_2S$	---	---	0.243	0.187	1.32	---	45.2
Hydroxyl	<i>OH</i>	1.76	1.27	---	----	1.384	0.489	--
Methane	$CH_4$	2.22	1.70	0.59	0.45	1.304	0.518	96.4

Methyl Chloride	$CH_3Cl$	--	---	0.240	0.200	1.20	---	30.6
Natural Gas	--	2.34	1.85	0.56	0.44	1.27	0.5	79.1
Neon	--	1.03	0.618	--	---	1.667	0.412	--
Nitric Oxide	$NO$	1.03	0.618	--	---	1.667	0.412	---
Nitrogen	$N_2$	1.04	0.743	0.25	0.18	1.400	0.297	54.99
Nitrogen tetroxide	--	4.69	4.6	1.12	1.1	1.02	0.09	--
Nitrous oxide	$N_2O$	0.88	0.69	0.21	0.17	1.27	0.18	35.1
Oxygen	$O_2$	0.919	0.659	0.22	0.16	1.395	0.260	48.24
Pentane	---	---	----	---	----	1.07	----	--
Propane	$C_3H_8$	1.67	1.48	0.39	0.34	1.127	0.189	35.0
Propene	$C_3H_6$	1.5	1.13	0.36	0.31	1.15	0.18	36.8
Water Vapour	---	1.93	1.46	0.46	0.35	1.32	0.462	---
Steam, (low pressure)	--	1.97	1.5	0.47	0.36	1.31	0.46	--
Steam, (High pressure)	--	226	1.76	0.54	0.42	1.28	0.5	--
Sulfure Dioxide	$SO_2$	0.64	0.51	0.15	0.12	1.29	0.13	24.1

### C. Properties Of Pyro Carbon

Parameter	Property
Density	2.0-2.3 gm/cm <sup>3</sup>
Electrical Conductivity	Varies Widely
Break down field	> 1E7 V/cm
Thermal Conductivity	0.01 W/cm K
Thermal Diffusivity	0.009cm <sup>2</sup> /sec
Coefficient of thermal exposition	0.5 ppm/K

Refraction index	1.46 [Thermal oxide]
Dielectric Constant	3.9 [Thermal oxide]

#### D. Model Settings

S.No	Model	Settings
1	Space	2D
2.	Time	Steady
3.	Viscous	Standard K-epsilon turbulence model
4.	Wall Temperature	Standard Wall Function
5.	Heat Transfer	Enable
6.	Solidification and Melting	Disable
7.	Radiation	None
8.	Species Transport	Disabled
9.	Coupled Dispersed Phase	Disabled
10.	Pollutants	Disabled
11.	Soot	Disabled

#### D1. Model Zones

S.No	Zones	Type
1.	Default Interior	Fluid
2.	Inlet	Velocity Inlet
3.	Outlet	Pressure Outlet
4.	Side walls	Walls
5.	Fuel Pebbles	Walls

#### E. Boundary Conditions

##### E1. Fluid

Condition	Value
Material Name	helium
Motion Type	0
X-Velocity (m/s)	0
Y-Velocity (m/s)	0
Rotational Speed (rad/s)	0

X-Origin of rotation-Axis (m)	0
Y-origin of rotation-Axis (m)	0
Deactivated Thread	No
Laminar zone	No
Set Turbulence Viscosity	Yes
Porous zone	No
X-Component of Direction-1 Vector	1
Y-Component of Direction-1 Vector	0
Direction-1 Viscous Resistance (1/m <sup>2</sup> )	0
Direction-2 Viscous Resistance (1/m <sup>2</sup> )	0
Direction-1 Inertial Resistance (1/m)	0
Direction-2 Inertial Resistance (1/m)	0
C <sub>0</sub> Coefficient for power law	0
C <sub>1</sub> Coefficient for Power-Law	0
Porosity	1
Solid Material name	Aluminum

## E2. Reactor Inlet

Conditions	Value
Velocity Specification Method	2
Reference Frame	0
Velocity Magnitude (m/s)	350
X-Velocity (m/s)	0
Y-Velocity (m/s)	0
X-Component of Flow Direction	1
Y-Component of Flow Direction	0
X-Component of Axis Direction	1
Y-Component of Axis Direction	0
Z-Component of Axis Direction	0
X-Coordinate of Axis Origin (m)	0
Y-Coordinate of Axis Origin (m)	0
Z-Coordinate of Axis Origin (m)	0
Angular velocity (rad/s)	0



Temperature (k)	1173
Turbulent Specification Method	0
Turbulent Kinetic Energy ( $m^2/s^2$ )	5
Turbulent Dissipation Rate ( $m^2/s^3$ )	1
Turbulent Intensity (%)	0.1
Turbulent Length Scale (m)	1
Hydraulic Diameter (m)	1
Turbulent Viscosity Ratio	10
Outflow Gauge Pressure (pascal)	0

### E3. Reactor Outlet

Condition	Value
Gauge Pressure (pascal)	0
Backflow Total Temperature (k)	1173
Backflow Direction Specification Method	1
X-component of Flow Direction	1
Y-Component of Flow Direction	0
X-Component of Axis Direction	1
Y-Component of Axis Direction	0
Z-Component of Axis Direction	0
X-Coordinate of Axis Origin (m)	0
Y-Coordinate of Axis Origin (m)	0
Z-Coordinate of Axis Origin (m)	0
Turbulent Specification Method	0
Backflow Turbulent Kinetic Energy ( $m^2/s^2$ )	1
Backflow Turbulent Dissipation Rate ( $m^2/s^3$ )	1
Backflow Turbulent Intensity (%)	0.1
Backflow Turbulent Length Scale (m)	1
Backflow Hydraulic Diameter (m)	1
Backflow Turbulent Viscosity Ratio	10
Specify targeted mass flow rate	No
Targeted mass flow (kg/s)	1

#### E4. Side Walls

Condition	Value
Wall Thickness (m)	0
Heat Generation Rate ( $w/m^3$ )	0
Material Name	steel
Thermal BC Type	0
Temperature (k)	1173
Heat Flux ( $w/m^2$ )	0
Convective Heat Transfer Coefficient ( $w/m^2-k$ )	0
Free Stream Temperature (k)	300
Wall Motion	0
Shear Boundary Condition	0
Define wall motion relative to adjacent cell zone?	Yes
Apply a rotational velocity to this wall?	No
Velocity Magnitude (m/s)	0
X-Component of Wall Translation	1
Y-Component of Wall Translation	0
Define wall velocity components?	No
X-Component of Wall Translation (m/s)	0
Y-Component of Wall Translation (m/s)	0
External Emissivity	1
External Radiation Temperature (k)	300
Wall Roughness Height (m)	0
Wall Roughness Constant	0.5
Rotation Speed (rad/s)	0
X-Position of Rotation-Axis Origin (m)	0
Y-Position of Rotation-Axis Origin (m)	0
X-component of shear stress (pascal)	0
Y-component of shear stress (pascal)	0
Surface tension gradient (n/m-k)	0
Specularity Coefficient	0

## E5. Fuel Pebbles

Condition	Value
Wall Thickness (m)	0
Heat Generation Rate (w/m3)	5.1999998
Material Name	Titanium
Thermal BC Type	2
Temperature (k)	1173
Heat Flux (w/m2)	882450
Convective Heat Transfer Coefficient (w/m <sup>2</sup> -k)	79.5
Free Stream Temperature (k)	1173
Wall Motion	0
Shear Boundary Condition	0
Define Wall motion to adjacent cell zone	Yes
Apply a rotational velocity to this wall	No
Velocity Magnitude (m/s)	0
X-Component of wall Translation	1
Y-Component of wall translation	0
Define wall velocity component	No
X-Component of wall translation (m/s)	0
Y-Component of Wall Translation (m/s)	0
External Emissivity	1
External Radiation Temperature (k)	300
Wall Roughness Height (m)	0
Wall Roughness Constant	0.5
Rotation Speed (rad/s)	0
X-Position of Rotation-Axis Origin (m)	0
Y-Position of Rotation-Axis Origin (m)	0
X-component of shear stress (pascal)	0
Y-component of shear stress (pascal)	0
Surface tension gradient (n/m-k)	0
Specularity Coefficient	0

**F. Linear Solver**

Variable	Solver Type	Residual Reduction	Tolerance
Flow	F-Cycle	0.1	Na
Turbulent Kinetic Energy	Flexible	0.1	0.7
Turbulent Dissipation Rate	Flexible	0.1	0.7

**G. Discretization Scheme**

Variable	Scheme
Flow	Second Order Upwind
Turbulent Kinetic Energy	Second Order Upwind
Turbulent Dissipation Rate	Second Order Upwind

**H. Material Properties**

**H1. Material: Titanium (Solid)**

Properties	Units	Method	Values
Density	Kg/m <sup>3</sup>	Constant	4850
C <sub>p</sub>	J/Kg-K	Constant	544.25
Thermal Conductivity	w/m-k	Constant	7.4400001

**H2. Material: Steel (Solid)**

Properties	Units	Method	Values
Density	Kg/m <sup>3</sup>	Constant	8030
C <sub>p</sub>	J/Kg-K	Constant	502.48
Thermal Conductivity	w/m-k	Constant	16.27

### H3. Material: Helium (Fluid)

Properties	Units	Method	Values
Density	Kg/m <sup>3</sup>	Constant	0.16249999
C <sub>p</sub>	J/Kg-K	Constant	5193
Thermal Conductivity	w/m-k	Constant	0.152
Viscosity	kg/m-s	Constant	1.9900001e-05
Molecular Weight	kg/kgmol	Constant	4.0026
L-J Characteristic Length	angstrom	Constant	0
L-J Energy Parameter	k	Constant	0
Thermal Expansion Coefficient	1/k	Constant	0
Degrees of Freedom	NA	Constant	0
Speed of Sound	m/s	None	#f

### H4. Material: Air (Fluid)

Properties	Units	Method	Values
Density	Kg/m <sup>3</sup>	Constant	1.225
C <sub>p</sub>	J/Kg-K	Constant	1006.43
Thermal Conductivity	w/m-k	Constant	0.0242
Viscosity	kg/m-s	Constant	1.7894e-05
Molecular Weight	kg/kgmol	Constant	28.966
L-J Characteristic Length	angstrom	Constant	3.711
L-J Energy Parameter	k	Constant	78.6
Thermal Expansion Coefficient	1/k	Constant	0
Degrees of Freedom	NA	Constant	0
Speed of Sound	m/s	None	#f

### H5. Material: Aluminum (Solid)

Properties	Units	Method	Values
Density	Kg/m <sup>3</sup>	Constant	2719
C <sub>p</sub>	J/Kg-K	Constant	871
Thermal Conductivity	w/m-k	Constant	202.4

### I. Solution Limits

Quantity	Limit
Minimum Absolute Pressure	1
Maximum Absolute Pressure	5e+10
Minimum Temperature	1
Maximum Temperature	5000
Minimum Turb. Kinetic Energy	1e-14
Minimum Turb. Dissipation Rate	1e-20
Maximum Turb. Viscosity Ratio	100000

### J. Hydrogen Production Source Analysis

Properties	Type I (%)	Type II (%)
<b>Proximate Analysis Standard Data</b>		
Moisture	27.1 %	27.0
Ash	10.1	8.0
Volatile Matter	33.0	36.0
Fixed Carbon	29.8	29.0
Total	100.0	100.0
<b>Ultimate Analysis</b>		
Carbon	70.4	69.5
Hydrogen	5.2	4.5
Nitrogen	1.3	--
Chlorine	0.0	--
Oxygen	22.8	24.8
Sulfur	0.3	0.3
Total	100.0	100.0
Heating Value(Btu/lb)	7650	7800

## K. Programs Used For Calculations

### K1. Program for the Calculation of Coolant Flow Rate, Heat Transfer Coefficient

```
#include<stdio.h>
#include<conio.h>
#include<math.h>
main()
{
float c,P,R,M,m,row,T,W,xP,v,A,Ac,pi,D,Dc,Sh,L,h,Q,xT,St,cp,He;
clrscr();
print("Enter the value of R:");
Scanf("%f",&R);
Printf("Enter the value of T:");
Scanf("%f",&T);
If(row=He)
{
printf(" Enter the He value:");
Scanf("%f",&He);
}
else
{
Printf(" Enter the compound name:");
Scanf( "%f",&c);
}
P=(r/m)*row*T;
printf("P=%f",P);
printf(" Enter the value of m:");
scanf("%f",&m);
printf("Enter the value of p1:");
scanf("%f",&p1);
printf("Enter the value of p2:");
```

```

scanf("%f", &p2);
xp=p1-p2;
printf("xP=%f",xp);
W=m*(xP/row);
printf("W=%f",W);
printf("Eneter the value of A:");
Scanf("%f",&A);
Printf("Eneter the value of: Ac");
Scanf("%f",&Ac);
v=A/Ac
printf("Enter the value of D:");
scanf("%f",&D);
Printf("Eneter the value of Dc");
Scanf("%f",&Dc);
v=(pie*D*D*)/(pie*Dc*Dc);
printf("v=%f",v);
printf("eneter the value of S:");
Scanf("%f",&S);
printf("enter the value of L:");
Scanf("%f",&L);
S=pie*D*L;
printf("S=%f",S);
h=(Q/(S*xT);
Printf("h=%f",h);
getch();
}

```

### **J1.C++ Program for Coolant Flow Rate Calculation**

```

#include<stdio.h>
#include<conio.h>
#include<math.h>
void main()

```



```

{
float row,v,A,m,Q,Cp,xT,xP,f,L,D;
clrscr();
printf("Enter the input parameters:v= row= A= Cp= xT= f= L= D=");
scanf("f%f%f%f%f%f%f%f",&row,&v,&A,&m,&Q,&Cp,&xT,&xP,&f,&L,&D);
m=row*v*A;
printf("m=%f",m);
Q=m*Cp*xT;
printf("Q=%f",Q);
xP=0.5*row*v*v*(4*f*L)/D;
printf("xP=%f",xP);
getch();
}

```

## **J2. C++ Program for Coolant Circulation Rate In Fusion Reactors**

```

# include<stuio.h>
#include<conio.h>
#include<math.h>
main()
{
float V,Q,Cp,Tm,Tin,del,qm,k,h,w,f,row,x;
clrscr();
printf("Enter the input parameters:");
Scanf("%f%f%f%f%f%f%f%f%f%f",&V,&Q,&Cp,&Tm,&Tin,&del,&qm,&k,
&h,&w,&f,&row,&x");
x=Cp*row*(Tmax-Tin-(del*qm/k)-(qm/h));
V=Q/x;
printf("x=%f",x);
printf("V=%f",f);
getch();
}

```